

2



2

1. AGENCY USE ONLY (leave blank)	2. REPORT DATE September 1992	3. REPORT TYPE AND DATES COVERED Final 1 Jun 91 - 31 Aug 91
4. TITLE AND SUBTITLE	5. FUNDING NUMBERS	

Symposium on Polymeric Materials for Photonic and Optical Applications

6. AUTHOR(S) Gary C. Bjorklund	61102F 2303 A3
-----------------------------------	----------------

7. PERFORMING ORGANIZATION NAME(S) AND ADDRESS(ES) American Chemical Society 1155 16th Street N.W. Washington, DC 20036-4801	8. PERFORMING ORGANIZATION REPORT NUMBER AFOSR-TR- 92- 0184
---	--

9. SPONSORING/MONITORING AGENCY NAME(S) AND ADDRESS(ES) AFOSR/NC Building 410, Bolling AFB DC 20332-6448	10. SPONSORING/MONITORING AGENCY REPORT NUMBER AFOSR-91-0275
---	---

11. SUPPLEMENTARY NOTES

12a. DISTRIBUTION/AVAILABILITY STATEMENT APPROVED FOR PUBLIC RELEASE; DISTRIBUTION IS UNLIMITED.	12b. DISTRIBUTION CODE
---	------------------------

13. ABSTRACT (Maximum 200 words) See Attached
--

DTIC ELECTE
S B D
OCT 0 1 1992

92

CH 750

92-26275



11894

14. SUBJECT TERMS	15. NUMBER OF PAGES 112
16. PRICE CODE	

UNCLASSIFIED

UNCLASSIFIED

UNCLASSIFIED

13. A symposium on Polymeric Materials for Photonic and Optical Applications was held as part of the 4th Chemical Congress of North America and 202nd ACS National Meeting during August 25-30, 1991 in New York, N.Y. This symposium was sponsored by the ACS Division of Polymer Chemistry and the ACS Division of Polymeric Materials: Science and Technology with the cooperation of the Optical Society of America. The symposium organizers were G. C. Bjorklund, G. Hadziioannou, J. Torkelson, and M. A. Winnik.

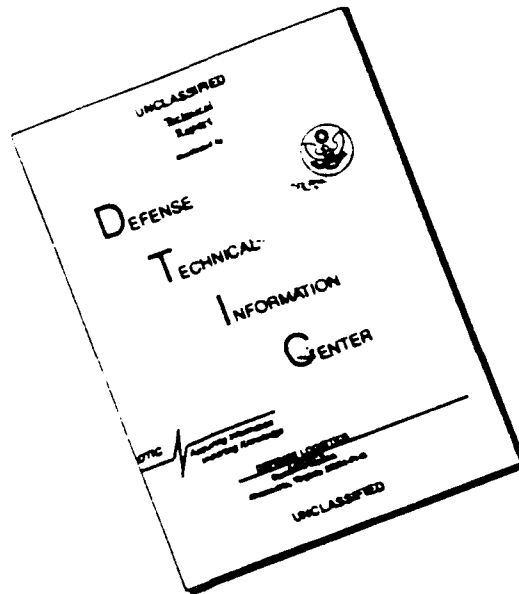
The goal of the symposium was to cover in depth the chemistry, characterization, and device application of polymers for photonics and optics. The major objective was to bring together leading experts from around the world to elucidate the major scientific challenges and hurdles that must be overcome for photonic polymers to reach their full potential and find major device applications.

The symposium consisted of a tutorial session, a poster session, and five oral sessions, extending over three full days. A total of 32 distinguished scientists presented invited papers. Of these, 21 were from North America, 9 from Europe, and 2 from Japan. In addition, 28 contributed papers were presented. Interactions among the attendees were quite good and the overall attendance was strong, with some of the sessions being held by more than 250 people.

DTIC QUALITY INSPECTED 3

Accession For	
NTIS GRA&I	<input checked="" type="checkbox"/>
DTIC TAB	<input type="checkbox"/>
Unannounced	<input type="checkbox"/>
Justification	
By _____	
Distribution/	
Availability Codes	
Dist	Avail and/or Special
A-1	20

DISCLAIMER NOTICE



THIS DOCUMENT IS BEST QUALITY AVAILABLE. THE COPY FURNISHED TO DTIC CONTAINED A SIGNIFICANT NUMBER OF PAGES WHICH DO NOT REPRODUCE LEGIBLY.

**SYMPOSIUM ON POLYMERIC MATERIALS FOR
PHOTONIC AND OPTICAL APPLICATIONS
- FINAL TECHNICAL REPORT**

**4th Chemical Congress of North America and
202nd ACS National Meeting**

New York, N.Y.

August 25-30, 1991

Approved for public release;
distribution unlimited.

SYMPOSIUM ON POLYMERIC MATERIALS FOR PHOTONIC AND OPTICAL APPLICATIONS

FINAL TECHNICAL REPORT

A symposium on Polymeric Materials for Photonic and Optical Applications was held as part of the 4th Chemical Congress of North America and 202nd ACS National Meeting during August 25-30, 1991 in New York, N.Y. This symposium was sponsored by the ACS Division of Polymer Chemistry and the ACS Division of Polymeric Materials: Science and Technology with the cooperation of the Optical Society of America. The symposium organizers were G.C. Bjorklund, G. Hadziioannou, J. Torkelson, and M.A. Winnik.

The goal of the symposium was to cover in depth the chemistry, characterization, and device application of polymers for photonics and optics. The major objective was to bring together leading experts from around the world to elucidate the major scientific challenges and hurdles that must be overcome for photonic polymers to reach their full potential and find major device applications.

The symposium consisted of a tutorial session, a poster session, and five oral sessions, extending over three full days. A total of 32 distinguished scientists presented invited papers. Of these, 21 were from North America, 9 from Europe, and 2 from Japan. In addition, 28 contributed papers were presented. Interactions among the attendees were quite good and the overall atmosphere was strong, with some of the sessions being held by more than 250 people.

GARY C. BJORKLUND
IBM ALMADEN RESEARCH CENTER
SAN JOSE, CALIFORNIA
SEPTEMBER 21, 1992

SYMPOSIUM ON POLYMERIC MATERIALS
FOR PHOTONIC AND OPTICAL APPLICATIONS

- FINANCIAL SUPPORT

AIR FORCE OFFICE OF SCIENTIFIC RESEARCH

ACS PETROLEUM RESEARCH FUND

DUPONT

IBM

KODAK

LOCKHEED

ACS DIVISION OF POLYMER MATERIALS SCIENCE AND ENGINEERING

ACS DIVISION OF POLYMER CHEMISTRY

POLYMER PREPRINTS

Volume 32

Number 3

August 1991

Published by The Division of Polymer Chemistry, Inc.

American Chemical Society

Papers presented at the New York, NY Meeting

Copyright © 1991 by The Division of Polymer Chemistry, Inc.
American Chemical Society. No papers may be reprinted without permission.
Publication Date: August 12, 1991

NEW YORK MEETING PROGRAM

Polymeric Materials for Photonic and Optical Applications

Organizers: G.C. Bjorklund, G. Hadziioannou, J. Torkelson and M.A. Winnik

Session 1. Tutorial

SUNDAY MORNING:

- 1 8:45 Introduction to Nonlinear Optics. G.C. Bjorklund.
- 2 9:30 Rational Design of Organic NLO Materials. T.J. Marks.
- 3 10:30 Characterization of NLO Materials. G.R. Meredith.
- 4 11:15 Materials Requirements for Active and Passive Devices. R. Lytel.
- 5 1:30 Introduction to Photorefractive Materials and Phenomena.
P. Gunter.

Session 2. Nonlinear Optical Properties of Polymers: Theory and Experiment

SUNDAY AFTERNOON

- 6 2:30 Orientation of Organic Molecules in Sol-Gel Matrices for Quadratic
Nonlinear Optics. G. Pucetti, E. Toussaere, I. Ledoux, J. Zyss,
P. Griesmar, C. Sanchez. 61
- 7 3:00 Electron Correlated States and Nonlinear Optical Properties of Linear
Chains. A.F. Garito, J.R. Heflin. 63
- 8 3:30 Linear and Nonlinear Optical Properties of Highly Ordered Conjugated
Polymers in Polyethylene: Orientation by Mesoepitaxy. C. Halvorson,
D. Moses, T.W. Hagler, K. Pakbaz, A.J. Heeger. 65
- 9 4:00 Determination of Third-Order Nonlinear Susceptibilities of
Semiconducting Polymers. Comparison with Theoretical Calculations.
J. Messier, F. Charra, C. Sentein. 67

10	4:30	A Survey of the NLO-Polymer Program at the MPI. C. Bubeck, G. Duda, A. Grund, W. Hickel, <u>W. Knoll</u> , A. Kaltbeitzel, A. Mathy, W.A. Meyer, D. Neher, T. Sauer, H.-U. Simmrock, G. Wegner, A. Wolf.	69
11	5:00	Cubic Nonlinear Optics of Polymer Thin Films. I. Molecular Engineering and Processing of Polymers with Large Third-Order Optical Properties for Photonic Switching. <u>S.A. Jenekhe</u> , A.K. Agrawal, C.J. Yang, J.A. Osaheni, W.-C. Chen, M.F. Roberts.	71

Session 3. Synthesis and Chemistry of NLO Polymers I

MONDAY MORNING

102	8:30	Highly Polarizable Metallic Complexes for Nonlinear Optics. T. Thami, M.A. Petit, <u>J. Simon</u>	73
103	9:00	Investigation of New Molecules and Materials for Quadratic Nonlinear Optics. <u>J.F. Nicoud</u>	74
104	9:30	Preparation of Polymeric Films for NLO Applications. R.P. Foss, <u>W. Tam</u> , F.C. Zumsteg.	76
105	10:15	Synthesis of Side-Chain and Main-Chain Nonlinear Optical Polymers with Sulfonyl Acceptor Groups. <u>D.R. Robello</u> , J.S. Schildkraut, N.J. Armstrong, T.L. Penner, W. Kohler, C.S. Willand.	78
106	10:45	Synthetic Approaches to NLO Polymers. <u>R. Twieg</u> , D. Burland, M. Lux, C.R. Moylan, C. Nguyen, P. Walsh, C.G. Willson, R. Zentel.	80
107	11:15	Novel Sidechain Polymers for Electro-optic Applications. <u>D.E. Allen</u> , R.A. Keosian, G. Khanarian, J. Hudop, S.J. Meyer.	82
108	11:45	Synthesis and Nonlinear Optical Characteristics of Chromophore-Functionalized Polymers Having Chromophore-Centered Hydrogen-Bonding and Crosslinking Groups. <u>Y. Jin</u> , S.H. Carr, T.J. Marks, W. Lin, G.K. Wong.	

Session 4. Synthesis and Chemistry of NLO Polymers II

MONDAY AFTERNOON

126	1:30	Synthesis of Controlled Structure Polyolefins. R.H. Gubbs	84
127	2:00	Chromophoric Self-Assembled Superlattices. Multilayer Construction of Thin Film Nonlinear Optical Materials. D.S. Allan , F. Kubota, Y. Orihashi, D. Li, T.J. Marks, T.G. Zhang, W.P. Lin, G.K. Wong.	86
128	2:30	A New Molecular Design Concept for the Poled Polymers — Utilizing the Off-Diagonal Tensor Components of the Molecule. T. Watanabe, M. Kagami, H. Yamamoto, A. Kidoguchi, S. Miyata , A. Hayashi, H. Sato.	87
129	3:15	Novel Polymers with Photorefractive and NLO Properties. G. Hadziioannou , J. Wildeman, J. Herrema, P. Soeteman, D. Hissink, J. Brouwer, R. Flipse.	90
130	3:45	Thermally Stable Electro-Optic Polymers. S. Ermer , J.T. Kenney, J.W. Wu, J.F. Valley, R. Lytel, A.F. Garito.	92
131	4:15	Design and Synthesis of a New Class of Photocrosslinkable Nonlinear Optical Polymers. S. Tripathy , B. Mandal, R.J. Jeng, J.Y. Lee, J. Kumar.	94
132	4:45	Towards High Susceptibilities in Soluble Polyacetylenes for Non-Linear Optics. J. Le Moigne , A. Hilberer, C. Strazielle.	96

Session 5. Processing and Characterization of NLO Polymers

TUESDAY MORNING

150	8:30	Second Harmonic Generation and Electrochromism Studies of Electrical Properties of Nonlinear Optical Polymers and Devices. C.S. Willand , M. Scozzafava.	
151	9:00	Orientation and Decay in Poled Polymer Nonlinear Optical Materials. K.D. Singer , L.A. King.	98
152	9:30	Second-Order Nonlinear Optical Onset and Decay and Their Relationship to Polymer Physics. A. Dhinojwala, G.K. Wong, J.M. Torkelson	100

153	10:15	Second-Order NLO and Relaxation Properties of Poled Polymers. <u>D.Y. Yoon</u> , D. Jungbauer, I. Teraoka, B. Reck, R. Zentel, R. Twieg, J.D. Swalen, C.G. Willson.	102
154	10:45	Nonlinear Optical Properties of Polymer/Silver Microsphere Composites. <u>M.P. Andrews</u> , M.G. Kuzyk.	105
155	11:15	The Photorefractive Effect in Non-Linear Polymers Doped with Charge Transport Agents. <u>J.C. Scott</u> , S. Ducharme, R.J. Twieg, W.E. Moerner.	107
156	11:45	Second-Harmonic Generation from Hyperpolarizable Amphiphiles at Polymer-Polymer Interfaces. <u>J.P. Gao</u> , G.D. Darling.	109

Session 6. Photonic Polymers for Device Applications

TUESDAY AFTERNOON

174	1:30	Low-Loss Graded-Index and Single-Mode Polymer Optical Fibers. <u>Y. Koike</u> , E. Nihei.	111
175	2:00	Planar Polymer Waveguides for Optical Interconnections. <u>B.L. Booth</u> , J.E. Marchegiano, C.T. Chang, T.K. Foreman, J.L. Hohman, S.L. Witman.	113
176	2:30	Guided-wave Nonlinear Optics in DCANP Langmuir-Blodgett Films. <u>P. Günter</u> , Ch. Bosshard, M. Küpfer, M. Flörsheimer.	115
177	3:15	Optically Nonlinear Polymers in Waveguiding Passive and Active Devices. <u>G.R. Möhlmann</u> , W.H.G. Horsthuis.	116
178	3:45	NLO Polymers for Frequency Doubling: Synthesis, Characterization and Photochemical Stability. <u>E.G.J. Staring</u> , G.L.J.A. Rikken, C.J.E. Seppen, S. Nijhuis, A.H.J. Venhuizen.	118
179	4:15	Recent Developments in Efficient Frequency Doubling in Poled Polymer Films. <u>G. Khanarian</u> , S. Meyer, R.A. Norwood, H.A. Goldberg, D. Holcomb, J. Stamatoff.	120
180	4:45	Photochemically Delineated Refractive Index Profiles in Polymeric Slab Waveguides. <u>K.A. Horn</u> , D.B. Schwind, J.T. Yardley.	122

Poster Presentations: Polymeric Materials for Photonic and Optical Applications

TUESDAY EVENING

5:30-7:30 PM

- 205 Cubic Nonlinear Optics of Polymer Thin Films. 2. Structure- $\chi^{(3)}$ Relationships in Rigid-Rod Polyquinolines. **A.K. Agrawal**, S.A. Jenekhe, H. Vanherzeele, J.S. Meth. 124
- 206 A Study of the Competition Between Electric Field Induced Molecular Ordering and Chemical Cross Linking in Vitrified Nonlinear Optical Polymer Films. **J.D. Bewsher**, G.R. Mitchel. 126
- 207 Metal Nanoclusters Within Block Copolymer Microdomains. **G.S.W. Craig**, R.E. Cohen, Y. Ng Cheong Chan, R.R. Schrock. 128
- 208 Nonlinear Optical Properties of Linear Epoxy Polymers with Pendant Sulfonyl Tolan Groups. **M. Ebert**, M. Lux, B.A. Smith, R. Twieg, C.G. Willson, D.Y. Yoon. 130
- 209 Synthesis and Characterization of Monomers and Polymers Containing Photoresponsive Azobenzene-based Sidegroups. **H.J. Haitjema**, G.O.R. Alberda v. Ekenstein, Y.Y. Tan, P.J. Werkman, A.J. Koldijk, T.S. Boer. 132
- 210 Poling and Chemical-Binding of Glass-Embodied Chromophores in Supported Sol-Gel Thin-Film Glasses for Second Harmonic Generation. Y. Haruvy, **J. Byers**, S.E. Webber. 134
- 211 Model Molecules with Donor-Acceptor Units Intermediated by Silicon Chains. **D. Hissink**, J. Brouwer, R. Flipse, G. Hadziioannou. 136
- 212 Novel Third Order NLO Materials from 96% Quinoline. **R.V. Honeychuck**. . . . 138
- 213 Cubic Nonlinear Optics of Polymer Thin Films. 5. Wavelength Dispersion of the $\chi^{(3)}$ of Poly(p-phenylene Benzobisthiazole) Based Molecular Composites. **S.A. Jenekhe**, M.F. Roberts, H. Vanherzeele, J.S. Meth. 140
- 214 Measurements of the Opto-Electric Properties of Molecules of Potential Use in Photoactive Polymers by Time Resolved Microwave Conductivity (TRMC). **S.A. Jonker**, J.M. Warman. 142
- 215 Macromolecular Chromophoric Assemblies with Enforced Polarity: Inorganic and Heterocyclic Linkages. **H.E. Katz**, M.L. Schilling, C.E.D. Chidsey, T.M. Putvinski, W.L. Wilson, G.R. Scheller, W.T. Lavell. 144

216	Synthesis, Poling, and Optical Characterization of Polyurethane Films Bearing NLO-Active Chromophores. P. Kitipichai, R. Laperuta, Jr., G.M. Korenowski, G.E. Wnek , I. Gorodisher.	146
217	Synthesis, Experimental, and Theoretical Studies of New Group 6 Pentacarbonyl-Based MLO Chromophores Exhibiting Large and Unusual Optical Nonlinearities. P. Larcroix , T.J. Marks, D.A. Kanis, M.A. Ratner, W. Lin, G.K. Wong.	
218	Optical Four-Wave Mixing in a Silver Colloid-Polymer Composite. R. LaPeruta , P. Kitipichai, G.E. Wnek, G.M. Korenowski.	148
219	Novel Photochromic Liquid Crystal Polymers. C.H. Legge , M.J. Whitcombe, A. Gilbert, G.R. Mitchell.	150
220	Synthesis of Block Copolymers of Poly(styrene) and Poly(arylate) and Their Optical Properties. H. Ohishi , S. Inaba, M. Kawabe, M. Kimura.	152
221	Cubic Nonlinear Optics of Polymer Thin Films. 4. Structure- $\chi^{(3)}$ Relationships in Polyanilines and Derivatives. J.A. Osaheni , S.A. Jenekhe, H. Vanherzeele, J.S. Meth.	154
222	Opto-Electronic Properties and Second Harmonic Generation by σ -Bond Separated Donor-Acceptor Molecules. W. Schuddeboom , B. Krijnen, J.W. Verhoeven, E.G.J. Staring, G.L.J.A. Rikken, H. Oevering, S.A. Jonker. . . .	156
223	Side Chain Copolymers for Third Order Nonlinear Optical Applications. J.R. Sounik , R.A. Norwood, J. Popolo, D. Holcomb.	158
224	Quantitative Study of Molecular Orientation of Hemicyanine Langmuir-Blodgett Films by Fourier Transform Infrared Spectroscopy and Second Harmonic Generation. W.-F. A. Su , T. Kurata, H. Nobutoki, H. Koezuka.	160
225	Internal Electric Field and Dye Orientation in PVDF/PMMA Blend. N. Tsutsumi , Y. Ueda, T. Kiyotsukuri.	163
226	Cubic Nonlinear Optics of Polymer Thin Films. 3. Structure- $\chi^{(3)}$ Relationships in Conjugated Aromatic Polyazomethins. C.-J. Yang , S.A. Jenekhe, H. Vanherzeele, J.S. Meth.	165

ORIENTATION OF ORGANIC MOLECULES IN SOL-GEL MATRICES FOR QUADRATIC NONLINEAR OPTICS.

Germain Puccetti, Eric Toussaere, Isabelle Ledoux and J.Zyss
Centre National d'Etudes des Télécommunications
196 Avenue Henri Ravera, 92220-Bagneux, France
Pascal Griesmar and Clément Sanchez
Laboratoire de Chimie de la Matière Condensée
Université Pierre et Marie Curie
4 Place Jussieu 75252-Paris, France

ABSTRACT: Orientation of nonlinear organic molecules in ion-free sol-gel matrices upon application of an external D.C. electrical field is being evidenced. The quadratic nonlinear response of silicon oxide and transition metal oxide based gels containing organic molecules have been determined from Electric Field Induced Second Harmonic (EFISH) measurements. Large concentrations of optically Nonlinear Organic Molecules (NOM) have been either incorporated inside the macromolecular network or chemically bonded to the oxide backbone of the gels. The feasibility of permanently corona poled films has subsequently been demonstrated. Moreover EFISH measurements offer an original point of view on conformational changes occurring in the process of sol-gel transformations.

The relevance of conjugated organic molecules towards the enhancement of nonlinear optical susceptibilities is now well documented and rests on the higher polarizabilities of eventually asymmetricized π electron systems which can be tuned to application requirements.⁽¹⁾ The unlimited possibilities of organic synthesis may then be fruitfully exploited following the indications of molecular engineering design rules. However, the next step aiming at the organization of molecular entities in macroscopic assemblies is mastered only to a lesser extent.

Although single crystals are of great interest as they allow to connect macroscopic observations to molecular phenomena, based on well defined crystallographic data, their structure is in general unpredictable and they may be difficult to grow. Besides, thin films and waveguides are required for integrated optics and may not be readily obtained in single crystalline format, although some promising early demonstrations have recently come out. These difficulties have spurred the introduction of organic polymers, mainly in the context of quadratic nonlinear optics, as a host passive matrix where active nonlinear molecules (subsequently referred to as NOM) are being either introduced as dispersed guest-entities at a limited concentration level, or anchored to the polymeric chain at higher concentrations. Subsequent electric field orientation above T_g , either via electrodes or corona poling is then possible to provide the required dipolar orientation for $\chi^{(2)}$ processes.⁽²⁾

It seems worthwhile to explore a similar strategy with a mineral matrix as the passive backbone; however, usual glasses are processed at temperatures precluding the incorporation of organic molecules which will not be able, in general, to sustain heating above 100°C. It is thus impossible to reach the glassy viscous phase required for poling without irreversibly damaging the material. Alternatively, sol-gel glasses offer attractive possibilities permitting to comply with the thermal requirements. Sol-gel chemistry is mainly based on inorganic polymerisation reactions at room temperature. Starting from molecular precursors, a macromolecular oxide network is formed via hydroxylation-condensation reactions.⁽³⁾ An additional important condition for the applications in view here, is to avoid the presence of charged entities, such as catalytic residues, that would prevent the application of a poling field as demanded by EFISH or subsequent permanent orientation of a thin film.

This condition can be met when perfectly transparent sol-gel matrices are synthesized without the participation of acid catalysts.⁽⁴⁾ We have thus been able, to demonstrate, for the first time to the best of our knowledge, electric field induced second harmonic (EFISH) generation in sol-gel glasses where non linear molecules are either incorporated as guests or anchored to the polymeric backbone. Moreover, the rheological properties of sols allow for the easy deposition of films on a variety of substrates such as glass, ceramics, semiconductors or polymers.

The fabrication of the polymeric gels requires a decrease of the functionality of the molecular precursor towards hydrolysis so as to allow for the decoupling of hydrolysis and condensation rates. Furthermore, condensation must be slowed down with respect to hydrolysis. Acid catalysis is a classical means, however inadequate in the present context, to activate the reactivity of $\text{Si}(\text{OR})_4$ silicon alkoxide precursors towards hydrolysis. Activation of silicon alkoxide precursors towards hydrolysis can also be performed by increasing the electrophilic character of the Silicon atom. This has been performed by adding dimethyl aminopyridine (DMAP) that catalyses the nucleophilic reaction via a mechanism named SNASi .⁽⁵⁾ $\text{SiH}(\text{OR})_3$ precursors which exhibit a higher reactivity towards hydrolysis probably due to the presence of SiH bonds have also been used for the synthesis of transparent polymeric gels within relatively short gelation times.

The synthesis of transparent polymeric Transition Metal Oxide (TMO) gels can be performed by using complexing ligands.⁽⁶⁾ Such a synthesis does not generate charged species. Alkoxy groups are replaced by new ligands that can be less easily removed upon hydrolysis. Thus alkoxy ligands are rather quickly removed at first upon hydrolysis while chelating ones (the modifiers) act as termination agents, that inhibit condensation reactions thus slowing down the polymerisation process. Complexation decreases the functionality of the precursor promoting anisotropic growth that favors the formation of transparent polymeric gels.

Following the synthetic routes undermentioned, gels having good transparency, reasonable mechanical integrity and relatively short gelation times were obtained without the presence of charged species which would prevent EFISH measurements.

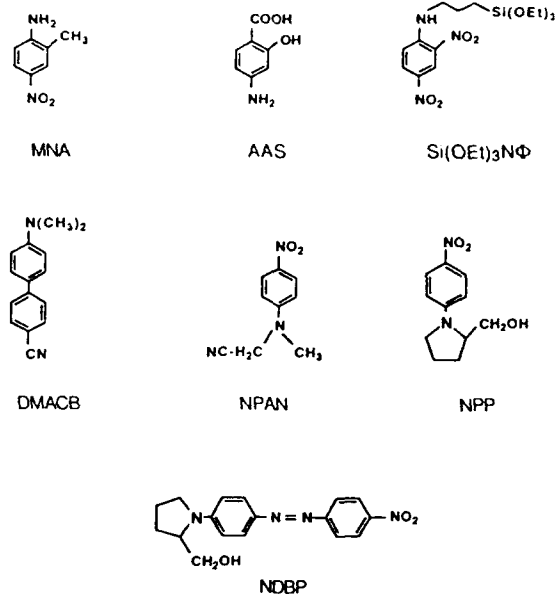


Fig.1 Nonlinear chromophores which have been inserted in the silica sol-gel matrices

The organic nonlinear chromophores investigated in this work are displayed in Fig.1. Their quadratic hyperpolarizabilities have been determined by the usual EFISH measurements performed in solution.

Organic groups can be bonded to an inorganic silica based network in two different ways, respectively as network modifiers or as network formers. Both functions have been recently achieved in the so-called ORMOSILS.⁽⁷⁾ The precursors of these compounds are organo-substituted silicic acid esters of general formula $\text{R}^1_n\text{Si}(\text{OR})_{4-n}$ where R^1 can be any organo-functional group. R^1 is a non hydrolysable organic group which can have a network modifying effect ($\text{R}^1 = \text{CH}_3$ or C_6H_5) or/and any desirable optical property.

However the chemical tailoring performed with silicon alkoxide precursors cannot be directly extended to transition metals or aluminium alkoxide precursors because the more ionic M-C bond would be cleaved upon hydrolysis. Chemical modifications could however be performed using complexing ligands preferably with β -diketones and allied derivatives or polyhydroxylated ligands such as α or β -hydroxyacids. These derivatives appear to be stable because of chelating and steric hindrance effects. Therefore, they are not removed during hydrolysis leading to new mixed organic-inorganic materials. Hybrid inorganic-organic transparent networks have been obtained using amino salicylic acid as complexing reagent for a transition metal alkoxide.

EFISH measurements have been undertaken following a well documented experimental procedure.⁽⁸⁾ The applied field value is of the order of 3-10 kV/mm over a plateau of 2 μs duration. The fundamental wavelength is generated by a Nd^{3+} -YAG laser emitting at 1.34 μm . The absorption of both fundamental and harmonic waves is then negligible. The SHG macroscopic third order susceptibility Γ originates from the contribution of microscopic susceptibilities γ attached to the organic chromophores (n molecules either doped or anchored per unit volume) to which the "background" susceptibility of the sol-gel medium must be further added following Eq.1:

$$\Gamma = \Gamma_{\text{sol}} + n\gamma \quad \text{Eq. 1}$$

Calling μ , β , and γ , the dipole and the first and second order hyperpolarizabilities of the NOM's, x and M their mass concentration and molecular weights, f the local field factor, ρ the density of the sol-gel medium, the following relation can be used to derive β :⁽⁹⁾

$$\gamma = \gamma_c + \frac{\mu\beta}{5kT} = [(1+x)\Gamma - \Gamma_{\text{sol}}] \frac{M}{Nf\rho x} \quad \text{Eq. 2}$$

γ_c may then be neglected for the conjugated molecular size of interest here.

The viscosity experienced by optical probes follows a Stokes-Einstein law. As soon as the reorientational correlation time of organic molecules surpasses the duration of the poling field plateau (i.e. 1 μs), the EFISH signal will vanish. Assuming a reorientational time of the order of 10^{-11} s for a mean molecular size of 5 Å, the EFISH signal at times $t \ll t_{\text{pol}}$ for molecules embedded in sols is comparable to that from molecules in regular solutions.

β values of the various nonlinear organic molecules shown in fig.1 (MNA, NPP, DMAP) have been measured in sol-gels and compared to those reported in the literature.^(10,12) The similarities between β values measured for N.O.M. dissolved in organic solvents and for N.O.M. embedded inside sol-gel systems also evidence the good stability of the non-linear molecules when embedded inside inorganic polymers. Detailed values are to be found in ref. 5. When large concentrations of N.O.M. (typically 0.5M) are incorporated inside wet sol-gel systems, drying lead to a partial crystallisation of the N.O.M. preventing measurements.

The functionalized silicon alkoxide ($\text{SiN}(\text{OEt})_3$) precursor exhibits a quite strong EFISH signal ($\beta = 13 \cdot 10^{-30} \text{esu}$, $\lambda = 1.34 \mu\text{m}$) close to that reported for MNA in dioxane ($\beta = 12.8 \cdot 10^{-30} \text{esu}$, $\lambda = 1.34 \mu\text{m}$). Large concentrations (0.2-0.5M) of chemically bonded N.O.M. ($\text{SiN}(\text{OEt})_3$) or ASA can be incorporated inside silica based sol-gel systems without any crystallisation even upon drying.

At longer timescales the different sol colloidal solutions lead to the formation of gels through a transformation process which can be also followed phenomenologically by changes in the viscosity. The evolution of a Zirconium oxide based system doped with MNA is described in Fig.2.

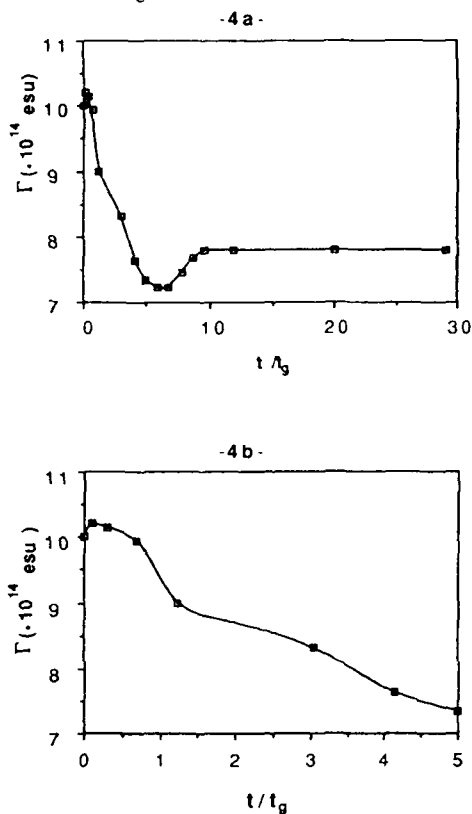


Fig.2 a. Evolution of the SHG macroscopic susceptibility Γ versus t/t_g for an MNA doped zirconium oxide based gel.
b. Expanded view for times up to $t/t_g = 1$.

There is only a slight change of Γ (10%) at the gelation point although the initial solution has turned to a solid amorphous material which does not exhibit macroscopic flow. Thus, in the case of solidification caused by gelation, the EFISH results show that the macroscopic rigidification of the sol does not extend down to the microscopic scale. The solvent phases at the gel point consists of propanol and water which account for the largest volume fraction of the gel (70%). The solid phase that causes the rigidity at the macroscopic level only represents a small percentage of the total volume of the gel. At this stage, the mobility of the MNA molecules is not significantly constrained by the open structure of the gel. Subsequently, the reorientational time of MNA is about the same in the gel and in the sol showing that MNA probes are weakly affected by gelation.

The next step of the process starting after $t=t_g$ corresponds to ageing. The decrease of the SHG macroscopic susceptibility Γ of MNA is observed until a minimum is reached at $5t_g$. The decrease of the SHG macroscopic susceptibility Γ can be assigned to the increasing restriction of dye motion as the connectivity of the oxide gel network extends. Molecular transport of reactants and products is however still possible through the interstitial liquid phase. Continued hydrolysis and condensation reactions will, therefore, go on. The molecular probe is not simply surrounded by the interstitial solvent and small oligomers as was the case during the gelation stage, but must now interact with numerous percolating medium size Zirconium oxide based polymers.

In the course of ageing (between $t/t_g = 7$ and $t/t_g = 10$) in a close vessel, the zirconium oxide based gels exhibit a slight increase of the SHG macroscopic susceptibility Γ . This increase can be accounted for either by a local depolymerisation occurring upon electrical and laser sollicitations or by condensation of smaller polymers along larger ones at the surface of the porous medium. This latter phenomenon must restrict the amount of polymeric species hindering rotation in the liquid phase of the gel and thus decrease the viscosity experienced by the MNA probe, consequently leading to an increase of Γ .

In the last sequence of the process, the macroscopic susceptibility Γ reaches a plateau which remains quite high (80% of the initial EFISH signal is still observed). This observation indicates that the fluidity around many dye molecules is important even a long time after the sol-gel transition has been passed ($> 30-40t_g$). EFISH measurements can lead therefore to an estimation of the wet porosity of gels.

EFISH of optical probes anchored at higher concentrations on siloxane based gels and transition metal oxide based gels has also been monitored versus the reduced gelation time t/t_g . The behaviour is then significantly different from that previously reported in the case of doped chromophores.

The macroscopic susceptibility Γ decreases as soon as the polymerisation reaction starts in contrast with the case of doped molecules where the decrease is smoother. When the N.O.M. is chemically bonded to the metallic center (Zr) the onset of the gelation is clearly detected by an immediate decrease of Γ until $t/t_g = 1$. This first transition observed by EFISH must reflect the percolation of a few larger polymers, those that lead to the macroscopic phenomenon of gelation. Then the evolution of Γ is roughly comparable to that previously reported. During the ageing period a decrease of Γ which reflects the crosslinking of the inorganic zirconium oxide based network is observed during a period of time extending from 1 to $10t_g$ (many ASA should be trapped in medium size polymeric clusters). After a long ageing period ($t/t_g > 100$), a slight decrease of Γ is observed showing that the crosslinking step has reached the microscopic level.

These results compared with those observed for MNA embedded in zirconium oxide based gels show that a molecule anchored on the metallic center (i.e. Zr) is a more intimate and sensitive probe of textural and structural changes occurring upon sol-gel transformations.

Furthermore, sol-gel glasses containing NPP molecules (0.310^{20} molecules/cm³) or anchoring ($\text{SiN}(\text{OEt})_3$) molecules (4.3310^{20} molecules/cm³) were spin coated on glass plates and oriented by corona poling. The matrices are mixed Zirconium oxide - organo-substituted silicic acid ester based materials. Maker fringe measurements were performed to measure the $\chi^{(2)}$ susceptibility. In the case of ($\text{SiN}(\text{OEt})_3$), a coefficient of 0.02 pm/V was obtained 1 month after poling. Optimisation of the content and poling conditions are currently under way.

In conclusion, we believe that investigations of sol-gel processes by nonlinear optical experiments will help further evidence, in conjunction with other methods, microscopic phenomena underlying rheological properties of importance for applications. Among these applications, nonlinear optics itself stand-out as a most promising area towards optoelectronics devices based on functionalized poled sol-gel thin films.

References

- 1) D.S. Chemla and J. Zyss, *Nonlinear Optical Properties of Organic Molecules and Crystals*, Academic Press (1987).
- 2) K.D. Singer, M.G. Kuzyk and J.E. Sohn, *J.Opt.Soc.Am. B*, 4, 968 (1987).
- 3) J. Livage, M. Henry and C. Sanchez, *Progress in Solid State Chemistry*, 18, 259 (1988).
- 4) C. Sanchez, J. Livage, M. Henry and F. Babonneau, *J. Non-Cryst. Solids* 100, 650 (1988).
- 5) P. Griesmar, C. Sanchez, G. Puccetti, I. Ledoux and J. Zyss, "Second harmonic generation from organic molecules incorporated in sol-gel matrices", to be published in *Mol. Eng.* (3), (1991).
- 6) R.J.P. Corriu, D. LeClercq, A. Vioux, M. Pauthe and J. Phalippou, in "Ultrastructure Processing of Advanced Ceramics", Eds J.D. Mackenzie and D.R. Ulrich 113 (J. Wiley N.Y., 1988).
- 7) G. Philipp and H. Schmidt, *J. Non-Cryst. Solids* 63, 283 (1984).
- 8) J.L. Oudar, *J.Chem.Phys.* 67, 446 (1977).
- 9) I. Ledoux and J. Zyss, *Chem.Phys.* 73, 203 (1982) and references therein.
- 10) J.F. Nicoud and R.J. Twieg in ref. 1, 255.
- 11) M. Barzoukas, D. Josse, P. Fremaux, J. Zyss, J.F. Nicoud and J.O. Morley, *J. Opt. Soc. Am. B*, vol.4, 977 (1987).
- 12) I. Ledoux, J. Zyss, A. Jutand, C. Amatore *Chem Phys.* 150, 117 (1991).

Electron Correlated States and Nonlinear Optical Properties of Linear Chains

by

A. F. GARITO and J. R. HEFLIN

Department of Physics

University of Pennsylvania, Philadelphia, Pennsylvania 19104

The electronic origin and mechanism of the comparatively large nonresonant second order $\chi_{ijk}^{(2)}(-\omega_3; \omega_1, \omega_2)$ and third order $\chi_{ijkl}^{(3)}(-\omega_4; \omega_1, \omega_2, \omega_3)$ nonlinear optical susceptibilities of conjugated organic and polymeric structures have been the center of intense scientific investigations for many years.¹ Fundamental understanding of the second order optical properties such as the linear electrooptic effect and second harmonic generation in terms of a microscopic many-electron description is fairly well established both theoretically and experimentally. In light of this fact, numerous new noncentrosymmetric molecular and polymeric structures with enhanced $\chi_{ijk}^{(2)}(-\omega_3; \omega_1, \omega_2)$ have been successfully designed and synthesized. Through efficient device designs and architectures, electrooptic polymers are now being implemented into novel electrooptic and nonlinear optical devices. In contrast to the considerable progress realized with second order optical processes, the first successful microscopic many-electron description has been achieved only recently for nonresonant third order optical processes such as third harmonic generation, degenerate four wave mixing, and the optical Kerr effect in conjugated structures, and it is this recent advance²⁻⁴ which is the main subject of this paper.

Up to the mid-1980's, progress in understanding third order optical processes in conjugated structures had been largely slowed due to incomplete descriptions based on noninteracting, independent particle models such as Huckel theory which, strikingly, in several important cases even fail to correctly predict the sign of $\chi_{ijkl}^{(3)}(-\omega_4; \omega_1, \omega_2, \omega_3)$, let alone the actual magnitude and dispersion. By natural development of the many-electron formalism and methodology established in the case of second order optical processes, a new successful microscopic description of third order optical excitations in interacting many-electron systems has been achieved that is generalizable to different conjugated organic and polymeric structures.^{2,3} The key central finding from this work is that repulsive Coulomb interactions natural to confined π -electron systems cause the electrons to be highly correlated in their motion, and it is these electron correlation effects among the many electrons that determine the sign, magnitude, and dispersion of $\chi_{ijkl}^{(3)}(-\omega_4; \omega_1, \omega_2, \omega_3)$ for third order optical processes in conjugated π -electron structures.

In this paper, we review the basic concepts and microscopic description for third order optical processes in conjugated structures based on comprehensive theoretical and experimental studies of the nonresonant molecular third order susceptibility $\gamma_{ijkl}(-\omega_4; \omega_1, \omega_2, \omega_3)$ in conjugated chains.²⁻⁴ We show how the origin of $\gamma_{ijkl}(-\omega_4; \omega_1, \omega_2, \omega_3)$ can be directly understood in terms of highly correlated virtual excitation processes and, in particular, the fundamentally important role of previously unknown, strongly correlated two-photon states energetically high-lying in the excited state manifold.

Electron correlation theory for $\gamma_{ijkl}(-\omega_4; \omega_1, \omega_2, \omega_3)$ of *trans* and *cis* polyenes reveals that for short polyene chains, $\gamma_{ijkl}(-\omega_4; \omega_1, \omega_2, \omega_3)$ is dominated by two competing third order virtual excitation processes that involve just three states. (Figure 1) For the $N = 6$ site chain hexatriene, for example, the largest virtual excitation process, which

makes a positive contribution to $\gamma_{ijkl}(-\omega_4; \omega_1, \omega_2, \omega_3)$, involves a previously unexpected, high-lying 5^1A_g state that is strongly coupled to the large oscillator strength 1^1B_u state and cannot be properly described by uncorrelated, independent particle models. This virtual process, together with a smaller, negative virtual process that involves only the 1^1B_u state and the 1^1A_g ground state, determines the sign, magnitude, and dispersion in this archetypal class of conjugated structures.

The same basic mechanism for $\gamma_{ijkl}(-\omega_4; \omega_1, \omega_2, \omega_3)$ holds for all chain lengths calculated from $N = 4$ to 16. For chains of increased length, there are a larger number of virtual excitation processes that make a significant contribution to $\gamma_{ijkl}(-\omega_4; \omega_1, \omega_2, \omega_3)$; but, in all cases, there is always at least one important highly correlated, two-photon 1^1A_g state. The dominant tensor component of the susceptibility, $\gamma_{xxxx}(-\omega_4; \omega_1, \omega_2, \omega_3)$ with all electric fields polarized along the molecular axis of the conjugation, can be diagrammatically represented in terms of transition density matrix diagrams that graphically illustrate the large charge separation that occurs upon virtual excitation between the 1^1B_u state and the strongly correlated, high-lying two-photon 1^1A_g state. (Figure 2)

It is found that $\gamma_{xxxx}(-\omega_4; \omega_1, \omega_2, \omega_3)$ increases dramatically with chain length as evidenced, for example, by the calculated power law dependence of the dc-induced second harmonic susceptibility $\gamma_{xxxx}(-2\omega; \omega, \omega, 0)$ on the number N of carbon atom sites in the chain with an exponent of 3.9 for the *trans* polyenes in the range $N = 4$ to 16. The supralinear chain length dependence of $\gamma_{xxxx}(-\omega_4; \omega_1, \omega_2, \omega_3)$ originates in the increased transition moments between the principal virtual states, the decreased excitation energies of those states, and the increased number of significant virtual excitation processes.

Comparison of calculations for the *cis* structural conformation of polyenes with results for the *trans* conformation demonstrates that the fundamental origin of $\gamma_{ijkl}(-\omega_4; \omega_1, \omega_2, \omega_3)$ remains basically the same, irrespective of the structural conformation. The only significant difference in the results for the two conformations is that, in all cases, the value of $\gamma_{xxxx}(-\omega_4; \omega_1, \omega_2, \omega_3)$ for a *cis* chain is smaller than that of the corresponding *trans* chain of the same number of sites. The results are unified by a power law dependence of $\gamma_{xxxx}(-\omega_4; \omega_1, \omega_2, \omega_3)$ on the physical end-to-end length of the chain L with an exponent of 3.5. (Figure 3) The *cis* conformation results in a smaller L for a given N than the *trans* conformation. Conformation affects $\gamma_{xxxx}(-\omega_4; \omega_1, \omega_2, \omega_3)$ only inasmuch as it affects the physical length of the chain. Furthermore, extrapolation of the power law dependence of $\gamma_{xxxx}(-\omega_4; \omega_1, \omega_2, \omega_3)$ on L indicates that the values of $\chi^{(3)}(-\omega_4; \omega_1, \omega_2, \omega_3)$ measured in conjugated polymers correspond to effective lengths of only 50 - 100 Å. We infer that $\gamma_{xxxx}(-\omega_4; \omega_1, \omega_2, \omega_3)$ must therefore deviate from the power law dependence and begin to saturate at a length shorter than 100 Å.

Experimental measurements of the dispersion of the isotropically averaged dc-induced second harmonic susceptibility $\langle\chi(-2\omega; \omega, \omega, 0)\rangle$ and the third harmonic susceptibility $\langle\chi(-3\omega; \omega, \omega, \omega)\rangle$ in two key polyene structures have demonstrated that the electron correlation theoretical description of the nonlinear optical properties of conjugated linear chains is quantitatively correct.⁴ The measured values of $\langle\chi(-2\omega; \omega, \omega, 0)\rangle$ and $\langle\chi(-3\omega; \omega, \omega, \omega)\rangle$ at the fundamental wavelengths $\lambda = 1907, 1543, \text{ and } 1064 \text{ nm}$ for hexatriene (HT), the $N = 6$ site chain, are in excellent quantitative agreement with the calculated magnitude, sign, and dispersion. (Figure 4) For example, while the dispersion of $\langle\chi(-2\omega; \omega, \omega, 0)\rangle$ is found to be weak in this wavelength region, experiment and theory are in agreement in the fact that $\langle\chi(-3\omega; \omega, \omega, \omega)\rangle$ at $\lambda = 1064 \text{ nm}$ is 1.8 times larger than the value at $\lambda = 1907 \text{ nm}$. For β -carotene, a substituted, $N = 22$ site chain, the nonresonant experimental values of $\langle\chi(-2\omega; \omega, \omega, 0)\rangle$ and $\langle\chi(-3\omega; \omega, \omega, \omega)\rangle$ are in

agreement with extrapolation of the calculated power law dependence of $\langle\gamma(-\omega_4;\omega_1,\omega_2,\omega_3)\rangle$ on chain length L . Thus, together with the results for HT, these measurements quantitatively validate the power law dependence on chain length L . Furthermore, based on our theoretical understanding of $\gamma_{ijkl}(-\omega_4;\omega_1,\omega_2,\omega_3)$, a three-level model was developed that adequately describes the experimentally measured dispersion of $\langle\gamma(-2\omega;\omega,\omega,0)\rangle$ and $\langle\gamma(-3\omega;\omega,\omega,\omega)\rangle$ for β -carotene. The basic origin and mechanism for $\gamma_{ijkl}(-\omega_4;\omega_1,\omega_2,\omega_3)$ of linear chains reviewed in this paper is generalizable to other conjugated structures, for example, cyclic rings, rigid-rod polymers, and polythiophenes. Finally, these results have led to the discovery that excited state nonlinear optical susceptibilities originating from the real population of electronic excited states can be enhanced by orders of magnitude compared to the usual ground state properties.⁵

This research was generously supported by AFOSR and DARPA (grant F49620-85-C-0105), Penn Research Fund, and partially by NSF/MRL (grant DMR-85-19059). The calculations were performed on the Cray Y-MP/832 of the Pittsburgh Supercomputing Center. We gratefully acknowledge the contributions of Drs. O. Zamani-Khamiri, K. Y. Wong, and Y. M. Cai and Mr. Q. L. Zhou to the work reviewed in this paper.

References

1. See, for example, *Nonlinear Optical Properties of Organic and Polymeric Materials*. D.J. Williams, ed., ACS Symp. Series, Vol. 233 (American Chemical Society, Washington, D.C., 1983); and *Nonlinear Optical Properties of Organic Materials III*, G. Khanarian, ed. (Proc. SPIE 1337, 1990).
2. J. R. Heflin, K. Y. Wong, O. Zamani-Khamiri and A. F. Garito, *Phys. Rev. B* **38**, 1573 (1988).
3. J. W. Wu, J. R. Heflin, R. A. Norwood, K. Y. Wong, O. Zamani-Khamiri, A. F. Garito, P. Kalyanaraman, and J. Sounik, *J. Opt. Soc. Am. B* **6**, 707 (1989).
4. J. R. Heflin, Y. M. Cai, and A. F. Garito, *International Quantum Electronics Conference 1990*, Technical Digest Series, Vol. 8 (Optical Society of America, Washington, D. C., 1990) p. 38; and *J. Opt. Soc. Am. B* (in press).
5. Q. L. Zhou, J. R. Heflin, K. Y. Wong, O. Zamani-Khamiri, and A. F. Garito, *Phys. Rev. A* **43**, 1673 (1991).

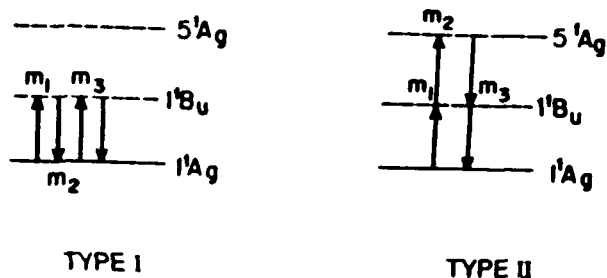


Figure 1. The two dominant third order virtual excitation processes for $\gamma_{xxxx}(-\omega_4;\omega_1,\omega_2,\omega_3)$ of *trans*-HT, $N = 6$. The positive type II process that involves the strongly correlated 5^1A_g state as the middle intermediate virtual state is larger than the negative type I process that has the 1^1A_g ground state as the middle intermediate state.

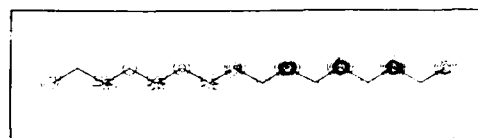


Figure 2. Transition density matrix contour diagram of *trans*-hexadecaoctaene (HDO), $N = 16$, for the 10^1A_g state with the 1^1B_u state. The corresponding x -component of the transition dipole moment is 19.38 D.

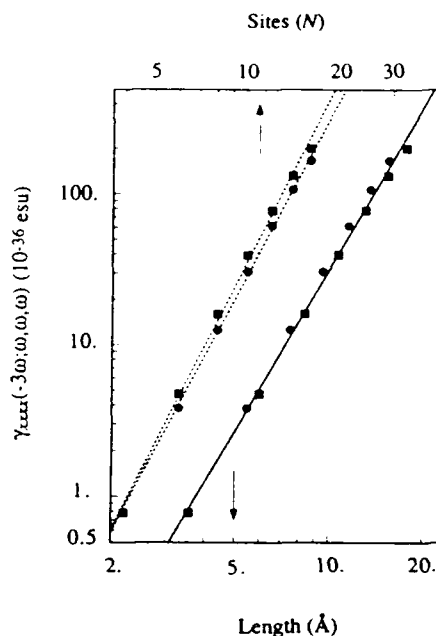


Figure 3. Log-log plot of $\gamma_{xxxx}(-3\omega;\omega,\omega,\omega)$ at $\hbar\omega = 0.65$ eV versus the number N of carbon sites (upper axis and dashed lines) and length L (lower axis and solid line). The values for *trans* chains are represented by squares; and the values for *cis* chains, by circles. The linear fit of the solid line corresponds to $\gamma_{xxxx}(-3\omega;\omega,\omega,\omega) \propto L^{3.5}$.

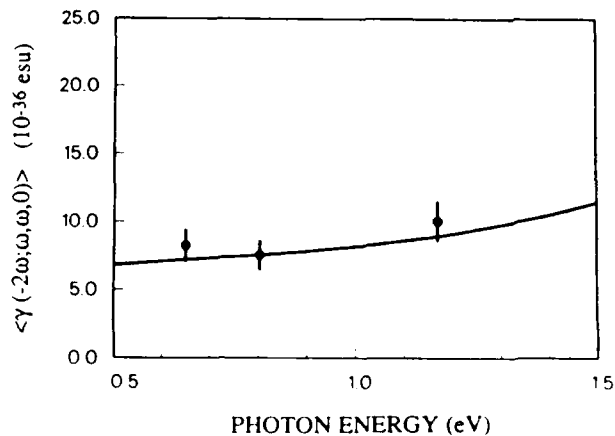


Figure 4. The experimentally determined values of $\langle\gamma(-2\omega;\omega,\omega,0)\rangle$ for HT at $\lambda = 1907, 1543,$ and 1064 nm and the theoretical dispersion curve.

Linear and Nonlinear Optical Properties of Highly Ordered Conjugated Polymers in Polyethylene: Orientation by Mesoeptaxy

C. Halvorson, D. Moses, T.W Hagler, K. Pakbaz and A.J. Heeger
Institute for Polymers and Organic Solids
University of California at Santa Barbara
Santa Barbara, CA 93103

There are two principal reasons for the interest in conjugated polymers as nonlinear optical materials:

- 1) **Delocalized** π -electrons of conjugated polymers provide a mechanism for a large third order nonlinear susceptibility, $\chi^{(3)}$, which leads directly to active device configurations by means of an intensity dependent index of refraction:

$$n = n_0 + n_2 I$$

where I is the intensity of the light and $n_2 = 4\pi^2\chi^{(3)}/cE_1$.

- 2) Sub-picosecond response time.

The sub-picosecond response has been demonstrated in a number of real systems and even in waveguide configurations. However, although polymers from this class have been shown to have relatively large $\chi^{(3)}$, the established values ($\sim 10^{-10}$ esu) are not large enough --- required values for use in digital optics are $\chi^{(3)} > 10^{-8}$ esu. In addition, the actual figure of merit (F) is the ratio of $\chi^{(3)}$ to the absorption coefficient, α , $F = \chi^{(3)}/\alpha$.

Typically α has been too large for constructing useful devices, and $\chi^{(3)}$ has been too small to allow the fabrication of small scale devices at moderately high densities (in waveguide configurations, etc).

A survey of the available materials shows that an increase in the magnitude of $\chi^{(3)}$ (or n_2) by one-to-two orders of magnitude is needed before conjugated polymers can satisfy the minimum material requirements.

Calculations¹ have predicted a dramatic increase in the nonlinear optical response with chain length; the results indicate that $\chi^{(3)}$ is proportional to N^v where N is the polymerization index, and v is in the range 4-5 (the precise value is sensitive to the detailed approximations in the method used). Since $\chi^{(3)}$ is an intrinsic quantity, it must saturate to a finite value in the thermodynamic (long chain) limit. The calculations imply, however, that this saturation does not occur until N reaches values of order 10^2 .

Thus, remarkable enhancements of $\chi^{(3)}$ are predicted for conjugated macromolecules compared with those of the corresponding short oligomers; i.e enhancements of order 10^v where v is in the range 4-5.

The achievement of ordered, chain-aligned films should lead to increases in the magnitude of $\chi^{(3)}$ over that of random material in two independent ways. First, since $\chi^{(3)}$ is a tensor, there is a simple geometric projection factor (the average of $|\langle \cos^3\theta \rangle|^2$, where θ is the angle between the electric field of the incident radiation and the chain axis) which ranges from 3 to 5 depending on whether the chains are random in a plane or in three dimensions.² Second, and more important, one can expect a major enhancement in $\chi^{(3)}$ from delocalization of the electronic wavefunctions.

The latter effect, with an implied enhancement of order 10^v compared with oligomers with $N=10$ is not evident in the data reported in the literature for conjugated macromolecules. This is perhaps not surprising in view of the well-known tendency for localization of the electronic wavefunctions in quasi-one-dimensional systems. Thus, the actual localization length, $l(E)$, may in fact be much less than the chain length, particularly at energies, E , close to the band edge where the localization lengths limited by disorder are particularly small. This same disorder-induced localization is responsible for the modest electrical conductivities in all but the most highly ordered samples of doped

conducting polymers.

There is evidence in the literature that the measured values for $\chi^{(3)}$ can be significantly increased through improvement in the structural order; the reported values for $\chi^{(3)}$ (from third harmonic generation) are greater by more than an order of magnitude in highly aligned samples of polyacetylene (mosaic spread of $\approx 3^\circ$) prepared by the Durham precursor polymer route³ than in samples with more moderate structural order (mosaic spread of $\approx 20^\circ$) prepared by other methods.

It is clear, therefore, that there is an important technological need for optical quality thin films of aligned and highly ordered conjugated polymers.

The simplest method of achieving chain extension and chain orientation of a polymer is by tensile drawing. Unfortunately, the relatively high density of entanglements present in most polymers limits the available draw ratios (λ) to modest values. A principal advantage of gel processing is that because of the dilution of the polymer in the gel (e.g., UHMW-PE forms gels at volume fractions even below 1%), the density of entanglements is far lower than in polymers prepared from the melt, etc.⁴ Moreover, the low entanglement density remains even after removing the solvent. Thus such gels (or gel-processed films and fibers) can be tensile drawn to remarkable draw ratios ($\lambda > 200$) during which the macromolecules are chain extended and aligned.

Can this high degree of structural order achieved through gel-processing be transferred to a conjugated polymer in a UHMW-PE blend? On first thought, this would seem unlikely, for the two component polymers are typically immiscible (since the entropy of mixing is essentially zero for macromolecules). However, there is evidence of a strong interfacial interaction when conjugated polymers are added to an UHMW-PE gel; the frequency dependent conductivity results⁵ suggest that the conjugated polymer adsorbs onto the PE and decorates the complex surface of the gel network, thereby forming connected (conducting) pathways at volume fractions nearly three orders of magnitude below the threshold for three-dimensional percolation.⁵ The implied strong interfacial interaction suggests that gel-processing of conjugated polymers in PE may lead to orientation of the conjugated polymer component.

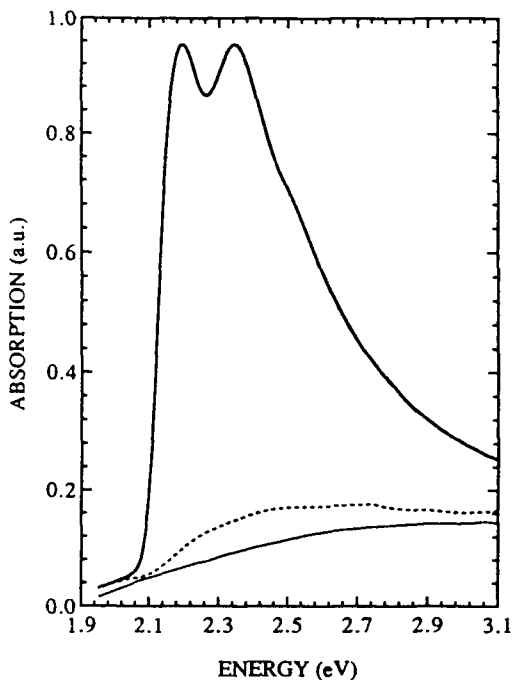
PE/MEH-PPV blends have been prepared and processed into highly aligned free standing films.⁶ Once processed, the films are found to be extremely durable; repeated thermal cycling and constant exposure to air caused no ill effects. This is presumably due to a combination of the stability of MEH-PPV and to the self-encapsulation advantage of utilizing polymer blends.

The absorption spectra⁶ for an oriented free standing film (draw ratio, $\lambda = 50$) of PE/MEH-PPV are shown in Figure 1 for polarization both parallel to (\parallel) and perpendicular to (\perp) the draw axis and for a spin-cast film (both at 80K). The spectra were scaled to that of $\alpha_{\parallel}(\omega)$ which has maximum value of $2.2 \times 10^3 \text{ cm}^{-1}$ at 2.2 eV (1% MEH-PPV in PE). A high degree of macroscopic orientation of the conjugated polymer has been achieved by tensile drawing the gel-processed blend. Moreover, $\alpha_{\parallel}(\omega)$ shows a distinct red shift, a sharper absorption onset, and a reduced total width compared to $\alpha(\omega)$ for the spin-cast film. These features, together with the appearance of resolved vibronic structure, indicate a significant improvement in the structural order of the conjugated polymer in the oriented blend.

The transverse "absorption" in Figure 1 is dominated by scattering from residual microstructure in the PE. This is demonstrated by comparing $\alpha_{\perp}(\omega)$ with the artificial "absorption", due to residual scattering, obtained from an undecorated UHMW-PE film of comparable thickness and draw ratio; the initial slope is the same and the overall spectral shape is similar. To circumvent the problem of residual scattering, the dichroism of selected IR-active modes associated with MEH-PPV have been studied as a function of the draw ratio; the dichroic ratio continues to improve

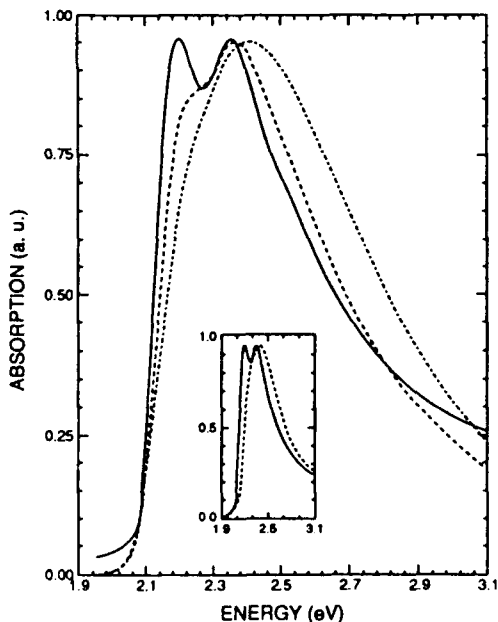
monotonically with λ to $\alpha_{\parallel}/\alpha_{\perp} > 100$.⁷

The PE scattering has been investigated⁶ by passing a He-Ne laser (632.8nm) through the various samples and examining the



speckle pattern. For oriented samples, analysis of the pattern indicates that the scattering is from elongated microstructure with length (along the draw ratio) more than 100 times the wavelength and diameter less than one-tenth of the wavelength. Efforts to modify the gel-processing to reduce the scattering by the oriented film are underway.

Figure 2 compares $\alpha(\omega)$ of a non-oriented free-standing film of PE/MEH-PPV, $\alpha_{\parallel}(\omega)$ of the oriented film of PE/MEH-PPV, and $\alpha(\omega)$ of the spin cast film (all at 80K).⁶



The spectrum obtained from the non-oriented blend is intermediate between that of the spin-cast film and the oriented blend; it shows the red shift, the sharper absorption onset, the reduced total band-width and the emergence of vibronic structure. Thus, even in the non-oriented blend, the MEH-PPV spectra are, in every way, consistent with a significant enhancement of microscopic order. Comparison of $\alpha_{\parallel}(\omega)$ of the oriented film of PE/MEH-PPV with $\alpha(\omega)$ of the non-oriented film of PE/MEH-PPV shows that there is a sharpening of all spectral features and a clear redistribution of spectral weight into the zero-phonon line. The data thus indicate a further enhancement of structural order by tensile drawing.

The inset to the previous figure compares $\alpha_{\parallel}(\omega)$ of an oriented free standing film of PE/MEH-PPV at 80K with that at 300K.⁶ As the temperature (T) is raised, the peak shifts (thermochromism), the onset of absorption broadens and there is both an overall loss of resolution as well as a clear redistribution of spectral weight out of the lowest energy vibronic feature. The changes in $\alpha_{\parallel}(\omega)$ at 300K are indicative of increased disorder, in many ways similar to the changes induced by the structural disorder of the spin-cast films.

The nonlinear optical properties of MEH-PPV have been investigated through third harmonic generation (THG) spectroscopy with the pump frequency varied over a wide range of frequencies within the gap. We have characterized the THG response in thin spin-cast films of MEH-PPV, in non-oriented MEH-PPV/PE blends and in ordered and in the most highly oriented MEH-PPV/PE blends (see Figures 1 and 2). The ordered blends exhibit large values for $\chi^{(3)}$ in the infrared. The results will be presented and analyzed in the context of the effect of disorder on the THG response.

REFERENCES

1. R. Silbey, in "Conjugated Polymeric Materials: Opportunities in Electronics, Optoelectronics and Molecular electronics", NATO ASI Series, Series E: Applied Sciences- Vol. 182, Ed. by J.L. Bredas and R.R. Chance; and references therein.
2. M. Sinclair, D. Moses, K. Akagi and A.J. Heeger, *Phys. Rev. B* **38**:10,724 (1988).
3. F. Kraus, E. Wintner, and G. Leising, *Phys. Rev. B* **39**:376 (1989)
4. P. Smith and P. Lemstra, *J. Mater. Sci.*, **15**:505 (1980).
5. A. Fizazi, J. Moulton, K. Pakbaz, S.D.D. Rughooputh, Paul Smith and A.J. Heeger, *Phys. Rev. Lett.* **64**:2180 (1990).
6. T. Hagler, K. Pakbaz, and A. J. Heeger, *submitted to Polymer Commun for publication*.
7. J. Van Schoot and K. Voss, *to be published*.

DETERMINATION OF THIRD-ORDER NONLINEAR SUSCEPTIBILITIES OF SEMICONDUCTING POLYMERS. COMPARISON WITH THEORETICAL CALCULATIONS.

J.MESSIER, F.CHARRA and C.SENTEIN

Laboratoire de Physique Electronique des Materiaux.CEA
GIF-SUR-YVETTE.91191 CEDEX.FRANCE

Third-order nonlinear optical phenomena are particularly important in polymers, or long molecules, having a one-dimensional π -electron system, the linear polarizability of which being much larger than that of polymers with saturated bonds.

We will be concerned here with the third-order phenomena responsible for harmonic generation, wave mixing, in the optical range and which are due to electronic hyperpolarizability. They should not be confused with those responsible for the variations of the index of refraction and which often originates from other phenomena (generation of charged species, thermal gratings produced by an energy absorption, etc...).

We will describe first the case of polydiacetylene which has the advantage of having well defined conformation in thin layer. Two- and three-photon resonances, vibronic contributions, are observed then easily in the variation of the $X^3(3\omega; \omega, \omega, \omega)$ coefficient with the frequency. One can give an account of it by a simple three-energy-level model where the nonlinear coefficient per monomeric unit $\chi(\omega)$ is given by the relation:

$$\chi(\omega) = \mu_{01}^2 \{ \mu_{12}^2 f(\omega) - \mu_{01}^2 g(\omega) \} \quad (1)$$

f and g are functions of the frequency and are given by the usual perturbation theories [1]. They depends on the energy of the one- and two-photon excited states E_1 and E_2 , on the dipolar transition moments between fundamental (0) and excited states (1,2) μ_{01} and μ_{12} .

In the general case however, the polymers have a large number of conformations to which corresponds broad dispersion of the optical spectrum and of the $\chi(\omega)$ values. The measurement of the generated intensity at 3ω , $I(3\omega)$, gives only an average of the module of $\chi(\omega)$ not very significant.

On the other hand the simultaneous measurement of the one-photon absorption spectrum and of the argument of $\chi(\omega)$ allows a better analysis of the experimental results. Indeed, with the reasonable assumption that the homogeneous linewidth is much smaller than the inhomogeneous one, the optical absorption spectrum permits to determine the function $P(\Omega) \cdot \mu_{01}^2(\Omega)$ where $P(\Omega)$ is the probability density of having an absorbent monomer at energy Ω [3]. One has

$$P(\Omega) \cdot \mu_{01}^2(\Omega) = \frac{hc n \ln(10)}{\pi K_1 t N} \cdot \frac{DO(\Omega)}{\Omega} \cdot \frac{1}{F} \quad (2)$$

where $DO(\Omega)$ is the optical density at Ω , K_1 a numerical factor taking account of three-dimensional orientation distribution of molecular axis ($K_1=1/3$), t the thickness of the thin layer or of the solution, N the number of molecules per unit volume, n the real part of the refractive index. The local-field factor F is taken equal to unity in one-dimensional system [2].

In addition it is important to point out that the imaginary part of $\chi(\omega)$, $Im\chi(\omega)$, is due only to the molecules having a resonance at 2ω or 3ω . With the above assumption that means that a very small number of molecules contribute to $Im\chi(\omega)$ at a given frequency ω . Hence it is possible to separate explicitly the contributions of two- and three-photon resonances as shown by the relation (3) below.

$$Im(\chi) = \left[\frac{\gamma_2}{(E_2 - 2\Omega)^2 + \gamma_2^2} \cdot \frac{2\mu_{01}^2 \mu_{12}^2}{(E_1 - 3\Omega)(E_1 + \omega)} \right]_{E_2 \approx 2\Omega} \quad (3)$$

$$+ \left[\frac{\gamma_1}{(E_1 - 3\Omega)^2 + \gamma_1^2} \cdot \frac{\mu_{01}^2}{(E_1 - \Omega)} \cdot \left(\frac{\mu_{12}^2}{(E_2 - 2\Omega)} - \frac{2\mu_{01}^2}{(E_1 + \Omega)} \right) \right]_{E_1 \approx 3\Omega}$$

Here γ_2 is the homogeneous linewidth of the two-photon state.

Taking into account equation (1), (2), and (3), one can express $\chi(\omega)$ as a sum of contributions of the various conformations using a small number of adjustable parameters concerning the two-photon excited states (E_2, μ_{12}). With the additional simplifying assumption that $E_2 - E_1$ and μ_{12} are independent of the individual conformation considered ($E_2 - E_1 = \delta$) one obtains the relation (4)

$$Im(\chi(\Omega)) = \pi \cdot \left[P(2\Omega + \delta) \cdot \mu_{01}^2(2\Omega + \delta) \cdot \frac{2\mu_{12}^2}{(\delta - \Omega)(\delta - 3\Omega)} \right. \quad (4)$$

$$\left. + P(3\Omega) \cdot \mu_{01}^2(3\Omega) \cdot \frac{1}{2\Omega} \left[\frac{\mu_{12}^2}{(\Omega - \delta)} - 2 \frac{\mu_{01}^2}{4\Omega} \right] \right]$$

FIG 1 shows as an example the absorption spectrum of two different soluble polythiophene having very different conformations in thin layer. The argument of $\chi(\omega)$ was determined by comparing the third harmonic generation due to the substrate and that of the covered substrate with the polymer layer [3,4,5].

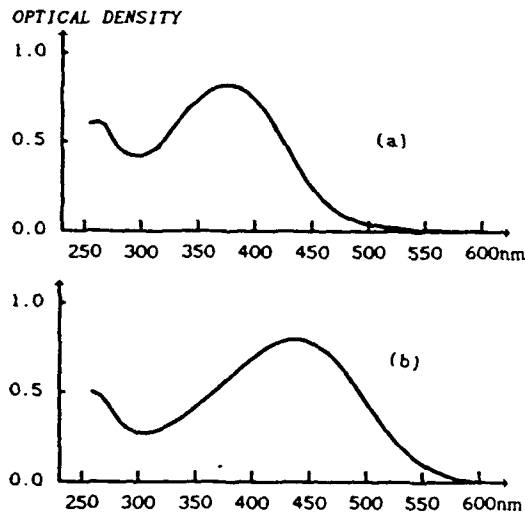


FIG.1 Linear absorption spectra: a) Al p-octylbithiophene. $t = 0.26 \mu m$
b) B1 p-octylthiophene. $t = 0.28 \mu m$

On FIG 2 the experimental data are compared with theoretical curves calculated with the parameters of TABLE 1.

	pDOBT A ₁	pOT B ₁
μ_{12}/e (Å)	4.0	4.4
δ (eV)	0.57	0.51
$\gamma(0)$ (10^{-59} SI)	3.1	5.7

TABLE 1

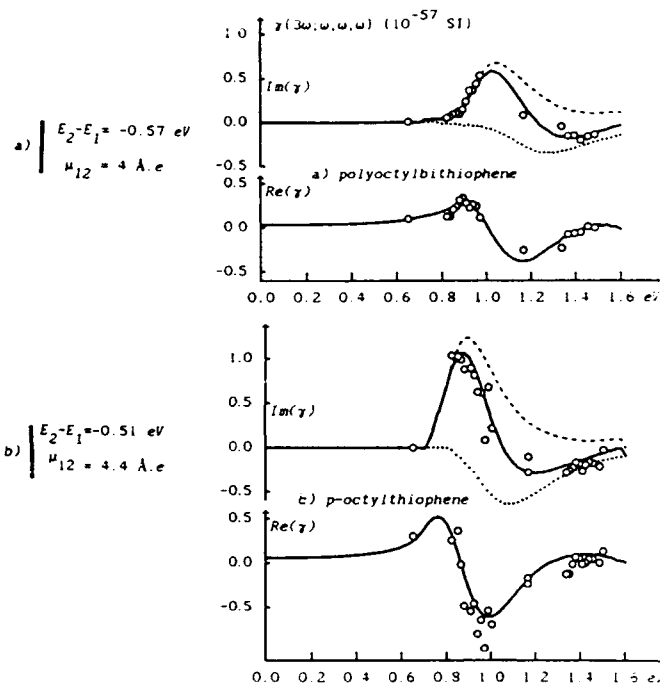


FIG.2

Experimental complex value of hyperpolarizability per thiophene unit $\gamma(3\omega; \omega, \omega, \omega)$ obtained by third-harmonic generation as a function of fundamental photon energy. The theoretical fit was obtained by a three-level model.

With the same parameters one can also determine the real part of $\gamma(\omega)$ by using the relation (3) and by summing on all conformations. One can then deduce the extrapolated value at zero frequency $\gamma(0)$ (cf TABLE 1). The values indicated in TABLE 1 are typical average values for conjugated polymers. As for polydiacetylene [4], polyacetylene [5], polyenes [6], the lowest two-photon energy level is located below the first one-photon excited level ($E_2 - E_1 < 0.6$ eV). The transition dipole moment μ_{01} lies generally between 1 and 2 e.Å and μ_{12} between 3 and 6 e.Å, and according to (1) $\gamma(\omega)$ is positive.

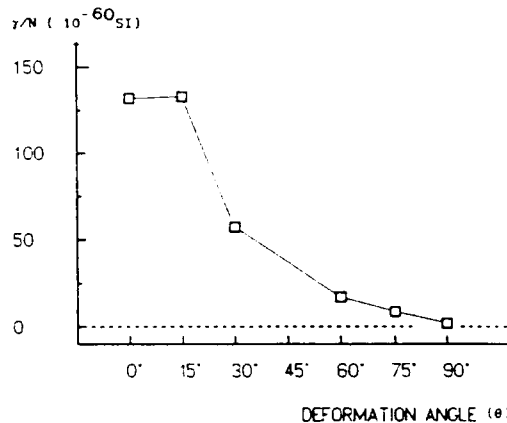


FIG.3 Variation of γ at zero frequency with θ . THEORETICAL CALCULATION OF THE NONLINEAR THIRD-ORDER COEFFICIENTS. By quantum chemical calculations (CNDO with configuration interaction) it is possible to calculate the variation with polymer length of the transition moments and the value of $\gamma(\omega)$ extrapolated for an infinite polymer.

For flat thiophene oligomers we have calculated the variation with the monomer unit number N of μ_{01}^2/N and μ_{12} . The first quantity is proportional to the polarizability per unit volume. These two quantities reach, as expected, a limit value when N tends to infinity, respectively $(1.35 \text{ e.Å})^2$ and 5.5 e.Å . On condition of renormalizing suitably [7], in the formula (1), the negative term proportional to $-\mu_{01}^2$, the hyperpolarizability per monomer unit, γ/N , also reaches a finite value.

The so calculated value for an infinite flat polymer of polythiophene $\gamma(0) = 15 \cdot 10^{-59}$ SI, is in reasonable agreement with the experimental data (cf TABLE 1) in view of the distortions of the polymers with respect to planarity in thin layer. Indeed it will be shown that this limit value depends on the localization of elementary excitations. In a flat polymer this results from electronic correlations (electron-hole pair interaction mainly). All distortion of the polymer backbone increases this localization. FIG 3 shows for example the reduction of the γ value produced in a helicoidal polythiophene by the increase in the torsion angle θ between two successive thiophene units.

In conclusion in conjugated polymers it is possible to determine experimentally and to model the variations with the frequency of the nonlinear coefficients due to electronic hyperpolarizability even when the polymer exhibits numerous conformations. The point in the interpretation of such measurements is the description of two-photon states. We have also shown that quantum calculations on the mono-electronic states permits to calculate some basic parameters with a good approximation.

REFERENCES

1. B.J. Orr and J.F. Ward, *Mol. Phys.* 20 (1971) p. 513
2. C. Cojan, G.P. Agrawal and C. Flytzanis, *Phys. Rev. B* 15 (1977) p. 909
3. F. Charra, J. Messier and C. Sentein, A. Proń and M. Zagórska, in *Organic Molecules For Nonlinear Optics and Photonics* NATO-ASI Series E vol. 194 p. 263 (Dordrecht-1991)
4. P.A. Chollet, F. Kajzar and J. Messier, *Synth. Metals* 18 (1987) p. 459
5. S. Etemad, G.L. Baker, D. Jaye, F. Kajzar and J. Messier, *SPIE proc.* Vol. 682. *Molecular and Polymeric Optoelectronic Materials: Fundamentals and Applications* (1986) p. 44
6. B.F. Kohler, C. Spangler and C. Westerfield, *J. Chem. Phys.* 89 (1988) p. 5422
7. F. Charra and J. Messier in *Conjugated Polymeric Materials: Opportunities in Electronics, Optoelectronics, and Molecular Electronics*, J.I. Bredas and R.R. Chance Ed NATO-ASI Series E vol. 182 p. 409 Kluwer (Dordrecht 1990)

A SURVEY OF THE NLO-POLYMER PROGRAM AT THE MPI

by
C. Bubeck, G. Duda, A. Grund, W. Hinkel, A. Kaltbeitzel
A. Mathy, W. A. Meyer, D. Neher, T. Sauer
H.-U. Simmrock, G. Wegner, A. Wolf and W. Knoll

Max-Planck-Institut für Polymerforschung
Ackermannweg 10, W-6500 Mainz/FRG

Introduction

The nonlinear optical polymer program at the Max-Planck-Institute for Polymer Research started about 5 years ago. Focusing mostly on phenomena related to the third order nonlinear optical susceptibility $\chi^{(3)}$, various polymeric materials with conjugated π -electron systems were developed and investigated by means of third harmonic generation (THG) and degenerate four wave mixing (DFWM). The $\chi^{(3)}$ -values obtained by THG in these materials increase strongly with the spectral position of their longest wavelength (linear) absorption, λ_{max} . The response times, τ , in most cases, were below the 1 ps resolution limit of the DFWM set-up. Interesting scaling behavior of $\chi^{(3)}$ at near resonance condition were found: For the π -conjugated polymers a linear increase of $\chi^{(3)}$ (from DFWM experiment) with increasing absorption coefficient, α , as one approaches a resonance seems to be adequately described by a recently developed phase-space filling model of 1D excitonic excitations. Contrary to this, localized two-level systems like rhodamine 6G or phthalocyanine thin films show a quadratic increase of $\chi^{(3)}$ as α increases. In addition, the latter systems show a strong dependence of the linear and nonlinear optical properties on the sample preparation condition resulting in different degrees of electronic coupling between individual chromophores.

Within this program, also a lot of work is devoted to the development and characterization of polymeric materials that might act as passive elements in future integrated optics devices. As most promising examples some results obtained with glassy polyelectrolytes based on quaternary ammonium salts are presented. Low-loss waveguide structures (2 dB/cm) can be fabricated, with indices of refraction n between 1.50 and 1.72 and with high Abbe numbers (low dispersion) up to $\nu_D > 70.0$. Another class of materials that can be manipulated at the molecular level to build supramolecular structures by the Langmuir-Blodgett-Kuhn technique includes polyglutamates, celluloseethers and polysilanes. These rod-like polymers with flexible side chains ("hairy rods") behave like molecularly reinforced liquids with excellent optical properties that allow also for a wide range of different functionalizations.

Experimental Section

THG experiments were performed with infrared light pulses ($\lambda = 1064$ nm, $P = 0.4$ mJ, duration ≈ 30 ps) from an actively/passively mode locked Nd: YAG laser¹¹. The pulses were focused on the sample mounted in a vacuum chamber on a rotary stage. Maker fringes were analyzed taking into account also back-reflection effects including all bound waves in the layer systems¹², and using fused silica with $\chi^{(3)}$ ($-3 \omega, \omega, \omega, \omega$) = $3.11 \cdot 10^{-16}$ esu at 1064 nm as a reference¹³.

DFWM experiments were done in a folded BOXCARS configuration¹⁴. The output of a synchronously pumped cavity dumped dye laser (wavelength variation between 560 nm and 760 nm) was split into three beams with variable delay and focused onto the thin film¹⁵. The intensity at the sample was ca. 1 GW/cm², the pulse duration \approx 1 ps. $\chi^{(3)}$ values were derived by comparison with CS₂, taking into account the effective sample thickness d , refractive index n , and the absorption coefficient α .

Waveguide properties of the thin film samples were studied with prism couplers in various configurations¹⁶⁻¹⁸. From angular measurements of the mode coupling conditions the (anisotropic) indices of refraction were obtained. Optical dispersion data were determined by using various lines of Ar+, Kr+, and HeNe-lasers. Mode-attenuation ("waveguide losses") were measured by imaging the straightlight of the guided beam onto a diode array¹⁹.

Thin polymer films were prepared by either spin-coating from solution (followed in some cases by thermal treatment, see results) or by the Langmuir-Blodgett-Kuhn technique²⁰. Film thicknesses were determined optically²¹ or with a mechanical step profiler.

Results and Discussion

a) Polymers with conjugated π -electron systems

Table 1 summarizes some of the results obtained by THG ($\chi^{(3)}$) and by DFWM (τ) for various conjugated polymers. Thin films of poly(*p*-phenylenevinylene) (PPV) and poly(naphthalenevinylene) (PNV) were prepared by spin-casting from precursor solutions followed by thermal treatment in vacuo¹⁰. Samples of poly(phenylacetylene) (PPA) derivatives prepared by the method of Masuda et al¹¹ were cast from solution. The observed $\chi^{(3)}$ -values are in the range typical for conjugated polymers. Despite possible resonance contributions in most cases the relaxation time τ derived from the decay of the transient grating in the DFWM experiments is shorter than the resolution limit given by the laser pulse width.

The spectral position of the linear absorption, λ_{max} , is also shown in Table 1 for comparison. Treating the conjugated polymers as one-dimensional systems with a π -electron delocalization length L_d , Agrawal²² and Flytzanis²³ derived a scaling law for the third order susceptibility

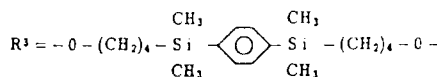
$$\chi^{(3)} \sim (L_d)^6 \quad (1)$$

If L_d is taken to be inversely proportional to the optical gap then $\chi^{(3)}$ should scale with $(\lambda_{max})^6$. This is qualitatively found for a wide range of polymers (Fig. 1) although for certain systems true non-resonant $\chi^{(3)}$ -values would be required for a rigorous testing of this theoretical approach¹⁴.

In view of possible applications of these materials for all-optical information processing where (non-resonant) $\chi^{(3)}$ -values in the range of 10^{-9} esu or larger are estimated to be required it is, however, highly doubtful whether linearly polyconjugated molecules allow to reach this non-resonant $\chi^{(3)}$ value at all. However, it is an open question if optimized figures of merit and larger device lengths can fulfill application requirements.

b) Electronic coupling between chromophores

The close interrelation between the detailed molecular structure of the chromophore, the supramolecular architecture of the matrix into which it is incorporated, and the linear and nonlinear optical properties of the resulting functionalized material is demonstrated for various thin film samples of phthalocyanines (PC). These dyes are of general interest because of their excellent light and temperature stability. The chemical structure and a few details of the different systems used in these studies are given in Table 2. For system 1, the interconnect, R₃, between different phthalocyanine rings had the following chemical structure:



In system 4 the phthalocyanine moieties were incorporated into a copolymer with styrene

Fig 2 shows the linear absorption spectra and the decay curves as obtained from DFWM experiments at $\lambda \approx 650$ nm. Remarkable differences for the various systems are found²⁴. An isolated PC molecule like, e.g., in system 4, gives a sharp absorption spectrum. This leads to a very slow decay time of the transient grating beyond the resolution of the set-up. Increasing aggregation eventually leads to an inhomogeneous broadening of the absorption band and a concomitant reduction of the transient time (by orders of magnitude!). Obviously, the electronic coupling between individual resonators affects both, the linear and the nonlinear, response of a chromophore system.

Various contributions to the observed phenomena may include i) fluorescence lifetime reduction by aggregational quenching, ii) energy migration²⁵, e.g. exciton diffusion into the not illuminated area, iii) energy trapping at lower states, iv) bimolecular exciton quenching²⁶, etc.

The response times of the conjugated polymers described above are presumably also related to the relaxation processes iii) and iv). The extended π -conjugation with a tight electronic coupling via intra- and interchain energy migration leads to the ultrafast transient times of these systems, even near resonances.

c) Scaling laws for $\chi^{(3)}$ near resonances

DFWM experiments (at various wavelengths λ_L with conjugated systems like PT- and PPV - thin films on one side and rhodamin-(R6G-) dye films cast from methanol solution on the other side show interesting differences as to the dependence of the nonlinear response $\chi^{(3)}$ on the linear oscillator strength¹⁷. This is shown in Fig. 3 where $\chi^{(3)}$ is plotted as a function of the extinction coefficient $\alpha = \alpha(\lambda_L)$ on a log-log scale.

For the R6G sample a scaling law $\chi^{(3)} \sim \alpha^2$ is derived. This can be understood on the basis of a theoretical model for the saturable absorption in a two level system¹⁸.

This is significantly different for the strongly delocalized excitations in 1D conjugated polymers like PPV or PT. In analogy to exciton theories in semi-conductors¹⁹ the recently developed model of phase-space filling by one-dimensional excitons²⁰ should be a more appropriate description. As shown by Greene et al. in this treatment, indeed, leads to a proportionality between the resonant $\chi^{(3)}$ and α , in agreement with the data of Fig. 3. Strong support for this picture comes also from the fact that this relation should be independent of the specific material, again in accordance with the data of Fig. 3.

As far as applications are concerned the important message of Fig. 3 is that it might be possible for certain systems to resonantly enhance the nonlinear response of an organic material into the required $\chi^{(3)}$ -range ($\geq 10^{-9}$ esu) by working at wavelengths near an electronic transition ($\chi^{(3)} \sim \alpha^2$) without burning the device because the heat deposition would increase only linearly with α . However, to obtain materials that can be operated at such high light intensities is still a severe problem.

d) Tailoring polymers for integrated optics

For future device applications not only the nonlinear "optically active" properties ($\chi^{(3)}$, $\chi^{(2)}$) of a polymeric material need to be optimized - what is equally urgently needed are passive units: materials that can be processed, e.g., in the form of planar waveguide structures, that can serve as substrates or superstrates, that can be further structured, e.g. to build-up channel waveguides, etc. Their linear optical properties need to be tuned either to low refractive index values, e.g. for cladding, or to high indices but with low dispersion. In addition, one needs highly transparent polymers for low-loss structures.

Polyelectrolyte glasses²¹ (ionenes) are promising candidates in this respect. Based on polymeric quaternary ammonium salts refractive indices a between 1.50 and 1.72 with high Abbe numbers (low dispersion) $\nu_D > 70.0$ have been described²². Matrix properties that determine, e.g., the transparency of the material are controlled by the polymeric backbone whereas the indices of refraction can be tuned over this wide range by the appropriate choice of suitable counterions.

An example for a planar waveguide structure (chemical composition of this material shown in the inset) with a series of guided modes is given in Fig. 4. In addition to these, a broad surface plasmon can be seen at a high coupling angle ($\theta_0 \approx 73^\circ$). From Fresnel calculations (full line in Fig. 4, for clarity somewhat shifted relative to the experimental data points) one thus obtains accurate thickness ($d = 1.85 \mu\text{m}$) and index of refraction data ($n = 1.49$)²⁴.

Another most critical property of waveguides is their scattering loss which determines for non-absorbing materials the propagation length of the guided modes. Fig. 5 shows the result for an optimized polyelectrolyte glass. Shown are attenuation data as obtained for various laser wavelengths. The full line corresponds to a λ^{-4} -proportionality given by a Rayleigh-Scattering mechanism. Losses in the range of 1 dB/cm can be achieved for wavelengths $\lambda > 650$ nm.

Other examples for materials with a controllable supramolecular structure and very interesting properties are rod-like polymers decorated by short flexible side chains ("hairy rods") that self-organize to form monolayers of nematic texture at the air-water interface of a Langmuir-rough^{25,26}. Applying the LBK-technique²⁷, layered structures of molecularly defined thickness and excellent optical quality can be build up. The type of layered architectures which has been tested in our Institute for wave-guiding properties²¹, for storage of optical information using surface plasmon excitation²⁸ and as a component of sensors²⁹ is depicted in Fig. 6. Here copoly(methyl, octadecyl-L-glutamate) in its helical form was used as the example. Other polymers which are also suitable are celluloseethers, poly(diphenylsilane), phthalocyaninatopoly-(siloxane)³⁰ etc. Physically, these layered polymer structures behave like molecularly reinforced liquids, since the rod-like backbones are embedded in a liquid-like matrix of the side chains. The macroscopic orientation of the layers is achieved by the flow-field induced orientation of the long rods in the monolayers at the air-water-interface during deposition in the LBK technique

Acknowledgement

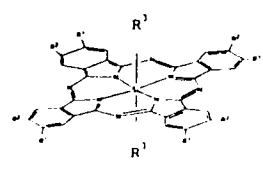
Helpful discussions with many colleagues at the Institute and even more visitors from many different countries are gratefully acknowledged. Financial support came from the Bundesministerium für Forschung und Technology (Project No. 03-M 4008 E9) and from the Deutsche Forschungsgemeinschaft.

REFERENCES

- 1) Bubeck, C.; Kaltbeitzel, A.; Neher, D.; Stenger-Smith, J.D.; Wegner, G.; Wolf, A.; in: *Electronic Properties in Conjugated Polymers III*, H. Kuzmany, M. Mehring, S. Roth, eds., Springer-Verlag, Berlin, Heidelberg 1989.
- 2) Neher, D.; Wolf, A.; Bubeck, C.; Wegner, G.; *Chem. Phys. Lett.* **163**, 116 (1989).
- 3) Kazar, F.; Messier, J.; *Phys. Rev. A* **32**, 2352 (1985).
- 4) Carter, G.M.; *J. Opt. Soc. Am* **B4**, 1018 (1987).
- 5) Kaltbeitzel, A.; Neher, D.; Bubeck, C.; Sauer, T.; Wegner, G.; Caseri, W.; in: *Electronic Properties in Conjugated Polymers III*, H. Kuzmany, M. Mehring, S. Roth, eds., Springer-Verlag Berlin, Heidelberg 1989.
- 6) Hickel, W.; Duda, G.; Jurich, M.; Kröhl, T.; Rochford, K.; Stegeman, G.I.; Swalen, J.D.; Wegner, G.; Knoll, W.; *Langmuir* **6**, 1403 (1990).
- 7) Hickel, W.; Knoll, W.; *Appl. Phys. Lett.* **57**, 1286 (1990).
- 8) Mathy, A.; Simmrock, H.-U.; Bubeck, C.; *J. Phys. D: Appl. Phys.*, in press.
- 9) Kuhn, H.; Möbius, D.; Bücher, H.; in: *Physical Methods of Chemistry*, A. Weissberger, B.W. Rossiter, eds., Wiley, New York 1972, Part II B, Chapter VII.
- 10) Stenger-Smith, J.D.; Lenz, R.W.; Enkelmann, V.; Wegner, G.; *Makromol. Chem.* **190**, 2995 (1989).
- 11) Masuda, T.; Hasegawa, K.; Higashimura, T.; *Macromolecules* **7**, 728 (1974).
- 12) Agrawal, G.P.; Cojan, C.; Flytzanis, C.; *Phys. Rev.* **B17**, 776 (1978).
- 13) Flytzanis, C.; in: *Nonlinear Optical Properties of Organic Molecules and Crystals*, Vol. 2, D.S. Chemla and J. Zyss, eds., Academic Press 1987.
- 14) Neher, D.; Kaltbeitzel, A.; Wolf, A.; Bubeck, C.; Wegner, G.; in: *Conjugated Polymeric Materials: Opportunities in Electronics, Optoelectronics, and Molecular Electronics*, J.L. Brédas and R.R. Chance, eds., Kluwer Academic Publishers, 1990, and references therein.
- 15) Salcedo, J.R.; Siegmund, A.E.; Dlott, D.D.; Fayer, M.D.; *Phys. Rev. Lett.* **41**, 131 (1987).
- 16) Ho, Z.Z.; Peyghambarian, N.; *Chem. Phys. Lett.* **148**, 107 (1988).
- 17) Bubeck, C.; Kaltbeitzel, A.; Grund, A.; LeClerc, M.; *Chem. Phys.*, in press.
- 18) Abrams, R.L.; Lind, R.C.; *Opt. Lett.* **2**, 94 (1978); *ibid.* **3**, 205 (1978); Caro, R.G.; Gower, M.C.; *IEEE J. Quantum Electronics* **QE-8**, 1376 (1982).
- 19) Schmitt-Rink, S.; Chemla, D.S.; Müller, D.A.B.; *Adv. Phys.* **38**, 89 (1999).
- 20) Greene, B.I.; Orenstein, J.; Millard, R.R.; Williams, L.R.; *Phys. Rev. Lett.* **58**, 2750 (1987); Greene, B.I.; Orenstein, J.; Schmitt-Rink, S.; *Science* **247**, 679 (1990).
- 21) Singh, B.P.; Samoc, M.; Nalwa, H.S.; Prasad, P.N.; *J. Chem. Phys.* **92**, 2756 (1990).
- 22) Kremer, F.; Dominguez, L.; Meyer, W.H.; Wegner, G.; *Polymer* **30**, 2023 (1989).
- 23) Simmrock, H.U.; Mathy, A.; Dominguez, L.; Meyer, W.H.; Wegner, G.; *Angew. Chem. Adv. Mat.* **101**, 1148 (1989).
- 24) Knoll, W.; Hickel, W.; Sawodny, M.; Stumpe, J.; Knobloch, H.; Fresenius J. *Anal. Chem.* **00**, 000 (1991).
- 25) Duda, G.; Schouten, A.J.; Arndt, T.; Lieser, G.; Schmidt, G.F.; Bubeck, C.; Wegner, G.; *Thin Solid Films* **159**, 221 (1988).
- 26) Hickel, W.; Duda, G.; Wegner, G.; Knoll, W.; *Makromol. Chem., Rapid Commun.* **10**, 353 (1989).
- 27) Sauer, T.; Caseri, W.; Wegner, G.; Vogel, A.; Hoffmann, B.; *J. Phys. D: Appl. Phys.* **23**, 79 (1990).
- 28) Embs, F.; Wegner, G.; Neher, D.; Albouy, P.; Miller, R.D.; Willson, C.G.; Schreppe, W.; *Macromolecules* **00**, 000 (1991).

Polymer	λ_{max} [nm]	THG $\chi^{(3)}$ [esu]	τ [ps]
PPV 	460	$1.2 \pm 0.6 \cdot 10^{-10}$	< 1
PNV 	440		6
PPA-1  R: Si(CH ₃) ₃	525	$1.9 \pm 0.4 \cdot 10^{-11}$	< 1
PPA-2  R: CH ₂ CH ₃	450	$8.4 \pm 1.7 \cdot 10^{-12}$	< 1
PPA-3  R: CH ₃	450	$1.5 \pm 0.4 \cdot 10^{-11}$	< 1

Table 1: List of conjugated polymers and survey of their linear and nonlinear optical properties.

Chemical Structure	System	R ³
	1 LB-Film of the polymer molecules 50 layers	see text
	2 LB-Film of the monomer, 80 layers	Cl
	3 Polystyrene doped by monomer	Cl
	4 Styrene copolymer in bulk	O-C ₆ H ₅

R¹ = O-CH₃, R² = O-C₆H₅, in all permutations

Table 2: Chemical structure and preparation method of the investigated phthalocyanine films

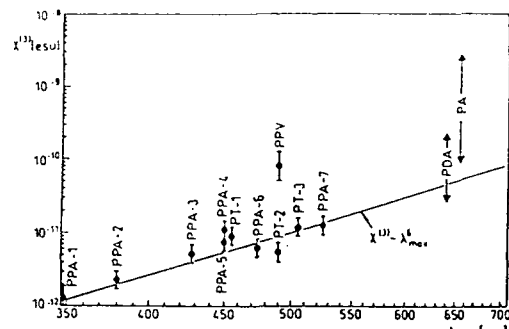


Figure 1: Survey of THG experiments with conjugated polymers. In addition to the systems listed in Table 1 $\chi^{(3)}$ -values for poly diacetylenes (PDA) and trans poly acetylenes (PA) taken from the literature⁽⁴⁾, as well as for poly(3-decyl thiophenes) (PT)⁽⁵⁾ are plotted as a function of the spectral position, λ_{max} , of the linear absorption. The higher $\chi^{(3)}$ -values found for PPV are explained as a consequence of the higher π -electron density due to the lack of bulky substituents (from Ref. 14).

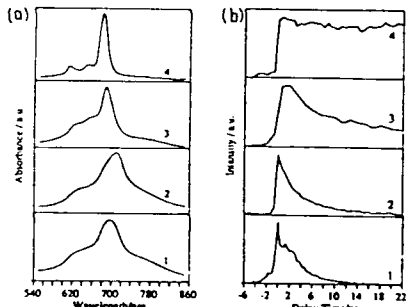


Figure 2: Absorption spectra (a) and decay of transient gratings (b) of some phthalocyanine thin films 1-4 as described in the text (from Ref. 5).

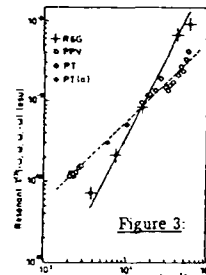


Figure 3: Double-logarithmic plot of resonant $\chi^{(3)}$ values determined by DFWM, if the laser wavelength is tuned in the low-energy tails of the absorption bands of the conjugated polymers PPV, PT and the dye R6G as described in the text. (a): data from Ref. 21. The full and dashed lines represent the slopes 2 and 1 respectively. Data from Ref. 17.

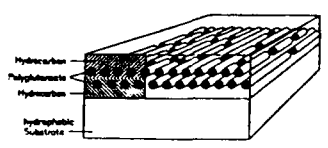


Figure 6: Schematic description of the organization of "hairy rod" polymers on solid supports as obtained by the Langmuir-Blodgett-Kuhn method.

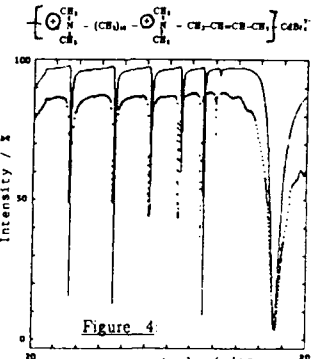


Figure 4: Waveguide mode pattern and surface plasmon resonance of a glassy polyelectrolyte thin film. Chemical structure given on top.

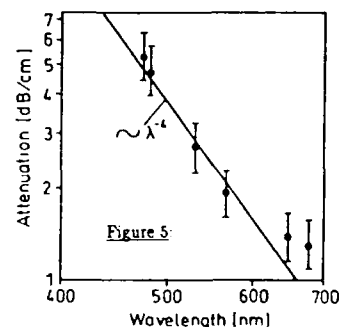


Figure 5: Waveguide losses of a glassy polyelectrolyte film as a function of the wavelength

CUBIC NONLINEAR OPTICS OF POLYMER THIN FILMS.
 1. MOLECULAR ENGINEERING AND PROCESSING
 OF POLYMERS WITH LARGE THIRD-ORDER OPTICAL
 PROPERTIES FOR PHOTONIC SWITCHING

Samson A. Jenekhe*, Ashwini K. Agrawal,
 Chen-Jen Yang, John A. Osaheni, Wen-Chang Chen,
 and Michael F. Roberts

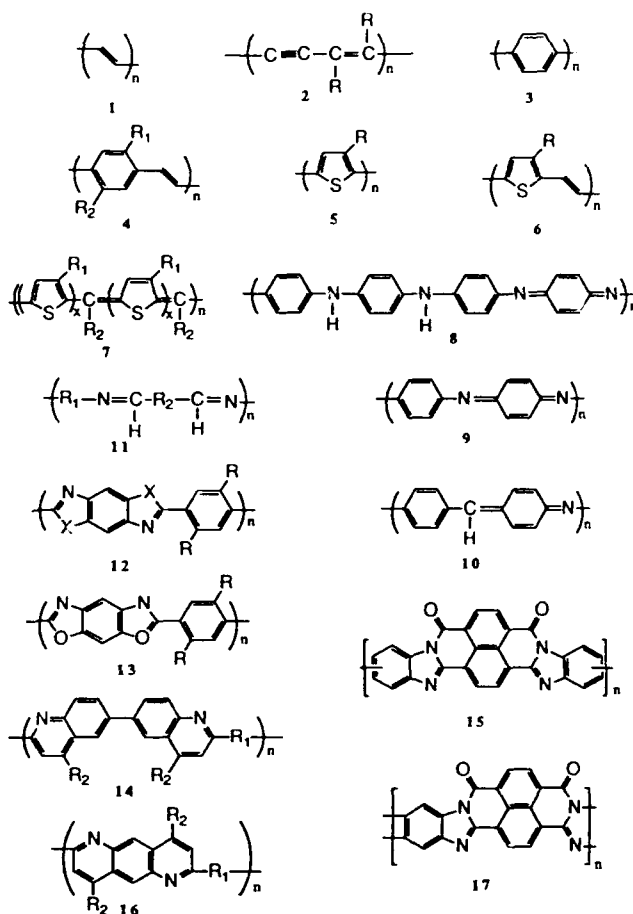
Department of Chemical Engineering and
 Center for Photoinduced Charge Transfer,
 University of Rochester, Rochester, NY 14627-0166

Introduction. Polymers with large cubic optical nonlinearities and picosecond or subpicosecond response time are among the important emerging photonic materials [1-8]. Envisioned applications of such materials in photonics and integrated optics include ultrafast photonic switching devices, optical interconnection of electronic devices, self-switching devices to protect optical and electrooptical sensors from laser radiation damage, and others [2]. However, research in the field is only in the early stages as significant advances in nonlinear optical (NLO) materials synthesis and optimization, thin film processing, fabrication of materials into device structures such as waveguides, and testing of device concepts and prototypes are all required for progress towards these important applications. In this and subsequent papers in the series [9], we will present results that exemplify our laboratory's approach to the molecular engineering and processing of polymers with cubic optical nonlinearities for photonic applications.

Molecular Engineering of Cubic NLO Polymers. One of the often cited advantages of organic nonlinear optical materials is the virtually limitless number of materials potentially accessible by synthetic chemistry and the possibility of materials by design. This assumes that the rules to guide such materials design or optimization are known, presumably from theory or experimental structure-property correlations. Although the third order optical susceptibility of many conjugated polymers has been reported [1,3-8], there is currently no detailed fundamental theory or experimental understanding of the underlying structure- $\chi^{(3)}$ relationships. Early studies [10-12] established the requirement of a conjugated molecule with a large electronic delocalization length, and hence a small optical band gap, to achieve a large second hyperpolarizability (γ) and bulk third order optical susceptibility $\chi^{(3)}$. These earlier or more recent theoretical studies do not provide a sufficient basis for a rational molecular engineering of materials.

The following structures 1-17 represent some of the main conjugated polymers whose NLO properties have been reported by others or under investigation in our laboratory. Most of the literature data on the $\chi^{(3)}$ of polymers consists of one wavelength measurements with little or no information about the wavelength dispersion of $\chi^{(3)}$. In fact, until recently the $\chi^{(3)}$ spectrum was reported for only polyacetylene (1) [13] and polydiacetylenes (2) [14]. Thus, a meaningful comparison of the currently known third order NLO properties of these conjugated polymers is nearly impossible. It is clear that without a rigorous comparison and systematic study of the $\chi^{(3)}$ spectra of conjugated polymers the underlying structure- $\chi^{(3)}$ relationships will remain obscure and there will be no rational basis for molecular engineering or optimization of the materials for devices. Also, without a common basis of assessing the NLO properties of the currently known polymers, the advantage of choice offered by organic NLO materials would turn into a disadvantage and slow progress towards photonic applications due to the problem of choice: i.e., how does one choose one or a small number of NLO polymers for a detailed device work from these polymers 1-17 and possibly scores of their derivatives or others?

Our approach to these problems is a systematic investigation of the $\chi^{(3)}$, and its wavelength dispersion, in different classes of conjugated polymers, e.g. 5-17, and their derivatives with the goal of establishing the structure- $\chi^{(3)}$ relationships and a $\chi^{(3)}$ (λ) data base for testing theoretical models. In addition to the effects of molecular and electronic structure on $\chi^{(3)}$, the effects of polymer chain structure, morphology, and composition is being investigated via copolymers I-III and blends or molecular composites. NLO results illustrating these approaches will be presented in this and the following papers.



.....ABABABABABABAB.....

I (ALTERNATING)

.....AAABABBABBBBAABAAABABB.....

II (RANDOM)

.....AAAAABBBBBAAAAABBBBB.....

III (BLOCK)

Processing of Conjugated Polymers. Advances in processing of conjugated polymers to thin films, coatings, or fibers will be crucial to developing cubic NLO materials for photonic applications for practical and fundamental reasons. An obvious practical consideration in selecting a material for a device application is the ability to reproducibly fabricate the material into the desired device structures. On the other hand, processing determines the bulk morphology of a polymer and hence both linear (α) and nonlinear ($\chi^{(3)}$) optical properties. The often used device figure of merit $\chi^{(3)}/\alpha$ is thus a sensitive function of processing, especially since a large contribution to the bulk optical loss is from scattering due to defects in morphology.

The problem of processing of conjugated polymers has been known to those in the field of conducting polymers for many years. There are currently three approaches to the solution processing of conjugated polymers: (1) soluble precursor polymers; (2) derivatization via long alkyl, alkoxy, or other bulky side chain; and (3) soluble complexes of the conjugated polymers. The precursor polymer approach [15] has been successfully used to process 1, 4, 6, 7 and 10. The derivatization approach has been used to prepare soluble derivatives of 2, 5, 7 and 11. A major drawback of the derivatization

by

Jacques SIMON, Thierry THAMI, Michel A. PETIT

ESPCI-CNRS

Chimie et Electrochimie des Matériaux Moléculaires
10, rue Vauquelin, 75231 Paris Cedex 05, France

Abstract. The synthesis of 1-p-phenylhydrazono-2-phenyl-imino-ethane derivatives unsymmetrically substituted in the para-position with an electron acceptor ($-\text{NO}_2$) and an electron donor ($-\text{OMe}$ or $-\text{NMe}_2$) are described and the corresponding cobaltous complexes are prepared. X-ray diffraction on a single crystal of the dimethylamino-complex has been performed (space-group : PI) showing that the coordinate site around the cobalt ion is nearly tetrahedral. The complex itself is approximately of C_2 symmetry. The inversion center of the space-group transforms one optical isomer into the other. The hyperpolarizability coefficients (β) of the ligands in their cis and trans-forms, and of the neutral cobaltous complexes, have been determined in solution by the Electric Field Induced Second Harmonic (EFISH) technique. The magnitude of the β -value obtained for the complex is larger than the value calculated from the tensorial addition of the molecular hyperpolarizability coefficients of the ligands. The importance of the cation on the nonlinear optical properties of metallo-organic complexes is outlined.

The use of organic molecules for second harmonic generation (SHG) in nonlinear optics (NLO) is well documented. The NLO properties of standard molecular units may be fairly accurately predicted from the donor/acceptor characteristics of the substituents and from the nature of the conjugation path linking these substituents. Only a few studies were concerned with metallic coordination complexes. Metallic coordination complexes may yield original NLO properties in two respects. Firstly, coordination complexes have geometries (tetrahedral, octahedral, square planar) which are extremely difficult to attain with purely organic molecules. Secondly, the molecular orbitals of metallo-organic complexes involve d-orbitals whose symmetry properties are different from s- and p-orbitals found in standard organic chemistry. In organic molecules, the charge transfer band which is the most efficient for SHG is either uniaxial or, more rarely, planar. In conventional disubstituted nitro-aniline derivatives (symmetry : C_{2v}), only the term β_{zzz} is colinear with the dipole moment is not negligible (Fig. 1).

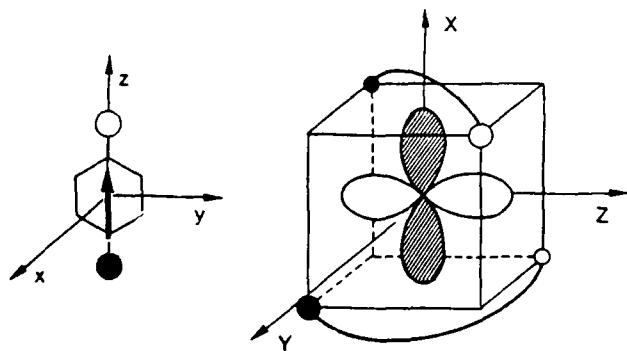


Figure 1. Charge transfers in tetrahedral complexes.

In the C_2 symmetry with two unidimensional polarization axes, the crossed terms $\beta_{YYZ} = \beta_{ZYY}$ appear. These coefficients may be related to the uniaxial molecular hyperpolarizability

coefficients (β_{MS}) by the equations :

$$\beta_{ZZL} = 2\beta_{MS} \cos^3 \alpha$$

$$\beta_{YYZ} = \beta_{ZYY} = 2\beta_{MS} \cos \sin^2 \alpha$$

where 2α is the angle between the charge transfer axes of the two molecular subunits. In this approach, the two polarization subunits are considered to be completely independent, the overall hyperpolarizability coefficients may be calculated from the tensorial sum of the individual hyperpolarizability coefficients.

In the case where the two molecular subunits are linked by a transition metal ion with d-orbitals, 5 other terms are introduced :

$$\beta_{ZXX} = \beta_{XXZ}$$

$$\beta_{XYZ} = \beta_{YZX} = \beta_{ZXY}$$

This paper describes the synthesis of highly polarizable didentate ligands : the hydrazono-imine glyoxal derivatives (Fig. 2).

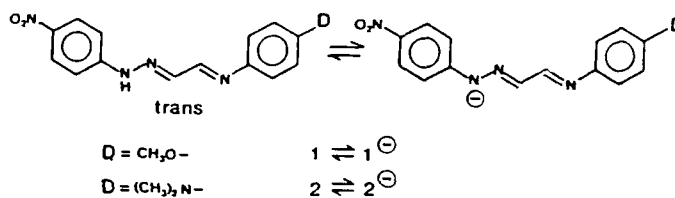


Figure 2. The ligands synthesized and the corresponding anions formed in basic media.

In basic conditions, the corresponding anions salts are prepared. They can be metallated with various metallic salts to form L_2M complexes (L: ligand ; M: first row divalent metallic ions). The X-ray structure of one of the complexes, $(2^-)_2\text{Co}^{II}$, has been determined. The second order hyperpolarizability coefficients of the various ligands and of the cobaltous complexes have been measured by the Electric Field Induced Second Harmonic generation (EFISH) method.

INVESTIGATION OF NEW MOLECULES AND MATERIALS
FOR QUADRATIC NONLINEAR OPTICS

by

J.F. Nicoud

Institut de Physique et Chimie des Matériaux de Strasbourg
Groupe des Matériaux Organiques
ICS- 6, rue Boussingault 7-67083 Strasbourg, France

Introduction

The search for organic materials with large second-order optical nonlinearities is presently intense owing to their potential use in various applications such as optical signal processing¹. To design such materials one must attempt firstly to achieve adequate molecular hyperpolarizability β relative to a given transparency range, and secondly correct alignment of the molecules in the bulk material in order to maximize each molecular contribution. A lot of work has been carried out on the first point since it is well established that a large hyperpolarizability β originates from the presence of a highly polarizable dissymmetric π -electron cloud. A typical nonlinear system consists of a compound bearing an electron acceptor group and a donor group at each extremity of a conjugated system. Such compounds present a typical intramolecular charge transfer electronic transition and are often considered as chromophores or dyes¹.

A good understanding of each effect that could influence the properties of such systems is useful as the next step in engineering suitable nonlinear optical materials, whatever the form of the bulk material that is investigated: crystal, polymer or LB films. Many chromophores have been examined for second-order nonlinear properties. The best known are 1,4-disubstituted benzenes or 2,5-disubstituted pyridines, which have led respectively to the discovery of the nearly optimized crystalline materials NPP² and PNP³. Then and still now, more extended conjugated systems have been investigated: 4,4'-disubstituted stilbenes⁴ and 4,4'-disubstituted tolans⁵. We wish to report here our recent results concerning both these kinds of conjugated systems.

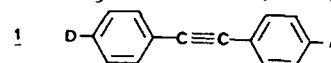
Results and discussion

Tolan derivatives. The tolan skeleton presents the advantage of avoiding the facile chemically and photochemically induced Z,E (cis-trans) isomerism that is often observed with the corresponding stilbenes. Some second harmonic generation (SHG) efficient derivatives have already been reported^{5,7}. We have synthesized a set of 4,4'-disubstituted ("push-pull") tolans **1**, and studied their nonlinear optical properties. All the compounds have been prepared using a palladium/copper catalyzed coupling reaction between an arylacetylene and an arylhalide in a dialkylamine solvent according Hagihara's procedure⁸. In some cases a catalytic phase transfer Pd/Cu coupling reaction proved useful⁹.

Classical considerations about conjugated systems reveal that the most stable conformation of each push-pull tolan is obtained when the phenyl rings lie both in the same plane. Contrary to the biaryl or stilbene analogues, no steric interactions between the ortho-hydrogens occur here. From calculations of the molecular structure and the heat of formation by using the AM1 semi-empirical method, it has been found that the resonance energy difference between an all planar geometry and an orthogonal orientation of the aryl rings is less than 0.3 kcal.mol⁻¹. The consequence is a quasi-free rotation around each aryl-ethynyl C-C bond and thus all conformers should coexist at room temperature. We predict from this result that we can observe any value of the interplanar angles in the crystalline state, since as is well known, the crystalline environment can effect such torsional changes easily. This has been actually observed recently by Desiraju and Krishna¹⁰ from a study of

unsymmetrically substituted tolans with moderate dipole moments. Their results show that these compounds are likely to adopt chiral non-planar conformations in the solid state, which in addition, leads to a high proportion of non-centrosymmetric space groups. The effect of the free rotational distortion of the diarylacetylene backbone on the molecular hyperpolarizability has been calculated by a Finite Field ANDO method. The results, reported elsewhere¹¹, show that even when the two aryl rings are perpendicular to each other, the charge-transfer interaction is still present, leading to a molecular hyperpolarizability of half the value of the maximum obtained for a full planar conformation. We can then conclude that whatever the conformation of the push-pull tolan in the solid state, it always retains an appreciable hyperpolarizability. We measured the β values of our ten samples using the EFISH technique¹¹. From the results, we pointed out that the thiomethoxy (Me-S-) group leads to a noticeable increase of β without loss of transparency in comparison with the methoxy (Me-O-) group. We also notice that the bromo (Br) substituent, though electronegative, can allow a relatively large β and good transparency when opposed to the cyano and nitro groups. The data together with the qualitative SHG powder tests at 1.06 μ m are summarized in Table I.

Table I. Qualitative SHG powder tests at 1.06 μ m, static $\beta(0)$ values (in 10⁻³⁰ esu) and maximum electronic absorption (λ_{max} in nm in CHCl₃) of 4,4'-diarylacetylenes **1**.



D	A = NO ₂	$\beta(0)$	λ_{max}	A = CN	$\beta(0)$	λ_{max}
Me ₂ N-	0	42	415	0	32	373
MeO-	++	25	357	0	13	328
MeS-	+++	29	362	0	15.5	334
Br-	++	21	335	+	9	310
CH ₃ -	++	21	342.5	+	10	314

Given the broad range of sizes of crystalline particles in the samples, and possible preferential orientation, the powder test were not quantified; + denotes a signal comparable to or a few times greater than that of urea, whereas ++ and +++ refer to one order and two orders of magnitudes greater signal respectively. 0 denotes no detectable SHG signal.

In summary, we indeed observed a high proportion of non-centrosymmetric crystal structures, especially for compounds bearing weak donors. Both the methyl and one bromo derivatives are new. The cyano derivatives are colorless and in this respect could be interesting for blue light frequency conversion.

Stilbazolium derivatives. Meredith¹² and Marder¹³ have demonstrated that a variety of 4-N-methylstilbazolium salts can give rise to large quadratic nonlinearities, when associated to the correct anion. This was due to the high molecular hyperpolarizability of the 4'-donor substituted 4-N-methylstilbazolium cation. Since these materials are ionic species the EFISH measurement of their hyperpolarizability is not possible. The only values reported so far for such chromophores come from D. Lupo et al.¹⁴. These authors determined $\chi^{(2)}$ values of Langmuir-Blodgett monolayers from second harmonic generation measurements at 1.06 μ m, then deduced the molecular β values by using an oriented gas model. For example the β value of compound **2** is 150 x 10⁻³⁰ esu, that is one order of magnitude greater than p-nitroaniline though having almost the same maximum absorption band (λ_{max} = 360nm). We therefore chose to examine the NLO properties of various derivatives bearing

Preparation of Polymeric Films for NLO Applications

R.P.Foss, W. Tam, and F.C. Zumsteg

Central Research and Development Department,
Du Pont, Experimental Station, P.O. Box 80328,
Wilmington, Delaware, 19880-0328

Introduction

The study of poled polymers is an active area of research because of the potential for large nonlinear optical coefficients, ease of fabrication, and high optical quality afforded by these polymers. Organic molecules with delocalized π -electronic structures and large charge-transfer resonances are known to be capable of having very large molecular hyperpolarizabilities. Materials with second-order nonlinear optical properties, suitable for nonlinear optical and electro-optic devices, can be prepared by incorporating organic molecules either in side-chain or in cross-linked polymer networks. Dipolar orientation has been induced by electric field poling of these systems (1,2,3). To obtain large nonlinear coefficients, the desired polymers should 1) have a large number density of nonlinearly active organic components, 2) contain molecules with large molecular dipole moment and hyperpolarizability product ($\mu\beta$), and 3) be able to sustain large electric poling fields to maximize orientation of nonlinearly active components. Of practical importance is the ability to form good films of the desired polymers, since device applications will most likely utilize the polymers in thin film configuration. To satisfy requirements 1 and 2 for side-chain polymers, one would like to have homopolymers containing pendent nonlinearly active molecules with large $\mu\beta$. Such molecules are derived from the use of strong donor and acceptor moieties attached to a conjugated π -electronic system; these molecules are generally highly colored (4,5). The good electron-transferring ability of these molecules and their deep colors make homopolymerization of derivatives containing nonlinearly active compounds difficult either by radical initiation or photolysis. The highly polar nature of these molecules may result in poor solubility of the homopolymers which makes casting of films from solution difficult or impossible. Better temporal stability has been observed for cross-linked polymer networks than for side-chain polymers (2,3). However, solubility problems prevent spin casting of these polymers from solution.

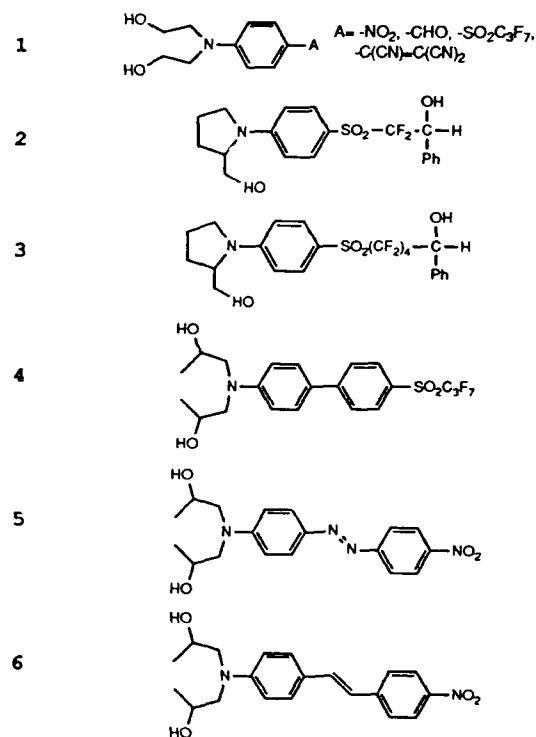
Our approach to preparing polymeric films suitable for NLO applications is initially to prepare a film from a solution containing a prepolymer with active pendant groups and a nonlinear dye, containing complementary reactive groups that can act as a cross-linking agent. The prepolymer must have the ability to form a film. In order for our approach to succeed, the dye must be miscible with the prepolymer so that phase separation does not occur at high doping levels when the mixture is spin cast. Once the film is formed, it is processed by heat to generate the final network. Due to the improved temporal stability of cross-linked systems, we have concentrated our efforts toward the use of dyes containing more than one reactive group.

Preparation of Prepolymers.

We have prepared homopolymers of isocyanatoethyl methacrylate, and isocyanatostyrene. Polyisocyanatoethyl methacrylate was prepared by free radical polymerization of isocyanatoethyl methacrylate using α,α' -azobis(isobutyronitrile) initiator in THF to give the desired polymers with $M_w(\text{ave})$ of 4,900 to 24,000. Polyisocyanatostyrene was prepared similarly by free radical polymerization in toluene of isocyanatostyrene, which had been prepared from the reaction of *p*-aminostyrene•HCl with phosgene. The $M_w(\text{ave})$ of the polyisocyanatostyrene was 3550. We have also prepared copolymers of styrene/isocyanatostyrene and methyl methacrylate/isocyanatoethyl methacrylate. These copolymers have $M_w(\text{ave})$ in the range of 11,550-25,300.

Preparation of Cross-Linking Agents

The following cross-linking agents have been prepared.

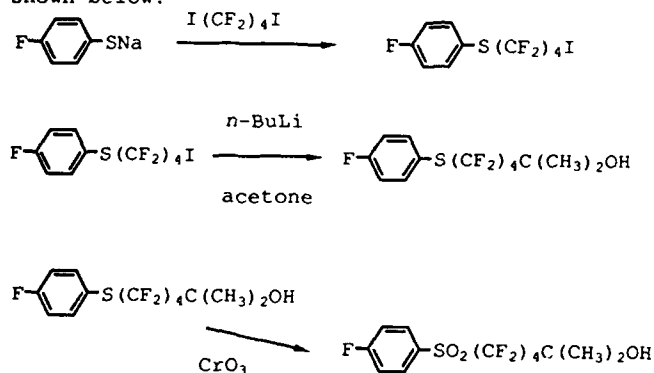


The bis(2-hydroxyethyl)aminophenyl derivatives (1) with nitro, fluorinated sulfone, and aldehyde acceptors were prepared from the reaction of *N,N*-diethanolamine with the corresponding 4-acceptor-1-fluorobenzene (6). Bis(2-hydroxyethyl)aminophenyl derivative with the tricyanovinyl acceptor was prepared from the reaction of bis(2-hydroxyethyl)aminobenzene with tetracyanoethylene using a literature procedure (7).

The derivative containing the 1-phenylsulfonylethanol acceptor (2) was prepared by nucleophilic substitution of fluoride from 2,2-difluoro-1-phenyl-2-(4-fluoro)phenylsulfonylethanol with (S)-(+)-2-pyrrolidinemethanol. Difluoro-1-phenyl-2-(4-fluoro)phenylsulfonylethanol was prepared according to a literature procedure (8).

[4-(2-hydroxymethyl-1-pyrrolydiny)phenyl]-[1,1,2,2,3,3,4,4-octafluoro-5-methyl-5-hydroxy-

hexyl]sulfone (3) was similarly prepared from [4-(1-fluorophenyl)-[1,1,2,2,3,3,4,4-octafluoro-5-methyl-5-hydroxy-hexyl]sulfone by nucleophilic substitution with (S)-(+)-2-pyrrolidinemethanol. The preparation of the starting fluoro compound is shown below.



The derivatives containing the bis(2-hydroxypropyl)amino donor (4,5,6) were prepared from the corresponding aminobiphenyl, aminoazobenzene, or aminostilbene with propylene oxide. The starting aminobiphenyl containing the fluorinated sulfone acceptor was prepared using the palladium-catalyzed cross coupling of (4-trimethyltin)phenylperfluoropropyl sulfone with 4-bromobis(*N,N*-acetyl)aminobenzene followed by deprotection with HCl(9). The azo compound with bis(2-hydroxypropyl)amino donor is more soluble than Disperse Red-19 (which leads to thicker films (1-2 μm)).

We have also examined commercially available materials including: Disperse Red-19, 4-nitrocatechol, 1-(4-nitrophenyl)glycerol, *p*-nitrophenyl- α -L-arabinofuranoside, and 4-nitro-1,2-phenylenediamine.

Preparation of Films and Properties of Final Polymers

In order to prepare good films with thicknesses of 1-2 μm , the dye must be relatively soluble in a solvent compatible with the prepolymer. Reaction must be slow enough to avoid precipitation of the final cross-linked polymers before spin casting. We have found THF to be a suitable solvent. All of the above cross-linking agents have been incorporated into films of the prepolymers with the ratio of reactive group (-OH or -NH₂) to active group (-NCO) in the range of 0.8 to 1 or higher, without phase separation. Monitoring of the reactions in the films by IR indicates that the intensity of the -NCO band decreases by 40-92% after heating at 150°C for one hour. The prepolymers themselves undergo little reaction (6-8%) under these conditions. Slower reactions occur with the dyes containing the propyl alcohol groups. The reaction can be catalyzed by the addition of dibutyltin dilaurate. Once cross-linking has been completed, the films are hard and brittle and are not soluble in common organic solvents (THF, CHCl₃, DMF, etc.).

The T_g of cross-linked films increases with processing temperature and time. For example, a film formed from polyisocyanatoethyl methacrylate and 4-bis(2-hydroxyethyl)aminonitrobenzene yielded a polymer with a T_g of 135°C after heating the film at 150°C for 1 hour. The T_g increased to 160°C after heating the film further at 180°C for 1 hour. After heating a film formed from polyisocyanatoethyl methacrylate and [4-(2-hydroxy-

methyl-1-pyrrolidinyl)-phenyl][1,1-difluoro-2-hydroxy-2-phenyl-ethyl]sulfone at 150°C overnight, a polymer with a T_g of 178°C was obtained.

Corona poling of these films can lead to materials with good orientational stability at 80°C for several weeks. Poling conditions are important for obtaining optimum nonlinearity and excellent orientational stability.

Summary

Our approach for the preparation of thin films for NLO applications appears to be general; incorporation of dyes containing various acceptors (-NO₂, -SO₂Rf, -CHO, -C(CN)=C(CN)₂) into cross-linked polymer networks has been demonstrated. Good orientational stability at 80°C has been achieved.

Literature cited

1. Meredith, G.R.; VanDusen, J.G.; and Williams, D.J., *Macromolecules*, 1982, 15,1.
2. Bjorklund, G.C.; Ducharme, S.; Fleming, W.; Jungbauer, D.; Moerner, W.E.; Swalen, J.D.; Twieg, R.J.; Willson, C.G.; and Yoon, D.Y. in *Materials for Nonlinear Optics*; Marder, S.R.; Sohn, J.E.; and Stucky, G.D. Eds., ACS, Washington, 1991, Chapter 13, 216.
3. Dai, D.-R.; Hubbard, M.A.; Li, D.; Par, J.; Ratner, M.A.; Marks, T.J.; Yang, J.; and Wong, G.K. in *Materials for Nonlinear Optics*; Marder, S.R.; Sohn, J.E.; and Stucky, G.D. Eds., ACS, Washington, 1991, Chapter 14, 227.
4. Cheng, L.-T.; Tam, W.; Meredith, G.R.; and Rikken, G.L.J.A. *Proc. of the Int. Soc. for Optical Eng.*, 1989, 1147, 61.
5. Katz, H.E.; Singer, K.D.; Sohn, J.E.; Dirk, C.W.; King, L.A.; and Gordon, H.M.; *J. Am. Chem. Soc.* 1987, 109, 6561.
6. DeMartino, R.N.; U.S. Patent, 4,757,130, 1988.
7. McKusick, B.C.; Heckert, R.E.; Cairns, T.C.; Coffman, D.D.; and Mower, H.F. *J. Am. Chem. Soc.* 1958, 80, 2806.
8. Stahly, G.P. U.S. Patent, 4,837,327, 1989.
9. Tam, W.; Cheng, L.-T.; Bierlein, J.D.; Cheng, L.K.; Wang, Y.; Feiring, A.E.; Meredith, G.R.; Eaton, D.F.; Calabrese, J.C.; and Rikken, G.L.J.A. in *Materials for Nonlinear Optics*; Marder, S.R.; Sohn, J.E.; and Stucky, G.D. Eds., ACS, Washington, 1991, Chapter 9, 156.

Synthesis of Side-chain and Main-chain Nonlinear Optical Polymers with Sulfonyl Acceptor Groups

Douglas R. Robello, Jay S. Schildkraut, Nancy J. Armstrong,
Thomas L. Penner, Werner Köhler, and Craig S. Willand
Corporate Research Laboratories, Eastman Kodak Company
Rochester, New York 14650-2109

Introduction

Practical second-order nonlinear optical (NLO) materials require many properties in addition to large nonlinear susceptibility ($\chi^{(2)}$), among these: ability to form thin films, low dielectric constant, negligible scattering and absorption of propagated light, chemical, photochemical, and thermal stability, etc. Organic materials may be successful in this area because they can possess very large $\chi^{(2)}$ values,¹⁻³ and their material properties can be tailored to meet the demands of the desired application using well-developed synthetic techniques.

In organic molecules, large molecular hyperpolarizabilities, β , are usually obtained with an extended π -conjugated system substituted at the extremes by electron-donating and electron-accepting groups. Sulfonyl acceptor groups are particularly advantageous because (unlike well-studied nitro and cyano groups) their *bifunctionality* allows for chemical substitution at the second valence. This synthetic flexibility permits the incorporation of NLO-active species into a number of different material embodiments.

We have demonstrated in model systems that sulfonyl-substituted compounds can possess relatively large hyperpolarizabilities, accompanied by significantly short wavelength absorbances.⁴ In this preprint, we present some aspects of our efforts to produce polymers that contain covalently-bound, sulfone-substituted NLO chromophores.

Side-Chain NLO Polymers

We have synthesized a number of homopolymers and copolymers that contain pendant 4'-amino-4-methylsulfonyl-azobenzene or -stilbene chromophores (Figure 1). Key in the synthesis is the ability to functionalize the sulfur atom to produce arbitrarily-substituted acceptor portions of the NLO dyes (Figure 2). A convergent strategy in which the donor and acceptor portions are later joined (Figure 3) allows for the "mixing and matching" of components to provide many different compounds from a common pool of intermediates.

High polymers were readily obtained from methacrylate esters of the sulfonyl-NLO dyes via free-radical polymerization. Both homopolymers and copolymers with conventional monomers were obtained (Table 1). The copolymers appear to be random because size exclusion chromatography (SEC) using differential refractive index and visible absorption detectors gave identical MW distributions. All of these side-chain sulfonyl-containing polymers were amorphous solids, in contrast to two analogous nitro-containing polymers that exhibited liquid crystallinity.⁵ (Although liquid crystalline polymers possess desirable order, grain boundaries often lead to an unacceptably large amount of light scattering in waveguide applications.) As noted by us⁵ and by others,^{6,7} stilbene-containing polymers crosslinked slightly when the concentration of monomeric dye was high.

High optical quality waveguides could be fabricated by spin-coating these polymers from solution. The only optical losses appeared to come from adventitious contaminants such as dust particles. The polymers were coated onto conductive substrates and poled at T_g using either a second electrode deposited on the polymer surface or a corona discharge. Typical poling fields were approximately 10^6 v/cm. After cooling to room temperature with the field on, second-order NLO susceptibilities were measured at 632 nm by an ellipsometric technique⁸ and at 830 nm by construction of a Mach-Zender interferometer. Relatively large electrooptic coefficients were found (Table 1), although it should be noted that the coefficients for azobenzene derivatives measured at 632 nm were subject to resonance enhancement (factor of 2-3) because of slight absorption by the chromophore.

Figure 1. Side-chain NLO polymers.

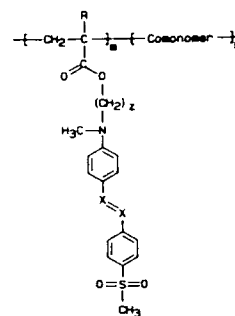


Table 1. Properties of side-chain NLO polymers.

Polymer	X	z	R	m/n	Comon.	M_w^a	T_g^b (°C)	r_{33}^c (pm/v)
1	N	2	CH ₃	1/0	—	46,000	140	—
2	N	6	CH ₃	1/0	—	89,000	99	38.7, ^d 12 ^e
3	N	6	CH ₃	1/5	MMA ^f	92,000	109	12.9 ^d
4	CH	6	H	1/9	<i>t</i> -Bu St ^g	177,000	127	2.6 ^d
5	CH	6	H	1/13	MMA ^f	111,000	109	—

^aBy SEC, PS stds. ^bBy DSC. ^cElectrooptic coeff. ^dAt 632 nm via ellipsometry. ^eAt 830 nm using a Mach-Zender interferometer.

^fMethyl methacrylate. ^g*t*-Butyl styrene.

Figure 2. Synthesis of acceptor portions of NLO dyes.

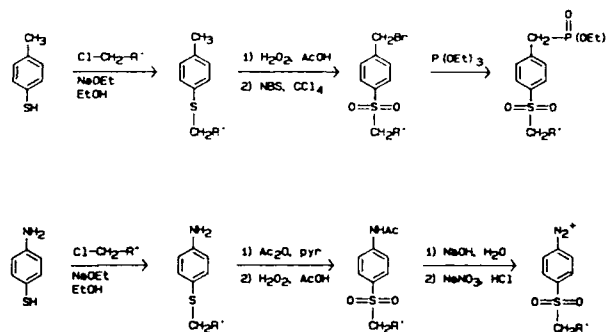
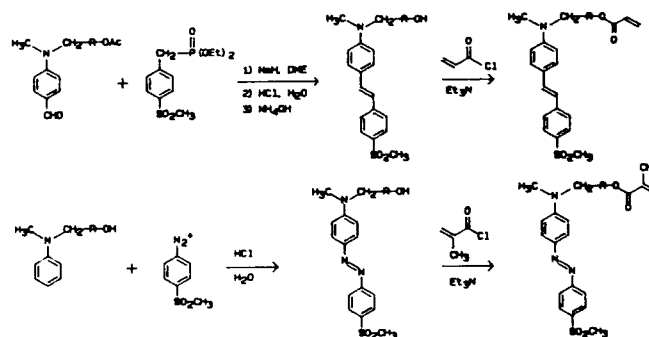


Figure 3. Synthesis of side-chain monomeric NLO dyes.



Langmuir-Blodgett Polymers

By a synthetic route analogous to that shown in Figure 2 and 3, we constructed side-chain polymers with long, nonpolar groups on the sulfone and polar spacer groups between the nitrogen donor and the polymer backbone (Figure 4).

These amphiphilic polymers formed excellent Langmuir monolayers when cast on water (Figure 4), and the films could be

transferred to solid supports.⁹ By alternating deposition with cadmium arichidate, multilayer noncentrosymmetric films were produced, in which the expected quadratic dependence of SHG intensity vs. thickness was found even for many layers (Figure 5).⁹ The SHG signals from these LB films remained unchanged even after weeks of storage at room temperature.

Figure 4. Amphiphilic NLO polymer 6 and its surface pressure-area isotherm on a Cd²⁺-containing subphase.

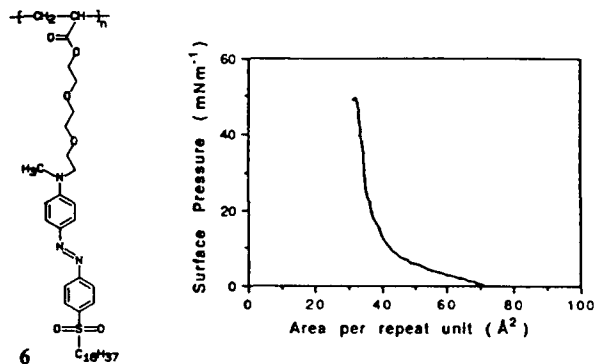
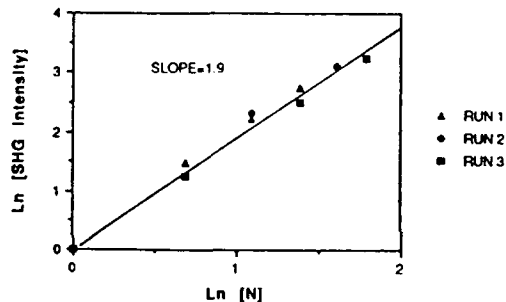


Figure 5. SHG intensity as a function of the number of layers of 6 alternated with cadmium arichidate.



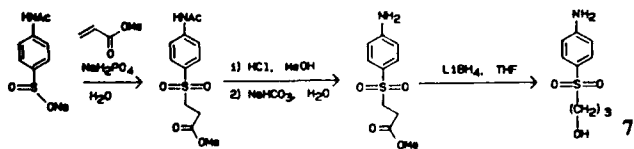
Main-Chain Polymers

By substituting the sulfone with an hydroxyl-bearing group and the nitrogen donor with an ester-bearing group, "AB-type" condensation monomers were prepared. The acceptor portion could be synthesized analogous to the method shown in Figure 2, but for 3-hydroxypropyl derivatives, we found that Michael addition of 4-acetamidobenzene sulfinate to methyl acrylate, followed by deprotection, and finally reduction of the ester gave superior yields of the desired sulfone 7 (Figure 6).

Isoregic main-chain NLO polymers were synthesized simply by heating the monomers in the melt under vacuum in the presence of a suitable catalyst (Figure 7).¹⁰ When the flexible spacer between chromophores was long or when a bulky side group was employed, these main-chain polymers were amorphous (Table 2), and could be easily processed into optically clear thin films.

After poling, the main-chain NLO polymers displayed significantly better orientational stability below T_g compared to side-chain polymers containing the same chromophore. In addition, simultaneous SHG and TSDC studies of the main-chain polymers suggested that the relaxation of the poling-induced order is comprised of two distinct mechanisms: a short-range motion at T_g that leads to little loss of SHG activity and a

Figure 6. Synthesis of 4-aminophenyl-(3-hydroxypropyl)sulfone.



long-range motion above T_g that causes the SHG decay (Figure 8).¹¹ This high temperature relaxation was absent in related side-chain and doped systems.

Figure 7. Polycondensation to form NLO main-chain polymers.

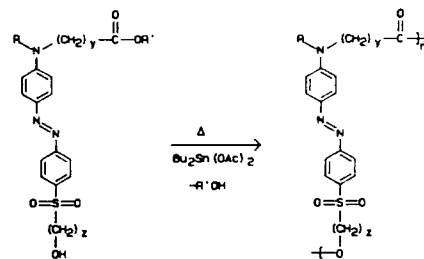
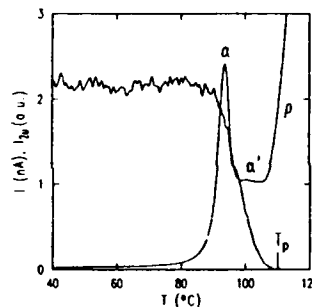


Table 2. Properties of main-chain NLO polymers.

Polymer	y	z	R	M_w^a	T_g^b (°C)	T_m^b (°C)
8	5	6	CH ₃	70,000	59	—
9	1	3	CH ₃	—	122	230
10	1	3	ⁿ C ₄ H ₉	39,000	92	—

^aBy SEC, PS stds. ^bBy DSC.

Figure 8. Simultaneous SHG and TSDC measurements as a function of temperature on main-chain NLO polymer 10.



Acknowledgments

We express our appreciation to the following members of Eastman Kodak Company: P. Dao and M. Scozzafava for sample preparation and poling studies, J. Revelli and J. Phelan for Mach-Zender experiments, T. Mourey and S. Miller for SEC data, and V. Mazzi and M. Moscato for DSC data. We also thank D. J. Williams and J. O'Reilly for helpful discussions.

References

- (1) Chemla, D. S.; Zyss, J. *Nonlinear Optical Properties of Organic Molecules and Crystals*; Academic Press: NY, 1987.
- (2) Prasad, P. N.; Williams, D. J. *Introduction to Nonlinear Optical Effects in Molecules and Polymers*, Wiley: NY, 1991.
- (3) Marder, S. R.; Sohn, J. E.; Stucky, G. D. *Materials for Nonlinear Optics*, Chemical Perspectives ACS Symposium Series No. 455; 1991.
- (4) Ulman et al., *J. Am. Chem. Soc.* **1990**, *112*, 7083.
- (5) Robello, D. R. *J. Polym. Sci., Polym. Chem.* **1990**, *28*, 1.
- (6) Griffin, A. C.; Bhatti, A. M., in *Organic Materials for Nonlinear Optics*, Spec. Publ. Roy. Soc. Chem., Hahn, R. A.; Bloor, D., eds.; 1989, p. 295.
- (7) Nijhuis, S.; Rikken, G. L. J. A.; Havinga, E. E.; ten Hoeve, W.; Wynberg, H.; Meijer, E. W. *Chem. Commun.* **1990**, 1093.
- (8) Schildkraut, J. S. *Appl. Opt.* **1988**, *27*, 329.
- (9) Penner, T. L.; Willand, C. S.; Robello, D. R.; Schildkraut, J. S.; Ulman, A. *Proc. SPIE* **1991**, *1436*, 169.
- (10) Köhler, W.; Robello, D. R.; Willand, C. S.; Williams, D. J. *Macromolecules* **1991**, in press.
- (11) Köhler, W.; Robello, D. R.; Dao, P. T.; Willand, C. S.; Williams, D. J. *J. Chem. Phys.* **1990**, *93*, 9157.

SYNTHETIC APPROACHES TO NLO POLYMERS

R. Twieg, D. Burland, M. Lux, C. Moylan,
C. Nguyen, P. Walsh, C.G. Willson, R. Zentel

IBM Research Division
Almaden Research Laboratory
San Jose, CA 95120

INTRODUCTION

A gradual enhancement of basic understanding and a corresponding optimization of the functional properties of second-order nonlinear optical polymers has brought them closer to practical applications in a variety of integrated optoelectronic devices, such as modulators and harmonic generators.¹⁻³ A wide range of polymer and nonlinear chromophore combinations have by now been evaluated and their structure and processing correlated with the resultant magnitude and stability of the poling induced macroscopic nonlinearity. Numerous additional combinations of polymers and chromophores can be envisioned; these systems may be classified by application of the following general criteria:

1) What is the bonding relationship between polymer and chromophore, no bond (guest-host) or covalently bonded? If the latter, is the chromophore attached as a mainchain or sidechain component? Exactly what is the nature of the linking group and how many and where are the points of attachment between chromophore and polymer?

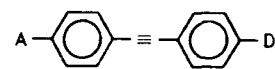
2) Is there any significant molecular weight change of the system during final processing, particularly during the electric field poling step? Does this change of molecular weight influence processing or function of the materials in particular as related to the magnitude and stability of the poled order?

3) In addition to the covalent interactions among the polymer and chromophore components, what other factors affect the macroscopic order? For example, does liquid crystallinity, hydrogen bonding or some other colligative interaction influence the magnitude and stability of the polar order?

RESULTS

Most of our own past effort on the synthesis and characterization of NLO polymers has focused on epoxy-based systems.⁴⁻⁷ In all cases we have examined thus far the chromophores are covalently bound to the polymer and both linear and crosslinking systems have been examined. Amongst the many opportunities for propagation chemistry typical of epoxy resins we have chosen the convenient reaction between aromatic amines and glycidyl ethers. This approach is *convenient* in the sense that the aromatic amine serves a dual role: first, it is a useful donor in the NLO chromophore sense and second, in the chemical sense it may serve as both the nucleophile (-NHR, primary or secondary aromatic amine) and also an intermediate for preparation of the glycidyl ether component. The reactivity of this aromatic amine and glycidyl ether pair is usually such that the molecular weight advancement can be staged to provide stable and soluble prepolymers of sufficient molecular weight for film processing by spin coating, in contrast to the much more reactive formulations containing aliphatic amines. The overall polymeric and nonlinear properties of these materials are a complex function of the exact nature, number and location of the polarizing substituents and reactive sites appended to the functionalized aromatic chromophores.

We have examined a variety of potential chromophores for introduction into these polymers, but tentatively have focused on utilization of the polar tolan (diphenylacetylene) chromophore. The tolan has a number of real (and perceived) virtues. There is little ambiguity in the direction of the microscopic nonlinear tensor along the director axis of these polar molecules. The thermal stability of the tolan unit is appreciable and at least commensurate with the epoxy backbone itself. The rigid tolan chromophore has a respectable aspect ratio which independent of the mode of attachment to the polymer will deter relaxation of the poled order. As a function of the particular acceptor (A) and donor (D) pair the chromophore and molecular hyperpolarizability can be systematically varied over an appreciable range and a wide variety of these polarizing pairs of groups are readily introduced by virtue of the synthetic methodology. The following table contains data for some of the tolan chromophores prepared and studied to date:



A	D	λ_{\max} (nm)	μ_g (D)	β (1.06)	β_0
NO ₂	NMe ₂	402	7.1	101	37
SO ₂ CH ₃	NMe ₂	358	7.5	40	19
SO ₂ CF ₃	NMe ₂	388	8.4	86	35
NO ₂	OCH ₃	-	-	-	16*
SO ₂ CH ₃	OCH ₃	310	5.9	11	7
SO ₂ CF ₃	OCH ₃	327	6.2	21	12

The β_0 is a two-level correction to β (1.06) both in units of 10⁻²⁰ esu, all measurements in dioxane except * in acetone (ref 18)

The sulfone acceptor group has found recent application in a variety of NLO polymer structures since this group seems to provide a good hyperpolarizability vs. transparency tradeoff and is bifunctional to permit "building through" the chromophore.⁸⁻¹¹ Like the nitro group (-NO₂), the alkyl sulfone, perfluoroalkyl sulfone, bisaryl sulfone and other relatives (-SO₂R, R = (CH₂)_nH, (CF₂)_nF, Ar, OR, NR'R', etc.) are well known electron-accepting groups from powder screening of single crystal SHG candidates.¹²⁻¹⁵ The large positive Hammett σ constants¹⁶ for these substituents containing the -SO₂R group are, of course, good indicators of their potential value as acceptors. This correlation is particularly true as the group R itself becomes more electrophilic and further enhances the inductive effect of the entire substituent. For example, as a function of R, the σ_p values for -SO₂R increase as follows: OH (0.50), NH₂ (0.57), CH₃ (0.68), CF₃ (0.93) (compare for the nitro substituent itself with σ_p = 0.78).

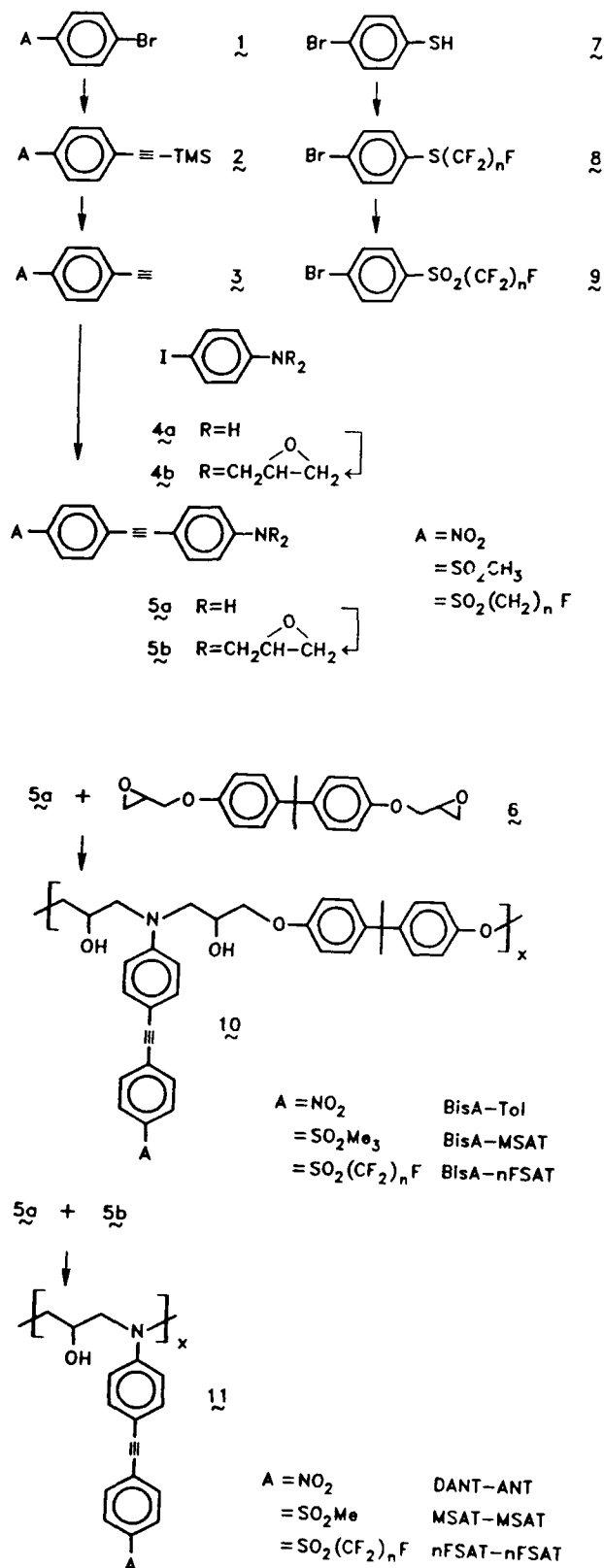
The synthesis of the tolan is very straightforward. Starting with an acceptor group (A) activated bromobenzene **1** the transition metal mediated ethynylation is done with a monoprotected acetylene and the intermediate **2** deprotected giving the acceptor substituted phenylacetylene **3**. This phenylacetylene is then reacted with iodocyaniline **4a** or its bisglycidylether **4b** to give **5a** or **5b** respectively. The bisglycidylation of the either aromatic amine **4a** or **5a** is straightforward in two steps via epichlorohydrin. Both the bromonitrobenzene (**1** A = NO₂) and the methylsulfonylbromobenzene (**1**, A = SO₂Me) are commercially available while the perfluoroalkylsulfonyl analogs (**1** A = SO₂(CF₂)_nF) are efficiently

prepared in two steps from bromothiophenol by reaction with a perfluoroalkyl iodide to give sulfide **7** which is subsequently oxidized to give sulfone **9**.¹⁷ The different lengths of perfluorocarbon tails ($n = 1, 2, 6, 12$) have been examined to assay any influence on important physical properties such as nonlinearity, dielectric constant, refractive index, and perhaps even the stability of poled order.

We have examined two general classes of linear tolan containing polymers. In the first class **10** only the amine component contains a high nonlinearity chromophore which is reacted with the diglycidylether of bisphenolA **6** (numerous other bisepoxides are obviously possible). The second class **11** have a nearly doubled loading of nonlinear chromophores and are prepared by condensation of the polar aminonitrotolan with is diglycylated counterpart. In both classes of linear tolan and related crosslinking systems very interesting behavior has been found in both dielectric and NLO studies.

REFERENCES

1. P. N. Prasad, D. R. Ulrich, Eds., "Nonlinear Optical and Electroactive Polymers" (Plenum, New York, 1988).
2. P. N. Prasad, D. J. Williams, "Introduction to Nonlinear Optical Effects in Molecules and Polymers" (John Wiley & Sons, Inc., New York, 1991)
3. S. R. Marder, J. E. Sohn, G. D. Stucky, Eds., "Materials for Nonlinear Optics, Chemical Perspectives" ACS Symposium Series 455 (ACS, Washington, D.C., 1991).
4. M. Eich, B. Reck, D. Y. Yoon, C. G. Willson, G. C. Bjorklund, *J. Appl. Phys.*, **66**, 2559 (1989)
5. B. Reck, M. Eich, D. Jungbauer, R. J. Twieg, C. G. Willson, D. Y. Yoon, G. C. Bjorklund, *Proc. SPIE*, **1147**, 74 (1990).
6. D. Jungbauer, B. Reck, R. J. Twieg, D. Y. Yoon, C. G. Willson, J. D. Swalen, *Appl. Phys. Lett.*, **56**, 2610 (1990).
7. I. Teraoka, D. Jungbauer, B. Reck, D. Y. Yoon, R. Twieg, C. G. Willson, *J. Appl. Phys.*, **69**, 2568 (1991).
8. S. Nijhuis, G.L.J.A. Rikken, E. E. Havinga, W. ten Hoeve, H. Wynberg, E. W. Meijer, *J. Chem. Soc. Chem. Comm.*, 1093 (1990).
9. A. Ulman, C. S. Willand, W. Kohler, D. R. Robello, D. J. Williams, L. Handley, *J. Amer. Chem. Soc.*, **112**, 7083 (1990); see also Chapter 10, pp 170-186 in ref. 3.
10. W. Kohler, D. R. Robello, P. T. Dao, C. S. Willand, D. J. Williams, *J. Chem. Phys.*, **93**, 9157 (1990).
11. W. Tam, L.-T. Cheng, J. D. Bierlein, L. K. Cheng, Y. Wang, A. E. Feiring, G. R. Meredith, D. F. Eaton, J. C. Calabrese, G. L. J. A. Rikken, Chapter 9, pp. 158-169 in ref. 3.
12. B. L. Davydov, et. al., *Opt. & Spec.*, **30**, 274 (1971).
13. L. G. Koreneva, "Molecular Crystals in Nonlinear Optics", (Nauka, Moscow, 1975).
14. B. L. Davydov, et. al., *Sov. J. Quant. Electron.*, **7**, 129 (1977).
15. R. Twieg, UCRL15706, DE86002596 (1985); CA106(8):57923q
16. J. A. Dean, "Handbook of Organic Chemistry", Table 7-1 (McGraw-Hill, New York, 1987).
17. A. E. Feiring, *J. Fluorine Chem.*, **24**, 191 (1984)
18. L.-T. Cheng, W. Tam, G. R. Meredith, G. L. J. A. Rikken, E. W. Meijer, *Proc. SPIE*, **1147**, 61 (1990)



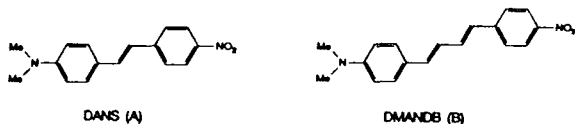
NOVEL SIDECCHAIN POLYMERS FOR ELECTRO-OPTIC APPLICATIONS

Diane E. Allen, Richard A. Keosian, Garo Khanarian,
Jane E. Hudop, Stephen J. Meyer.
Hoechst-Celanese Corporation
86 Morris Ave
Summit, NJ 07901.

A tremendous amount of interest surrounds the use of organic and polymeric materials for advanced electro-optic device and systems applications. The appeal of organic compounds lies in the flexibility in which one can tailor the molecular and macroscopic properties to achieve high activity, desirable mechanical characteristics, and processibility.

Numerous studies on the factors affecting the second order response have documented that the nature of the electron donor and acceptor substituents, the conjugation length, and the type of conduit all contribute to the nonlinear optic activity.¹ In general activity increases with the strength of the donor/acceptor groups and with increasing conjugation length. To realize bulk second order activity the molecular dipoles must be aligned non-centrosymmetrically. Since NLO active small molecules tend to crystallize with their dipoles paired, resulting in the loss of second order properties, it is desirable to incorporate the active units into a polymer and orient the dipoles via an external field.

In a logical extension of our work with the stilbene sidechain polymers,² our attention turned to increasing the length of the conduit between the donor and acceptor groups since it is known that increasing the conjugation length increases the second order hyperpolarizability. In a direct analogy to DANS (A), 1-[4-dimethylaminophenyl]-4-[4'-nitrophenyl]-1,3-butadiene (DMANPB) (B) was synthesized as model compound in order to demonstrate the concept and to provide a straightforward comparison with the stilbene. Solvatochromism measurements for DMANPB gave a β value of 121×10^{-30} esu, which represents approximately a 70% increase in activity over DANS as a result of increased conjugation length.³ EFISH measurements of DMANPB vs. DANS appear to be solvent dependent. In nitromethane DMANPB shows a slight increase in activity relative to DANS with a value for $\mu \times \beta = 500 \times 10^{-48}$ esu vs. 470×10^{-48} esu for DANS. However, in cyclohexanone $\mu \times \beta = 327 \times 10^{-48}$ esu for DMANPB and 436×10^{-48} esu for DANS.⁴ The lower activity of DMANPB compared to DANS is at odds with solvatochromism data but is not inconsistent with the EFISH observations of other researchers.^{1b,c}



The diphenylbutadiene moiety was incorporated into a polymethacrylate system via the multistep sequence in Figure 1 in order to evaluate the material's poling characteristics and device-worthiness. Equimolar amounts of the monomer C, 1-[4-(N-2-methacryloxyethyl-N-methylamino)phenyl]-4-[4'-nitrophenyl]-1,3-butadiene, and methyl methacrylate were copolymerized under radical polymerization conditions to provide copolymer 1 of low molecular weight ($M_w=25,000$) and a $T_g = 123^\circ\text{C}$. A thin film of the material spun out of cyclohexanone was electroded and poled at low fields near T_g and exhibited an electro-optic coefficient, r , 25% greater than that for copolymer 2 (Figure 2). The magnitude of the increase in activity is in close agreement with guest-host measurements of r for the monomer C and the stilbene monomer D as shown in Table 1.⁵

Experimental Procedure

Instrumentation: NMR spectra were obtained on either a Varian XL200 or a Bruker MSL300 spectrometer, and chemical shifts were reported in ppm downfield relative to TMS. All NMR samples were solutioned in CDCl₃ unless noted otherwise. Polymer molecular weights were determined on a Waters 201

GPC equipped with a Waters 410 RI and a Viscotek Model 100 differential viscosity detector, and the mobile phase was THF. Molecular weights were calculated from a Universal calibration curve. T_g was determined on a DuPont 9900-910 Thermal Analyzer. Melting points were obtained on a Thomas Hoover Capillary Melting Point Apparatus and are uncorrected. Elemental analyses were performed by Robertson Laboratory, Madison, NJ.

Materials: NMP was distilled from CaH₂ prior to use. Methyl methacrylate was passed through a styrene/DVB ion exchange resin to remove inhibitor prior to use. All other reagents were used without further purification. All reactions were run under an inert atmosphere in oven-dried glassware.

Synthesis of 1-[4-dimethylaminophenyl]-4-[4'-nitrophenyl]-1,3-butadiene

To a stirred solution of 1.0 g (5.7 mmol) of 4-dimethylaminocinnamaldehyde, 0.52 mL (5.7 mmol) of aniline, and 10 mg of toluenesulfonic acid monohydrate in 40 mL of toluene was heated at reflux for 16 hours with the azeotropic removal of water. After cooling the reaction to room temperature, the solvent was removed in vacuo. The residue was dissolved in 35 mL of glacial acetic acid, and 1.03 g (5.7 mmol) of 4-nitrophenylacetic acid was added to the solution with stirring. The reaction was then stirred at room temperature for 16 hours and at 50°C for 96 hours. After cooling to room temperature the solution was poured into water, and the solid product was collected by filtration, washed with water and ether, and vacuum dried. The reaction yielded 0.93 g (55%) of product as copper crystals. mp = $246-247^\circ\text{C}$. ¹H NMR 2.98 (s, 6H), 6.56 (d, 1H), 6.67 (d, 2H), 6.75 (d, 1H), 7.08 (dd, 2H), 7.32 (d, 2H), 7.48 (d, 2H), 8.14 (d, 2H).

Synthesis of copolymer 1:

1-[4-(N-2-hydroxyethyl-N-methylamino)phenyl]-4-[4'-nitrophenyl]-1,3-butadiene

A stirred solution of 20 g (96 mmol) of 4-[N-2-hydroxyethyl-N-methylamino]cinnamaldehyde, 8.8 mL (96 mmol) of aniline, and 0.2 g of toluenesulfonic acid monohydrate in 600 mL of toluene was heated at reflux with the azeotropic removal of water for 16 hours. After cooling to room temperature, the imine product was collected by filtration and washed with additional portions of toluene.

The crystalline imine was then dissolved in 590 mL of glacial acetic acid, and 17.6 g (96 mmol) of 4-nitrophenylacetic acid was added to solution with stirring. The reaction was stirred at room temperature for 2 days and at 50°C for 5 days. After cooling to room temperature the solution was poured into 2500 mL of water, and the solid product was collected by filtration. Recrystallization from methanol gave 12.61 g of a mixture of diphenylbutadiene alcohol and diphenylbutadiene acetate.

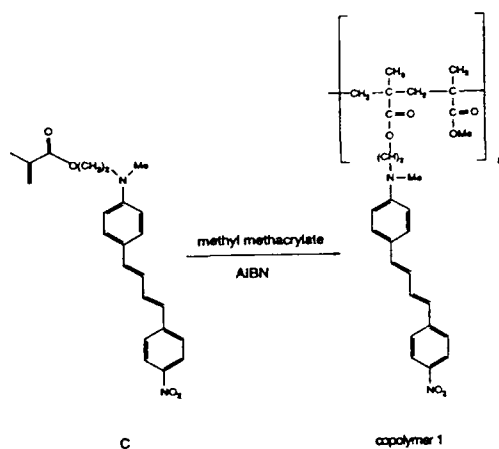
The above acetate/alcohol mixture was dissolved in 260 mL of THF. To the stirring solution were added 260 mL of water, 260 mL of methanol, and 9.8 g of potassium carbonate, and the reaction was stirred at room temperature overnight. As the reaction progressed the product precipitated from the solution. Upon completion of the reaction the product was collected by vacuum filtration, and recrystallized from methanol to give 9.12 g of a brown solid. ¹H NMR 3.05 (s, 3H), 3.55 (t, 2H), 3.85 (t, 2H), 6.60 (d, 1H), 6.70 (d, 2H), 6.75 (d, 1H), 7.10 (dd, 2H), 7.35 (d, 2H), 7.50 (d, 2H), 8.16 (d, 2H). Calculated for C₁₉H₂₀N₂O₃: C, 70.3; H, 6.2; N, 8.6; O, 14.8. Found: C, 69.11; H, 6.26; N, 8.31; O, 14.73.

1-[4-(N-2-methacryloxyethyl-N-methylamino)phenyl]-4-[4'-nitrophenyl]-1,3-butadiene (structure C, figure 1)

To a stirred solution of 8.77 g (27.0 mmol) of 1-[4-(N-2-hydroxyethyl-N-methylamino)phenyl]-4-[4'-nitrophenyl]-1,3-butadiene in 266 mL of pyridine were added 8.04 mL (54.0 mmol) of methacrylic anhydride and 180 mg of DMAP. After 16 hours at room temperature, the reaction mixture was poured into 1 L of water, and the solid monomer was collected by filtration. The product was then stirred in 600 mL of water for 2 hours, and the product was again isolated by vacuum filtration. Recrystallization from ethyl acetate gave 7.79 g of the monomer as a red solid. mp = $146-150^\circ\text{C}$. ¹H NMR 1.92 (s, 3H), 3.05 (s, 3H), 3.69 (t, 2H), 4.34 (t, 2H), 5.56 (d, 1H), 6.17 (d, 1H), 6.59 (d, 1H), 6.72 (d, 2H), 6.82 (d, 1H), 7.10 (dd, 2H), 7.36 (d, 2H), 7.5 (d, 2H), 8.16 (d, 2H).

Copolymer 1

A solution of 6 g of the comonomer C in 72 mL of dry, distilled NMP was degassed with argon for 45 minutes at room temperature. This was followed by the addition of 1.62 mL of methyl methacrylate and argon degassing for 30 minutes. Finally 0.05 g of AIBN as an initiator was added, the solution was degassed with argon for 5 minutes more, and the reaction vessel was placed in an oil bath heated at 68°C. After 2 days at 68°C, some monomer remained, and an additional 0.05 g of AIBN was added. The polymerization proceeded no further so the solution was precipitated into MeOH. The polymer was dissolved in hot THF, and MeOH was added dropwise with stirring until the solution went cloudy. The solids were collected by filtration, and the process was repeated. The material was then dissolved in ethyl acetate, and MeOH was added dropwise until the solution again became cloudy. The polymer was collected by filtration. 1.76 g (This is the result of the combination of material in the precipitation step from two equal size runs.) $T_g = 123^\circ\text{C}$; $M_w = 25,000$ and $M_n = 14,000$. Calculated for $\text{C}_{28}\text{H}_{32}\text{N}_2\text{O}_6$: C, 68.28; H, 6.55; N, 5.69; O, 19.49. Found: C, 68.20; H, 6.52; N, 5.87; O, 19.39.



Acknowledgments: We wish to thank Jim Sounik and Jackie Popolo for the polymer thin films used in the poling studies and the analytical department for the characterization of the materials. We also want to thank P. Kalyanaraman for supplying us with the starting aldehyde.

References

- Some examples: (a) Leslie, T. M.; DeMartino, R. N.; Choe, E. W.; Khanarian, G.; Haas, D.; Nelson, G.; Stamatoff, J. B.; Stuetz, D. E.; Teng, C. C.; Yoon, H. N. *Mol. Cryst. Liq. Cryst.* 1987, 153, 451. (b) Singer, K. D., et al. *J. Opt. Soc. Am.* 1989, 6, 1339. (c) Sohn, J. E., et al. in *Nonlinear Optical Effects in Organic Polymers*; Messier, J. et al., Eds.; Kluwer Academic Publishers, 1989; 291-297. For general reference see *Nonlinear Optical Properties of Organic and Polymeric Materials*; Williams, D. J., Ed.; ACS Symposium Series 233, 1983. and *Nonlinear Optical Properties of Organic Molecules and Crystals Vols. 1 and 2*; Chemla, D. S. and Zyss, J., Eds.; Academic Press, Inc., 1986.
- DeMartino, R. N. and Yoon, H. N., U. S. Pat. 4865430 (1989). DeMartino, R. N. and Yoon, H. N., U. S. Pat. 4808332 (1989).
- Buckley, A., et al. *Polymeric Materials Science & Engineering Proceedings of the ACS Division of Polymeric Materials: Science & Engineering* 1986, 54, 502.
- Measurements are made at 1.34 microns, and the values are corrected for resonance enhancement.
- Guest-Host samples were prepared as a solution of 12% dye in polymethylmethacrylate and spun into thin films.

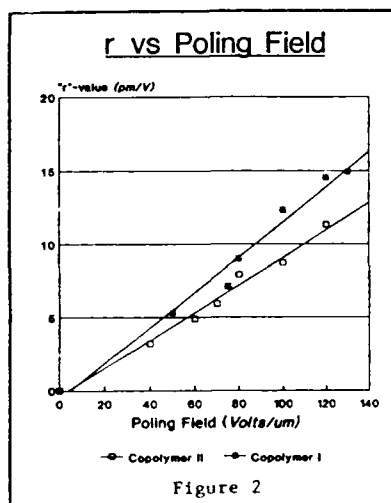
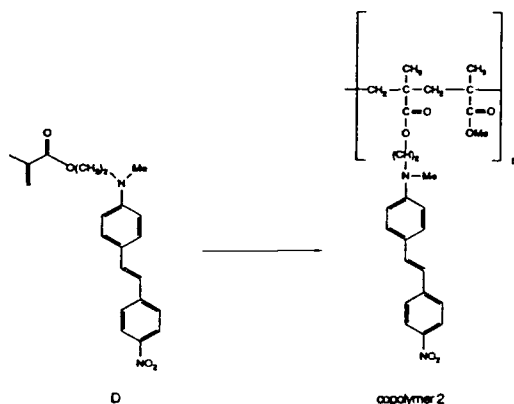


Figure 2

Table 1

compound	field (V/micron)	r (pm/V)
C	50	1.4
	70	1.8
	90	2.2
D	50	1.0
	70	1.37
	90	1.66

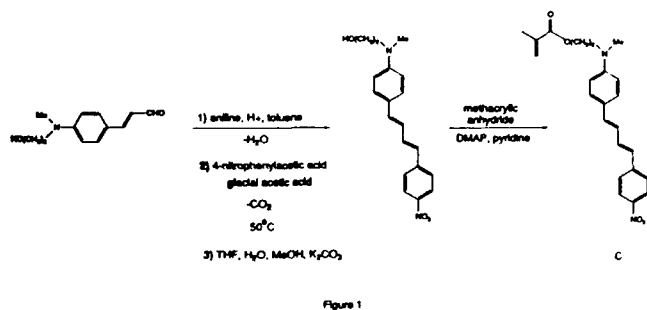


Figure 1

SYNTHESIS OF CONTROLLED STRUCTURE POLYOLEFINS

ROBERT H. GRUBBS

*Division of Chemistry and Chemical Engineering
California Institute of Technology
Pasadena, California 91125 USA*

ABSTRACT: As a result of the developments in organometallic chemistry, new catalysts are available for the synthesis of polymers with high levels of control of structure. Outstanding success has been achieved in the area of Ziegler catalysis for polyolefin synthesis. Parallel developments have been made in ring opening metathesis polymerization (ROMP).¹ Some developments in this area will be reviewed.

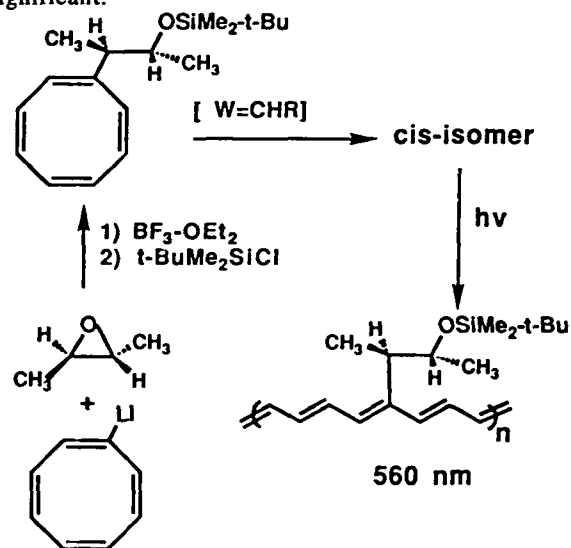
SYNTHESIS OF POLYACETYLENE

Over the past few years we have demonstrated that cyclooctatetraene (COT) can be polymerized using ROMP² (ring opening metathesis polymerization) catalysts to form excellent quality polyacetylene. These techniques have been used to prepare polyacetylene based devices.^{3,4} A major emphasis has been placed on the synthesis of substituted polyacetylenes that have controllable properties. The factors that control solubility, conductivity and optical properties in these systems have been examined and modeled. To date, the major substituent effects that have been probed are associated with the steric effects of the substituents on the polymer chain conformation.⁵ Random copolymers were prepared to study the effect of conjugation length on conductivity and block polymers were prepared to examine the effects of phase separation on conductivity and optical properties.

SUBSTITUTED POLYACETYLENES

The polymerization of monosubstituted COT derivatives produces polymers with substituents that are on the average every eight carbons apart on the PA backbone. It has been found that primary alkyl substituents produce cis-PA that is soluble. However photoisomerization to the trans isomer results in

insoluble material. This material displays many of the characteristics of the parent system. Substituents that bear a secondary substituent adjacent to the chain produce polymers that are soluble in both isomeric forms and show moderate conductivities on doping with iodine. Tertiary substituents give highly soluble polymers that show very low conductivities on iodine doping. Modeling studies show that solubility and conductivity are both related to the degree of twisting induced by the substituent.⁵ The greater the twist angle, the higher the solubility in the trans form and the lower the conductivity on doping. The full range of substituents that should result in changes due to steric effects has been explored. Of major interest are chiral substituents. Chiral substituents could increase solubility by producing stereo random polymers or, if the substituents are enantiomerically pure, the substituents could induce a helical twist to the conjugated backbone. This effect has been examined using the following set of substituents. The amount of helical chromophore formation appears to be significant.⁶



The photoisomerization of the high cis polymers is of considerable theoretical as well as practical interest. The cis polymer isomerizes to the trans with an isobestic point. This shows that the polymer isomerizes without the formation of stable intermediates and is consistent with the excited state of the cis polymer relaxing to an isomerized segment of polymer that is the ultimate conjugation length.

Only preliminary results have been obtained with substituents that should result in large polar effects on

the polyCOT properties. It has been found that alkoxy derivatives of COT are straightforward to prepare and can be polymerized to high molecular weight materials. The conductivities of these materials are low.

An electrochemical application in which soluble poly-COT materials may be used to great advantage is the fabrication of semiconductor based devices. The ease with which semiconductor surfaces can be coated with soluble polyacetylene contrasts the more technically challenging methods of film preparation used presently. We have already reported on the fabrication of solar cells from the solvent deposition of poly-trimethylsilyl-COT onto silicon surfaces. After doping of the thin polymer layer to the metallic regime, a solar cell results, whose performance rivals that of conventional semiconductor/metal solar cell devices.⁴ These devices hold great promise, and continue to be studied. The advantage of poly-COT materials may be further demonstrated in cases where polar substituents significantly alter the work function of the doped polymer, thus effecting the solar cell performance. In this way, it may be possible to optimize cell performance by tuning the organic metal. This is not possible for traditional semiconductor/metal systems.

It was earlier demonstrated that the copolymerization of cyclooctadiene and COT resulted in a polymer whose composition was near that of the feed ratio. Independent measurements of reactivity ratios suggested that the polymerization was nearly random. Since the introduction of a cyclooctadiene into the chain introduces an sp^3 defect, the probability of forming a given conjugation length with a specific feed ratio can be calculated. Preliminary measurements were made of the conductivity and doping levels as a function of the copolymer feed.⁷

As has been shown in the styrene-butadiene triblock polymers, the periodicity of the morphological features is controlled by the regularity of the polymer structure. For the synthesis of new materials with interesting macrostructures new techniques are required that will allow the synthesis of triblock polymers with nearly monodispersed blocks of controlled length. One such system has been studied. The synthesis of this material is based on a difunctional initiator. The difunctional initiator insures that the block segments are uniform.⁸

References

- (1) R.H. Grubbs and W. Tumas, *Science* **1989**, *243*, 907-915.
- (2) F.L. Klavetter and R.H. Grubbs, *J. Am. Chem. Soc.* **1988**, *110*, 7809-7813.
- (3) D.V. McGrath, B.M. Novak, and R.H. Grubbs, in *Olefin Metathesis and Polymerization Catalysts*, Y. Imamoglu, Ed., Kluwer Academic Publishers: the Netherlands, 525-536 (1990).
- (4) R.H. Grubbs, C.B. Gorman, E.J. Ginsburg, J.W. Perry, S.R. Marder, in *Materials for Nonlinear Optics*, S.R. Marder, J.E. Sohn, G.D. Stucky, Eds, American Chemical Society: Washington D.C., pp. 672-682 (1991).
- (5) C.B. Gorman, E.J. Ginsburg, S.R. Marder, R.H. Grubbs, *Angew. Chemie* **1989**, *101*, 1603-1606.
- (6) J.S. Moore, C.B. Gorman, R.H. Grubbs, *J. Am. Chem. Soc.* **1991**, *113*, 1704-1712.
- (7) S.R. Marder, J.W. Perry, F.L. Klavetter, R.H. Grubbs, *Chemistry of Materials* **1989**, *2*, 171-173.
- (8) F. Stelzer, O. Leitner, K. Pressl, G. Leising, R.H. Grubbs, *Synthetic Metals* **1991**, in press.

**CHROMOPHORIC SELF-ASSEMBLED SUPERLATTICES.
MULTILAYER CONSTRUCTION OF THIN FILM
NONLINEAR OPTICAL MATERIALS**

by
D. S. Allan, F. Kubota, Y. Orihashi, D. Li, and T. J. Marks
Department of Chemistry and the Materials Research Center
Northwestern University, Evanston, IL 60208

T. G. Zhang, W. P. Lin, and G. K. Wong
Department of Physics and the Materials Research Center
Northwestern University, Evanston, IL 60208

INTRODUCTION

Key requirements in the design of efficient macromolecular second-order nonlinear optical (NLO) materials include maximizing the number density of constituent high- β molecular chromophores as well as achieving and preserving maximum acentricity of the microstructure. We recently reported a new approach to such materials which utilizes the sequential construction of covalently self-assembled, NLO chromophore-containing multilayer structures (Figure 1).^{1,2} The result is a robust new family of thin film NLO materials with bulk $\chi_{zzz}^{(2)}$ values near 2×10^{-7} esu at $\lambda = 1064$ nm. These materials represent a complement to, and possible improvement upon, NLO materials composed of either poled, cross-linked chromophore-functionalized polymers,^{3,4} or acentric Langmuir-Blodgett films.^{5,6} In this contribution, we

of the resulting films are indistinguishable). Multilayer assembly was carried out under inert atmosphere in an apparatus⁸ that allows the simultaneous preparation of 6-10 specimens. Progress of the surface reactions was monitored by advancing contact angle measurements using DI water as the probe liquid. Ion exchange experiments on assembled films were carried out in 0.1 M acetonitrile solutions using gentle sonication. Second harmonic generation (SHG) measurements were carried out at $\lambda = 1064$ nm^{3,4} with automated, computer-interfaced instrumentation for angle-dependent data acquisition and analysis.⁸ Single-sided samples for angle-dependent transmission SHG measurements were prepared by diamond polishing to remove films from the back of double-sided, as-prepared samples. The SHG reaction cell and instrumentation for the *in situ* observation of the NLO film assembly process will be described elsewhere.⁹ All other physical measurements (advancing contact angle, optical spectroscopy, X-ray photoelectron spectroscopy, FTIR-attenuated total reflectance spectroscopy) employed apparatus described previously.^{1,2}

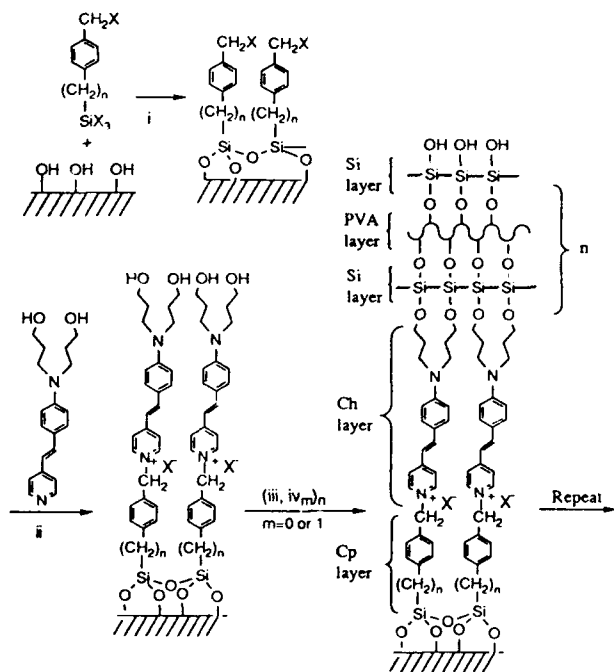
RESULTS AND DISCUSSION

The present chemical strategy for the construction of self-assembled chromophoric multilayer NLO materials is shown in Figure 1.^{1,2} Important aspects of this approach include the use of a stilbazole chromophore precursor, which becomes a high- β chromophore upon quaternization, and transverse structurally stabilizing/planarizing layers introduced using silicone self-assembly technology originally developed by Sagiv.^{10,11} Our initial synthetic approach employed $X = I$ in step i, and $m=1, n=1$ or 2 in steps iii and iv.^{1,2} We now focus upon the degree to which the parameters in Figure 1 can be modified and the properties of the resulting films. Key issues discussed here are the substrate generality, the efficiency with which multilayer structures can be built up, and the susceptibility of the X^- ion to controlled exchange.

In our initial work, we reported that multilayer construction could be carried out on clean glass surfaces to yield chromophoric assemblies with high structural uniformity as judged by SHG interference patterns from double-sided samples and the quadratic dependence of $I^{2\omega}$ on the number of chromophore layers.^{1,2} Angle-dependent SHG data could be fit¹² to a structural model in which the average deviation of the chromophore dipoles from the substrate surface normal (Ψ) is in the range 35-39°. We now find that multilayer construction can also be carried out on the oxidized (110) surface of single crystal silicon. As assessed by reflectance SHG measurements, the NLO characteristics of such films are very similar to those deposited on glass, and we find that $\Psi = 44^\circ$. In preliminary experiments, we also find that chromophoric layers can be formed on the oxidized surface of single crystal germanium (for FTIR-ATR studies) as well as on ITO-coated glass surfaces.

In regard to maximizing the chemical efficiency of the construction process, which is essential for building up micron-scale films, we find that step i (Figure 1) can be readily carried out with the commercially available $X = Cl$ silyl reagent. As judged by advancing contact angle measurements, step i is complete on glass after 2-3 minutes reaction time followed by curing in air at 115°C. By XPS, we find that the benzylic chloride produced in step i ($X = Cl$) can be readily converted to the more reactive benzylic iodide by exchange with KI in CH_3CN . However, we also find that the $X = Cl$ derivative is sufficiently reactive to readily effect quaternization step ii. Defining the exact rate of this chromophore-forming step is crucial to optimizing the assembly process, and we have therefore developed *in situ* SHG measurement methods to monitor the quaternization.⁹ As illustrated by Figure 2, the rate of chromophore layer evolution is satisfactory for efficient multilayer synthesis at 60°C, but impractically slow at 20°C. *In situ* SHG techniques should be invaluable in monitoring many other temporal and structural aspects of the self-assembly process.

Steps iii and iv in Figure 1 effect a transverse "capping off" of the chromophore layer so that the i,ii reaction sequence can be repeated. Earlier work showed that the iii,v sequence involving both a chlorosilane reagent and polyvinylalcohol is also essential for chromophore alignment and the ultimate temporal stability thereof.^{1,2} We now find that step iv can be eliminated if the product of chlorosilane step iii is cured in air at 115°C for short periods of time (~15 min). Advancing water contact angles indicate that the curing affords a more hydrophilic surface. As judged by relative film SHG intensity (an increase of 18(6)% and derived Ψ values (40.6(42)° vs. 43.8(55)°) eight-layer films prepared with the aforementioned cure but without polyvinylalcohol layers have comparable or superior chromophore alignment and have a significantly higher chromophore number density. Importantly, the temporal stability of chromophore alignment is unchanged.



- i. Benzene, 25°C followed by cure at 115°C
- ii. Reflux in n-PrOH
- iii. $Cl_3SiOSiCl_2OSiCl_3$ in THF followed by cure at 115°C
- iv. Polyvinylalcohol in DMSO

Figure 1. Scheme for the construction of chromophoric self-assembled multilayer NLO materials.

provide an account of our continuing efforts to elaborate/streamline the multilayer construction methodology and to assess/understand the effects thereof on film microstructure and NLO characteristics.

EXPERIMENTAL

The sources and purification of all reagents were as described previously.^{1,2} Substrate surfaces were cleaned as reported before,¹ but with $H_2O_2 + H_2SO_4$ substituted for an O_2 plasma where appropriate (properties

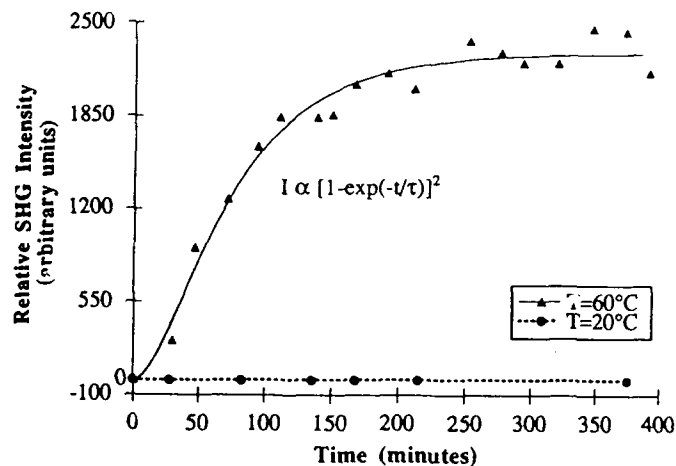


Figure 2. Time dependence of chromophore introduction (step ii in Figure 1) at two different temperatures as monitored by in situ SHG techniques.

Finally, the salt-like nature of the chromophore layers in these materials raises the intriguing question of whether ion exchange processes can be effected and, if so, how the properties of film microstructure respond. For single chromophore layer films, we find that Cl^- or I^- can be readily exchanged by solution dipping for a variety of anions of differing size, shape, and polarizability.⁹ As illustrated in Figure 3, XPS can be employed to monitor the exchange of I^- for *p*-toluenesulfonate. Here, diminution of the $\text{I}(3d_{5/2}, 3d_{3/2})$ signals is accompanied by growth of the $\text{S}(2p)$ signal. The SHG characteristics of these ion exchanged materials are presently under examination.

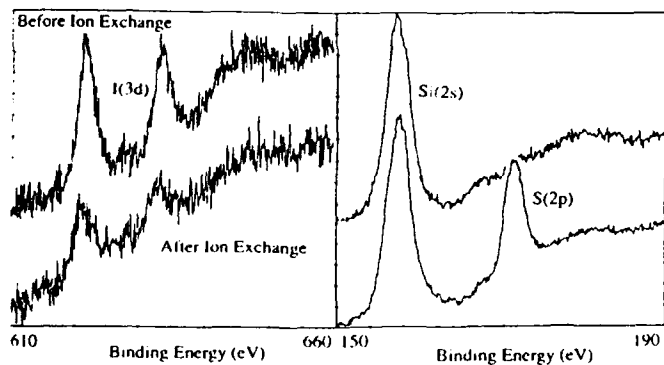


Figure 3. Ion exchange of $\text{X}^- = \text{I}^-$ for $\text{X}^- = p$ -toluenesulfonate in a single chromophore layer material as assessed by X-ray photoelectron spectroscopy. Intensities are ratioed to the $\text{Si}(2s)$ feature.

REFERENCES

1. Li, D.; Ratner, M. A.; Marks, T. J.; Zhang, C.; Yang, J.; Wong, G. I. *J. Am. Chem. Soc.*, **1990**, *112*, 7389-7390.
2. Li, D.; Marks, T. J.; Zhang, C.; Yang, J.; Wong, G. K. *SPIE Proc.*, **1990**, *1337*, 341-347.
3. Dai, D.-R.; Hubbard, M. A.; Li, D.; Park, J.; Ratner, M. A.; Marks, T. J.; Yang, J.; Wong, G. K. *ACS Sympos. Series*, **1991**, *455*.
4. Dai, D.-R.; Hubbard, M. A.; Park, J.; Marks, T. J.; Wang, J.; Wong, G. K. *Mol. Cryst. Liq. Cryst.*, **1990**, *189*, 93-106.
5. Bosshard, C.; Küpfer, M.; Günter, P.; Pasquier, C.; Zahir, S.; Seifert, M. *Appl. Phys. Lett.* **1990**, *56*, 1204-1206.
6. Popovitz-Biro, R.; Hill, K.; Landau, E. M.; Lahav, M.; Leiserowitz, L.; Sagio, J.; Hsiung, H.; Meredith, G. R.; Vanherzeele, H. *J. Am. Chem. Soc.* **1988**, *110*, 2672-2674.
7. Wasserman, S. R.; Whitesides, G. M.; Tidswell, I. M.; Ocko, B. M.; Pershan, P. S.; Axe, J. D. *J. Am. Chem. Soc.*, **1989**, *111*, 5852-5861.
8. Allan, D. S.; Wong, G. K.; Marks, T. J., unpublished results.
9. Allan, D. S.; Zhang, C.; Wong, G. K.; Marks, T. J., manuscript in preparation.
10. Ulman, A. *Adv. Mater.*, **1990**, *2*, 573-582, and references therein.
11. Pomerantz, M.; Segmüller, A.; Netzer, L.; Sagiv, J. *Thin Solid Films*, **1985**, *132*, 153-162.
12. Zhang, T. G.; Zhang, C. H.; Wong, G. K. *J. Opt. Soc. Am. B*, **1990**, *7*, 902-907.

CONCLUSIONS

These results demonstrate that the scope of thin film NLO materials that can be synthesized via the scheme in Figure 1 is very broad in terms of substrate identity, layer formation methodology, and charge-compensating counterions. Our results also demonstrate that considerable improvements in the efficiency of the multilayer assembly process are achievable without degradation of the NLO characteristics.

ACKNOWLEDGMENTS

This research was supported by the NSF-MRL program through the Materials Research Center of Northwestern University (Grant DMR8821571) and by the Air Force Office of Scientific Research (Contract AFOSR-86-0105). We thank Dr. E. P. Plueddemann for helpful suggestions.

A NEW MOLECULAR DESIGN FOR THE POLED POLYMERS
-UTILIZING THE OFF-DIAGONAL COMPONENT OF THE MOLECULES-

T. Watanabe, M. Kagami, H. Yamamoto, A. Kidoguchi, A. Hayashi, H. Sato and S. Miyata
Department of Material Systems Engineering
Tokyo University of Agriculture and Technology,
Japan

1. INTRODUCTION

Recently, there is a rapidly growth of interest in guest-host polymer materials due to their large nonlinear optical effects and as a means of the introduction of the noncentrosymmetric structures¹⁾. However, these systems show a decay of SHG activities²⁾. In order to overcome this problem, we propose a new molecular design for the poled polymers whose nonlinear susceptibilities of the poled molecules possessing large off-diagonal components such as β_{xyy} decay only a few, even if the order parameter of the dipole is relaxed from 0.26 to 0.15. In this presentation, the nonlinear susceptibilities of molecules, possessing off-diagonal components will be discussed according to the theoretical calculation as well as some preliminary experimental results.

2. THEORY

The nonlinear polarization at frequency 2ω induced in the bulk media can be expressed by Eq. (1).

$$P_{\alpha}^{2\omega} = \epsilon_0(1/2) \chi_{\alpha IJK}^{(2)}(-2\omega; \omega, \omega) E_{\alpha}^{\omega} E_{\beta}^{\omega} \quad (1)$$

where $\chi^{(2)}(-2\omega; \omega, \omega) = 2d(-2\omega; \omega, \omega)$

The relationship between the macroscopic molecular hyperpolarizability $\langle \beta_{\alpha IJK} \rangle$ which is related to the averaging of the molecular hyperpolarizability and nonlinear optical coefficient can be expressed by the following equation³⁾

$$d_{\alpha IJK}^{2\omega} = N f_{\alpha}^{\omega} f_{\beta}^{\omega} \langle \beta_{\alpha IJK} \rangle \quad (2)$$

where N is the number density of the dopant molecules. The f terms are the local field factors. $\langle \beta_{\alpha IJK} \rangle$ cooperated to the electrically poling, can be calculated from the integral of the molecular tensor properties ($\beta_{\alpha IJK}$) over all the possible orientations weighted by the distribution function which is given as follows⁴⁾.

$$\langle \beta_{\alpha IJK} \rangle = \int d\phi \int \sin \theta d\theta \int d\psi b_{\alpha IJK} G(\theta) \quad (3)$$

where rotation matrices $a_{\alpha IJK}$ between the molecular frame and the laboratory frame is given by the Euler angles (ϕ , θ and ψ), and $b_{\alpha IJK}$ is the inverse matrices of $a_{\alpha IJK}$. $G(\theta)$ is the distribution function. In the case of two-directional charge-transfer molecules, large β_{xyy} still remain as well as β_{xxx} .

Finally, the macroscopic hyperpolarizability can be derived by the following equation.

$$\beta_{\alpha\alpha\alpha} = L_3(p) * \beta_{xxx} + 1.5 \{ L_1(p) - L_3(p) \} \beta_{xyy} \quad (4)$$

where $L_1(p)$ and $L_3(p)$ present first and third order Langevin functions respectively.

3. EXPERIMENT

The molecular hyperpolarizabilities were calculated according to the finite field method, which gives a off-resonant β value at frequency 0. A model compound, N,N'-bis-(p-nitrophenyl)-methanediamine(abbreviated as p-NMDA), of a two-directional charge transfer molecule, possessing a β_{xyy} component, was synthesized by reacting p-nitroaniline(p-NA) with formaldehyde in methylalcohol. The obtained material was characterized by nuclear magnetic resonance(NMR), infrared absorption spectroscopy(IR), and differential scanning calorimetry(DSC).

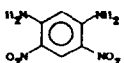
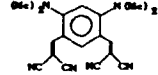
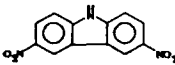
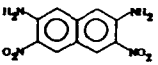
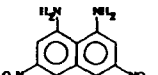
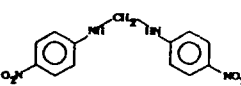
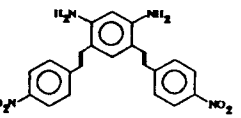
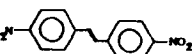
Both p-NMDA and PMMA were desolved in N,N-dimethylformamide(DMF) and the nonlinear optical films were prepared by spin-coating from the mixed solutions.

The electric field is applied above 90 °C by corona poling method. The refractive index of the host-guest films was measured by m-line method at 532nm and 1064nm. The nonlinear optical coefficient of the poled polymer including p-NMDA, $d_{\alpha\alpha\alpha}$ and $d_{\alpha\alpha 1}$, was measured according to the Maker fringe method.

4. RESULTS AND DISCUSSION

Table 1 shows the calculated molecular hyperpolarizabilities of different kinds of molecules possessing two pairs of donor and acceptor. In these calculations, x axis of molecule is directed along a dipole moment and y is perpendicular to the dipole moment, within the molecular plane. Two-directional charge transfer molecules possess a large off-diagonal tensor components such as β_{xyy} instead of β_{xxx} or β_{yyy} . Especially for 1,3-diamino-4,6-bis-(2-4'-nitrophenyl)-benzene(abbreviated as DABNP), the β_{xyy} value is larger than the β_{xxx} value of 4-amino-4'-nitrostilbene(abbreviated as ANST). The β_x value of ANST obtained from the electric field induced second harmonic generation (EFISH) is larger than that of calculated value because of the resonance effect. The dipole moment of DABNP is higher than that of ANST which is preferable to the electrical poling, since the nonlinear coefficient is proportional to the absolute value of dipole moment at weak electrical field. Figure 2 shows the macroscopic hyperpolarizabilities of DABNP and ANST that were theoretically calculated according to Eq. (4) as a function of poling electric field. At weak electric field, the slope of $\beta_{\alpha\alpha\alpha}$ of DABNP is almost proportional to the poling field, and the $\beta_{\alpha\alpha\alpha}$ value is larger than that of ANST. However, the DABNP shows a saturation of $\beta_{\alpha\alpha\alpha}$ at 4MV/cm electric field and hereafter almost keeps constant. On the contrary, the $\beta_{\alpha\alpha\alpha}$ of ANST is still increasing above this poling electric field and exceeds the $\beta_{\alpha\alpha\alpha}$ of DABNP at 6MV/cm. Compared with ANST, in the case

Table 1. Calculated molecular hyperpolarizabilities of two-directional charge transfer molecules.

SAMPLE	β Components ($\times 10^{-30}$ esu)	
	x_{xx}	x_{yy}
 (ADA)	-0.28	-7.85
 (DDCV)	-2.85	-20.30
 (DNCBz)	-0.66	7.40
 (OANN)	0.37	11.86
 (MANN)	0.03	11.87
 (p-NMDA)	-0.02	11.35
 (DABNP)	-9.40	-47.36
 (ANST)	-46.27	1.91

since the half-wave voltage also would not be changed.

In order to confirm these theoretical calculations, the macroscopic hyperpolarizabilities of two-directional charge transfer molecules, p-NMDA with PMMA, was measured and compared with the result of one-directional charge transfer molecules such as p-aminobenzoic acid (abbreviated as ABA) in a PMMA matrix. Figure 2. shows the nonlinear optical coefficient of these molecules as a function of the applied electrical field.

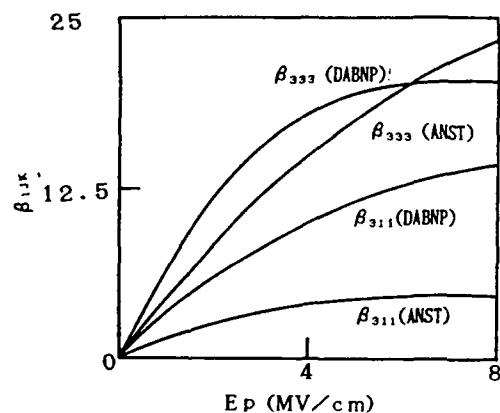


Figure 1. Calculated macroscopic hyperpolarizabilities of DABNP and ANST.

of DABNP, the main contribution to β_{333} is β_{xyy} resulting in a higher difference in the orientation of the molecules as a function of the applied electric field. In the actual poling process, 6MV/cm electric field cannot be applied because of the electrical break down of the host polymer, therefore, DABNP still possess larger nonlinear coefficient than that of ANST. Moreover, DABNP decays a little even if the order parameter of the dipole is relaxed. These results suggest that molecules, possessing large off-diagonal components, are preferable for optical devices.

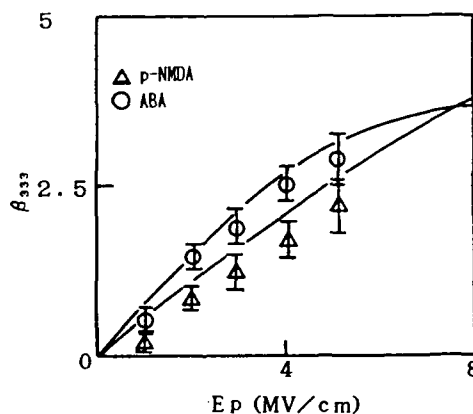


Figure 2. Macroscopic hyperpolarizabilities of p-NMDA and ABA.

The obtained β_{333} almost corresponds to the calculated values as expected. However, the saturation of β_{333} of p-NMDA as a function of applied electric field cannot be observed, since the dipole moment of these molecules is smaller than that of DABNP. The more precisely discussions about this theory will be published in elsewhere by using molecules with much larger dipole moment.

5. CONCLUSION

We found that the molecules possessing large off-diagonal components are preferable for optical devices, since the $\chi^{(2)}$ values of these molecules decay only a few, even if the dipolar orientation is relaxed. Therefore, two-directional charge transfer molecules will be a good candidate for nonlinear poled polymers.

6. ACKNOWLEDGEMENTS

We thank Dr. H. Knobloch for helpful discussions, and Dr. T. Minato for the calculations of the molecular hyperpolarizabilities.

7. REFERENCES

- 1) K. D. Singer, J. E. Sohn and S. J. Lalama, Appl. Phys. Lett., 49, 248 (1986).
- 2) C. Ye, T. J. Marks, J. Yang and G. K. Wong, Macromolecules, 20, 2324 (1987).
- 3) J. L. Oudar and J. Zyss, Phys. Rev. A, 26, 2016 (1982).
- 4) M. G. Kuzyk, K. D. Singer, H. E. Zahn and L. A. King, J. Opt. Soc., Am. B, 6, 742 (1989).

"Novel Polymers with Photorefractive and NLO Properties"

Georges HADZIIOANNOU, Jurjen WILDEMAN,
Jan HERREMA, Pieter SOETEMAN, Diny HISSINK,
Jeannet BROUWER and Rien FLIPSE.

Laboratory of Polymer Chemistry,
Department of Chemistry, University of Groningen,
Nijenborgh 16, 9747 AG Groningen, The Netherlands

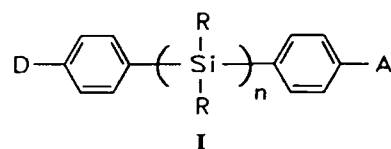
Recent effort on the synthesis of hybrid Organic-Inorganic small molecules and macromolecules towards materials with the desired Optical and Electrical properties will be described. More specifically the design of materials with high microscopic and macroscopic optical nonlinearities with the appropriate transmittance thus leading to various trade-offs between efficiency and transparency (1). The final goal within our research effort is the design of new high performance functional polymer materials for various optical and electronic components for the present macroscopic and the future Molecular Optoelectronic Devices.

In order to accomplish the above goal we employ the following methodology. First we imagine the molecules with the necessary desired functions, then we synthesize them and then we characterize their properties and correlate them to the a priori desired functions. The second step will be to put these functional molecules in the required material form for the device application by incorporating them into a supramolecular structure such as an amorphous polymer matrix or an organized mesomorphic structure which can be achieved by appropriate self-assembling processes (e.g. block copolymers). Then the properties have to be studied again in order to see if the resulting material has the prerequired function also at this level. The third and final step will be the incorporation of the functional material into the device, thus integrating it with the other components and evaluate once more its functions. On this paper we will present the first results of the first step for two kinds of molecules. A) The synthesis and characterization (structural and optical) of small molecules with unusually high second order molecular hyperpolarizability and transparent for the most part in the visible spectrum. B) The synthesis and structural characterization of macromolecules with possible a) high third order molecular hyperpolarizability, b) high conductivity upon doping but sufficiently transparent for its use as material for transparent electrodes and c) the same macromolecules can be imagined to behave photorefractively either by appropriate external doping or internal self doping.

A) The quadratic nonlinear effects are usually obtained with highly polarizable molecules which are doted with electron donor and electron acceptor groups linked via a π -conjugated molecular system. Typically these molecules are disubstituted stilbenes and push-pull polyenes which exhibit large molecular hyperpolarizabilities but usually are not transparent. For many applications (optical processing, frequency doubling, etc.) new compounds combining high nonlinear optical activities (NLO) with good transparency are needed.

Thus we have chosen to synthesize a new class of highly polarizable molecules where the electron donor and electron acceptor groups are linked via silicon backbone, because of its good transparency and σ - σ' conjugation through the Si-Si bonds.

The general formula of this new class of materials is:



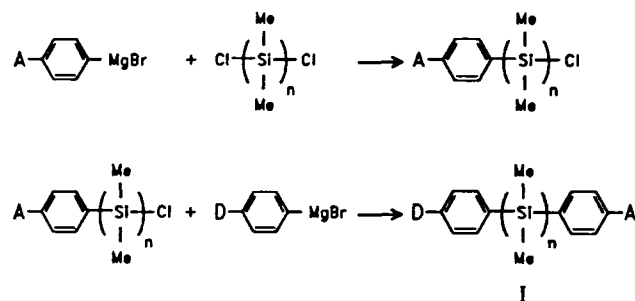
$n = 2, 3, 4$ etc

$\text{R} = \text{Me}, \text{Et}, \text{Pr}$ etc

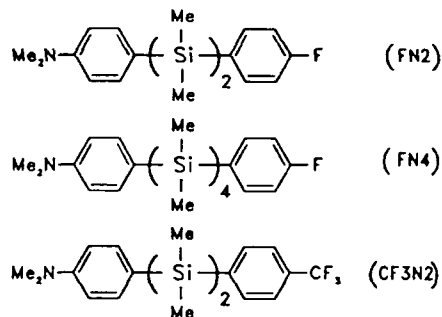
$\text{D} = \text{NMe}_2$

$\text{A} = \text{F}, \text{CF}_3, \text{SO}_2\text{Ph}, \text{CH}=\text{C}(\text{CN})_2$

All synthetic manipulations were performed under a dry argon atmosphere with the standard Schlenk techniques and following the general scheme:



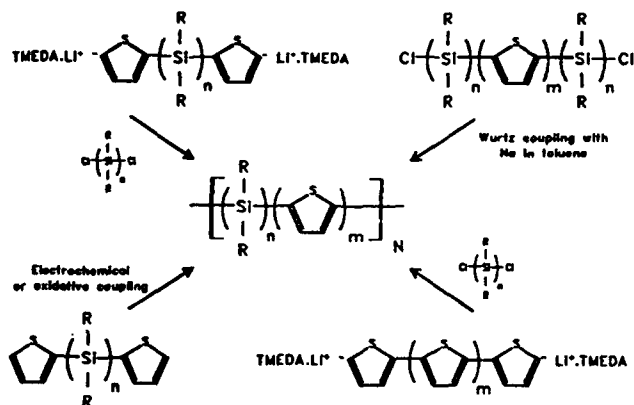
We have prepared successfully so far three compounds:



All of the above materials were characterized with spectroscopic techniques: NMR (^1H , ^{13}C , ^{29}Si , ^{19}F), IR (CCl_4), MS and DSC (melting points, FN2: 58°C; FN4 42°C; CF3N2: 88°C). The results are in agreement with their proposed structure. We have determined also the crystal structure with X-Ray diffraction. Again the results confirm the proposed molecular structure and gave us the supplemental information that in the FN2 crystal the molecules are arranged in the head to head configuration, however in the CF3N2 the molecules are arranged in the head to tail configuration, indicating the higher charge delocalization in the CF3N2 molecules. The electronic properties of these new materials and their relation to their structure were investigated with the use of the absorption (UV) and emission (fluorescence) spectra in different solvents. The UV-spectra of all compounds show an absorption maximum at about 273 nm with small solvatochromic shifts. The maximum can be assigned to a local excitation of the π -electrons of the dimethylaminophenyl ring. In the fluorescence spectra (excited at 263 nm) we observed an emission band at about 350 nm, from a local excited state. The solvatochromatic shifts are small.

Only CF3N2 shows a charge-transfer emission band with a large solvatochromatic shift of 350 nm (cyclohexane) and 520 nm (acetonitrile). Preliminary measurements and calculations of the second order molecular hyperpolarizabilities show promising results comparable to the recently reported values on similar compounds (2). Extensive EFISH measurement and ab-initio calculations are under the way.

B) Relatively high values of third order hyperpolarizabilities are obtained usually with highly conjugated linear macromolecules (3). For the most part all investigated materials having the above properties were homopolymers with entirely π - or σ -conjugation. Recently the synthesis of poly[(silanyl)diethynylene]s polymers which become conducting (4) upon oxidative doping have been reported. For optoelectronic properties it is of interest to see whether these polymers exhibit delocalization of the π -electron density along the main chain through the Si atoms, achieving thus highly conjugated systems with relatively good transparency in the visible. In this context we synthesized alternating copolymers of mono-, di- or tetrasilanyl units as one block and thiophene, 2,2'-bithiophene or 2,2' : 5',5''-terthiophene as the other block. Similar type of polymers and their conducting properties have been reported recently (5). We have used different synthetic routes as is depicted in scheme 1 (6).



Some of the properties and spectral data of the synthesized polymers are listed in the Table below.

Polymer ^a	\bar{M}_n ^b	\bar{M}_w/\bar{M}_n	\bar{N}	mp.(°C)	λ_{max} (nm)
(SiT) _N	4350	1.4	30	120-130	252
(SiSiT) _N	3700	1.6	17	155-165	270
(SiSiSiSiT) _N	4150	1.7	14	110-115	248/274
(SiTTSiT) _N	4200	1.5	16	120-130	250/270
(SiSiTT) _N	4600	1.6	15	190-200	254/327
(SiTTT) _N	2700	1.3	10	200-215	256/372

a: Si = SiMe₂ and T = thienyl

b: relative to polystyrene standards

All polymers showed a red shift of their UV absorption maxima compared to the corresponding monomers (Fig 1 and 2). The extent of this shift seems to be dependant on the degree of polymerization (6).

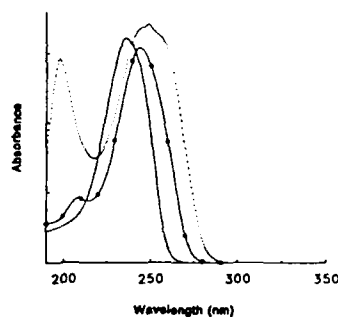


Fig 1. UV spectra of (SiT)_N (—),

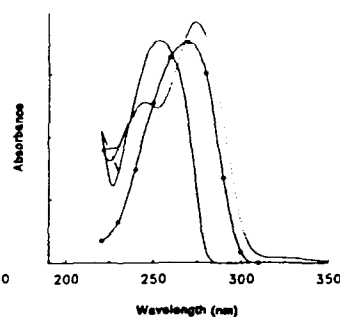


Fig 2. UV spectra of TSiT (—) (Si₂)_N (---) and (Si₄T)_N (.....) TSi₂T (---) and TSi₄T (.....)

All the above suggest that a σ - π coupling and delocalization through the Si-Si bonds is present, the extent of which is dependant on the silanyl unit between the thiophene groups (Fig 1 and 2).

This extent of delocalization is comparable with the results obtained by West (4a) for poly[(disilanyl)ethynylene]s. More detailed studies on the spectral properties of these polymers are currently pursued in order to elucidate the origin of the red shift. Also investigations of the conducting and the NLO-properties of the reported polymer materials are currently in progress.

In summary two new types of material components, with interesting preliminary results on their spectroscopic behaviour, signature of promising opto-electronic properties, have been synthesized. Further investigations are in progress following our initial scheme described in the beginning of this abstract.

Acknowledgement. This work was financially supported by the Dutch Ministry of Economic Affairs, Innovation Oriented Research Program on Polymer Composites and Special Polymers (IOP-PCBP Project BP108).

BIBLIOGRAPHY

- 1) J. Zyss in "Conjugated Polymer Materials: Opportunities in Electronics, Optoelectronics and Molecular Electronics." J.L. Brédas, R.R. Chance, Ed. NATO ASI Series 182, p.545 (Kluwer, Dordrecht 1990)
- 2) G. Mignani et al. *Organometallics*, 9, 2640 (1990)
- 3) D. Neher, A. Kaltbeitzel, A. Wolf, C. Bubeck, G. Wegner in "Conjugated Polymer Materials etc." J.L. Brédas, R.R. Chance Ed. NATO ASI Series 182, (Kluwer, Dordrecht 1990)
- 4) (a) T. Iwakara, S. Hayase and R. West, *Macromolecules*, 23, 1298 (1990) (b) R.J. Corriu, C. Gurein, B. Henner, T. Kuhlmann and A. Jean, *Chem. Mater.*, 2, 351 (1990) (c) I. Ohsihita, D. Kanaya, M. Ishikawa and T. Yamanaka, *J. Organomet. Chem.*, 369, C18 (1989)
- 5) P. Chicart, R. Corriu, I. Moreau, F. Garnier and A. Yassar, *Chem. Mater.*, 3, 8-10 (1991)
- 6) J. Wildeman, J.K. Herrema, G. Hadziioannou, E. Schomaker, *J. Inorg. Organomet. Chem.*, accepted, september issue 1991

THERMALLY STABLE ELECTRO-OPTIC POLYMERS

Susan Ermer,* John T. Kenney, Jeong W. Wu, John F. Valley and Rick Lytel

Lockheed Missiles and Space Co., Inc.
Research and Development Division
Palo Alto, CA 94304

and

Anthony F. Garito

Department of Physics, University of Pennsylvania
Philadelphia, PA 19104-6396

INTRODUCTION

Recently the development of higher speed electronic systems has led to proposals for the application of organic electro-optic polymers in integrated optical devices, which include electro-optic modulators and optical waveguides.¹ In addition to the intrinsic low dielectric constant essential to high speed operation, organic polymers are attractive because their ease of processibility as thin films is compatible with semiconductor device processing techniques. These same techniques are also suitable for the fabrication of single mode electro-optic devices. In device applications, thermal stability is one of several major criteria in selecting appropriate polymers for optical applications because electronic assembly (e.g., solder) temperatures easily exceed 300°C. This thermal requirement is met by a class of polymers known as polyimides, which already receive wide spread use in the microelectronic industry as dielectric insulators for semiconductor chips, die attach adhesives, and interlayer dielectrics for thin film interconnects. In the field of photonics, the application of polyimides as passive optical waveguide materials for optical interconnects has been reported.² The fabrication of micron-size structures in polyimide films suitable for single mode devices has been demonstrated using integrated circuit process technology.³

For active optical waveguide structures, poled electro-optic (EO) polymer thin films have emerged in the photonics field as a promising new class of EO materials.⁴ The net alignment of molecular dipoles induced by the electric field poling of a polymer system doped with nonlinear optical (NLO) guest molecules gives rise to a linear EO effect.⁵ In this way, it is possible to make high speed active EO modulators for electronic systems including, for instance, phase shifters, directional couplers, and intensity modulators (e.g. Mach-Zehnder interferometers).⁶ Such an active EO waveguide is very attractive in a new architecture of high speed inter-chip interconnections because of the high bandwidth operation (low dielectric constant) as well as the relative ease of processibility characteristic of organic polymers. The integration of opto-electronic technology into the current semiconductor electronics, however, has only been demonstrated at a research level and was not feasible in electronic system fabrication. This has been mainly due to the failure of existing EO polymers to meet the thermal stability requirements dictated by standard electronic assembly processes. It is now realized that thermal stability of EO materials, and of the poled EO response in these materials, is a critical issue in meeting the thermal stability requirements of an integrated device as a whole.⁷

We have already reported a new poling process for creating active EO polyimide waveguide structures based on molecular doping of polyimide thin films with NLO guest molecules.⁸ In an initial proof of principle study, the resulting polyimide guest-host film was cured at 250°C to demonstrate a thermally stable EO response at 150°C. We have recently demonstrated an improvement in the thermal stability of the EO response to temperatures of 200°C and 300°C, respectively, for poled polyimide systems cured at 360°C.⁹ These results have been achieved by using a new approach to the design of guest-host EO polymer systems.

GUEST-HOST SYSTEM DESIGN

The preferred approach for EO polymer materials has been the synthesis of side chain polymers based primarily on ester, vinyl, and other linkages used in glassy polymers such as polyacrylates and polystyrenes.¹⁰ The EO moiety, consisting of donor and acceptor groups connected by a conjugated π -electron system,¹¹ has been attached as a side group to the polymer main chain. Initially these moieties, such as dimethylaminonitrostilbene (DANS), Disperse Red 1 (DR1), etc., were mixed into polymethyl methacrylate (PMMA) and other polymers as guests in the polymer host system. These guest-host systems had limited thermal stability and limited miscibility kept the concentration of the active optical moieties below 15%. The side chain polymers increased thermal stability and allowed loadings of up to 60%. Other approaches to increasing thermal stability include crosslinking the active moiety into the polymer system,¹² and constructing covalently self-assembled superlattice structures containing oriented chromophores.¹³

We have taken the approach of regarding the guest as a solute in a polymeric host solvent. By matching solubility parameters for the guest and host we have achieved >50% loadings of the active EO molecule in polyimides. To increase thermal stability of the guest in the host, we consider the way the active EO molecule fits into the free volume of the polymer. By choosing the appropriate molecular Van der Waals (VDW) volume of the guest and polymeric free volume of the host, we have achieved thermal stability of EO response at 300°C for 2 hours and 200°C for over 80 hours in polyimide guest-host systems.

Host Selection

Selection of a host polymer for use in a thermally stable EO guest-host system is governed by several major criteria. First, the polymer chosen must have the inherent thermal stability to withstand electronic processing conditions without structural deterioration. The polymer must also be optically clear at the operating wavelengths of the device, and must be compatible with other materials and processes used in electronic assembly. Finally, the morphology of the polymer must be such that the guest is constrained after orientation is induced by electric field poling. Based on these requirements we have chosen to investigate the polyimides as host polymers.

Polyimides are well-known polymers used in the semiconductor industry as thin film dielectric insulators. They are chemically stable at temperatures as high as 400°C. Polyimides are available which have high optical transparency, a coefficient of thermal expansion comparable to silicon, and refined micro-electronics process compatibilities.¹⁴

Available as polyamic acid solutions, which are the initial condensation product of the reaction between an aromatic dianhydride and an aromatic diamine in aprotic solvents such as N-methyl pyrrolidinone (NMP), these resins are easily coated as thin films using a variety of techniques (e.g., spin and spray coating). During final heat curing, the polyamic acid resin completes the condensation process to irreversibly form imide ring linkages which account for the high degree of thermal and mechanical stability achieved with this class of polymer. This thermal cure process results in a film thickness change of the order of 40%, and essentially all of the volume loss is in one dimension. The resulting morphology of these thin imidized films prepared by spin coating closely resembles that of smectic liquid crystal, in which the long axis of the polymer chain is preferentially oriented parallel to the film surface.¹⁵ Polyimide films consequently exhibit substantial optical, mechanical, and diffusion anisotropies.¹⁶ This implies that the free volume available for guest molecule occupation is highly oblate. The size of the free volume is influenced by the structure of the polymer. Polyimides based on tightly packed rod-like structures exhibiting small free volumes and low coefficients of thermal expansion have been reported.¹⁷

Guest Selection

The optimal size and shape of the guest for a given host system is determined by the free volume present in the polymer after cure. By using a guest that closely matches the host free volume in overall size, rotational diffusion resulting in loss of alignment can be significantly reduced. In the original guest-host systems, the typical optical moieties had VDW volumes of 200 Å³ or less.

Segmental motion in PMMA-type molecules involves the side chain for the β transition and main chain motion for α transitions.¹⁸ The loss of dipole alignment, which is associated with the α transition in these systems, occurs due to a rotational diffusion which is related to the free volume through the polymer conformation and morphology changes propagating along the chain.¹⁹ The effective rotational free volume for an optical molecule disalignment is reduced by bonding to the main chain; therefore side-chain attachment results in enhanced thermal stability. By addressing the relative free volume of the polymer and EO moiety high thermal stability can be achieved in guest-host systems without side chain attachment. When the free volume of the polymer at a specific temperature is less than the VDW volume of the molecule, rotational diffusion is significantly reduced and the active EO moieties retain their poling-induced alignment.

The VDW size of NLO molecules that undergo rotational diffusion from an aligned state should be treated as a series of temperature activated segmental size dependent motions, rather than as a rigid body. This is analogous to the treatment of segmental motion in polymer systems that give rise to the α , β , γ , etc., transitions at different temperatures.¹⁸ This leads to a lower VDW volume when adding the segment sizes than when treating the molecule as a single unit that undergoes rotational diffusion about a central rotation axis.

Because polyimides are highly anisotropic, the shape of the guest molecule is also a factor in guest selection. An elongated molecule can be effectively trapped in the oblate free volume of a densified polyimide. We have therefore chosen relatively planar dye molecules in order to take advantage of this anisotropy in free volume of the polyimide. We have examined a series of dyes belonging to the fluorescein class. The chemical structures of four of these dyes are shown in Figure 1. Figure 2 depicts two views of a space-filling model of the free-acid form of Erythrosin B, the dye that was used in the thermal stability studies described in the preceding section. It can be seen from this model that the structure of Erythrosin B molecule deviates only slightly from planarity and occupies a relatively large VDW volume (ca. 350 Å³).

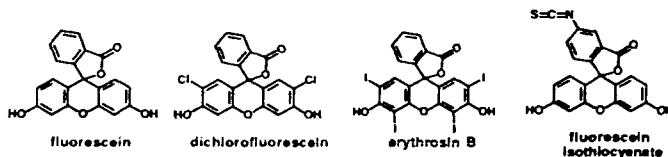


Figure 1. Structures of Fluorescein Dyes (lactone isomers shown)

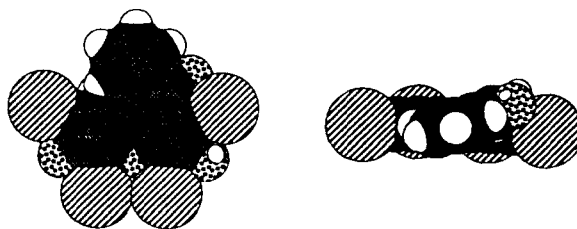


Figure 2. Space-filling Model of Erythrosin B (front and side views)

Another criterion in guest selection is resistance of the guest molecule to thermal decomposition at the temperatures required for polyimide cure and densification. We have studied the decomposition of a series of fluorescein dyes by UV-visible spectra in polyimide materials. As can be seen in Figure 3, the intensity of the optical absorption near 500 nm of Erythrosin B is significantly diminished after high-temperature cure in polyimide, indicating decomposition of the dye. Other members of the fluorescein class are more thermally stable, however. On the right this region of the absorption spectrum of fluorescein isothiocyanate in polyimide is shown, before and after cure. In this case, the oscillator strength remains relatively unchanged after the same curing procedure, along with a uniform dielectric shift.

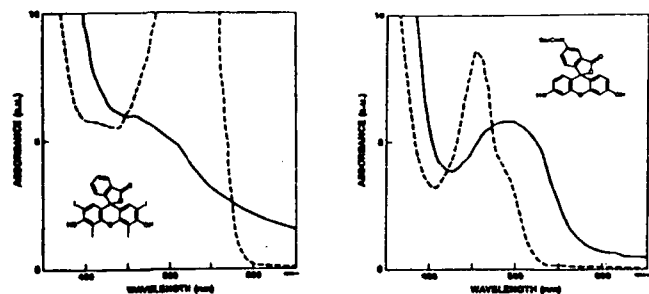


Figure 3. Erythrosin B (left) and Fluorescein Isothiocyanate (right) in polyimides (30%) before (---) and after (—) curing at 360°C for 30 min.

EXPERIMENTAL

We have investigated a series of fluorescein and other dyes in polyimide hosts. Compatibility of dye and polyimide was studied by mixing guest and host and checking for the formation of crystals or domains by optical microscopy and optical waveguide attenuation. In some cases the active EO moiety is more compatible with the polyimide than with the polyamic acid solution or film and thus time from dissolution to cast and cure and imidization is a relevant parameter for generation of optically clear films. In each case, the sample was cured while a dc poling field was applied to the film. This field was maintained after imidization during the high-temperature densification of the films as well.

The following procedure describes an example in which the guest molecule is erythrosin B and the host polymer is Pyralin 2611D. The guest molecule was dissolved in NMP. Films were prepared by spin coating the erythrosin/polyamic acid solutions (erythrosin/2611D) on the etched chromium electrodes (100 nm thick) deposited on fused quartz substrates. The poling electrode geometry was a coplanar structure, and the experimental measurement set-up has been described in Ref. 6. Residual NMP solvent was removed by vacuum soft-baking at 120°C for a few hours.

The curing temperature profiles are shown in Figure 4. The 250°C for 1 hour profile (curve 1, adopted for sample curing as reported in Ref. 6) is shown as a reference. The temperature profile adopted for the fluorescein series is 250°C for 1 hour plus 360°C for 2 hours (labeled (2)) or 360°C for 1/4 hour plus 300°C for 1/3 hour (labeled (3)). For curing process (2), the films were imidized by heating to 250°C at a rate of 5°C/min with a dc poling field applied. After holding the sample at 250°C for 1 hour, the sample was heated again up to 360°C (10°C/min) and held there for 1/2 hour with a dc poling field applied. For curing process (3), the film was heated to 360°C (10°C/min) and held there for 1/4 hour and cooled down to 300°C (12°C/min) and held for 1/3 hour for annealing. In both processes (2) and (3), the dc field was removed upon reaching room temperature.

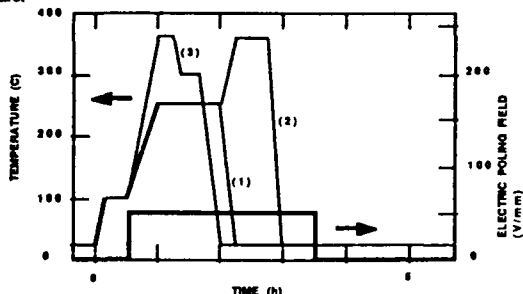


Figure 4. Temperature profiles of thermal curing are shown. Profiles (1), (2), and (3) correspond to 200°C for 1 hour, 200°C for 1 hour plus 360°C for 1/2 hour, and 360°C for 1/4 hour plus 300°C for 1/3 hour, respectively. The temporal profile of the poling electric field is also shown.

We have measured the EO response at 633 nm as a function of time for an erythrosin/2611D coplanar-electrode sample poled at 50 V/μm with curing profile (2). Except for an initial decay of around 30% after 20 hours at 200°C, virtually no decay was observed in the EO signal over 60 hours at 200°C. Samples cured using temperature profile (3) were also tested. In this case the initial decay was 35% in the first hour, followed by no further decay in the EO signal over another 1 hour at 300°C.

DISCUSSION

Our approach to increasing EO thermal stability is based on the recognition that, in polyimides, there actually exist two distinct stages in the curing process with corresponding different temperature ranges. The first stage is the imidization stage in which the polyamic acid condenses to form the imide rings at temperatures around 170–300°C; and the second is a densification stage in which the polyimide densifies to further shrink the available free volume at around 340–380°C.²⁰ The existence of this second ring stage suggests that through densification at temperatures higher than 250°C during a poling process, EO thermal stability at 300°C in polyimide guest-host systems may be achieved. This is evidenced in thermal aging tests carried out at temperatures higher than the imidization curing temperatures. Thus, for example, polyimide guest-host films cured at 250°C exhibit EO thermal stability at 150°C for many hours as previously reported, but, after 1 hour of thermal aging at 300°C, no EO signal is detectable. Such thermal aging results suggest that imidization alone without densification is inadequate to

obtain EO thermal stability at 300°C in polyimide guest-host systems, and that a densification curing step should be included in the poling process in order to reduce the free volume and inhibit the guest NLO molecules from becoming unaligned.

We have also determined that two conditions in the poling process are of major importance for the EO thermal stability that we report here. First, the poling field is applied during the cure process so that the dipole alignment is achieved before imidization when the available free volume is much larger and the film is less rigid; and second, the guest molecules are aligned in the same orientation as the conforming morphology of the host polymer. That is, the material poled is located between coplanar electrodes which lie in the plane of the spun polyimide and thus, for many linear or planar dye molecules, this results in a coincidence of the aligned NLO molecule with the fully cured polyimide's highly oblate free volume.

Experimentally, the high temperature curing with a high poling electric field (order of 100 V/μm) becomes more challenging due to the change in electrical conductivity of polyamic acid and polyimide over a wide range of temperatures.²¹ The presence of guest molecules inside the host polyamic acid further complicates the conductivity at high temperatures; this is often due to the increased mobility of undesirable ionic impurities present in the guest-host system. We find that the high conductivity leads to dielectric breakdown of the thin film samples resulting in unsuccessful poling. By selecting cleaner, lower ionic impurity NLO molecules as guest, we succeeded in curing at 360°C with a poling electric field applied.

It should also be noted that we observed an EO signal in the cured Erythrosin B/polyimide film despite the decrease of the absorption peak for Erythrosin B after high temperature curing which was described earlier. This result indicates that either decomposition of the dye was incomplete or that the molecule fragmented to produce products with some EO activity. We are currently addressing the issue of thermal stability of the active guest moiety by evaluating a number of different classes of compounds in polyimide systems.

CONCLUSIONS

In summary, we have described an approach in which the active EO moiety is treated as a solute in a host polymer solvent. Loading levels are increased by selecting guests and hosts with compatible solubility parameters. By matching the Van der Waals volume of the guest to the free volume and morphology of the polyimide host, the thermal stability of these guest-host systems is enhanced. The films are imidized and densified during high temperature curing under an applied dc poling field. Using this approach we have demonstrated thermally stable EO response in poled polyimide films at temperatures up to 300°C.

ACKNOWLEDGMENTS

The authors gratefully acknowledge the cooperative efforts of the Lockheed Photonics and Lightwave Technology Group and ROI Technologies, Inc.

REFERENCES

- Author to whom correspondence should be addressed
- 1) A.F. Garito, J. Wu, G.F. Lipscomb, and R. Lytel, *Materials Research Society Symp. Proc.* Vol. 173, 467 (1990).
 - 2) R. Selvaraj, H.T. Lin and J.F. MacDonald, *J. Lightwave Tech.*, 6, 1084 (1988).
 - 3) See, for example, *SPIE Proceedings, Excimer Laser Materials Processing and Beam Delivery Systems*, SPIE Conf. 1377, 1990 (to be published), Husain, *Microelectronic Interconnects and Packaging: System Integration*, SPIE Conf. 1390, 1990 (to be published).
 - 4) J.I. Thackara, G.F. Lipscomb, M.A. Stiller, A.J. Ticknor, and R. Lytel, *Appl. Phys. Lett.* 52, 1031 (1988); See also G.F. Lipscomb, R.S. Lytel, A.J. Ticknor, T.E. Van Eck, S.L. Kwiatkowski, and D.G. Garton, *Nonlinear Optical Properties of Organic Materials III*, SPIE Conf. 1337, 23 (1990).
 - 5) See, for example, J.W. Wu, *J. Opt. Soc. Am.*, B8, 142 (1991) and references therein.
 - 6) T. E. Van Eck, A. J. Ticknor, R. S. Lytel, and G. F. Lipscomb, *Appl. Phys. Lett.* 58, 1558 (1991); D.G. Garton, S. Kwiatkowski, G.F. Lipscomb, and R. Lytel, *Appl. Phys. Lett.*, 58, 1730 (1991).
 - 7) R. Lytel, G.F. Lipscomb, E.S. Binkley, J.T. Kenney, and A.J. Ticknor, *The 199th ACS National Meeting, Inorganic Division, Tutorial on Nonlinear Optics, Paper #8, American Chemical Society, Washington, D.C.*, (1990).
 - 8) J.W. Wu, J.F. Valley, S. Ermer, E.S. Binkley, J.T. Kenney, G.F. Lipscomb, and R. Lytel, *Appl. Phys. Lett.*, 58, 225 (1991).
 - 9) J.W. Wu, E.S. Binkley, J.T. Kenney, R. Lytel and A.F. Garito, *J. Appl. Phys. Comm. Sec.*, 62 (1991) in press.
 - 10) See, for example, R.N. DeMartino et al., in *Nonlinear Optical and Electroactive Polymers*, Proc ACS Symposium on Electroactive Polymers, Denver, CO, Plenum Press, New York, 169 (1988); C. Ye, N. Minami, T.J. Marks, J. Yang and G.K. Wong, *Mat. Res. Soc. Symp. Proc.*, 102, 263, (1988); G.R. Mohlmann et al., *SPIE Conf.* 1147, 245 (1989).
 - 11) S.J. Lalama and A.F. Garito, *Phys. Rev. A* 20, 1179 (1979); K.D. Singer and A.F. Garito, *J. Chem. Phys.* 75, 3572 (1981).
 - 12) D. Jungbauer, B. Reck, R. Twieg, D. Y. Yoon, C. G. Wilson, and J. D. Swalen, *Appl. Phys. Lett.* 56, 2610 (1990).
 - 13) D. Li, T.J. Marks, C. Zhang, J. Yang, and G.K. Wong, *Nonlinear Optical Properties of Organic Materials III*, SPIE Conf. 1337, 341 (1990).
 - 14) *Polymeric Materials for Electronics Packaging and Interconnection*, J.H. Lupinski and R.S. Moore, eds., Vol. 407 of *American Chemical Society Symposium* (ACS, Washington, D.C., 1989). See also *Polyimides*, Vol. 1 & 2, K.L. Mittal, ed. (Plenum Press, New York (1984)).
 - 15) N. Takahashi, D.Y. Yoon, and W. Parrish, *Macromolecules* 17, 2583 (1984).
 - 16) T.P. Russell, H. Guggen, and J.D. Swalen, *Journal of Polymer Science: Polymer Physics Edition* 21, 1745 (1983).
 - 17) S. Numata, T. Miwa, Y. Misawa, D. Makino, J. Imazumi and N. Kinjo, *Mat. Res. Soc. Symp. Proc.*, 108, 113 (1988).
 - 18) N.G. McCrum, B.E. Read and G. Williams, *Anelastic and Dielectric Effects in Polymeric Solids*, John Wiley & Sons, London (1967).
 - 19) See, for an introduction, H. Scher, M.F. Schlesinger, and J.T. Bendler, *Physics Today*, 44, 26 (1991) and references therein.
 - 20) S. Isoda, H. Shimada, M. Kochi, and H. Kambe, *Journal of Polymer Science: Polymer Physics Edition*, 19, 1293 (1981).
 - 21) G.M. Sessler, B. Hahn, and D.Y. Yoon, *J. Appl. Phys.*, 60, 318 (1986).

DESIGN AND SYNTHESIS OF A NEW CLASS OF PHOTOCROSSLINKABLE NONLINEAR OPTICAL POLYMERS

Sukant Tripathy, Braja Mandal, Ru Jong Jeng, Jun Young Lee and Jayant Kumar*

Departments of Chemistry and *Physics
University of Lowell
Lowell, Massachusetts 01854

Nonlinear optical (NLO) polymers have attracted much attention due to their application possibilities in a number of photonics technologies¹. We have developed a new class of photocrosslinkable polymers with stable second and third order nonlinear optical properties². The polymers have significant processing advantages over their inorganic counterparts.

The NLO polymers have been designed as guest-host systems and as polymers with the NLO and photocrosslinkable units in the main chain and in the side chain. Each of these classes of materials presents unique features and advantages.

A guest host photocrosslinkable NLO polymer has been designed where the host polymer is polyvinylcinnamate (PVCN), a commercially available photosensitive polymer. A new azo dye, 3-cinnamoyloxy-4-[4-(N,N-diethylamino)-2-cinnamoyloxy phenylazo] nitrobenzene (CNNB-R) has been designed as the guest NLO molecule. The photocrosslinking groups are present in both the host polymer and the NLO dye, facilitating intermolecular linkings. An azo dye appropriately substituted with donor-acceptor groups is selected for its large molecular hyperpolarizability and ground state dipole moment. Presence of the bulky photocrosslinking groups was also expected to inhibit trans-cis isomerization and improved compatibilization with the polymer is possible. The system as synthesized meets all these design expectations.

Figure 1 shows the diazo linked π -extended system (i and ii) that has been synthesized by diazo coupling reaction of aromatic molecules appropriately substituted with donor-acceptor groups and hydroxyl groups. Nitro- and N,N-diethylamine are chosen as efficient acceptor and donor groups, respectively, and placed at either end of the π -extended molecule, in order to obtain large second-order electro-optic effects. Likewise, one hydroxyl group in each aromatic ring is appropriately substituted for coupling with the photosensitive chromophores (ia and iia). The preparation of i, ia, ii and iia (shown in Figure 1) was achieved via the reactions of Figure 2.

Crosslinks are formed by 2 + 2 photo-dimerization between an excited cinnamoyl group of one chain with a ground-state cinnamoyl group belonging to another chain. The photo-dimerization between two CC double bonds of cinnamoyl groups is very effective because of the adjacent carbonyl group which provides desirable polarization towards the reactivity of the double bond. The phenyl group, on the other hand, increases the polarizability and the absorption coefficient of the chromophore. The intermolecular photocrosslinking reaction between the photosensitive chromophores of the polymer and the active molecules is represented in Figure 3.

The conventional spinning technique used in microfabrication was employed for coating thin films of various combinations of the NLO molecules and PVCN over different

substrates such as glass, quartz, thermally grown silicon dioxide on silicon, etc. Thickness ranging from 0.5 to 2.5 μm was obtained by optimizing the spinning speed and the viscosity of the solution. Non-centrosymmetric organization of NLO molecules in the polymer matrix was introduced by corona poling³. The poling temperature was properly selected as dictated by the concentration of NLO molecules in the polymer matrix. This temperature is usually close to T_g of the polymer matrix.

Main chain NLO polymers with the photocrosslinking groups on the side chain have also been synthesized. One of the representative structures is shown in Figure 4. These polymers are produced by reacting an epoxy with an NLO unit containing an amine group. This prepolymer is subsequently derivatized using cinnamoyl chloride to provide the photocrosslinking groups functioning as guests. These polymers can be processed, poled and subsequently photocrosslinked. They also allow incorporation of different types of NLO chromophores. The number density of NLO units in these polymers can be significantly increased. These polymers are also used as host in guest host systems with NLO dyes functionalized with the photocrosslinking groups. In addition to the cinnamoyl group which is reactive at 250 nm, styrylacrylate groups have been used, allowing photocrosslinking at 360 nm. The second order nonlinear coefficients, d_{33} , have been measured for the poled, crosslinked system by second harmonic generation. Electrooptic coefficient has been measured using interferometric techniques.

The stability of the poled and crosslinked polymers has been investigated by monitoring the decay of the second harmonic signal. No measurable decay in optical nonlinearity is observed for one of the photocrosslinked polymers up to temperatures of 160 °C for a period of several hours. These results are also confirmed by monitoring the stability of the UV-visible absorption spectrum at these temperatures⁴. Channel waveguides and diffraction gratings have been fabricated using lithographic techniques.

Acknowledgement

We acknowledge the Office of Naval Research for their support of this research.

References

1. R.D. Small, K.D. Singer, J.E. Sohn, M.G. Kuzyk, S.J. Lalama, in: "Molecular and Polymeric Optoelectronic Materials: Fundamentals and Applications", edited by G. Khanarian, Society of Photo-Optical Instrumentation Engineers 682 160 (1986).
2. B.K. Mandal, J. Kumar, J.C. Huang and S.K. Tripathy, "Novel Photo-crosslinked Nonlinear Optical Polymers", Makromol. Chem., Rapid Commun. 12 63-68 (1991).
3. G.M. Sessler, "Electrets", Springer-Verlag, Berlin 1987.
4. B.K. Mandal, Y.M. Chen, J.Y. Lee, J. Kumar and S.K. Tripathy, "Crosslinked Stable Second Order Nonlinear Optical Polymer by Photochemical Reaction", Applied Physics Letters, to be published, June 3, 1991.

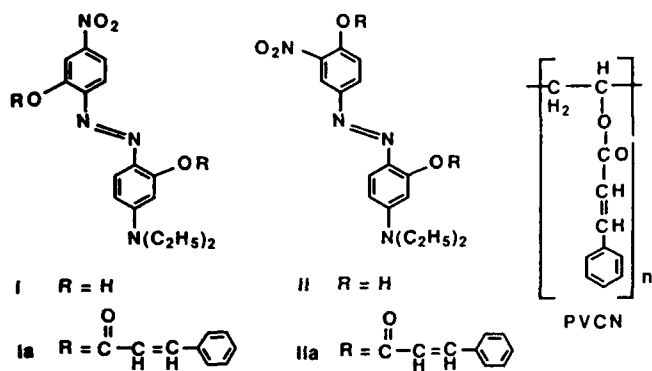


Figure 1. **i** and **ii**) Diazo linked π -extended systems. **ia** and **iia**) Diazo linked π -extended systems functionalized by cinnamoyl groups.

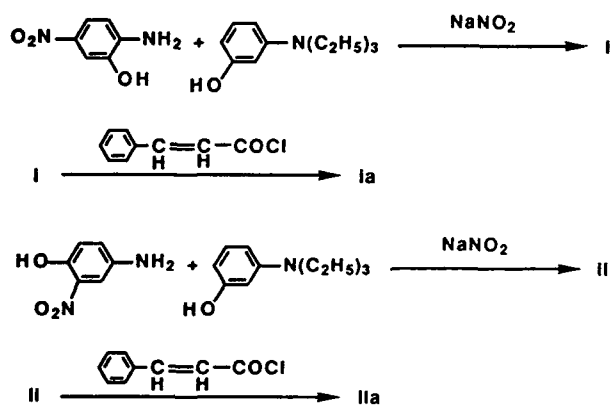


Figure 2. Reaction steps for the preparation of diazo linked π -extended systems.

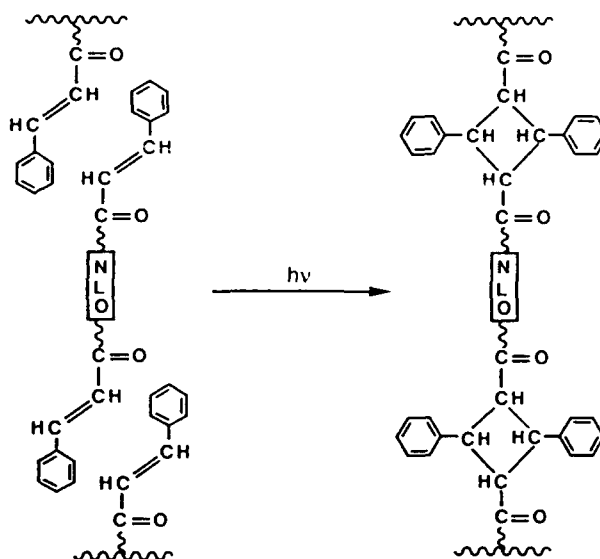


Figure 3. Intermolecular photocrosslinking reaction between photosensitive chromophores of the polymer and active molecules.

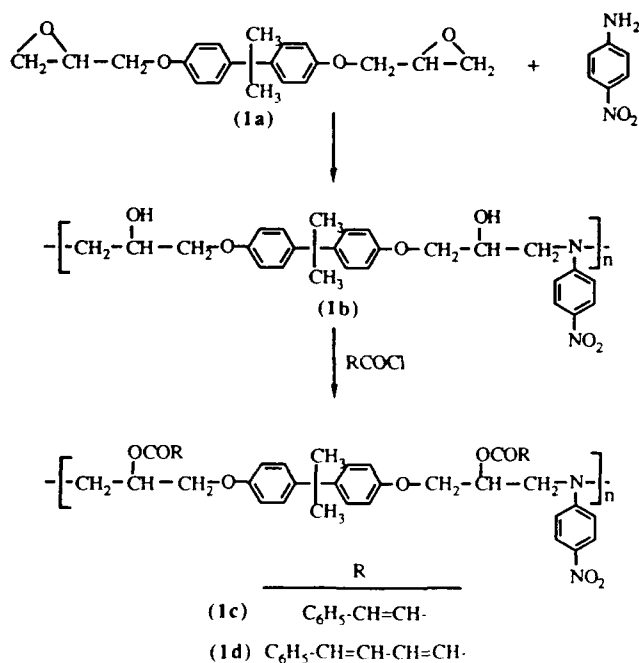


Figure 4. Structure of a photocrosslinkable polymer with a NLO group in the main chain.

continuous line the polyPEBC₁₆ chromatogram. The shift of the maximum of the polyPEBC₄ curve indicates a lower molecular weight than that of the C₁₆ derivative (polyPEBC₁₆, $M_w = 12.0 \times 10^4$, polyPEBC₄, $M_w = 7.2 \times 10^4$). While the two polymers are obtained in the same polymerization conditions, the low molecular weight of the short chain polymer may be due to the "bond solvent effect", i.e. the short chain does not give enough solubility to allow the high molecular weight of the C₁₆ polymer.

The figure 3 represents the relationship between the intrinsic viscosity and the molecular weight for the polyPEBC₄ and polyPEBC₁₆. The calculated intrinsic viscosities $[\eta]$, calculated from the universal law, are plotted versus the molecular weight from light scattering, respectively for polyPEBC₄ and polyPEBC₁₆, for cholesteryl derivative of ref (3) and for the polystyrene standards. The values of α in the Mark-Houwink equation $[\eta] = k M^\alpha$, estimated from the last square fit of the logarithmic representation gives $\alpha = 0.92$, the same for the two polyPEBC_n with $n=4$ and 16. This value is significantly different from the polyacetylene with cholesteryl groups at the end of a flexible spacer where $\alpha = 0.66$.

The results of the viscosity law imply that the polyPEBC_n derivatives are more rigid than the previous derivatives with a flexible spacer and mesogenic groups. The stacking of lateral phenyl rings increases the stiffness of the backbone and, at the local range, the electrons are delocalized over a longer conjugated length. Nonlinear optical measurements on the thin solid films of the polyPEBC_n series are in progress in order to confirm these results.

REFERENCES

1. F. Kajzar, S. Etemad, G.L. Baker, J. Messier, *Synth. Met.* **17**, 563, (1987)
2. M.R. Drury, *Sol. State Comm.*, **68**, 417, (1988)
3. J. Le Moigne, A. Hilberer, F. Kajzar, A. Thierry, in *Organic Molecules for Nonlinear Optics*, J. Messier et al (eds), *Nato, ASI Series*; **194**, 327, (1991)
4. J. Le Moigne, A. Hilberer, F. Kajzar, *submitted to Makromol. Chem.* (1991)
5. K. Sonogashira, Y. Tohda, N. Hagihara, *Tetrahedron Lett.* **50**, 4467, (1975); T. Masuda, T. Higashimura, *Adv. Polym. Sci.*, **81**, 121, (1987)
6. L. Beltzung, C. Strazielle, *Makromol. Chem.*, **185**, 1155, (1984)
7. M. Ballauf, *Angew. Chem.* **28**, 253, (1989)

Table 1. Polymerization yield of different lengths of side-chain in the monomer series, PEBC_n, by different catalyst/solvent couples.

Monomer	catalysts/solvent	polym. yield%
PEBC ₁	WCl ₆ /dioxane	40
	WCl ₆ /toluene	95
	MoCl ₅ /dioxane	ε
	MoCl ₅ /toluene	ε
PEBC ₂	WCl ₆ /toluene	70
PEBC ₄	WCl ₆ /toluene	60
PEBC ₈	WCl ₆ /dioxane	40
	WCl ₆ /toluene	96
PEBC ₁₆	WCl ₆ /toluene	67

Figure 1. UV-visible absorption spectra of polyPEBC₁₆ in THF.

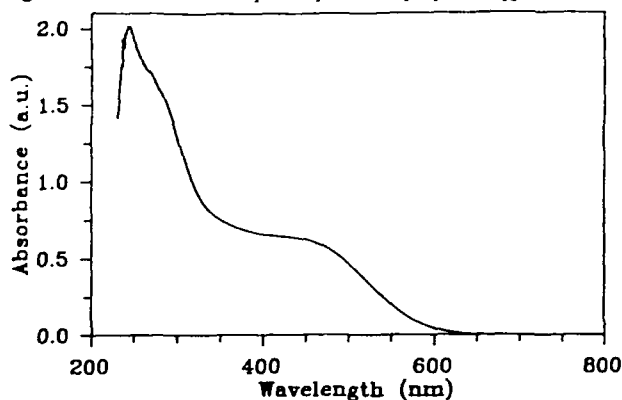


Figure 2. GPC chromatograms of polyPEBC₄, and polyPEBC₁₆, respectively dashed line and continuous line.

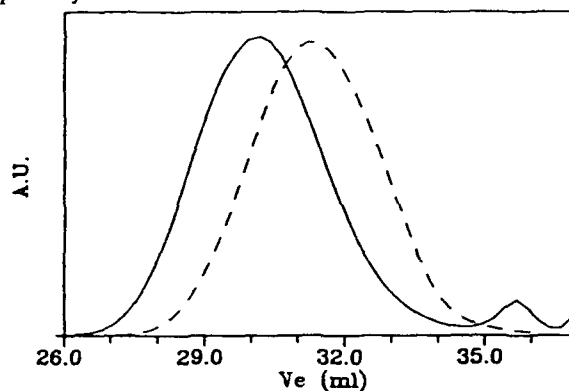
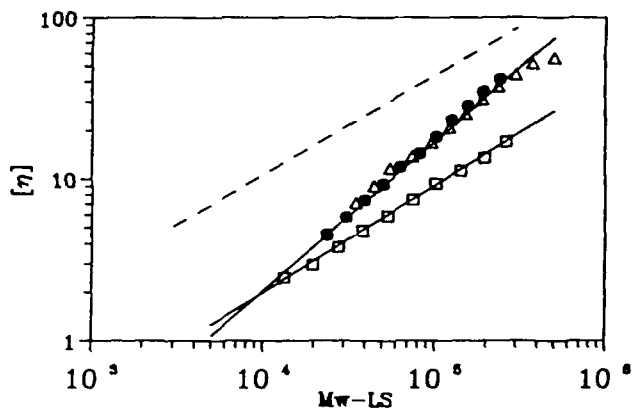


Figure 3: GPC characterization of polyPEBC₄ and polyPEBC₁₆ in THF, intrinsic viscosity versus molecular weight $[\eta] = f(M_w - LS)$, ● and Δ for polyPEBC₄ and polyPEBC₁₆, open squares for poly(cholesteryl pentynoate) (ref.3), dashed line for polystyrene.



Orientation and Decay in Poled Polymer Nonlinear Optical Materials

by
Kenneth D. Singer
Department of Physics
Case Western Reserve University
Cleveland, Ohio 44106

and
Lori A. King
AT&T Bell Laboratories
P.O. Box 900
Princeton, NJ 08540

Poled polymer materials for second-order nonlinear optics have become the subject of intense interest due to their potential application as electro-optic and frequency conversion materials. [1] The electric field poling process is necessary in order to break the center of symmetry of the polymer so that it can exhibit second-order nonlinear optical effects. In this process, dipolar nonlinear optical moieties which are incorporated in the polymer rotate through the coupling of the dipole to the electric field when the polymer is in a state allowing the rotation. After the dipoles are aligned, the polymer must be put into a state where the dipole rotation is inhibited in order to minimize the orientation decay.

It is generally assumed and found that in the rubbery state, the molecular dipoles associated with a variety of nonlinear optical moieties exhibit rotational motion consistent with that found in liquids, and the nonlinear optical properties follow a local field corrected oriented gas model. In this model, the polymer electric polarization is related to the molecular polarization by [2]

$$P_i(t) = N \langle p_i(t) \rangle, \quad (1)$$

where N is the number density of the nonlinear optical moieties. The angle brackets denote that a statistical average over the molecular orientations is performed. Thus, the second order susceptibility is given by [2]

$$\chi_{ijk} = N \beta_{ijk}^* \int d\Omega a_{iI} a_{jJ} a_{kK} G(\Omega, E_p), \quad (2)$$

where β_{ijk}^* is the local field dressed molecular nonlinear optical susceptibility, the a_{uV} are coordinate transformations from the molecular (IJK) to the laboratory (ijk) systems. The $G(\Omega, E_p)$ is the poling field dependent orientational distribution function. The integral can be partially evaluated by expanding in Legendre polynomials, $P_l(\cos \theta)$ yielding for the nonlinear susceptibility

$$\chi_{333} = N \frac{\beta_{333}^* m_z^* E_p}{kT} \times \left(\frac{1}{5} + \frac{4}{7} \langle P_2 \rangle + \frac{8}{35} \langle P_4 \rangle \right), \quad (3)$$

where m_z^* is the local field dressed molecular dipole moment, and kT the Boltzmann factor. The values $\langle P_2 \rangle$ and $\langle P_4 \rangle$ are microscopic order parameters which are statistical averages of the appropriate Legendre polynomials. These order parameters describe the degree of axial order of the molecule in the polymer due to forces independent of the poling field, such as stresses in a polymer or liquid crystalline forces. This oriented gas model has been shown relevant to a variety of polymeric and stressed polymeric systems.

This oriented gas model describes the static behavior of the orientation in the polymer. The nonlinear susceptibility it describes will be observed just after the poling field is removed. It is found that the nonlinear optical susceptibility decays with time due to relaxation processes in the polymer. [3,4,5,6,7] In addition, the process of poling is a dynamic process involving a time, temperature, and electric field program. It is found that the orientation dynamics depends on both time and temperature. We have studied the nonisothermal electric field poling process as well as the subsequent isothermal decay using second harmonic generation. [8]

Figure 1: Electric field induced second harmonic generation coefficient as a function of temperature for a constant heating rate of 1.7°C/min for DR1/PMMA system. Line is function fit to Equation 6 with parameters in Table I.

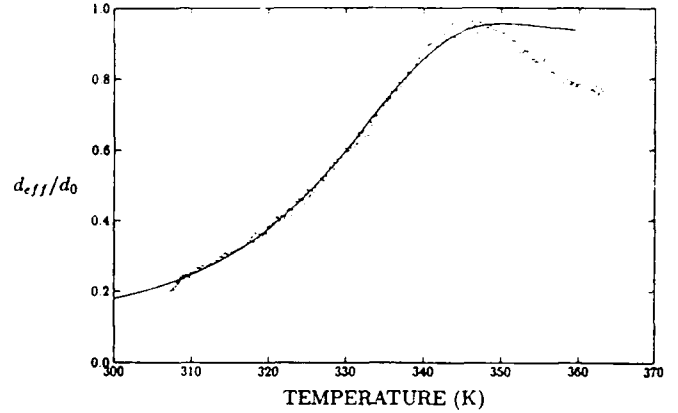
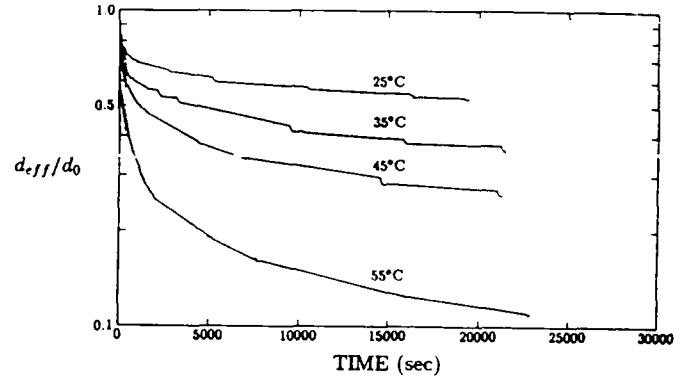


Figure 2: Isothermal decay of the second harmonic coefficient for a series of temperatures.



Samples were prepared by dissolving purified Disperse Red 1 dye (DR1) in polymethylmethacrylate (PMMA) to 10% by weight in a common solvent, and spin coating thin films on indium tin oxide coated glass slides. A double electrode structure was formed by placing two of these films face to face and fusing them. The films were placed in a temperature controlled cell in a second harmonic generation apparatus. The second harmonic intensity from a 1.58 μm fundamental wavelength was monitored while the sample temperature was heated at a constant rate with a 30 V potential applied. The sample was then cooled to a fixed temperature, the potential removed and the electrodes shorted. The decay of the second harmonic intensity was monitored over time. This measurement was repeated for several final temperatures.

The data during the heat ramp are shown in Figure 1 where the heating rate, h , was 1.7°C/min. The data for the isothermal decays are shown in Figure 2. In both figures, the vertical scale is the square root of the intensity which is proportional to the nonlinear optical polarization, and thus the second harmonic coefficient. The data of Figure 2 cannot be fit to a single exponential, a biexponential, or a simple single diffusion model. The data suggests behavior consistent with a distribution of local relaxation rates. These relaxation rates would be

Table 1: Activation energies, A/k , exponential prefactors, $-\ln \tau_0$, and slopes, m , and intercepts, b , of β versus temperature derived from isothermal decay data and from a fit of temperature ramped EFISH.

	A/k (1/K)	$-\ln \tau_0$	m	b
Isothermal decay	2.16×10^4	-59.4	0.00317	-0.795
Ramped EFISH	2.22×10^4	-57.	0.0033	-0.73

determined by the distribution of free volume. In this type of model, the relaxation would follow the set of differential equations [9]

$$\frac{dP_i(t)}{dt} + \alpha_i(T)P_i(t) = 0, \quad (4)$$

where $P_i(t)$ is the nonlinear optical polarization of the i th relaxing dipole with relaxation rate $\alpha_i(T)$ in the distribution of temperature dependent relaxation rates. The relaxation for each dipole follows a simple Debye relaxation for a local relaxer. A continuous distribution of relaxation rates can be described in a variety of ways. We have found it convenient to describe it by a Williams-Watt-Kohlrausch stretched exponential where [10]

$$P(t) = P_0 \exp[-(\alpha(T)t)^\beta] \quad (5)$$

where the parameter β describes the width of the distribution.

We fit the data to the relaxation time, $\tau = 1/\alpha$, and β by plotting $\ln[-\ln(d_{eff}/d_0)]$ versus $\ln(t)$ for each data set. The width parameter was found to be relatively temperature insensitive, and describes a rather broad distribution for this material system. A linear temperature dependence fit the data for β with the regression parameters given in Table 1. The relaxation time τ fit well to an Arrhenius plot with the fit parameters also given in Table 1.

The nonisothermal temperature ramp data would follow a related differential equation for each relaxation which leads to the following expression for the temperature dependent poling process [9]

$$P(t) = \frac{P_f}{T} \{1 - \exp[-(\alpha(T)t)^\beta]\}. \quad (6)$$

where P_f is an amplitude constant proportional to the applied electric field. With a constant heating rate, h (leading to $T = ht$), and again with the relaxation time obeying Arrhenius behavior, and assuming the width parameter β linear in temperature in this range, we fit the data of Figure 1 to Equation 6 with the resulting parameters given in Table 1. The fitted line shown in Figure 1 describes the data well except at high temperatures where the increased space charge due to the rise in polymer conductivity screens the poling field.

Examination of Table 1 reveals that both experiments result in the same phenomenological parameters indicating that the dynamical behavior is locked in during the poling process. Thus, an experimental program varying the poling process while monitoring the susceptibility will directly measure the expected lifetime. For example, a poling rate leading to a higher temperature peak, a higher glass transition temperature, or a steeper temperature dependence will result in a longer lived polarization. This was directly verified for a side-chain copolymer. [8] This process involves a rather broad distribution of local Debye relaxation rates which may follow Arrhenius behavior. The exact form of the distribution which governs these processes cannot be discerned from the data obtained here, due to a limited dynamic range. Typical distributions differ most in the distribution tails. The rates are related to the rotational binding forces in the polymer such as the steric forces between the molecule and the local polymer environment. Understanding of the underlying physical mechanisms requires further study.

References

- [1] K.D. Singer and J.E. Sohn, "Organic Materials for Second-Order Nonlinear Optics" in *Electroresponsive Molecular and Polymeric Systems*, T. Skotheim, ed. (Marcel-Dekker, 1991).
- [2] K.D. Singer, M.G. Kuzyk, and J.E. Sohn, *J. Opt. Soc. Am. B* **4**, 968 (1987).
- [3] C. Ye, T.J. Marks, J. Yang, and G.K. Wong, *Macromolecules* **20**, 2322 (1987).
- [4] K.D. Singer, M.G. Kuzyk, W.R. Holland, J.E. Sohn, S.J. Lalama, R.B. Comizzoli, H.E. Katz, and M.L. Schilling, *Appl. Phys. Lett.* **53**, 1800 (1988).
- [5] B. Reck, M. Eich, D. Jungbauer, R.J. Twieg, C.G. Willson, D.Y. Yoon, and G.C. Bjorklund, *Proc. SPIE* **1147**, 74 (1989).
- [6] H.L. Hampsch, J. Yang, G.K. Wong, and J.M. Torkelson, *Polym. Commun.* **30**, 40 (1989).
- [7] M. Eich, H. Looser, D.Y. Yoon, R. Twieg, G. Bjorklund, and J.C. Baumert, *J. Opt. Soc. Am. B* **6**, 1590 (1989).
- [8] K.D. Singer and L.A. King (to be published).
- [9] J. van Turnhout, "Thermally Stimulated Discharge of Electrets", in *Electrets*, G.M. Sessler, ed. (Springer-Verlag, 1980).
- [10] F. Kohlrausch, *Pogg. Ann. Physk.* **119**, 352 (1863); G. Williams and D.C. Watts, *Trans. Faraday. Soc.* **66**, 80 (1970).

Second-Order Nonlinear Optical Onset and Decay

and Their Relationship to Polymer Physics

Ali Dhinojwala^a, George K. Wong^b, and John M. Torkelson^{a,c}
^aDept. of Chemical Engr., ^bDept. of Physics, and
^cDept. of Materials Science and Engr.
 Northwestern University
 Evanston, IL 60208

Recent experimental studies¹⁻⁵ have indicated that second-order nonlinear optical properties of doped, poled amorphous polymers are sensitive to the basic physics associated with polymers in both glassy and rubbery states. In particular, effects of temperature, physical aging, polymer species, and dopant size have been documented. However, much of this work²⁻⁴ was performed with corona poling which complicates the analysis of the second harmonic generation (SHG) data (often reported in terms of the second-order nonlinear susceptibility, $\chi^{(2)}$), as the SHG decays reflect a complex combination of effects from corona poling (surface and space charges) and polymer physics.³

In the work reported here, contact poling has been used to impose a noncentrosymmetric orientation of an SHG dopant, 4,4'-dimethylaminonitrostilbene (DANS), in polymethylmethacrylate (PMMA). Preliminary investigations by us and others⁵ indicate that, in contrast to corona poling, contact poling (with chrome electrodes) results in at most small effects on the observed SHG decay behavior, i.e., the SHG decay may be ascribed largely if not exclusively to polymer physics and not to extraneous poling factors. Based on the work reported here, a "two-phase" model has been developed to explain both $\chi^{(2)}$ onset (poling field on) and decay (poling field off) results in terms of local "liquid-like" and "glassy" sites surrounding the dopants. Alternative formalisms^{5,6} are available for interpreting at least some part of the data reported here, and we acknowledge the influence these formalisms have had in the development of the model presented here.

Fig. 1 shows the effect of temperature on the decay of $\chi^{(2)}$ for 3 wt. % DANS in PMMA when the poling (SHG onset) and SHG decay measurements are done at the same temperature. This figure demonstrates that as long as the decay is measured at the same temperature as used in poling the sample, regardless of being in the glassy (30°C) or rubbery state (115°C), the decay of $\chi^{(2)}$ upon removal of the electric field is extremely rapid, resulting in total loss of SHG signal within 1.5 min. Given that only those dopant sites which have sufficient mobility and/or local free volume to allow some net orientation of dopant will contribute to the signal at 30°C or 115°C, once the electric field is removed, these mobile or "liquid-like" sites will allow rapid randomization of dopant orientation. As the $\chi^{(2)}$ observed by poling at 30°C is only about 37% of that observed by poling at 115°C, this indicates that only a fraction of the dopants are in liquid-like sites in the macroscopic glassy state. Those dopants not in liquid-like sites may be described as being in locally "glassy" sites.

Using this two-site formalism, the liquid-like site fraction, f , may be determined from SHG onset and decay data assuming that the liquid-like sites obey Boltzmann statistics. In terms of SHG onset data, the following equation may be derived:

$$f = (\chi_G^{(2)}/\chi_R^{(2)})(T_G/T_R) \quad (1)$$

where T_G and T_R represent poling temperatures in the macroscopic glassy and rubbery states, respectively, and $(\chi_G^{(2)}/\chi_R^{(2)})$ is the ratio of the steady-state $\chi^{(2)}$ for samples poled at T_G to that for samples poled at T_R . For 3 wt.% DANS in PMMA, $f = 0.29$ at $T_G = 30^\circ\text{C}$.

Similar information on f may be obtained from SHG decay if poling is done in the macroscopic rubbery state, followed by quenching into the macroscopic glassy state, followed by removal of the electric field. Fig. 2 shows results for a system poled at 115°C, followed by quenching to 55°C, followed by removal of the field. Assuming that the liquid-like sites follow Boltzmann statistics,

$$f = A(\chi_G^{(2)}/\chi_L^{(2)})(T_G/T_L) \quad (2)$$

In eqn. (2), $\chi_G^{(2)}/\chi_L^{(2)}$ is the ratio of $\chi^{(2)}$ obtained after quenching (with the field still applied) from the already poled rubbery state to that obtained in the poled rubbery state. (This ratio is about 1.13 in Fig. 2.) A is the fast decay fraction of the $\chi^{(2)}$ at T_G .

Regardless of the details of how A is determined (biexponential fit or relative decay of $\chi^{(2)}$ 1.5 min after removal of the poling field), similar values of A are obtained. For the system in Fig. 2, $A = 0.41 - 0.42$ resulting in $f = 0.39$ to 0.40 at 55°C. When samples are poled at 115°C followed by quenching to 30°C, the SHG decay data yield $f = 0.27$ to 0.289 at 30°C. This is in excellent agreement with SHG onset results at 30°C which yielded $f = 0.29$. This suggests that this model holds significant promise in explaining the relationship between SHG onset and decay results and between SHG results and the basic physics of doped polymer systems.

Finally, Fig. 3 illustrates the relative $\chi^{(2)}$ decays of systems poled for several minutes at 115°C followed by quenching to various temperatures in the macroscopic glassy state. In contrast to previous studies³ on in-situ corona-poled systems which did not allow for adequate modeling of the $\chi^{(2)}$ decays by a Williams-Watt stretched exponential (often used to model glassy polymer relaxations), all of the data in Fig. 3 may be fit with the Williams-Watt model, including the rapid decay features at $t < 1.5$ min. This further indicates that careful analysis of the results of contact-poled samples can result in a direct understanding of the SHG of doped, poled polymers and the governing polymer physics.

REFERENCES

- Hampsch, H.L.; Yang, J.; Wong, G.K.; Torkelson, J.M. *Macromolecules* 1988, **21**, 526.
- Hampsch, H.L.; Yang, J.; Wong, G.K.; Torkelson, J.M. *Polym. Commun.* 1989, **30**, 40.
- Hampsch, H.L.; Yang, J.; Wong, G.K.; Torkelson, J.M. *Macromolecules* 1990, **23**, 3640; 1990, **23**, 3648.
- Hayden, L.M.; Sauter, G.F.; Ore, R.; Pasillas, P.L.; Hoover, J.M.; Lindsay, G.A. *J. Appl. Phys.* 1990, **68**, 456.
- Boyd, G.T.; Francis, C.V.; Trend, J.E.; Ender, D.A. *J. Opt. Soc. B.*, in press.
- Kuzyk, M.G.; Moore, R.C.; King, L.A. *J. Opt. Soc. B.* 1990, **7**, 64.
- Victor, J.G.; Torkelson, J.M. *Macromolecules* 1987, **20**, 2241; 1988, **21**, 3490.
- Royal, J.S.; Victor, J.G.; Torkelson, J.M. *Macromolecules*, in press.
- Royal, J.S.; Torkelson, J.M. *Macromolecules* 1990, **23**, 3536.

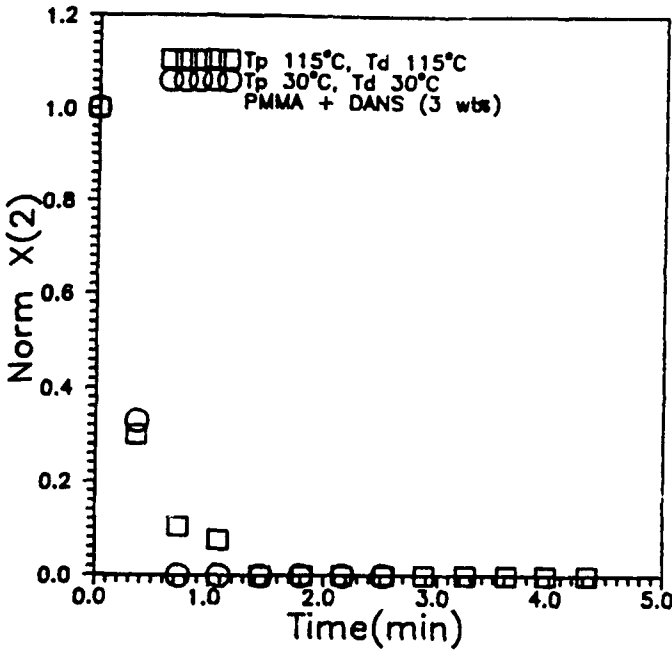


Fig. 1. Decay of $\chi^{(2)}$ upon removal of electric field. Decays are measured at the same temperature used in poling the sample. Normalized $\chi^{(2)}$ is relative to $\chi^{(2)}$ when the electric field is first removed. (Applied field = 2.2×10^4 V/cm.)

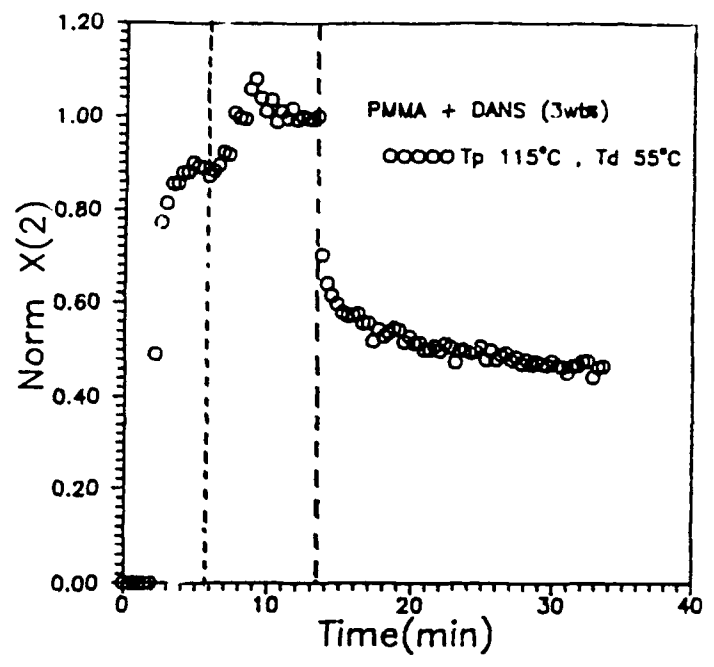


Fig. 2. Normalized $\chi^{(2)}$ for sample poled at $T = 115^\circ\text{C}$ ($0 < t < 5.7$ min), quenched (with the field applied) to 55°C (5.7 min $< t < 13.4$ min), followed by removal of the field ($t > 13.4$ min). (Applied field is the same as in Fig. 1.)

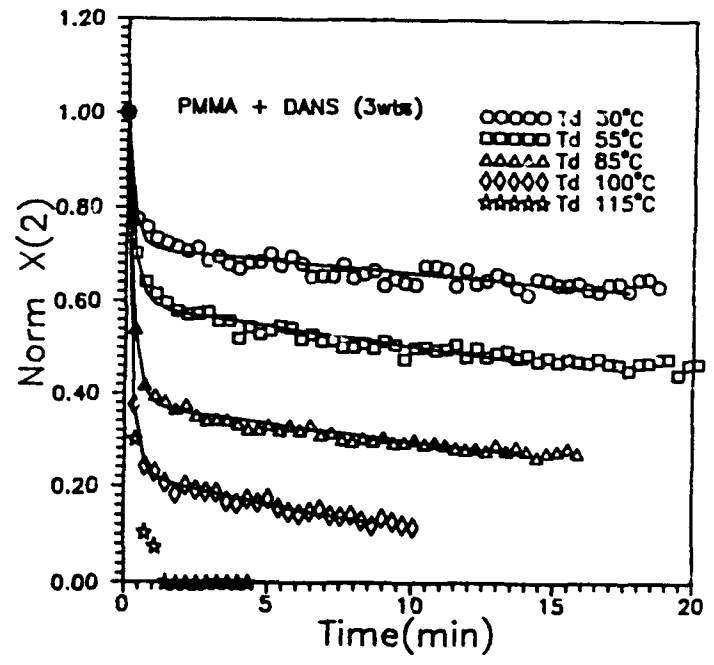


Fig. 3. Decay of normalized $\chi^{(2)}$ for samples poled at 115°C and quenched to various temperatures. (Applied field is the same as in Fig. 1.)

SECOND-ORDER NLO AND RELAXATION PROPERTIES OF POLED POLYMERS

D. Y. Yoon, D. Jungbauer, I. Teraoka, B. Reck,
R. Zentel, R. Twieg, J. D. Swalen, and C. G. Willson

IBM Almaden Research Center
650 Harry Road, San Jose, CA 95120-6099

Poled amorphous polymeric materials for second-order nonlinear optical (NLO) devices have been intensely investigated in recent years,^{1,2} owing to their advantages over conventional inorganic crystalline NLO materials, such as higher figures of merit, easy processibility into thin films, and low manufacturing cost. However, their NLO properties, arising from the noncentrosymmetry of chromophores achieved by electric-field poling above the glass transition temperature T_g , are usually subject to thermal relaxation in the glassy state.³⁻⁶ Hence, initial high values of their nonlinear optical susceptibilities tend to show a slow decay even at ambient temperature well below T_g , unless prevented by extensive chemical crosslinking.^{7,8}

The stability of the poling-induced alignment in linear epoxy polymers which incorporate one end of each NLO-active moiety to the chain backbone was recently reported.⁶ Their stability characteristics were studied in detail by relating the decay of NLO doubling coefficients to the measured decay of birefringence at ambient temperature and the dielectric relaxation results. One of the polymers has 4-nitroaniline (NA) as its NLO-active group, designated as BISA-NA (see Fig. 1).

Here we first compare the NLO and relaxation properties of BISA-NA with a new linear epoxy NLO polymer of the same chain backbone, containing relatively long rodlike chromophores of 4-amino-4'-nitrotolane (ANT), designated as BISA-ANT.⁹ It has nearly double the length of 4-nitroaniline, and its π electrons can be extended over the full length. We will then present results on new polymers containing nearly twice as large number densities of substituted aminonitrotolane NLO moieties as that in BISA-ANT.

Experimental

The detailed characterizations of the molecular weights of BISA-NA and BISA-ANT, referenced to polystyrene standards, and their glass transitions, determined by DSC, are also shown in Fig. 1.

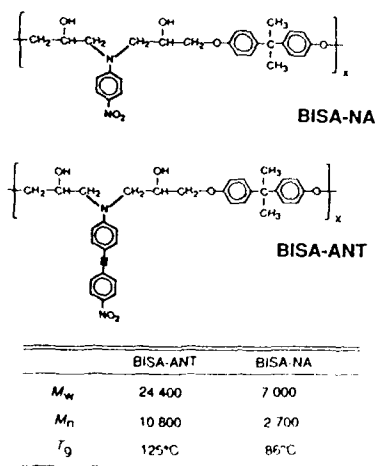


Figure 1. Molecular structures, molecular weights (referenced to polystyrene standards), and glass transition temperatures of BISA-NA and BISA-ANT polymers.

The nonlinear optical doubling coefficients d_{31} and d_{32} for the second harmonic generation (SHG) were determined from Maker-fringe measurements for incident light of 1.06 μm wavelength using a quartz reference; the details of experiments and data analyses were described previously.^{2, 5-7} A Metricon PC 2000 prism coupler was used to measure the refractive indices for *s*- and *p*-polarized light. Temperature dispersions of the dielectric response were measured in the heating process at 100Hz, 400Hz, 1kHz, 4kHz, 10kHz, 40kHz, and 100 kHz, using the HP 4274A LCR meter, employing the heating rate of 1.0 ~ 2.0 K/min.

Further details of our experimental setups and corona poling are described elsewhere.^{2, 5, 8}

Nonlinear Optical Properties

For corona poled BISA-ANT polymer, second harmonic generation at fundamental wavelength of 1.06 μm gave the nonlinear doubling coefficients $d_{31} \approx 89$ pm/V and $d_{32} \approx 25$ pm/V, respectively, from the analysis of Maker-fringe data. These values of the nonlinear susceptibility are to be compared with those of BISA-NA for which $d_{31} \approx 31$ pm/V. Among various factors which determine the doubling coefficients, the number density of NLO moieties is almost the same for both BISA-ANT and BISA-NA. Also, the ground-state dipole moment attached to the NLO moieties (4-amino-4'-nitrotolane or 4-nitroaniline) should not be much different, since its magnitude shows only a slight dependence on the NLO species when they belong to a similar class of NLO moieties.¹⁰ It appears that the larger nonlinear susceptibility of BISA-ANT can be accounted for primarily by a larger molecular hyperpolarizability due to a longer conjugation length and a larger contribution from resonance enhancement in the tolane moiety.

Decay of Poling-Induced Alignment

As discussed in detail in references 6 and 11, the change in poling-induced alignment can be followed most carefully by the birefringence Δn , defined as a difference of refractive indices between the TE and TM modes. This is due to the fact that the linear polarizability tensors of the NA and ANT moieties have their principal axes parallel to the permanent (ground-state) dipole axes. The birefringence of poled BISA-ANT polymers did not show any decay in two weeks at room temperature, whereas the BISA-NA polymer exhibited a considerable decay in birefringence at room temperature (see Fig. 2). So, we raised the temperature to 100 °C (still below $T_g \approx 125$ °C) and obtained a decay of Δn , plotted in Fig. 2. The data points are well fitted by a stretched exponential function (Kohlrausch¹²-Williams-Watts¹³ [KWW] equation):

$$\Delta n(t)/\Delta n(0) = \exp[-(t/\tau)^\beta], \quad (1)$$

with parameters $\tau \approx 448$ hrs and $\beta \approx 0.446$, plotted by the solid line in the same figure.

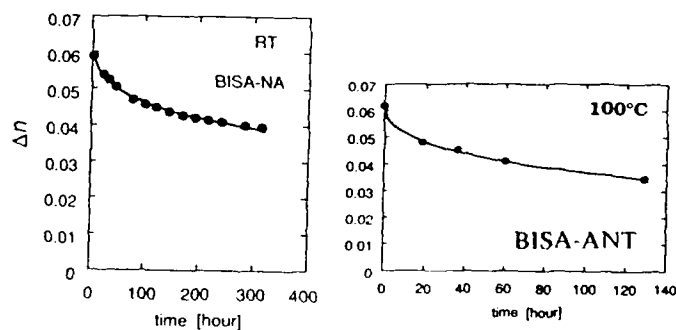


Figure 2. Decay characteristics of the birefringence Δn at 633 nm for a poled BISA-NA film (a) and BISA-ANT film (b) as a function of annealing time at room temperature and 100 °C, respectively; this decay is well fitted by a stretched exponential function, Kohlrausch-Williams-Watts equation, shown by the solid lines with the relaxation time $\tau = 2,400$ hrs and the broadening index $\beta = 0.317$ for BISA-NA and $\tau = 448$ hrs and $\beta = 0.446$ for BISA-ANT.

Dielectric Relaxations

Temperature dispersions of dielectric relaxations of BISA-ANT were measured from -70°C to 205°C upon heating. Fig. 3 shows temperature dispersions of the dielectric constant ϵ' and the dielectric loss ϵ'' for an unpoled BISA-ANT film of $1.78\ \mu\text{m}$ thickness at the frequencies indicated. Two dispersions are observed; the relaxation in the lower temperature range below T_g is denoted as β relaxation, and the higher temperature relaxation above 130°C with a large dielectric increment $\epsilon \sim 7$ is designated as α relaxation according to the well-established procedure.¹⁴

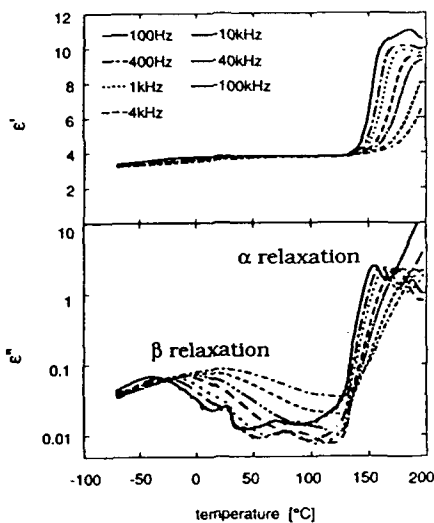


Figure 3. Temperature dispersions of the dielectric constant ϵ' and the dielectric loss ϵ'' for an unpoled BISA-ANT film measured in the heating process. The frequencies are 100 Hz, 400 Hz, 1 kHz, 4 kHz, 10 kHz, 40 kHz, and 100 kHz.

It was shown previously that for BISA-NA the peak temperatures are shifted toward lower temperatures by at least several degrees by the poling.⁶ Furthermore, this tendency was more conspicuous for thinner films, probably due to a higher electric field experienced by thinner films in a corona discharge. However, in the dielectric relaxations of BISA-ANT, we could not observe any lowering of the peak temperatures due to the poling. In Fig. 4, circles connected by solid lines represent peak temperatures T_p of α relaxation for the unpoled BISA-ANT samples. In the same figure, peak temperatures of α relaxation for the poled samples are shown by squares connected by dashed lines. Different lines are for different samples with various thicknesses. All of them show peak

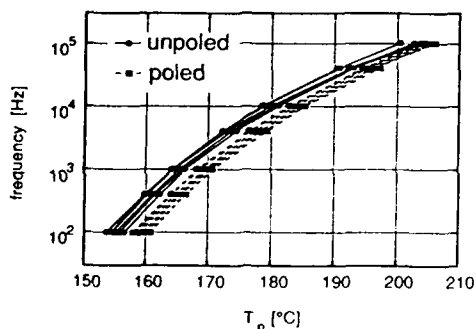


Figure 4. Plot of $\log(\text{frequency})$ vs. peak temperature T_p of the dispersions of ϵ'' for the α relaxation of BISA-ANT. Circles connected by solid lines and squares connected by dashed lines represent those of unpoled samples and poled samples, respectively.

temperatures of WLI-type. We can see clearly that the peak temperatures of the poled samples are shifted by several degrees toward higher temperatures as compared to the unpoled samples. This is in remarkable contrast to the opposite tendency observed for poled BISA-NA. Also, there was no significant dependence on the film thickness ranging between $1.2\ \mu\text{m}$ and $10\ \mu\text{m}$. This shows that the poling-induced alignment of the ANT groups is not accompanied by increased mobility. On the contrary, the poling appears to reduce the mobility of NLO moieties and raise the glass transition temperature.

Relaxation Diagram

Next we compare the time constants of the dielectric α and β relaxations of poled BISA-ANT with those of the decay in the birefringence Δn and the nonlinear optical susceptibility d_{33} at 100°C . In Fig. 4 are plotted the frequencies of both α and β relaxations of a poled sample (circles and squares) and the relaxation frequency associated with the birefringence decay (open triangle) against $1000/T$, where T is the absolute temperature. The relaxation frequency f_n associated with the birefringence decay⁶ was calculated by $f_n = 1/6\pi\tau_n$. Also shown in the same figure by closed triangle is a rough guess of the relaxation frequency f_β of the d_{33} decay, estimated from the KWW equation assuming the same value of β as obtained for the birefringence data and $f_n = 1/2\pi\tau_n$. (τ_n and τ_β are the relevant relaxation times in the KWW equation.) In Fig. 4, it is clear that the α relaxation is well extrapolated to the birefringence decay (and the d_{33} decay); the solid line in the figure is for eye-guide.

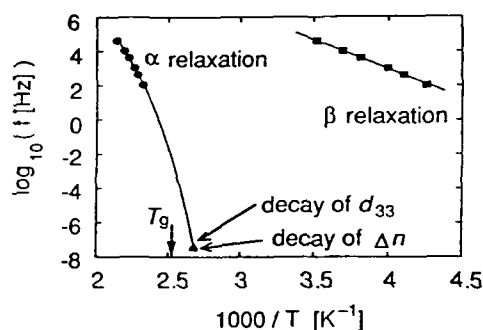


Figure 5. Relaxation frequencies of the dielectric α and β relaxation modes (circles and squares) and the relaxation frequencies associated with the decay in the birefringence (open triangle) and the d_{33} (closed triangle) for poled BISA-ANT are plotted against $1000/T$, where T is the absolute temperature.

Discussions

The longer pendant NLO moiety in BISA-ANT is responsible for the increased glass transition temperature by 40°C , as compared with that of BISA-NA. More importantly, the poling does appear to decrease the mobility associated with the glass transition for BISA-ANT, while an opposite effect was found for BISA-NA. Therefore, it seems that the poling induces more than alignment of NLO moieties in the amorphous polymers, possibly by the interaction of high electric field with the electrostatic forces and the Maier-Saupe thermotropic forces¹⁵ between the neighboring NLO moieties.¹⁶ In this regard, the decreased mobility in BISA-ANT due to poling, in contrast to the increased mobility in BISA-NA, may be attributed to the larger polarizability anisotropy of the ANT moiety, that favors parallel alignment of adjacent NLO moieties.

Consistent with this conjecture, the oligomers with double the number density of aminonitrotolane chromophores, prepared by reacting 4-amino-4'-nitrotolane (ANT) with the diepoxy containing a substituted ANT (see Fig. 6a), exhibit a smectic liquid crystalline structure.¹⁷ However, this liquid crystalline phase can be suppressed by the incorporation of chemical crosslinking by reacting this diepoxy with the tetrafunctional diamine of nitrotolane (see Fig. 6b). The resultant poled crosslinked polymer exhibited a large birefringence, as large as ca. 0.15 at 633 nm, and little decay in alignment during extended annealing at $80 - 90^{\circ}\text{C}$ for 30 days, as monitored by the birefringence results shown in Figure 6.¹⁷

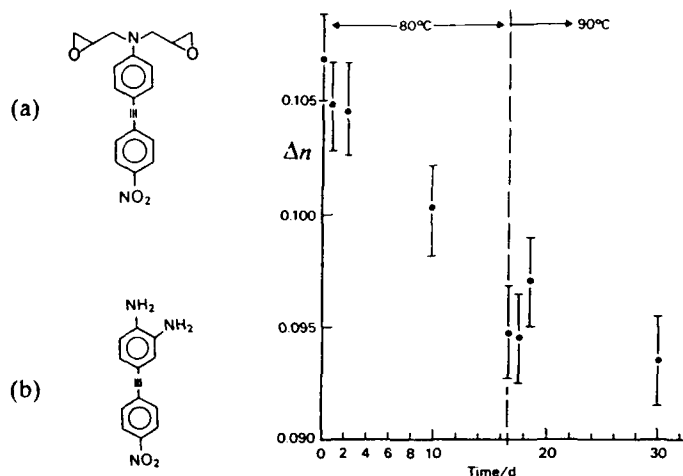


Figure 6. Schematics of the chemical structures of the dipoxy (a) and diamine (b) both containing substituted aminonitrotolane NLO chromophores, and the change in birefringence of the poled crosslinked polymer prepared by the two reactants of Figure 6, measured as the sample was annealed at 80 °C for ca. 16 days followed by annealing at 90 °C for additional ca. 14 days.

References

1. See, for example, *Nonlinear Optical and Electroactive Polymers*, P.N. Prasad and D.R. Ulrich, Eds., Plenum, New York (1988).
2. M. Eich, G. C. Bjorklund, and D. Y. Yoon, *Polymers for Advanced Technologies* 1, 189 (1990).
3. C. Ye, N. Minami, T.J. Marks, J. Yang, and G.K. Wong, *Macromolecules* 21, 2899 (1988).
4. K.D. Singer, M.G. Kuzyk, W.R. Holland, J.E. Sohn, S.J. Lalama, R.B. Comizzoli, H.E. Katz, and M.L. Schilling, *Appl. Phys. Lett.* 53, 1800 (1988).
5. M. Eich, A. Sen, H. Looser, G. C. Bjorklund, J. D. Swalen, R. Twieg, and D. Y. Yoon, *J. Appl. Phys.* 66, 2559 (1989).
6. I. Teraoka, D. Jungbauer, B. Reck, D. Y. Yoon, R. J. Twieg, and C. G. Willson, *J. Appl. Phys.*, 69, 2568 (1991).
7. M. Eich, B. Reck, D. Y. Yoon, C. G. Willson, and G. C. Bjorklund, *J. Appl. Phys.* 66, 3241 (1989).
8. D. Jungbauer, B. Reck, R. J. Twieg, D. Y. Yoon, C. G. Willson, and J. D. Swalen, *Appl. Phys. Lett.* 56, 2610 (1990).
9. D. Jungbauer, I. Teraoka, D. Y. Yoon, B. Reck, J. D. Swalen, R. Twieg, and C. G. Willson, *J. Appl. Phys.*, in press.
10. M. S. Paley, J. M. Harris, H. Looser, J. C. Baumert, G. C. Bjorklund, D. Jundt, and R. J. Twieg, *J. Org. Chem.* 54, 3774 (1989).
11. R. H. Page, M. C. Jurich, B. Reck, A. Sen, R. J. Twieg, J. D. Swalen, G. C. Bjorklund, and C. G. Willson, *J. Opt. Soc. Am. B* 7, 1239 (1990).
12. R. Kohlrausch, *Pogg. Ann. Physik* 91, 198 (1854).
13. G. Williams and D. C. Watts, *Trans. Faraday Soc.* 66, 80 (1970).
14. N. G. McCrum, B. E. Read, G. Williams, *Anelastic and Dielectric Effects in Polymeric Solids*, John Wiley and Sons, New York (1967).
15. W. Maier and A. Saupe, *Z. Naturforsch.* 14a, 882 (1959); *Ibid.* 15a, 287 (1960).
16. C. P. J. M. van der Vorst and S. J. Picken, *J. Opt. Soc. Am. B* 7, 320 (1990).
17. R. Zentel, D. Jungbauer, D. Y. Yoon, R. Twieg, and C. G. Willson, in preparation.

NONLINEAR OPTICAL PROPERTIES OF POLYMER/SILVER MICROSPHERE COMPOSITES

M.P. Andrews
Department of Chemistry
McGill University
801 Sherbrooke St. West
Montreal, Quebec, Canada
H3A 2K6

M.G. Kuzyk
Department of Physics
Washington State University
Pullman, Washington
USA

Introduction

Inhomogeneous composites of semiconductor or metallic microstructures offer new opportunities for studying optical nonlinearities as functions of size and volume fraction of the nonlinear material and guest/host chemical composition. Such studies can be combined with examinations of composite material properties including mechanical, chemical and optical stability that are important for long term applications. Recent research has explored the possibility that enormous enhancements in cubic susceptibilities can be expected from inclusions of Rayleigh limit ($<200 \text{ \AA}$) metallic spheres.^[1] The enhancement is accomplished by increasing the local field within the particle by exciting surface plasmon resonances. Quantum mechanical^[2] and mean-field (effective medium) theories^[3] have emerged to describe the response of the particle or the composite. Degenerate four wave mixing has been the dominant spectroscopic probe of media ranging from water, plastic or glass. We have chosen to study the third order response of a accessible poly(methylmethacrylate) (PMMA) composite consisting of 10-8 nm diameter silver spheres dispersed in PMMA. We introduce a new, intrinsically clean batch technique for preparing the composite by depositing atomic silver into solutions of the polymer.

Integrated nonlinear optical devices such as Mach-Zehnder interferometers and directional couplers rely on the electrooptic effect. These devices can be made from materials with third order nonlinearities. For our investigations, a quadratic electrooptic phase modulation technique was used to explore the nonlinear response of the medium.^{[4],[5]} QEO phase modulation spectroscopy appears to probe the electronic response of the surface of the spherical particles because the modulated DC field cannot penetrate the interior of the silver spheres. The polarization relevant to the optical Kerr effect would then be non-zero only at the surface of the sphere. In the present work, we show that the off-resonant third order susceptibility of a dilute dispersion of metal spheres in the polymer is much larger than the susceptibility of pure PMMA and may be attributed to electronic excitations of the metal.

Experimental

The PMMA host was selected because it is optically transparent in the region of interest in this experiment, it is commonly used to make optical devices,^[6] and it is a macroscopically rigid material suitable for stabilizing silver particles against agglomeration. PMMA (Aldrich, $M_w = 5 \times 10^4$) was purified by reprecipitation 3 times from tetrahydrofuran (THF) into hydrous methanol. The polymer was then dried at room temperature under vacuum.

The measurement of the third order susceptibility relies on a Mach-Zehnder interferometric technique. Because high electric fields are used to modulate the refractive index of the sample, conventional methods for producing silver colloids that lead to adventitious charged species cannot be used. Instead, atomic silver was evaporated quantitatively into cold, turbulently mixed organic solvent solutions of PMMA.^[7] The procedure yields silver organosols and PMMA/Ag composites directly.^[8]

The silver rod (99.998%) was obtained from Johnson-Mathey. The metal was evaporated from a Sylvania alumina coated tungsten strand spiral crucible (S1007). A quartz crystal microbalance positioned nearby was used to monitor the Ag deposition rate. Atomic silver was vaporized over periods of 0.75-2 h into 200 ml volumes of 2-5% w/v solutions of PMMA in THF,

cooled to 150 K in an evacuated rotatable glass cryostat. The rate of Ag evaporation was held constant from run to run. The total loading in the polymer depended on the duration of the evaporation. Particles grew to a maximum size of 15 nm by diffusion and aggregation in the liquid organic medium. Typically, enough metal was evaporated to give metal loadings in the PMMA of less than 0.1%. The resulting golden-yellow silver organosol was filter-cannulated at 150 K through a column of Celite A (4x5 cm) held in a special low-temperature filter flask. Pressurized argon was used to force the liquid through the Celite. A 500 ml Schlenk flask maintained at 200 K collected the filtrate. Solvent was removed with a rotary evaporator over a period of 2 h, while the flask warmed gradually to 273 K. An intensely colored orange to red-orange solid polymer film eventually deposited on the walls of the Schlenk tube. The PMMA/Ag composite was removed from this container in an argon-filled ($<2 \text{ ppm O}_2$) dry-box. The composite could be reversibly dissolved in THF and propylene glycol methyl ether acetate (PGMEA) with no evidence of decomposition or aggregation of the metal particles.

Electronic absorption spectra were collected from solid films or solution of the composite in organic solvents. Manipulations were conducted in a clean room. For the QEO measurements, a robust sample cell was fabricated. Solid PMMA/Ag composite was dissolved in PGMEA to give a final concentration of 15% w/v. An aliquot of the solution was filtered by syringe through a 0.2 micron membrane and deposited onto a glass plate patterned with transparent indium-tin-oxide (ITO) electrodes. A 3 micron thick film was spun from this solution and baked at 373 K to remove PGMEA. Two square sections were cut from the plate, overlapped and compressed in an oven programmed to cycle the sample through a temperature ramp from 298 K to well above the glass transition of the polymer (403 K). This thermal treatment bonds the ITO plates into a sandwich, providing a nearly hermetic environment for study of the polymer-metal composite.

The third order nonlinear optical susceptibility was determined with electrooptic phase modulation. The sample was placed in one arm of a Mach-Zehnder interferometer with the film perpendicular to the laser beam. The electric field polarization was in the plane of the film while the modulating field was applied with the transparent ITO electrodes perpendicular to the film plane. The experimental layout has been previously discussed.^{[4],[5]} The phase modulation results in an intensity modulation of the light out of the interferometer. An apertured silicon detector collected the light and the output was sent to a lock-in amplifier. A computer controlled interface was used to measure the amplitude of the modulated beam at both the modulating frequency and at twice the modulating frequency as a function of phase difference between the two arms of the interferometer. The relationship between the measured interferograms and the third order susceptibility is described in detail elsewhere.^{[4],[5]}

Results and Discussion

Figure 1 shows a linear absorption spectrum of the silver spheres embedded in a thin film of the polymer. The absorption profile is characteristic of the dipolar surface plasmon mode of small silver particles in a dielectric host.^[9] The arrow at 633 nm locates the frequency of the He-Ne laser used in the electrooptic modulation experiment. The absorption spectrum is fairly well reproduced by the Maxwell-Garnet expression^[8] for the absorption coefficient of the PMMA/Ag composite medium. The expression requires that the bulk dielectric function of silver be weighted by the distribution in particle size, and that the imaginary part of the dielectric function be corrected for the reduced mean free path of the conduction electrons. Figure 2 shows the particle size distribution determined from electron micrographs of films containing 0.045 weight % of silver in PMMA. Before compression, the microspheres are observed to be associated into clusters that are for the most part non-contiguous. After compression they aggregate and evolve into somewhat larger sized particles. The bright field image of the silver particles showed that they are grouped in colonies of 200 to 500 non-overlapping spheres, some of which exhibit dark bands from twin dislocations and/or stacking faults. The colonies are separated over distances greater than 100 nm. The mean particle size before processing between the ITO patterned plates is 7.9 nm, with a standard deviation of 3.6 nm. After processing we observed that both the average particle size and also the number density of particles increased. The colloid was then more evenly distributed throughout the PMMA matrix. This suggests diffusion and growth of spheres smaller than 2.0 nm in diameter

when the medium is annealed above the polymer glass transition temperature.

The film thickness in the sandwich was $d = 6.8 \times 10^{-6}$ microns and the light intensity at the detector at twice the modulating frequency ($\Omega = 4.0$ kHz) is shown as a function of phase difference in Figure 3 for an R.M.S. modulating voltage of $V_{RMS} = 83.4$ V. The arrows show the phase difference where the modulating efficiencies are expected to be the greatest as determined from the phase difference dependence of the light output from the interferometer with no modulation.

The measured value of the quadratic electrooptic coefficient of the composite is $s_{1133} = 2.0 (\pm 0.5) \times 10^{-22} \text{ m}^2 \cdot \text{V}^{-2}$. A similar measurement of pure PMMA shows that the coefficient is smaller than $s_{1133} = 4.2 (\pm 0.5) \times 10^{-23} \text{ m}^2 \cdot \text{V}^{-2}$. The laser wavelength of both measurements was at $\lambda = 633 \text{ nm}$, located away from the absorption maximum at $\lambda = 435 \text{ nm}$ (see Figure 1). Although the enhancement is expected to be much smaller here than for a resonant measurement, the third order susceptibility of the composite at low levels of loading (0.045 weight % or a volume fraction of $f = 4.5 \times 10^{-4}$) was at least 5 times larger than that of undoped PMMA.

Ricard^[1], Hache^[2] and coworkers consider two mechanisms that produce a third order susceptibility in plasmon-enhanced optical phase conjugation: an enhanced electronic susceptibility from the metal and an enhanced susceptibility of the dielectric host. They conclude that the nonlinear response is dominated by the electrons in the metal particles. More recent studies indicate that conjugate reflectivity relaxation times depend on particle size through a temperature dependent contribution to the third order susceptibility. This effect appears to be limited to particles having diameters $\geq 15 \text{ nm}$. We consider the former two effects in the off-resonant quadratic electrooptic measurement of silver-doped PMMA. The enhancement of the square of the modulating field in the polymer host at low loading gives an expression that is similar to the average dielectric function as predicted by Maxwell-Garnet theory, and is of the form

$$E_{av}^2 = E_0^2 [1 + 2/3 f \{ \epsilon - 1/\epsilon + 2 \}^2]$$

where E_{av} is the average field amplitude, E_0 the field with no metal, f the volume fraction of the metal, and ϵ is the composite medium dielectric function. Here the modulating frequency is far away from the plasmon resonance and f is so small $E_{av} \approx E_0$, and there is little enhancement. Because the third order susceptibility of PMMA is much smaller than the measured susceptibility of the composite, enhanced host effects can not account for the signal. However, there are several mechanisms that can produce an electric field dependence of the refractive index.^[4] These include electrostriction, trapped charge movement, electrode attraction, and heating. We have eliminated these sources as causes of the modulation. Our resistivity measurements revealed the current response of the sample to be independent of He-Ne laser illumination. Photoelectrons therefore do not contribute to the signal. Electrostriction effects are calculated to contribute $5 \times 10^{-26} \text{ m}^2 \cdot \text{V}^{-2}$ to S_{1133} , and so cannot account for the response. The electrooptic measurement is less sensitive to heating effects than a pulsed nanosecond pump-probe experiment. The heating contribution to the Kerr coefficient,^[5] J_{1133} , for typical modulating frequencies of 4 MHz is less than $0.3 \times 10^{-23} \text{ m}^2 \cdot \text{V}^{-2}$. Electrode attraction also cannot explain the presence of signal. The interferometric experiment is sensitive to changes in sample dimensions through a change in phase of the light. Indeed, determinations show that the contribution to S_{1133} due to electrode attraction can dominate; however, motion of the polymer film is strongly clamped by the heavy mass of the electrodes and the contribution due to changes in path length turns out to be smaller than the nonlinearity of undoped PMMA.

The third order susceptibility calculated from the quadratic electrooptic coefficient is $\chi^{(3)}_{1133} = 2.4 \times 10^{-9} \text{ esu}$.^[11] Using optical phase conjugation techniques^[1], a third order susceptibility, enhanced at the maximum of the plasmon absorption, was calculated to be $\chi^{(3)}_{1133} = 1.6 \times 10^{-14} \text{ esu}$.^[1] The enhancement factor as determined by the quotient of the phase conjugation measurement and our measurement, is 8.5×10^5 when the difference in concentration between the two samples is taken into account. This compares favorably with the predicted enhancement factor of 3.6×10^6 .^[11] The difference in the enhancement factors may be accounted for if the QEO experiment is most sensitive to changes at the surface of the spheres. We are presently examining this possibility. Precluding any other nonlinear mechanisms, it appears likely that the resonant measurement results from the electronic mechanism in the metal as predicted from Maxwell-Garnet theory as applied to the third order dielectric function.

In summary, we have used quadratic electrooptic modulation to measure the nonresonant third order susceptibility of a composite medium comprising Rayleigh-limit silver particles dispersed in PMMA. The mechanism of the nonlinearity is consistent with electronic effects intrinsic to the metal.

Acknowledgements

We thank Debbie Fish for help with sample preparation, T.T. Sheng for the transmission electron microscopy.

References

1. Ricard, D.; Roussignol, Ph.; Flytzanis, C. *Optics Lett.* **1985**, *10*, 511.
2. Hache, F.; Ricard, P.; Flytzanis, C. *J. Opt. Soc. Am. B* **1986**, *3*, 1647; Hache, F.; Ricard, D.; Flytzanis, C.; Kreibig, U. *Applied Phys. A* **1988**, *47*, 347.
3. Haus, J. W.; Kalyaniwalla, N.; Inguva, R.; Bloemer, M.; Bowden, C. M. *J. Opt. Soc. Am. B* **1989**, *6*, 797.
4. Kuzyk, M. G.; Dirk, C. W. *Applied Phys. Lett.* **1989**, *54*, 1628.
5. Kuzyk, M. G.; Sohn, J. E.; Dirk, C. W. *J. Opt. Soc. Am. B* **1990**, *7*, 842.
6. Thackara, J. I.; Lipscomb, G. F.; Stiller, M. A.; Ticknor, A. J.; Lytel, R. *Appl. Phys. Lett.* **1988**, *52*, 1031.
7. Andrews, M. P. *Using Metal Atoms and Molecular High Temperature Species in New Materials Synthesis*, in *Experimental Organometallic Chemistry*, Wayda, A. L.; Darensbourg, M. Y., Eds.; ACS Symposium Series 357; Washington, DC: 1987, ch. 7, p. 158.
8. Andrews, M. P.; Ozin, G. A. *J. Phys. Chem.* **1986**, *90*, 2929.
9. Kreibig, U. in *Contribution of Cluster Physics to Materials Science and Technology*, Devenas, J.; Rabette, P. M., Eds.; NATO ASI Series 104, Martinus Nijhoff Publ., Dordrecht: 1986.

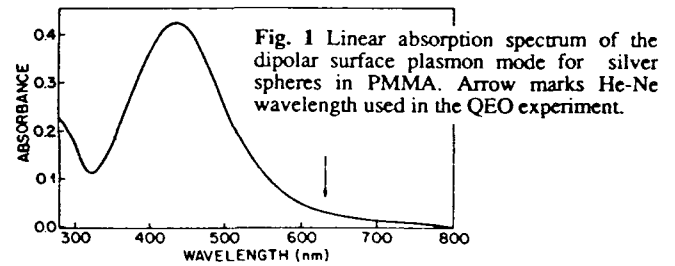


Fig. 1 Linear absorption spectrum of the dipolar surface plasmon mode for silver spheres in PMMA. Arrow marks He-Ne wavelength used in the QEO experiment.

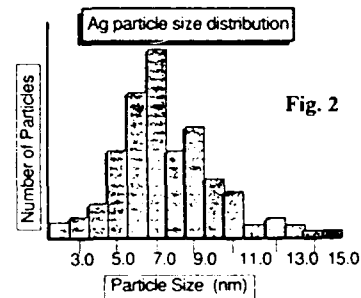


Fig. 2

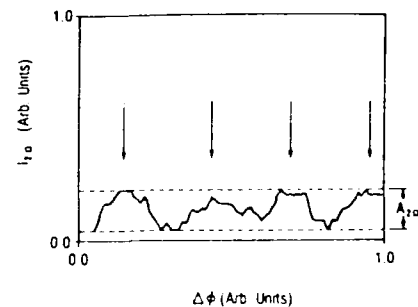


Fig. 3 Electrooptic modulation as a function of phase difference between two arms of the interferometer. Arrows show positions where phase difference is expected to be a maximum.

THE PHOTOREFRACTIVE EFFECT IN NON-LINEAR POLYMERS DOPED WITH CHARGE TRANSPORT AGENTS

J. Campbell Scott, Stephen Ducharme, Robert J. Twieg
and W.E. Moerner

IBM Research Division
Almaden Research Center
San Jose, CA

Introduction

Polymeric photorefractive materials offer a number of potential advantages over inorganic ones, particularly low cost of components, low dc dielectric constant, ease of fabrication, and compatibility with integrated optics. However until recently,^{1,2} no such materials were available. This paper describes an approach to formulating polymeric photorefractive materials, presents data which demonstrates the photorefractive effect and discusses the differences between the mechanisms involved in amorphous organic materials and in crystalline inorganic materials.³

Photorefraction occurs in certain materials which both photoconduct and exhibit second-order optical non-linearity. The effect arises when charge carriers, photoexcited by a spatially modulated light intensity, separate to produce a non-uniform space charge distribution. The resultant space charge field, via the electro-optic effect, then modulates the refractive index to create a phase grating which can diffract a light beam.

The formulation of a photorefractive polymer therefore requires the combination of chemical species to perform four physical functions: charge generation, charge transport, trapping and optical non-linearity. We have chosen to use polymers which contain covalently bonded non-linear chromophores, and to dope them with small-molecule charge transport agents. Second-order non-linearity is achieved by poling, i.e. aligning the dipolar chromophore in an electric field. Thus the polymer provides both the charge generation and the second-order non-linearity; charge transport occurs via the dopant molecules; trapping sites, although not deliberately added, turn out to be sufficiently abundant in this amorphous medium. The experimental proof that materials formulated in this way behave as expected relies on a combination of absorption, photoconductivity, electro-optic, and four-wave mixing measurements.

It should be noted that transport molecule doping of a non-linear polymer is not the only conceivable approach. One might instead dope a charge transporting polymer with a non-linear small molecule, or both species might be made part of the polymer structure. In addition, the photorefractive response could be optimized by addition of a more efficient charge generation dye or pigment (sensitizing agent⁴) and of trapping sites for the charge carriers. Our early attempts to achieve photorefraction did employ all four ingredients, but since only two are sufficient, we have concentrated on more complete characterization of the simpler system.

Materials

To date, we have results on four combinations of two different non-linear polymers and three hole transport agents. The polymers (see Figure 1) are diglycidylether derivatives of bis-phenol-A or nitroaniline partially crosslinked with non-linear chromophores which are nitroaniline derivatives. The molecular dopants are hydrazones, which because of their low oxidation potentials and extended π -electron systems, are hole transport agents.

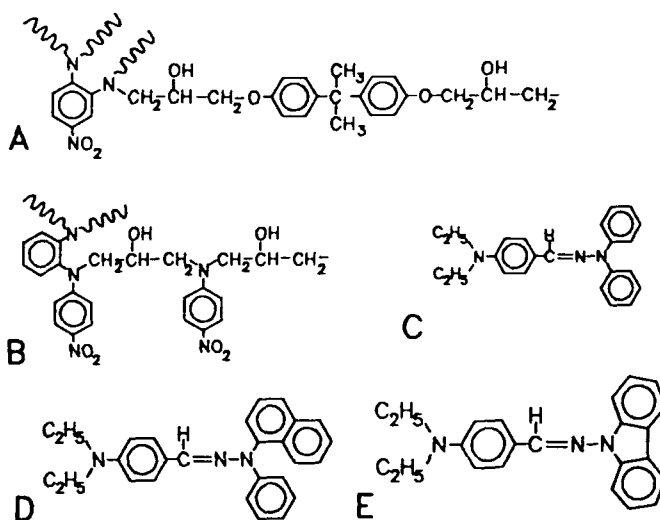


Figure 1: Polymers and transport molecules studied in this work

Polymer binders are (A) bisA-NPDA and (B) NA-APNA. Crosslinking occurs at the multifunctional amines. The transport molecules are (C) DEH, (D) DENH, and (E) DECH.

As a particular example, we report here data for the combination: DEH in bisA-NPDA.^{1,5} The component materials were dissolved in propylene glycol monomethyl ether (or its acetate) in various weight ratios and films cast by either spin or draw-bar coating techniques. For the thick (several hundred micron) films required for demonstration of grating formation, a special coating technique was used: the solution was fed drop-wise onto a two heated ITO-glass slides, with partial drying between drops, and 30 minutes of further drying and curing at 95°C when sufficient material had accumulated. Then the two glass slides were pressed together to form a sandwich structure with electrodes on either side of the polymer. Crosslinking of the epoxy groups was deliberately limited by ensuring that the samples never exceeded 95°C. Such light curing retains considerable molecular motion, and permits alignment of the non-linear moieties by an external electric field. Thus it is possible to switch on and off the electro-optic response.

Experiments and Results

Photoconductivity was measured by two different techniques. First, a conventional two electrode sandwich arrangement was used to determine the conductivity change resulting from illumination with a dye laser. Second, the rate of decay of a corona-deposited surface charge was measured. This second method gives a much more accurate determination of the conductivity at low intensity, and eliminates the possibility of sample heating. There was no significant difference between the results from the two methods.

The photoconductivity increases with concentration of DEH, up to 10^{-12} (Ωcm)⁻¹ per W/cm^2 at 30% by weight, and its spectral response follows the absorption spectrum of the NPDA chromophore. Therefore we conclude that NPDA is acting as the charge generation material, with transport occurring, as expected, via the DEH dopant molecules.

The electro-optic coefficient ($r = r_{13}\cos^2\alpha_0 + r_{33}\sin^2\alpha_0$ where α_0 is the angle between the direction of propagation and electric field) was determined in a Mach-Zehnder interferometer, reaching 90% of its long term value within a few minutes. This response can be attributed to the time required to establish equilibrium dipolar orientation of the NLO chromophore. The steady-state electro-optic coefficient, plotted as (n^3r) at each value of applied electric field is shown in Figure 2 (right abscissa).

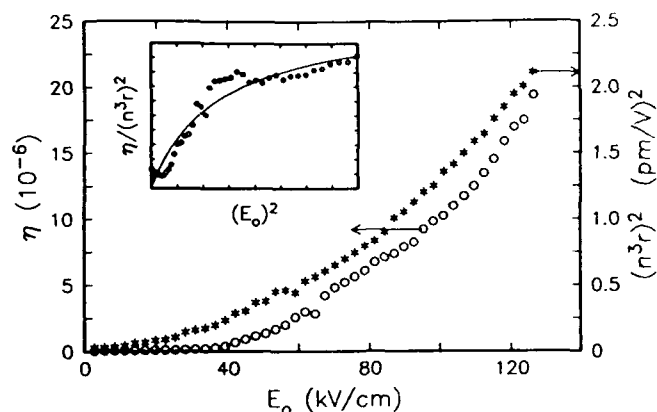


Figure 2: Electro-optic coefficient and diffraction efficiency as a function of applied electric field

The inset shows the ratio of the two quantities. The line is the fit described in the text.

Thus three of the four properties necessary for photorefraction are established by independent measurements, namely charge generation, transport and electro-optic response. We have no independent measure of the trapping, but this is provided by the photorefractive effect itself, generated as follows. Two coherent writing beams (wavelength $\lambda = 647$ nm) were incident on the sample (e.g. thickness $L = 350$ μm , between electrodes) at angles 30° and 60° on the same side of normal, such that the resulting grating had a component of its normal along the electric field. This geometry is necessary in order that the applied field assist in separation of photogenerated charges. A third, p-polarized, reading beam counterpropagated along the 60° beam, and the fraction η of its intensity diffracted (at an angle given by the Bragg condition) determined. The diffraction efficiency is shown in Figure 2.

The standard theory⁶ of diffraction for a phase grating gives $\eta = (g_1 \pi L \Delta n / \lambda)^2$ (where g_1 is a known geometric factor). The index modulation, due to the electro-optic effect, is proportional to the space charge field, ($\Delta n = \frac{1}{2} n^3 r_{\text{eff}} E_{\text{sc}}$) The effective electro-optic coefficient (r_{eff}) depends on the geometry. For diffusion only,⁷ E_{sc} has a value $E_d = k_g k T / e$ (where k_g is the grating wavenumber, and k , T , and e are Boltzmann's constant, temperature and electric charge), and on the ratio of ϵ_{13} to ϵ_{33} . The space charge is enhanced by drift in the externally applied field, with a component E_{0g} along k_g . In the standard model,^{7,8}

$$E_{\text{sc}}^2 = \frac{E_d^2 + E_{0g}^2}{(1+A)^2 + A^2(E_{0g}/E_d)^2}$$

Fitting the ratio $\eta / (n^3 r)^2 \sim E_{\text{sc}}^2$ permits the determination of the trap density $N_T = k_g^2 \epsilon \epsilon_0 k T / A e^2 = 2 \times 10^{-15}$ cm^{-3} , with $\epsilon = 2.9$ the dielectric constant. In an applied field of 126 kV/cm the space charge field reaches 26 kV/cm.

Preliminary results for several other material combinations are presented in Table 1.

It is observed that the external field is required for generation of a detectable diffractive grating. However, once the grating (i.e. the space charge field) is established the diffracted signal switches on and off with field induced poling of the sample (independent of the sign of the polarization) demonstrating that the electro-optic response is also a necessary component of the diffraction. Finally, the diffraction grating is erased, most readily in an applied field, by uniform illumination. These features, together with the independently measured photoconductivity and electro-optic response, prove that the diffraction observed is due to the photorefractive effect and not to some other mechanism such as photochromism, photochemical bleaching or isomerization.

Material Property	bisA-NPDA /DEH	bisA-NPDA /DENH	bisA-NPDA /DECH	NA-APNA /DEH
$\sigma_{ph} 10^{-12} (\Omega \text{cm})^{-1} / \text{Wcm}^{-2}$	0.06-12.0	0.02-0.7	0.33	0.2-2.8
$n^3 r$ (pm/V)	0.1-5	0.2-1	0.15-1.2	1.4-17
η	5×10^{-7} to 5×10^{-5}	4×10^{-6} to 10^{-5}	9×10^{-6}	1.2×10^{-5} to 1×10^{-3}
at field (kV/cm)	125	110	110	85

Table 1: Photoconductivity, electro-optic and diffraction efficiency data for several materials combinations

Discussion

Several of the details of the photorefractive mechanism must be different in these organic polymers than in the inorganic crystals studied most extensively to date.³ Charge generation is expected to be highly field dependent, with Onsager behavior⁸ modified by the hopping transport in the surrounding matrix. The mobility is relatively low (e.g. DEH in polycarbonate has a mobility of 10^{-7} to 10^{-6} cm^2/Vs for this concentration range at room temperature⁹) and may set a limit to the speed of response. Traps have not been deliberately added to the materials discussed here, but are presumably provided by defects intrinsic to the amorphous state. Lastly, the second-order nonlinearity appears only when the polymer is poled to break its inversion symmetry. In this work, we have taken advantage of ability to turn the polarization on and off in a material with a low glass transition temperature. The dipolar relaxation is highly dispersive. It is also possible to freeze in permanent polarization by fully curing the epoxy in the presence of an electric field⁵ or by using other optically non-linear binders poled above a high glass transition temperature.

References

1. S. Ducharme, J.C. Scott, R.J. Tweig and W.E. Moerner, Phys. Rev. Lett. **66**, 1846 (1991).
2. The photorefractive effect has also been observed in a doped organic crystal: K.Sutter and P. Gunter, J. Opt. Soc. Am. B **7**, 2274 (1990).
3. P. Günter and J.-P. Huignard *Photorefractive Materials and Their Applications*, Vols I and II (Springer Verlag, Berlin, 1988, 89).
4. The sensitization of non-linear polymer has been described by J.S. Schildkraut, Appl. Phys. Lett. **58**, 340 (1990).
5. M. Eich, B. Reck, D.Y. Yoon, C.G. Willson and G.C. Bjorklund, J. Appl. Phys. **66**, 3241 (1989).
6. H. Kogelnik, Bell Syst. Tech. J., **48**, 2909 (1969).
7. V.L. Vinetskii and N.V. Kukhtarev, Sov. Phys. Solid State **16**, 2414 (1975).
8. A. Twarowski, J. Appl. Phys. **65**, 2833 (1989).
9. J.X. Mack, L.B. Schein and A. Peled, Phys. Rev. B **39**, 7500 (1989).

SECOND-HARMONIC GENERATION FROM HYPERPOLARIZABLE AMPHIPHILES AT POLYMER-POLYMER INTERFACES

Jian Ping Gao and Graham D. Darling*

Department of Chemistry, McGill University

801 Sherbrooke St. W., Montreal, QC, Canada H3A 2K6

INTRODUCTION

Organic molecules with conjugated π -bonds connecting electron-donating to electron-withdrawing groups possess large hyperpolarizabilities (β). Efficient second-harmonic generation (SHG) becomes possible only if such molecules are arranged in a non-centrosymmetric fashion. Past approaches to such arrangement used materials which spontaneously form non-centrosymmetric crystals or liquid crystals, or which have been "poled" in strong electric fields; or oriented thin films, self-assembled or deposited with a Langmuir-Blodgett apparatus¹⁻³. We report here the preparation, by a relatively simple and inexpensive spin-coating technique, of robust SHG-active samples in which amphiphilic hyperpolarizable molecules are permanently oriented between solid layers of hydrophobic and hydrophilic polymers.

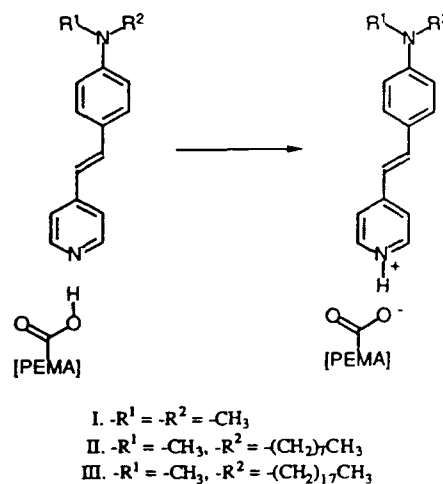
EXPERIMENTAL

Organic dyes shown in Fig. 1 were synthesized and characterized according to literature procedures⁴. Poly(ethylene/maleic acid) ("PEMA") solution was prepared by dissolving 10% w/w of commercial 1:1 ethylene/maleic anhydride copolymer (Aldrich) in distilled water and filtering through a 0.45 μm membrane. Samples for SHG measurements were prepared thus: a few drops of PEMA solution were placed on a circular glass cover slip (Fisher, 18 mm x 0.21 mm), which was then spun at 3000 rpm for 2 min., and dried at 20°C under vacuum for 1 hour to give a smooth and uniform clear coating about 0.5 μm thick (Dektak profilometer). The film was then wetted with 0.1-0.2 mL of dye solution (0.01-0.05% w/w in MeOH:toluene 1:9), spun dry, rinsed with toluene, dried by spinning and in vacuo. Polystyrene ("PS"; Sp² Inc. "45,000 g/mol") was overlaid in similar fashion from a 10% w/w toluene solution.

Contact angle was measured by the sessile-drop method with a home-made video microscope system (Concordia University, Montreal), using 1 μL drops of distilled water measured within 4 seconds of application.

SHG measurements were made using s- or p- linear polarized light from a Q-switched Nd-YAG laser (1064 nm, 10 ns pulse duration, 5 mJ pulse energy) directed at a 45° angle onto the sample. The SHG signal $I_{2\omega}$ (532 nm) was isolated and resolved into p- and s- polarized components using 3 interference filters and a polarizer, and quantitated by a photomultiplier (Hamamatsu R928). Each output signal was normalized by dividing by the square of the corresponding input signal, as measured with a photodiode.

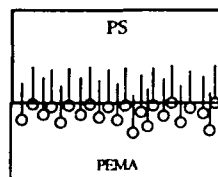
Figure 1. Structures of Hyperpolarizable Amphiphilic "Dyes"



RESULTS & DISCUSSION

Scanning electron micrographs (75,000X, Au + Pd coating), front-on and in cross-section, confirm the surface of PEMA films to be very flat and smooth both before and after application of dye. The change in colour from yellow to red-orange ($\lambda_{\text{max}} = 470 \text{ nm}$) confirms protonation of the basic dye as it bonds (ionically) to the acidic hydrophilic polymer; this "chemisorbed" species tenaciously remains while toluene easily washes away the excess free dye. The optical density ($\lambda = 470 \text{ nm}$) of the final coloured film increases from 0.05 to 0.30 with increasing content of dye and/or methanol (in which the hydrophilic polymer is soluble) in the colouring solution ($\text{O.D.}_{470} = 0.02$ in known monolayers of similar molecules⁵ - hence, Fig. 2). Spectral characteristics (and SHG intensity) of the dye change little with application of the PS layer, which, besides providing a sharply distinct hydrophobic environment for "solvation" of long alkyl tails to induce (with hydrophilic PEMA) net orientation of the amphiphilic dye, can also act as a protective coating for the "active" dye layer, as a substrate upon which to deposit further PEMA/dye/PS layers for multiplied SHG efficiency in the "vertical" direction (Figure 2); and as a medium for "horizontal" propagation/SHG of IR/visible light ("organic waveguide").

Figure 2. Arrangement of Dye Molecules at Interface



Contact angles θ which start (Table 1) and remain (with time) large for dye-treated films confirm the presence of coatings which are outwardly hydrophobic ("water-repellant"), particularly with longer alkyl chains (Dye III).

Table 1. Contact Angle θ of PEMA Films Before and After Dye Treatment

Film	PEMA	PEMA-I	PEMA-II	PEMA-III
θ	35-40°	50-55°	75-80°	85-90°

SHG signals $I_{2\omega}$ of PEMA-I,II,III films in p-p and s-p geometries at 45° incident angle were recorded and compared. The relative intensities were: PEMA-III > PEMA-II >> PEMA-I. Glass or glass-plus-PEMA alone showed no SHG. The PEMA film coloured with dye I (shortest alkyl) showed only a very weak SHG signal. $I_{2\omega}$ values of PEMA-II and -III fluctuated between zero and maximal intensities as incident angles were varied. Under the assumptions of β_{zzz} being dominant and a sharp distribution of the molecular axes characterized by an angle α (tilt angle) from the perpendicular, Eqn. 1 applies⁶:

$$\frac{I_{2\omega}^{p-p}}{I_{2\omega}^{s-p}} = \frac{[(2/\tan^2\alpha) - 1]^2}{8} \quad \text{Equation 1}$$

Our results show that this ratio is between 5 and 3 for PEMA-III and PEMA-II, implying an average orientation angle α in the range of 28-30° from the vertical, which compares favourably with materials prepared by Langmuir-Blodgett techniques^{3,6,7}.

In summary, we have demonstrated a very simple method to prepare thin films with second-order nonlinear optical properties. The results suggest that amphiphilic dyes II and III are adsorbed on PEMA surface in an oriented fashion, with a certain degree of penetration of the hydrophilic end, and with the long alkyl chain extending to the top of the surface (Fig. 2).

ACKNOWLEDGMENTS

Special thanks are due to Physics professor J. F. Lee for laser time and technical assistance. Thanks also to A. Eisenberg, D. Simkin, F. Buchinger and J. Wang for the use of equipment, and to Dr. J. Y. Yuan for useful discussions. This work was supported by the Natural Sciences and Engineering Research Council of Canada.

REFERENCES

- (a) Bosshard, C.; Kupfer, M.; Gunter, P.; Pasquier, C.; Zahir, S.; Seifert, M. *Appl. Phys. Lett.* y1990 v56 p1204. (b) Lupo, D.; Prass, W.; Scheunemann, U.; Laschewsky, A.; Ringsdorf, H.; Ledoux, I. *J. Opt. Soc. Am. B* y1988 v5 p300. (c) Cross, G. H.; Peterson, I. R.; Girling, I. R.; Cade, N. A.; McRoberts, A. M.; Scrowston, R. M.; Toyne, K. J. *Thin Solid Films* y1988 v156 p39.
- (a) Singer, K. D.; Kuzyk, M. G.; Sohn, J. E. *J. Opt. Soc. Am. B* y1987 v4 p968. (b) Park, J.; Marks, T. J.; Yang, J.; Wong, G. K. *Chem Mater.* y1990 v2 p229.
- Li, D.; Ratner, M. A.; Marks, T. J. *J. Am. Chem. Soc.* y1990 v112 p7389.
- Kost, A. N.; Sheinkman, A. K.; Rozenberg, A. N. *J. Gen. Chem. USSR (Engl. Transl.)* y1964 v34 p4106.
- Steinhoff, R.; Chi, L. F.; Marowsky, G.; Möbius, D. *J. Opt. Soc. Am. B* y1989 v6 p843-847.
- Marowsky, G.; Gierulski, A.; Steinhoff, R.; Dorsch, D.; Eidenschnik, R.; Rieger, B. *J. Opt. Soc. Am. B* y1987 v4 p956.
- Williams, D. J.; Penner, T. L.; Schildkraut, J. J.; Tillman, N.; Ulman, A.; Willand, C. S. In *Nonlinear Optical Effects in Organic Polymers*; J. Messier et al, Eds.; Kluwer Academic Publishers: Boston y1989 p195-218.

Yasuhiro Koike and Eisuke Nihei

Faculty of Science and Technology
Keio University, Yokohama 223, Japan

INTRODUCTION

There has been considerable interest^{1,2} in the development of a polymer optical fiber (POF) as a short distance communication such as local area network (LAN), datalink, ultranodded bus network, etc., because of its easy processing and handling. In short distance communication, many junctions and connections of optical fibers would be necessary. In the single-mode glass fiber, the core diameter is about 5 μm, so when connecting two fibers a slight amount of displacement such as ± a few μm causes a significant coupling loss. Polymer optical fiber with a large diameter such as 1 mm is one of the promising candidates to solve this problem. However, all commercially available POFs have been of the step-index (SI) type. Therefore, even in short-range optical communication (e.g. indoor use), the SI POF will not be able to cover the whole bandwidth of the order of hundreds of MHz which will be necessary in LAN, or datalink, because the bandwidth of the SI POF is only about 5MHz·km.

On the other hand, graded-index (GI) POF is expected to give a much higher bandwidth than that of SI POF, while maintaining a large diameter. In this paper, the author describes a graded-index POF in which the bandwidth is more than 500MHz·km, and a single-mode POF which has been developed by us very recently.

GI POLYMER OPTICAL FIBER

In the SI POF, lights pass through the fiber by reflecting off the wall at different angles, which spreads an impulse over time interval that is equal to the difference of the arrival times of the slowest and fastest modes. On the other hand, in the GI POF, if the index profile is optimum, all modes propagate at the same velocity without spreading an impulse, which remarkably increases the bandwidth.

It is well known that the bandwidth can be maximized by optimizing the shape of the graded-index distribution of the fiber core. When the index distribution is expressed by a power law of the form

$$n(r) = n_0 [1 - (r/a)^\alpha \Delta] \tag{1}$$

the bandwidth is maximized for

$$\alpha = 2 - (12/5) \Delta \tag{2}$$

where this formula Δ is a parameter that measures the relative-index difference, Δ = (n₀ - n_c)/n₀, where n₀ and n_c are the index values at the core center and in the fiber cladding respectively, and a is the radius of the core. The parameter α is the exponent of the power law. Since Δ is 0.01-0.02 for the GI POF, the maximum bandwidth is achieved when α is about 2.

Such a GI POF has been developed recently at Keio University^{3,4}. The GI preform rod is obtained by the interfacial-gel copolymerization process³, and is heat-drawn at 190-280 °C into the GI POF. A pure PMMA tube filled with M₁ and M₂ monomer mixture is placed in a furnace at 80-100 °C. As the inner wall of the polymer tube is slightly swollen by the monomer mixture, then a gel phase is formed on the inner wall of the tube. It is well known that the reaction of the polymerization is accelerated in the gel state. Then, the polymer is gradually formed from the inner wall of the tube, finally solidifying up to the center axis of the tube.

The refractive index distribution is obtained by the following two mechanisms: The M₂ monomer which has a higher refractive index than that of the M₁ monomer is gradually concentrated in the center region of the tube. The other

mechanism is the gradual diffusion of the PMMA molecules dissolved from the PMMA tube into the center region. Here MMA is used as the M₁ monomer, and vinyl benzoate (VB), vinyl phenylacetate (VPAC) or benzyl methacrylate (BzMA) etc. are used as the M₂ monomer.

The refractive index distribution of the GI POF for the MMA-BzMA monomer system is shown in Fig.1, in which the monomer feed composition, MMA/BzMA (wt/wt), is 3, 4, and 5, respectively. Here R_p is the radius of the fiber. The preform rods of these GI POFs were polymerized at 95 °C for 24h. The normalized index distributions of these fibers are almost the same as those of the preform rods.

The bandwidth of the GI and SI POFs was measured as follows: A pulse of 10-MHz from an InGaAlP laser diode (wavelength = 670 nm) was injected (N.A.=0.5) into a 20-m length fiber. The output pulse was detected by a sampling head. The result for the MMA-BzMA GI POF is shown in Fig.2, compared with the commercially available SI POF. Although the output pulse through the 20-m length SI POF is quite spread, the pulse through the GI POF is almost the same as the input pulse.

The bandwidth of the SI POF estimated at 3dB level in pulse-response-function is 6 MHz·km, while the bandwidth of the MMA-BzMA GI POF in Fig.2 is about 500 MHz·km. Figure 3 summarizes the normalized bandwidths of the various GI POFs

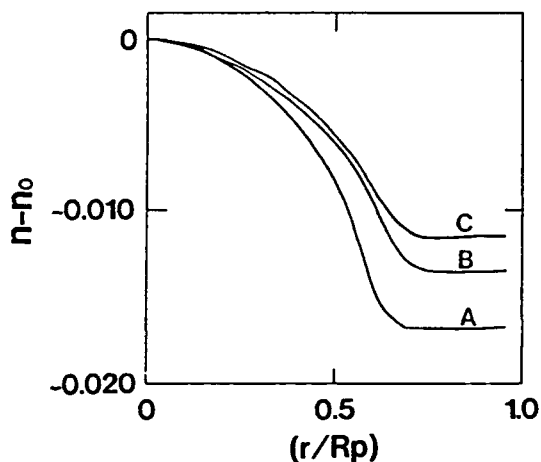


Fig.1. Refractive-index distribution of the MMA-BzMA GI POF. Monomer feed composition MMA/BzMA (wt/wt): (A), 3.0 (wt/wt); (B), 4.0 (wt/wt); (C), 5.0 (wt/wt).

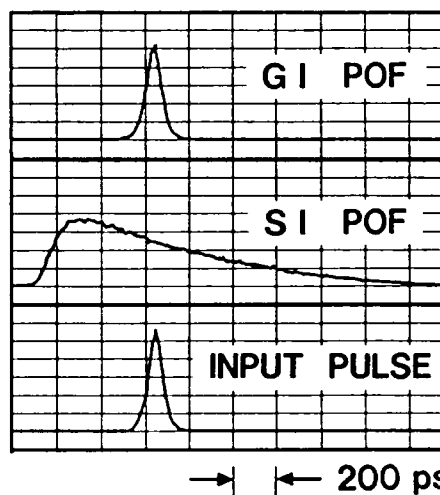


Fig.2. Bandwidth measurement by spreading of the output pulse through both GI and SI POFs with a 20-m length.

against the α in Eq.(2), along with that of the SI POF. The bandwidth around $\alpha = 2$ achieved by the MMA-BzMA fiber is about 500MHz·km which is one hundred times larger than that of the SI POF.

The total attenuation of the light transmission through these GI POFs is 150–200 dB/km at 652-nm wavelength. It should be noted that these values are comparable with the attenuation (100–300 dB/km) of the commercially available SI POF. The MMA-BzMA GI POF is especially flexible and the tensile strength is 1600 kg/cm² which is comparable to that of the commercially available SI POF.

SINGLE-MODE POLYMER OPTICAL FIBER

A single-mode POF in which the core diameter was 3–15 μ m and the attenuation of the transmission was about 200 dB/km at 652-nm wavelength was successfully obtained⁵. As far as we know, this is the first single-mode POF.

The basic mechanism for forming the index distribution in the preform rod of the single-mode POF is the same as in the GI POF. The preform rod which was heat-treated to complete the polymerization was heat-drawn at ca. 200°C to obtain the single-mode POF (One-step process). When the core diameter was larger than the single-mode condition, the resulting fiber was inserted into a PMMA tube, filling gaps with MMA monomer, and this was polymerized. This second preform rod was again heat-drawn into the fiber to satisfy the single-mode condition (Two-step process).

Figure 4 shows the end-surface of the single-mode POF with a 50-m length and the intensity display of the core, in which the fiber diameter is 600 μ m and the attenuation of the transmission at 652 nm wavelength was 190 dB/km. Figure 5 shows the index distribution of the POF prepared by the two-step process as follows: The graded-index (GI) preform rod was prepared by the interfacial-gel copolymerization technique under the condition of MMA/BzMA=4/1(wt/wt) and was heat-drawn into the GI POF, followed by the two-step process mentioned above to obtain the single-mode POF. The core and clad diameters are 5 μ m and 250 μ m respectively, and the index difference Δn is ca. 0.003, which satisfies the single-mode condition (V parameter), Eq.(3):

$$V = \pi \frac{2a}{\lambda} \sqrt{2\Delta} < 2.405 \quad (3)$$

where a is the radius of the core and λ is the wavelength of the light. Equation (3) is for the case in which the core index distribution is of an SI type. Since the index distribution of the fiber in Fig.5 is of a GI type single-mode, the cut-off wavelength is shorter than the value estimated by Eq.(3). The single mode was also confirmed by the far field pattern measurement.

CONCLUSION

It is experimentally and theoretically confirmed that the GI POF is quite superior to the conventional SI POF in the bandwidth, while the attenuation and mechanical properties of both fibers are comparable. The low-loss single-mode POF in which the core diameter was 3–15 μ m was successfully obtained, we believe, for the first time.

REFERENCES

1. C.Emslie, J. Mater. Sci., 23, 2281 (1988).
2. W.Groh, D.Lupo, and H.Sixl, Angew. Chem. Int. Ed. Engl. Adv. Mater., 28, 1548 (1989).
3. Y.Koike, E.Nihei, N.Tanio, and Y.Ohtsuka, Appl. Opt., 29, 2686 (1990).
4. Y.Koike, E.Nihei, and Y.Ohtsuka, ECOC'90, Amsterdam, Vol.1, 513 (1990).
5. Y.Koike and E.Nihei, Soc. Polym. Sci. Japan, Spring Meeting (1991).

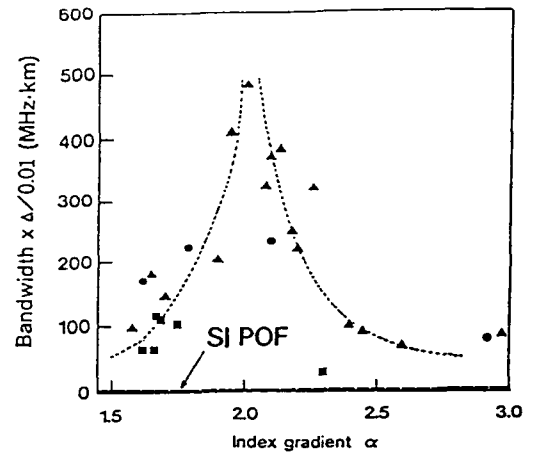


Fig.3. Bandwidth of the GI POFs against the exponent of the power law in Eq.(2). (●), MMA-VB system; (▲), MMA-BzMA; (■), MMA-VPAC.

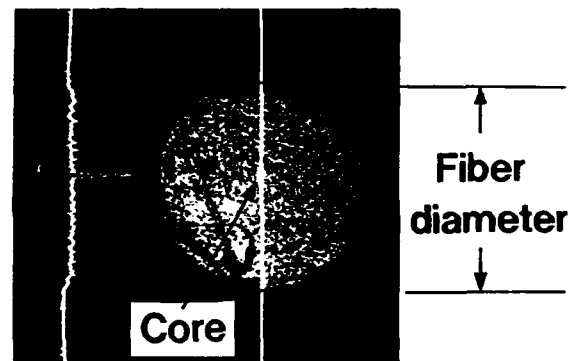


Fig.4. Photograph of the end-surface of the single-mode POF. The fiber diameter is 600 μ m.

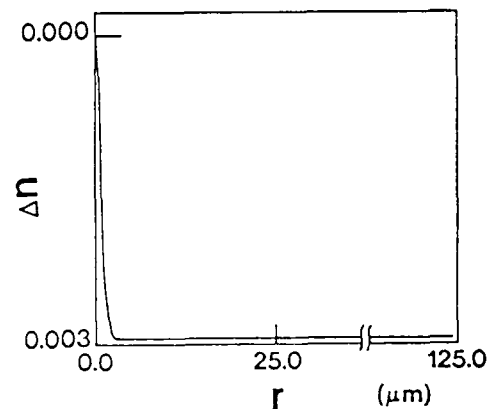


Fig.5. Representative index-distribution of the single-mode POF.

PLANAR POLYMER WAVEGUIDES FOR OPTICAL INTERCONNECTIONS

by
B. L. Booth, J. E. Marchegiano, C. T. Chang, T. K. Foreman,
J. L. Hohman, S. L. Witman
E. I. du Pont de Nemours & Co. (Inc.)
Wilmington, Delaware 19880-0357

Optical interconnect technology is being increasingly considered as necessary to resolve the bottlenecks resulting from high circuit densities, multiple pin outs, high data and processing rates, electromagnetic interference, and the growing demand for data and services. To satisfy these applications low-cost, versatile optical and system performance capabilities are required involving backplane-to-backplane, board-to board, and within-board optical interconnections utilizing optical fibers, connectors and integrated optics. A number of polymeric materials have been explored for integrated optical systems that indicate considerable potential to meet many perceived requirements. This paper reviews the polymer integrated optic system technology referred to as Polyguide* that is currently under development at Du Pont. Polyguide refers to a core technology currently employing a polymeric binder and acrylate monomers precast on Mylar® polyester film carrier layers. Using multilayer lamination techniques, a symmetric structure is assembled around an embedded waveguide photolithographically created by a UV-to-blue light exposure process. A specific effort will be made to relate polymeric properties to the resulting optical or applications-specific requirements. The intent is to demonstrate the versatility of polymers and, specifically, Polyguide for integrated optical interconnection applications.

A high-index waveguide region results from photopolymerization-induced monomer diffusion into the polymerizing guide region through the exposed waveguide layer. The core technology noted above plus solvent-free photopolymerizable liquid Polyguide formulations (LPG) and excimer-laser machining all combine to provide a broad range of optical, physical, and mechanical properties. Formulation and process variations exploit the broad and unique properties of Polyguide to satisfy diverse integrated optical interconnect requirements.

Creation of the waveguide regions in Polyguide is achieved by lamination of the waveguide-forming layer directly to the photomask, followed by waveguide exposure. This initiates a primary diffusion reaction whereby monomer and other low-molecular-weight constituents move into the guide region. A secondary diffusion reaction results when Polyguide buffer layers of similar or different formulation are laminated on both sides of the waveguide layer, having removed both the mask and the Mylar® carriers. These buffer layers come from adjoining regions of the cast material roll and are thus identical in thickness, ensuring a highly-centered buried waveguide. Diffusion from these layers further enhances the magnitude and profile of the refractive index of the waveguide relative to the surround. The structure is then totally photopolymerized, followed by the addition of subsequent layers, creating different adhesion and/or mechanical properties. Process control is achieved through exposure energy, power, temperature, and time variations which can directly modify the diffusion into the guide region.

Singlemode guides are typically around 7 μm thick and 6 to 7.5 μm wide. The refractive index of the guide relative to the surround is approximately 0.004 at 1300 nm. This is essentially equivalent to the relative core-to-cladding index of glass optical

fibers to optimize guide-to-fiber optical coupling. Multimode guides typically have 50- μm -square cross sections with a relative guide index in excess of 0.04, through use of higher-index constituents such as aromatic monomers, and process conditions with higher temperatures and exposure levels for enhanced diffusion. Exposure energies range from 10 to 100 mJ/cm^2 for the initial primary exposure. The ratioing of monomers of different molecular structure and functionality combined with selected process conditions noted above results in excellent guide-index control. Excellent waveguide properties, as well as performance of all splitting and coupling functions, have been achieved for both multimode and singlemode waveguiding and will be summarized in the presentation.

The primary critical issue for creating practical optical interconnects is the ability to effectively couple light between two waveguides, between waveguides and fibers, and between waveguide and electro-optic components. Matching of both the in/out optical cross sections referred to as overlap and the allowed angle of guide propagation or numerical aperture is required for efficient coupling from one guiding system to another. Compromises must be made to achieve overall system optimization since, typically, waveguides may have a higher numerical aperture than fibers to facilitate, for example, high-radius-of-curvature guides and maximize input coupling of diode laser light.

Fiber-to-waveguide self-alignment is achieved in Polyguide by first creating and then inserting the fiber in an open square alignment channel. This is accomplished by first excimer-laser ablating at 248 nm a 500- μm -long by 120- μm -wide slot in a 120- μm -thick structure containing a centered buried waveguide. All these dimensions are tolerant to plus or minus several microns. Thick outer layers are then laminated on top and bottom of the waveguide structure. This creates a square opening with the waveguide located precisely ($\pm 0.5 \mu\text{m}$) in the center with $\pm 0.2^\circ$ angular deviation. A beveled 125- μm glass fiber is inserted into the smaller, nominally 120- μm , square channel, which provides equal self-centering pressure for alignment. The fiber is bonded permanently with a silanated photopolymerizable and/or thermally polymerizable LPG to complete the low-optical-loss, robust coupling. The process is amenable to automation and thus low cost.

Waveguide-to-waveguide coupling is achieved using ablated slots described above without the laminated outer layers. Slots at the ends of two buried waveguide structures are inserted into each other when they are first oriented at 90° . This form of waveguide-to-waveguide "slot" coupling permits construction of optical board-to-board coupling systems and connectors which will be described in the presentation.

Diode lasers have been embedded and permanently interfaced, via LPG, directly to waveguides, enabling construction of robust components and connectors. Performance of these systems will also be reviewed.

The permanent attachment of Polyguide waveguide structures to both ceramic and fiber-reinforced circuit board materials has been achieved that is stable over a -65°C to 150°C range. No change in optical propagation of the guides has been observed with these configurations. Low-modulus formulations were developed to buffer the widely different thermal expansion coefficients associated with board attachment. Additionally, using cross-linked Polyguide, heat spiking for 30 seconds, typically used for IR solder operations to attach surface mount electronic components, has demonstrated no loss in guide properties with repeated cycles to 230°C . Compatibility with higher spike temperatures appears likely and is under investigation. Finally, to optically interface surface mounted electronic components on boards to optical waveguide layers, excimer-laser-ablated reflecting mirrors are constructed and are under ongoing investigation.

* Du Pont trademark

Overall, a number of formulation variations readily available to the Polyguide system have been developed and utilized to achieve the results for singlemode and multimode waveguiding, interconnection, and board-associated applications. Although Polyguide technology is still evolving, to date we have created a versatile polymeric approach to form integrated optical interconnects, connectors, and components, with a goal of demonstrating real-world applications. The Polyguide system capitalizes on the significant potential of polymer chemistry to create, in a dry, light-exposure-induced process, well-controlled, interconnectible waveguides highly compatible with many electronic processing and optical requirements.

Guided-wave nonlinear optics in DCANP Langmuir-Blodgett films

P. Günter, Ch. Bosshard, M. Küpfer and M. Flörsheimer

Institute of Quantum Electronics, Nonlinear Optics Laboratory, Swiss Federal Institute of Technology, ETH Hönggerberg, CH-8093 Zürich, Switzerland

2-Docosylamino-5-nitropyridine (DCANP) is a molecule displaying strong nonlinear optical effects in Langmuir-Blodgett (LB) films. DCANP is a molecule having a chromophore which is tilted with respect to the long chain alkyl axis used for ordering the molecules before deposition. LB films made from these tilted chromophore molecules (TC-molecules) can have a net dipole moment in the plane of the substrate which is advantageous for the deposition of high quality multilayer films. Its linear and nonlinear optical properties have been described in [1] and [2]. Due to its ability to form multilayers (up to 600) of high optical quality, waveguiding with low attenuation has been observed in these films [2].

We will review the preparation of DCANP LB films and its physical properties, including the measurement of dispersion of refractive indices, nonlinear optical susceptibilities and waveguide attenuation losses. For the first time guide-wave second-harmonic generation of Nd:YAG lasers in a nonlinear optically active LB film will be reported. The first waveguiding experiments were carried out using a grating coupler. The grating was first etched into the pyrex substrate through ion etching. Subsequently the LB film was deposited with the dipping direction parallel to the grating grids. TM_0 - and TE_0 -modes were observed for layer thicknesses between 177 nm and 442 nm.

Phase-matched frequency-doubling was investigated in these LB films employing the Cerenkov-type configuration. This method is simpler than phase-matching of guided modes where very strict conditions on the waveguide thickness are required and where both fundamental and second-harmonic waves have to be guided. In Cerenkov-type phase-matching with DCANP only the fundamental beam is guided in the LB layer, whereas the second-harmonic beam is radiated into the substrate. Since the charge-transfer axis of the DCANP molecules lies in a plane parallel to the dipping direction, the largest nonlinear optical coefficient $d_{33} = 8$ pm/V could be used with guided TE modes. Experiments at different wavelengths and waveguide dimensions and efficiency studies of the frequency-doubling process were performed. In addition the dipping process was adjusted for optimized waveguiding.

- [1] G. Decher, B. Tieke, Ch. Bosshard and P. Günter, *Ferroelectrics* **91**, 193-207 (1989)
- [2] Ch. Bosshard, M. Küpfer, P. Günter, C. Pasquier, S. Zahir and M. Seifert, *Appl. Phys. Lett.* **56** (13), 1204-1206 (1990)

OPTICALLY NONLINEAR POLYMERS IN
WAVEGUIDING PASSIVE AND ACTIVE DEVICES

by
G.R. Möhlmann and W.H.G. Horsthuis
Akzo Research Laboratories Arnhem, Corporate Research,
P.O. Box 9300, 6800 SB Arnhem, The Netherlands

Introduction: Optically nonlinear side chain polymers, containing hyperpolarizable molecules as the side groups, have been developed over the past years. These optically nonlinear (nlo) polymers have been applied for making electro-optically active devices [1,2]. In electro-optic devices, the nlo-active material exhibits a shift of refractive index if placed in electric fields thus influencing the propagation and permitting the manipulation of light; in this way, optical functions can be performed.

Polymeric nlo-devices such as phase shifters, Mach-Zehnder interferometers, directional mode couplers, etc., are usually made by starting with a multilayer sandwich structure containing the nonlinear polymer, in which channel waveguides can be realised via UV irradiation. By electric field poling of the polymer in the sandwich, electro-optic coefficients in excess of 20 pm/V have been induced. Device switching and modulation voltages achieved, are of the order of 10 Volts; the corresponding modulation ratio's are in excess of 10 dB. By applying different nlo-polymers, device operation in specific parts of the optical spectrum (400 - 600 nm) can be achieved. Active and passive waveguides can be made, applying virtually the same processing techniques.

Optically Nonlinear Polymers: In order to show second order nonlinear effects (e.g. the electro-optic effect and frequency doubling), the nlo (side group) molecules as well as the bulk nlo-materials, are subject to a symmetry constraint: only noncentrosymmetric systems are useful. Noncentrosymmetry on the molecular level can be obtained via asymmetric substitution by electron donating groups such as alkoxy, amino, etc., and by electron attracting groups such as cyano, nitro, etc. These groups are often asymmetrically substituted to conjugated π -electron systems; the resulting molecules are called: D- π -A molecules. Typical examples are 4-alkoxy-4'-nitro-stilbene and 4-dimethylamino-4'-nitro-stilbene (DANS). The D- π -A groups are covalently attached to polymerizable moieties; after polymerisation, a nlo-polymeric material is obtained (see Figure 1). The concentration of the covalently attached nlo-side groups in polymers can be up to 60-70 %, and is much larger than can be achieved in solid solutions of nonlinear molecules in polymer hosts. By varying the side group, mainly the functionality of the polymer is determined; by varying the backbone or the spacer connecting the nlo-group to the backbone, mainly the mechanical properties (glass transition temperature Tg, etc.) can be varied. To achieve noncentrosymmetry on the macroscopic (bulk) level, electric field induced polar orientation of the permanent dipole moments of the side groups is carried out.

It is now widely believed that nlo side chain polymers offer the best compromise with respect to desired optical, mechanical, electrical, processing, etc., properties as compared to other forms of organic nonlinear materials such as: organic single crystals (difficult to grow and process);

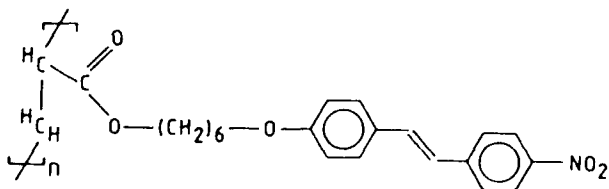


Figure 1. Schematic representation of a side chain polymer.

Langmuir-Blodgett layers (time consuming processing, low optical quality); polymeric solid solutions (segregation, small nonlinear effects) and main chain polymers (intractable, difficult to process systems thus far). The attractive features of nlo-side chain polymers are: large nonlinear effects; fast switching and modulation; easy processing into thin film multilayer structures; channel waveguide formation by UV-irradiation; large compatibility with other materials permitting integration; low dielectric constant permitting high speed operation; tailorability of optical, mechanical, electrical, etc properties by organic synthesis and molecular engineering. Moreover, in nature only a limited number of materials possesses spontaneously noncentrosymmetry and nlo-properties, whereas virtually every nlo-group containing polymer can be converted by electric field poling into an nlo-polymer.

Thin Film Multilayer Structures: The basic structure for making the waveguiding devices, consists of a polymeric thin film multilayer, comprising: a substrate (glass, silicon, III-V, etc.); a lower metal electrode (gold, silver, etc.); a lower polymeric optical cladding; a central (core) polymeric nonlinear layer; the polymeric upper cladding, and the top metal electrode (see Figure 2 left side). The polymer layers are deposited via spincoating or dipping, applying polymer solutions. The thickness of the different layers are of the order of micrometers. The central (nonlinear) layer possesses the highest refractive index of the various polymeric layers and acts, therefore, as an optical waveguide. By heating the sandwich structure close to the Tg of the central layer (a typical Tg value is 140°C), the polymer becomes soft enabling the side groups to move. Application of a strong electric field (of the order of 100's V/ μ m) causes the side groups to reorient owing to the interaction between their dipoles and the field, yielding a net polar order. By cooling down to sufficiently below Tg, the induced polar order is frozen in. Electro-optic coefficients up to 34 pm/V have been achieved in poled polymers [1], which is close to the value of the often applied inorganic single crystal lithium niobate (32 pm/V).

Thermal Stability of the Electro-optic Effect: Since the electro-optic effect can be obtained via electric field induced molecular segmental reorientation at Tg, it is expected that thermally induced relaxation of the effect will occur if, later on, the temperature of the poled polymers approaches Tg. The electro-optic effect in polymers, in principle, suffers from thermal instability. Measurements have been carried out on the thermal stability of poled polymers. For a poled polymer with a Tg of 142°C, the time required for a 50 % decrease of the effect (half life), as a function of temperature (T), is presented in Table I.

T (°C)	ϕ (years)	ϕ (days)
40	$9 \cdot 10^{+6}$	$3 \cdot 10^{+9}$
60	$2 \cdot 10^{+4}$	$7 \cdot 10^{+6}$
80	$2 \cdot 10^{+1}$	$7 \cdot 10^{+3}$
100	$5 \cdot 10^{-2}$	$2 \cdot 10^{+1}$

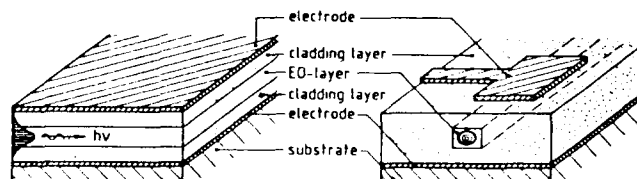


Figure 2. Examples of (patterned) multilayer structures.

It can be seen in Table I that nlo-polymers with a T_g of 142°C are reasonably stable up to 60°C. However, it is highly desired that nlo-polymers with improved thermal stability become available. Two possibilities are currently tried to improve the thermal stability, both aiming at reducing the mobility of the side groups after poling by: 1) increasing the T_g; 2) introduction of a crosslinks. Both methods are explored by various workers and have yielded promising results and are continued; it has not yet become clear which is the preferred one. For passive devices, thermal stability is less of a problem (no poling required).

Waveguide Realisation: By irradiating the nlo-polymers with UV light, a photo-induced process, causing a decrease of the refractive index, occurs. For DANS containing polymers, the original refractive index of 1.63 is lowered by values ranging from 0.001-0.09 depending on the (monitoring) wavelength, intensity and bleaching time used. By applying proper masks and UV bleaching conditions, monomode and multimode channel waveguides can be realised (see Figure 2, right hand side). For optimised combinations of channel widths (typically 3-5 μm) and refractive index contrast (typically 0.003-0.001), monomode waveguides result at 1.3 μm. The intensity contour plot of the monomode output of a passive 1*2 splitter, as measured with an infrared camera, is shown in Figure 3. Increasing channel widths or refractive index contrasts, convert the channels from monomode into multimode waveguides. Depending on whether the poling step is applied, passive or active waveguides are obtained.

Electro-Optic Devices: A variety of polymeric electro-optical devices has been made by starting from the multilayer sandwich structure as shown in Figure 2, including DANS containing polymers.

Arrays of active linear waveguides, performing as phase modulators arrays, have been made by poling the nlo-polymer at a temperature close to the T_g of 142°C with an electric field of 170 V/μm for about 10 minutes and by applying a mask for bleaching. The best half wave voltage (V_π) measured thus far for a 28 mm long device was about 2 Volts at 1.3 μm wavelength; this V_π value corresponds to a r₃₃ of 34 pm/V in the channel of the device. The optical loss in the waveguide was equal to about 0.9 dB/cm at 1.3 μm.

Similarly, after poling at slightly lower temperature with 205 V/μm and bleaching, an array of 30 integrated polymeric Mach-Zehnder interferometers has been made. The switching voltage on the 14 mm long active arm, was about 8 Volts, corresponding to a r₃₃ of 18.5 pm/V; the intensity modulation ratio was about 20 dB. A schematic view of a single element of the device is given in Figure 4.

Another type of polymeric switching device, that has been made similarly to the process as mentioned above, is the directional mode coupler which can be regarded as a 2*2 switch. The switching voltage for going from the bar to the

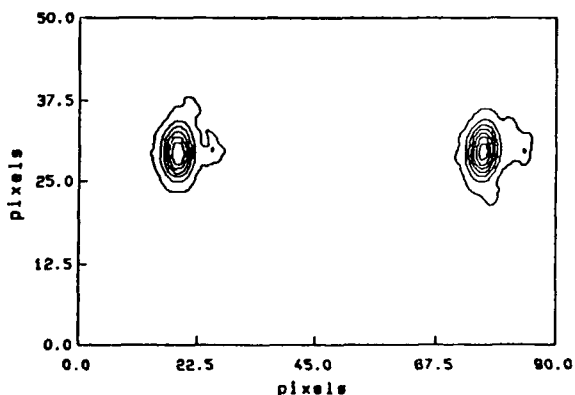


Figure 3. Output intensity plot of a passive 1*2 splitter.

cross state, was about 10 Volts; the intensity modulation ratio's were in excess of 15 dB.

Thermo-Optic Switching and Biasing: Instead of the electro-optic effect, the thermo-optic effect can be applied to vary the refractive index for switching. The switching electrodes are then used to carry electric currents instead of fields only, and act as heating elements raising the temperature of the polymer underneath. The refractive index decreases up to 0.1 have been measured for increasing temperatures. A disadvantage of the thermal effect is the low speed: 1 kHz versus >>1 GHz for electro-optic effects. Various integrated polymeric waveguiding switches and modulators have been made, requiring a few milliwatts only of electrical power for switching.

The thermo-optic effect can be applied to fine-tune the bias point of polymeric electro-optic devices. In (high speed) Mach-Zehnder interferometers, bias tuning has been thermo-optically achieved, while (high speed) modulation has simultaneously been performed by electro-optic means. The electrode covering one arm of the interferometer is used as a strip heater, thereby changing the refractive index and phase velocity in the arm, hence shifting the bias point of the interferometer. The electrode system at the other arm of the interferometer is used for (fast) electro-optic modulation; a voltage difference here, will generate an electric field across the waveguide and permitting (fast) electro-optic phase shifting and thus output intensity and modulation.

Thermo-optically biased Mach-Zehnder interferometers (similar to that in figure 4 but with optimised electrodes) have been realised and tested. Typical electrical power values needed for a π-radians phase shift are about 0.25 W/cm². This corresponds to a current of 0.5 mA for a 5 μm wide strip heater. Geometries with strips up to 200 μm wide, required currents up to 90 mA. The electro-optic V_π was equal to 20 V for this particular device with an electrode length of 20 mm. An advantage of using the thermo-optic effect instead of the electro-optic effect for DC bias tuning is that no compensation for electrical drift is required. Such drift phenomena, owing to electrical stress in polymeric integrated optic devices, have been observed.

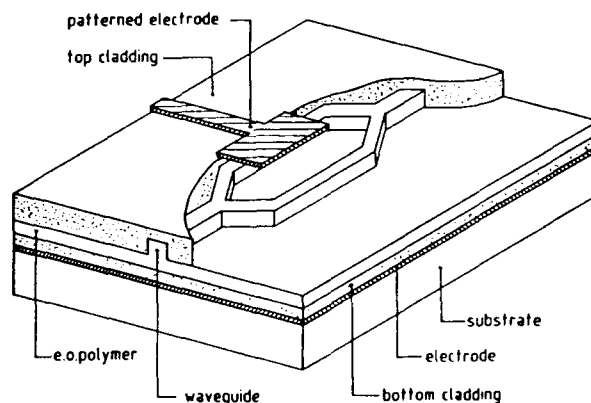


Figure 4. Schematic view of a Mach-Zehnder interferometer.

References:

- 1 G.R. Möhlmann, W.H.G. Horsthuis, A. McDonach, M.J. Copeland, C. Duchet, P. Fabre, M.B.J. Diemeer, E.S. Trommel, F.M.M. Suytem, E. Van Tomme, P. Baquero and P. Van Daele in 'Nonlinear Optical Properties of Organic Materials III', ed. G. Khanarian, Proc. Spie Vol.1337, 215-225(1990).
- 2 G.F. Lipscomb, R.S. Lytel, A.J. Thicknor, T.E. Van Eck, S.L. Kwiatkowski and D.G., Girton in 'Nonlinear Optical Properties of Organic Materials III', ed. G. Khanarian, Proc. Spie Vol.1337, 23-24 1990).

**NLO Polymers for frequency doubling:
Synthesis, characterization and photochemical stability.**

Emiel G.J. Staring, G.L.J.A. Rikken, C.J.E. Seppen,
S. Nijhuis, A.H.J. Venhuizen
Philips Research Laboratories, P.O.Box 80.000
5600 JA Eindhoven, The Netherlands

Introduction

An important potential area of application of second order nonlinear optical (NLO) effects is frequency doubling or second harmonic generation (SHG) of the emission of a common GaAs/AlGaAs semiconductor diode laser in order to achieve a 4-fold increase of information density in optical data storage systems. For this application highly nonlinear materials are required with zero absorption at the fundamental wavelength around 820 nm and at the second harmonic wavelength around 410 nm. At our Labs the NLO research program is aimed at obtaining poled polymer side-chain materials for frequency doubling of these diode lasers. In our view, complete transparency around 410 nm can only be achieved if the wavelength of maximum absorption λ_{max} of the charge transfer (CT) absorption of the chromophore lies well below that wavelength. Because of the transparency-high nonlinearity trade-off [1,2] efficient molecules and materials of this type are difficult to obtain. Our investigations showed that NLO molecules containing the sulphone electron acceptor group are especially suitable [3,4,5]. The narrow CT absorption band of these NLO molecules [4] allows a small energy separation between λ_{max} and the second harmonic wavelength, which is advantageous because of the resonance enhancement of β .

Results and Discussion

We now report on polymethylmethacrylate (PMMA) copolymer side-chain materials based on the 4-(dimethylamino)-4'-(alkylsulphonyl)biphenyl chromophore. The parent chromophore 5 represents one of the best examples that combines transparency around 410 nm with a high nonlinearity. For this chromophore, λ_{max} is 342 nm, $\lambda_{cut-off}$ is 410 nm and β is 110×10^{-30} esu at 820 nm.

The synthesis of the monomeric chromophore is summarized in Scheme 1. The commercially available 4-nitrobiphenyl 1 is converted into the sulphonic acid salt 2 [6], which allows the preparation of various 4'-(ω -hydroxyalkyl)-sulphonyl substituted biphenyls. We prepared compounds 3, 4 and 5 with respectively C₇, C₈ and C₉-alkylchains. Several copolymers 6 were prepared from the methacrylate of 5 ($n=6$) and methylmethacrylate (MMA), by thermal radical polymerization in chlorobenzene, at 100 °C. Colourless materials were obtained by precipitation with methanol. The results of these polymerization reactions are summarized in Table 1. The molar mass \bar{M}_w of the polymers, as determined by GPC was in the range of 66 - 207 $\times 10^3$ g/mol (vs PMMA standards). All polymer materials listed in Table 1 are amorphous, glassy materials, with T_g values varying from 100 to 110 °C. Measurements of SHG to determine d₃₃-values were performed on corona-poled films of 1 μ m thickness. The d₃₃-values increase super-linearly with the chromophore concentration. At the highest concentration (75 % w/w of the

methacrylate of 5) the value of d₃₃ was 46 pm/V, at 840 nm, for the 75 % w/w copolymer. This value exceeds that of the best inorganic NLO material LiNbO₃ (d₃₃ = 30 pm/V [7]) at that wavelength.

For application of these poled polymer materials in frequency doubling devices the temporal stability of the induced polar order is essential. Relaxation of the polar order arises from thermal randomization processes due to the molecular mobility in the amorphous polymers. This mobility is a function of (1) the structure of the polymer backbone and chromophore, (2) the amount of free volume frozen in the glassy state and (3) the temperature of storage. A suitable approach to an increased temporal stability of the polar order is to increase the T_g of the polymeric materials [8,9]. For most practical purposes, a T_g of ≥ 130 °C will result in sufficient temporal stability, even at elevated temperatures [9]. We have prepared copolymers of MMA and the methacrylates of 3, 4 and 5 to investigate the influence of the spacer length on the temporal stability of the polar order. Polymers were prepared in the molar ratio 0.81:0.19, by the procedure described above. Again, these polymers are amorphous, glassy materials. The highest T_g was observed for $n=2$: 127 °C. For $n=4$ the T_g is 109 °C. All three polymeric materials have, within experimental error, identical d₃₃-values of 10 pm/V at 1064 nm after poling just below their T_g. Experiments to compare the temporal stability of these copolymers at elevated temperatures are currently underway.

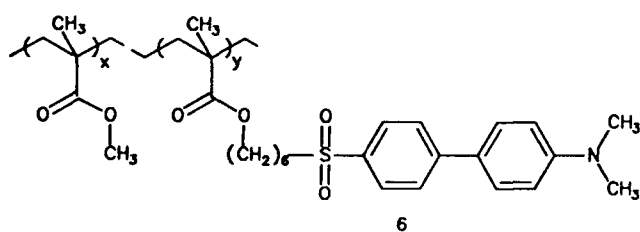
Sofar few experiments have been described in literature about the photochemical stability of NLO polymeric materials. Organic materials are reportedly able to withstand high intensity radiation. However, the demands on these materials are truly phenomenal in frequency doubling devices. For write applications in optical recording systems power densities larger than 0.1 MW/cm² are required, at a wavelength close to the absorption band of the NLO chromophore. Therefore we have started a systematical inquiry into the photochemical stability of chromophores and polymers to be used in frequency doubling. Our preliminary experiments have been performed with copolymer 7 which we described earlier [3,4,5]. This NLO material was irradiated with focussed 413 nm radiation from a CW Kr-ion laser, this wavelength being just above $\lambda_{cut-off}$ for this material. According to the Grotthus-Draper principle [10] a photochemical reaction only takes place if light is absorbed. The CT band in the UV-VIS spectrum of our material is a measure of the concentration of the chromophore and thus a measure of the nonlinearity of the material. Figure 2 shows a strong and irreversible decrease of the CT band for a power density of about 0.1 kW/cm² for a period of 26 minutes, although the residual absorption of the chromophore at 413 nm is less than 1 cm⁻¹. The pure polymer PMMA is effectively ablated in seconds at power densities of 0.3 MW/cm² and poly(α -methylstyrene) at 1 MW/cm². Probably a radical mechanism is responsible for the degradation of these pure polymers. This idea is supported by the fact that pure poly(bis-phenol-A-carbonate), which is not formed by a radical polymerization, does not show any ablation up to the highest available power densities of 60 MW/cm². Since the presence of radicals in the NLO materials may be of negative influence on the lifetime of the NLO chromophore we are currently studying (1) NLO side-chain polymers that are based on polycondensation or polyaddition reactions (polyesters, polyepoxides, polyurethanes) and (2) the influence of radical scavengers on the photochemical stability of NLO chromophores and polymers.

Conclusions

We have prepared various PMMA copolymer side-chain materials based on the 4-(dimethylamino)-4'-(alkylsulphonyl)biphenyl chromophore system. These materials are especially designed for application in frequency doubling. The copolymers are amorphous materials up to 75 % w/w of the methacrylate of the chromophore. The d_{33} -value of this material exceeds that of LiNbO₃. By variation of the spacer-length, the T_g could be raised from 106 °C to 127 °C. Therefore the temporal stability of the polar order in these materials is expected to be sufficient for practical purposes. However, the photochemical stability of the chromophore and of the polymer backbone under the strenuous conditions in frequency doubling must be improved.

References

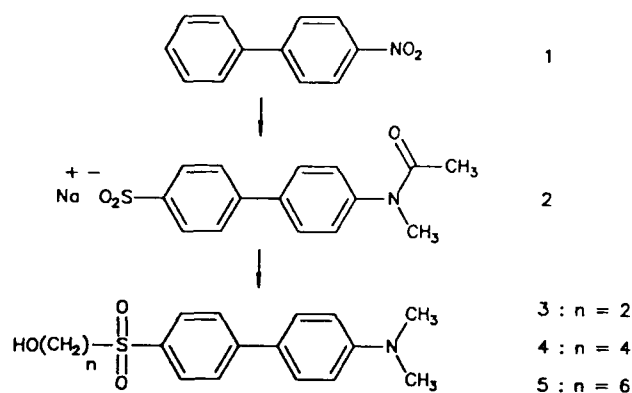
1. L.-T.Cheng, W.Tam, G.R.Meredith, G.L.J.A.Rikken, E.W.Meijer in "Nonlinear Optical Properties of Organic Materials II", Garo Khanarian, Editor, Proc. SPIE 1147, 61 (1989).
2. L.-T.Cheng, W.Tam, A.Feiring, G.L.J.A. Rikken, in "Nonlinear Optical Properties of Organic Materials III", Garo Khanarian, Editor, Proc. SPIE 1337, 203 (1990).
3. S.Nijhuis, G.L.J.A.Rikken, E.E.Havinga, W.ten Hoeve, H.Wynberg, E.W.Meijer, J.C.S., Chem.Commun. 1093 (1990).
4. G.L.Rikken, C.J.Seppen, S.Nijhuis, E.Staring, in "Nonlinear Optical Properties of Organic Materials III", Garo Khanarian, Editor, Proc. SPIE 1337, 35 (1990).
5. G.L.J.A. Rikken, C.J.E. Seppen, S. Nijhuis, E.W. Meijer, Appl.Phys.Lett. 58, 435 (1991).
6. Neth.Appl. 6,516,582, 1966 to American Cyanamid Co.
7. S.K.Kurz, J.Jerphagnon, M.M.Choy, Landolt-Bornstein Numerical Data and Functional Relationships in Science and Technology, Springer, New York, Volume 11, pp.671 (1979).
8. G.R.Mochlmann, W.H.G.Horsthuis, A.Mc.Donach, M.J.Copeland, C.Duchet, P.Fabre, M.B.J.Diemeer, E.S.Trommel, F.M.M.Suyten, E.Van Tomme, P.Baquero, P.Van Daele in "Nonlinear Optical Properties of Organic Materials III", Garo Khanarian, Editor, Proc. SPIE 1337, 215 (1990).
9. H.T.Man, K.Chiang, D.Hass, C.C.Teng, H.N.Yoon, in "Photopolymer Device Physics, Chemistry, and Applications" R.A.Lessard, Editor, Proc.SPIE 1213, 7 (1990).
10. J.F.McKellar, N.S.Allen, "Photochemistry of Man-made Polymers", ASP Ltd., London (1979).



x mol %	y	\bar{M}_w 10 ³ g/mol	T_g °C	d_{33} pm/V ^a
0.91	0.09	207	107	10.4
0.87	0.13	191	110	15.2
0.81	0.19	143	106	20.0
0.74	0.26	94		24.5
0.58	0.42	66	100	46.0

^a, at 840 nm

Table 1. Structure and properties of polymer 6, designed for frequency doubling of GaAs/AlGaAs diode lasers.



Scheme 1. Schematic representation of chromophore synthesis.

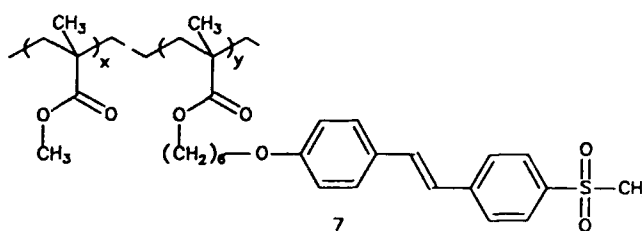


Figure 1. Structure of copolymer 7.

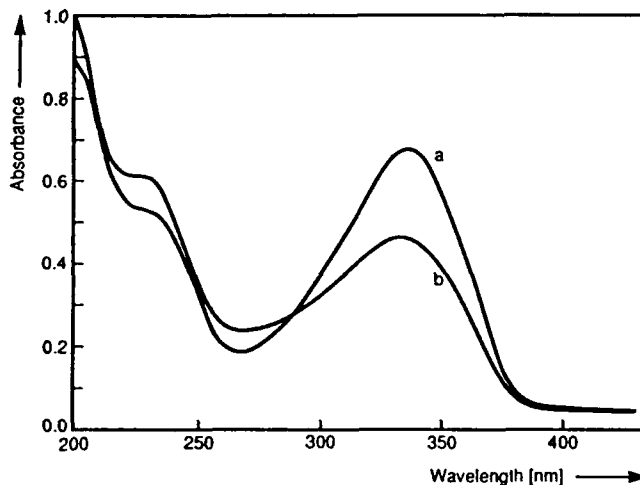


Figure 2. Absorption spectrum of NLO copolymer 7 before (curve a) and after irradiation with 0.1 kW/cm² of 413 nm radiation during 26 minutes (curve b).

RECENT DEVELOPMENTS IN EFFICIENT FREQUENCY DOUBLING IN POLED POLYMER FILMS. G. Khanarian, S. Meyer, R.A. Norwood, H.A. Goldberg, D. Holcomb and J. Stamatoff, Hoechst Celanese, 86 Morris Ave., Summit, N.J. 07901

Introduction

Frequency doubling is becoming increasingly important in a number of areas such as optical data storage and displays. However compact solid state lasers are only available at 0.63 μm and longer wavelengths which limit their application. For this reason there are great efforts underway to frequency double existing near-infrared light sources to the blue/violet region of the spectrum. Frequency doubling is inherently a weak and inefficient process because the transfer of energy from the fundamental to the harmonic is limited by dephasing due to the mismatch of refractive indices at the fundamental and harmonic. A number of techniques have been developed to match the effective indices at the fundamental and harmonic wavelengths and the process is called *phase matching*.

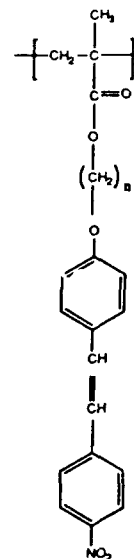
Waveguides are attractive for efficient doubling because high power intensities result from low power lasers in channel waveguides, long interaction lengths are possible (several millimeters) without diffraction and the waveguide dispersion properties can be used for phase matching. Also waveguide doublers can be integrated with other sources, detectors and other waveguide components to make a compact light weight system.

Waveguide frequency doublers have been fabricated from many materials. It presents a special challenge to chemists and material scientists to create nonlinear optical materials that are transparent at both the fundamental and harmonic wavelengths. They must also be processible to form thin films whose refractive indices can be accurately controlled. The condition of phase matching puts additional demands on the material such as the need to periodically pole. Amongst the materials under study for waveguide frequency doublers are inorganic crystals such as KTP, organic crystals and most recently polymers.

Nonlinear Optical Dyes and Polymers

Recently nonlinear optical polymers have been studied for electrooptical and frequency doubling applications. They present an interesting challenge to chemists to design dyes that have large activity whilst being transparent at the harmonic wavelength (0.4-0.5 μm) They must also be photolytically stable. Cheng et al [1] have made an extensive EFISH study of activity versus transparency and conclude that 4-methoxy 4'-sulphoxide stilbene (MOSO₂S) has good activity ($\mu\text{b} = 292 \times 10^{-48}$ esu at 0.8 μm) with a $\lambda_{\text{max}} = 0.336 \mu\text{m}$.

Then the dye can be attached to a polymer backbone in order to increase the number density of dyes and obtain a spin coatable polymer which also has good mechanical properties. An example of a nonlinear optical polymer that has been used in frequency doubling is shown in Fig. 1. The active dye is 4-methoxy 4'-nitrostilbene [2] which has a $\lambda_{\text{max}} = 0.370 \mu\text{m}$, $\chi^{(2)} = 8 \text{ pm/V}$ when poled at 70 V/ μm and measured by SHG using 1.3 μm fundamental wavelength. Rikken et al. [3] have also made a copolymer incorporating the MOSO₂S dye and they obtain $\chi^{(2)} = 18 \text{ pm/V}$ when poled at 120 V/ μm and measured at 0.8 μm .



4,4'-Oxynitrostilbene Copolymer for Frequency Doubling
Fig. 1

Phasematching in Frequency Doubling Waveguides

Polymer waveguides are made by spin coating a polymer solution onto a substrate such as a silicon wafer. The active nonlinear optical guide has cladding polymers of lower index to confine the radiation. Then the waveguide is poled to obtain a $\chi^{(2)}$ waveguide. It is a well known result from waveguide theory that the effective indices N^ω and $N^{2\omega}$ of the fundamental and harmonic are dependent on the waveguide parameters such as the guide/cladding indices and thickness of the waveguide [4]. In order to obtain efficient second harmonic generation (SHG) the effective indices must be equal or the mismatch of indices must be compensated (phase matching). Also one tries to optimize other properties such as phase matching the largest nonlinear optical (NLO) coefficient, maximizing the overlap of the optical fields of the fundamental and harmonic radiation and finally designing the waveguide to be insensitive to fabrication variabilities such as index and thickness fluctuations. The last aspect of quasi phase matching enables the fabrication of longer frequency doublers. [5]

One approach that meets the above criteria for efficient SHG is quasi phase matching [2,6,7,8]. The basic idea is to modulate periodically the NLO waveguide to compensate for the mismatch of refractive indices. This allows one to phase match the largest NLO coefficient, use zeroth order modes for the fundamental and harmonic waves with a resultant large overlap of optical fields and, finally, the waveguide parameters can be adjusted to make it relatively insensitive to random thickness/index variabilities (noncritical quasi phase matching). This approach has been implemented in two ways. Khanarian et al [2,8] have fabricated periodically poled slab waveguides using the polymer shown in Fig. 1 and used 1.34 μm fundamental radiation to observe the highest reported efficiencies to date. Rikken et al. [9] made a slab waveguide from a polymer containing the MOSO₂S dye, poled it uniformly, etched the top electrode and then periodically bleached the NLO polymer. They observed phase matching using 0.8 μm radiation. The efficiencies of these two demonstrations is given in Table 1.

A classic approach to phase matching is using the modal dispersion properties of waveguides such that the fundamental is in the zeroth order mode and the harmonic is travelling along a higher order mode[4]. This approach has been used by Sugihara et al [10] to observe phase matched SHG in a slab waveguide guest host film of MNA in PMMA. This approach utilizes the largest nonlinear optical coefficient d_{33} but there is small overlap of optical fields and it is critically important to have very smooth waveguides. Another approach is to use collinear phase matching where the fundamental is split into two and brought together again at a small angle in the slab waveguide. Again the fundamental is in the zeroth order mode and the harmonic in the third order mode. By varying the angle Shuto et al. [11] were able to phase match in a slab waveguide made from the polymer shown in Fig. 1. The efficiencies are given in Table 1.

Competing Materials

KTP[7] and LiNbO₃[6] are inorganic crystals that have been used to fabricate periodic frequency doublers. The result in KTP is the highest reported for any waveguide frequency doubler and results from the fact that the modulation depth of $\chi^{(2)}$ is high, the radiation is confined to a channel, the waveguides are low loss and also noncritically phase matched.

Table 1

Comparison of Polymer Frequency Doubling Results with KTP and LiNbO₃

Material	Waveguide Format	Length (P.M) (mm)	Efficiency (%/watt)	Ref
KTP	channel	5	10	7
LiNbO ₃	channel	1	0.24	6
Oxynitrostilbene Copolymer	Slab	5	0.01	8
Oxynitrostilbene Copolymer	Slab	0.1-1	3×10^{-7}	11
Oxysulphoxidesilbene Copolymer	Slab			9
MNA/PMMA Guest/Host	Slab		1.7×10^{-4}	10

Conclusions

Preliminary studies of frequency doubling in slab waveguides show that it is a promising approach to making efficient doublers. It presents a challenge to chemists to design high intensity dyes that are also transparent at the second harmonic, and also to the polymer material scientists to fabricate smooth waveguides which can be phase matched. More work remains to be done on different phase matching schemes such as periodic poling and bleaching and the fabrication of smooth low loss channel waveguides in polymers.

References

1. L.T.Cheng, W.Tam, A.Feiring and G.Rikken, Proc. SPIE, 1990, 1337, 203
2. G. Khanarian, R. A. Norwood, D. Haas, B. Feuer and D. Karim, Appl. Phys. Lett. 1990, 57, 977
3. G. Rikken, C. Seppen, S. Nijhuis and E. W. Meijer, Appl. Phys. Lett. 1991, 58, 435
4. G. I. Stegeman, J. J. Burke and C. T. Seaton, Chapter 9 in "Integrated Optical Circuits and Components", Ed. L. D. Hutcheson, Marcel Dekker, N. Y. 1987
5. E. Lim, M. Matsumoto and M. M. Fejer, Appl. Phys. Lett. 1991
6. E. J. Lim, M. M. Fejer, R. L. Beyer and W. J. Kozlovsky, Elect. Lett. 1989, 25, 731
7. C. J. van der Poel, J. D. Bierlein, J. B. Brown and S. Colak, Appl. Phys. Lett. 1990, 57, 2074
8. R. A. Norwood and G. Khanarian, Elect. Lett. 1990, 26, 2105
9. G. Rikken, C. Seppen, S. Nijhuis and E. Staring, Proc. SPIE, 1990, 1337, 35
10. O. Sugihara, T. Kinoshita, M. Okabe, S. Kunioka, Y. Nonaka and K. Sasaki, to appear in Appl. Optics, 1991
11. Y. Shuto, H. Takara, M. Amano and T. Kaino, Jap. J. Appl. Phys. 1989, 28, 2508

PHOTOCHEMICALLY DELINEATED REFRACTIVE INDEX
PROFILES IN POLYMERIC SLAB WAVEGUIDES

by
Keith A. Horn, David B. Schwind, and James T. Yardley
Allied-Signal Inc.
Research and Technology
101 Columbia Road
Morristown, NJ 07962-1021

Introduction

Thin organic polymeric films are promising materials for planar integrated optical waveguides and devices.¹ Several recent papers²⁻⁴ have described a direct one-step ultraviolet photolithographic method for the formation of polymer waveguides via lamp exposure through a mask. In general the polymeric systems utilized in these systems require high fluences (10-1000 J/cm²) to achieve waveguiding. Two fundamental phenomena combine to cause this low sensitivity or photospeed. In the cases described to date, the quantum yields (Φ) for photochemical reaction are low ($\ll 10^{-2}$) thereby requiring the high doses reported. In addition these systems often contain high oscillator strength chromophores resulting in large optical densities at the wavelengths used to induce the photochemical reaction responsible for the refractive index change. The lithographic light is not uniformly absorbed by these highly absorbing films and graded refractive index (GRIN) structures result. In order to model the propagation of light in organic thin film waveguides and devices it is important to be able to model the GRIN profile produced by these photochemical reactions and to calculate the propagation constants for such structures.

For a slab waveguide film of thickness d , which contains a photochemically reactive chromophore, the light intensity as a function of depth and the number density as a function of time are related by the Beer-Lambert equation and the rate equation

$$\frac{dI}{dx} = -\left(\frac{N}{V}\right)\sigma I \quad (1)$$

$$\frac{d\left(\frac{N}{V}\right)}{dt} = -\Phi\sigma\left(\frac{N}{V}\right)I \quad (2)$$

where σ is the absorption cross section, N/V is the number density and Φ is the quantum yield for the photochemical reaction. Eqs. 3 and 4 are the integrated analytical solutions to these equations⁷ ($\alpha = \sigma(N/V)$) for the case in which the chromophore bleaches to give photoproducts which are transparent to the lithographic source.

$$\frac{I}{I_0} = \frac{e^{-\alpha x}}{e^{-Kt}(1-e^{-\alpha x}) + e^{-\alpha x}} \quad (3)$$

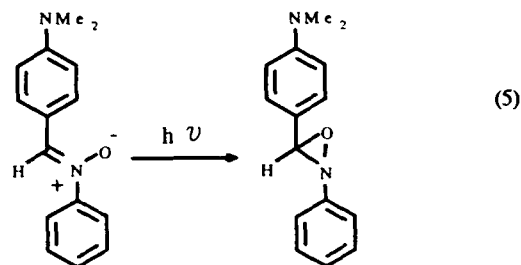
$$\frac{(N/V)}{(N/V)_0} = \frac{e^{-Kt}}{e^{-Kt}(1-e^{-\alpha x}) + e^{-\alpha x}} \quad (4)$$

Few photochemical reactions are sufficiently free of absorbing photoproducts for verification of these exact solutions. These rate equations have, however, been adapted to describe the growth of phase holograms.^{8,9} Use of this photochemical model to determine N/V as a function of

position in the film and photochemical dose allows us to apply a "WKB model" to determine the effective index of the propagating modes in slab waveguides generated in this manner.

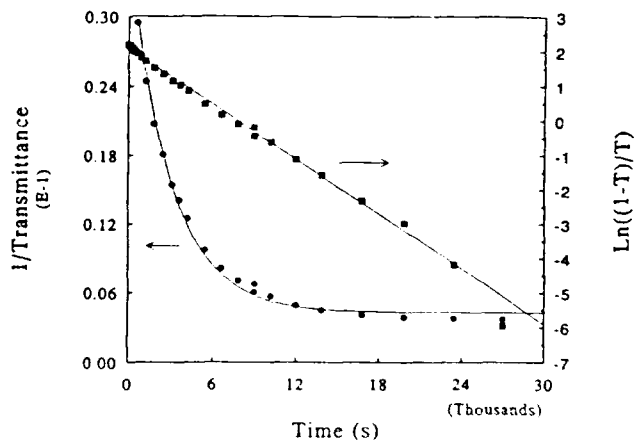
Results and Discussion

We have previously described a model system for the photochemical delineation of waveguides in polymeric films which consists of a monomeric nitron dissolved in a polymeric film such as PMMA. The photochemical reaction of (4-dimethylaminophenyl)-*N*-phenyl nitron (DMAPN) is shown in Eq. 5. The quantum yields for the conversion of nitrones such as DMAPN to the corresponding oxaziridines typically range from 0.1 to 1.0. Since the oxaziridine absorption maximum is at ca. 270nm, irradiation with 410nm light results in a clean bleach of the nitron absorption without interference by the photoproduct.



Thin films of DMAPN/PMMA were spin coated on quartz substrates and irradiated at 410nm (xenon lamp/monochromator source, 10nm bandpass). The transmitted intensity was monitored as a function of time. Figure 1 shows the fit of Eq. 3 to the transmitted intensity data. From this fit the absorption coefficient α and K were determined to be 3.1 cm⁻¹ and 3.4 x 10⁻⁴ s⁻¹. Substitution of the transmittance T for $e^{-\alpha d}$ in Eq. 3 and rearrangement suggests that a plot of $\ln((1-T)/T)$ vs time should be a straight line with a slope of $-\Phi\alpha I_0$ as shown in Figure 1.

Figure 1

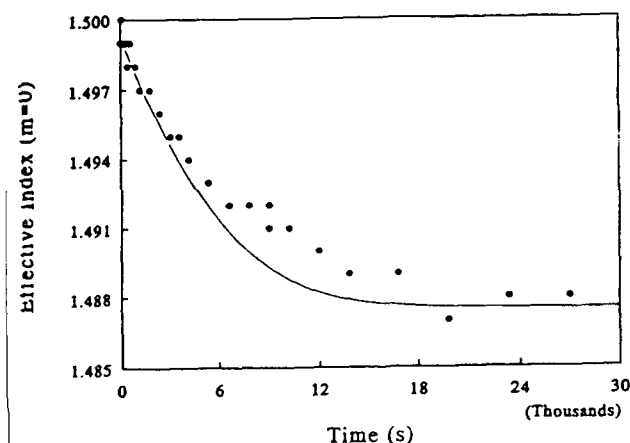


The refractive index profile determined from this photochemical bleaching model was then used to determine the slab waveguiding properties of this film at 815nm using the WKB approximation.¹⁰ The effective indexes of the single slab mode carried by this 0.68 micron thick film (measured as a function of irradiation time) are plotted in Figure 2. The conditions for guided waves in the WKB approximation are given by Eq. 6

$$k_0 \int_0^{x_2} [n(x)^2 - (n_{eff}^m)^2]^{\frac{1}{2}} dx = \left(m + \frac{1}{2}\right)\pi \quad (6)$$

where $k_0 = 2\pi/\lambda_0$, m is the mode index and the x axis is the depth direction in the film. The solid line in Figure 2 is a fit of Eq. 6 for $m = 1$ (the lowest order guided mode) to the measured effective indexes.

Figure 2



Conclusions

Graded refractive index profiles generated by photolithographic processes in thin organic polymer films can be effectively modelled (in the absence of absorbing photoproducts) by the integrated rate expressions given by Simmons.⁷ Use of the WKB approximation allows the effective indexes of the guided modes to be efficiently calculated.

References

1. Stegeman, G.I.; Seaton, C.T. and Zanoni, R., *Thin Solid Films*, **1987**, 152, 231.
2. Rochford, K.B.; Zanoni, R.; Gong, Q. and Stegeman, G.I., *Appl. Phys. Lett.*, **1989**, 55, 1161.
3. Wells, P.J. and Bloor, D. in *Organic Materials for Non-Linear Optics*, Eds. R.A. Hann and D. Bloor (The Royal Society of Chemistry, London, 1989), p.398.
4. Diemeer, M.B.J.; Suyten, F.M.M.; Trommel, E.S.; McDonach, A.; Copeland, J.M.; Jenneskens, L.W. and Horsthuis, W.H.G., *Electron. Lett.*, **1990**, 26, 379.
5. Hornak, L.A.; Weidman, T.W. and Kwock, E.W., *Appl. Phys.*, **1990**, 67, 2235.
6. (a) Horn, K.A.; Beeson, K.W.; McFarland, M.J.; Nahata, A.; Wu, C.; Yardley, J.T., *Abstracts of the 1989 International Chemical Congress of Pacific Basin Societies*, Honolulu, Hawaii, Dec. 17-22, 1989, Macr. 0082. (b) Beeson, K.W.; Horn, K.A.; McFarland, M.; Nahata, A.; Wu, C.; Yardley, J.T., ACS Symposium Series No. 455 *Materials for Nonlinear Optics*,

Chemical Perspectives, S.R. Marder, J.E. Sohn, and G.D. Stucky, Eds., American Chemical Society, 1991, 303. (c) Beeson, K.W.; Horn, K.A.; McFarland, M.; Yardley, J.T., *Appl. Phys. Lett.*, **1991**, in press.

7. Simmons, E.L., *J. Phys. Chem.*, **1971**, 75, 588.
8. Bjorklund, G.C.; Burland, M. and Alvarez, D.C., *J. Chem. Phys.*, **1980**, 73, 4321.
9. Burland, D.M. and Brauchle, C., *J. Chem. Phys.*, **1982**, 76(9), 4502.
10. Hocker, G.B. and Burns, W.K., *Appl. Opt.*, **1977**, 16, 113 and references therein.

CUBIC NONLINEAR OPTICS OF POLYMER THIN FILMS.

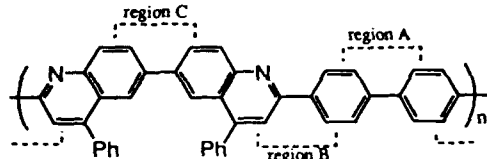
2. STRUCTURE- $\chi^{(3)}$ RELATIONSHIPS IN RIGID-ROD POLYQUINOLINES.

Ashwini K. Agrawal and Samson A. Jenekhe, Department of Chemical Engineering and Center for Photoinduced Charge Transfer, University of Rochester, Rochester, N.Y. 14627-0166. Herman Vanherzeele and Jeffrey S. Meth, Du Pont Central Research and Development Department, Wilmington, DE 19880-0356.

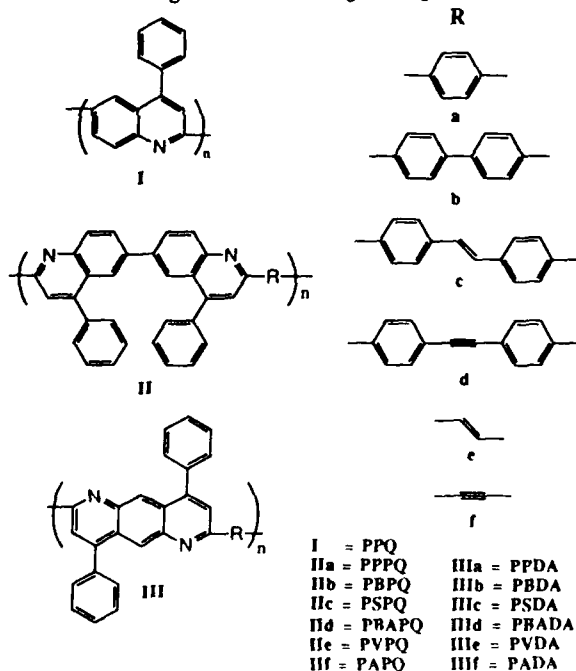
Many conjugated polymers have been tested for their third order nonlinear optical properties but fundamental understanding of the structure- $\chi^{(3)}$ relationships is not yet established. It is important to investigate the wavelength dispersion of $\chi^{(3)}$ in series of systematically synthesized polymers to establish such structure- $\chi^{(3)}$ correlations. The present results are part of such an on going research effort in our laboratory[1].

Conjugated rigid-rod polyquinolines are thermally stable (500-600°C), high mechanical strength, film- and fiber-forming materials[2] that can be doped to a high electronic conductivity (10 S/cm)[3]. These polymers are soluble in high concentration in their usual polymerization solvent, di-m-cresyl phosphate (DCP)/m-cresol[4] or in Lewis acids ($AlCl_3$, $GaCl_3$, etc./nitroalkanes[5]) to form lyotropic liquid crystalline solutions and hence are processable to thin films and fibers. One of the most attractive features of this class of conjugated polymers is the flexible synthetic scheme with which the basic polyquinoline molecular structure can be modified. This makes the conjugated polyquinolines an ideal class of polymers, or model systems, for the investigation of structure- $\chi^{(3)}$ relationships.

We propose a series of conjugated polyquinolines in which molecular structures have been modified to vary the extent of effective π -electron delocalization along the backbone of the polymer chain. In the molecular structure of the most commonly studied rigid-rod polyquinoline, poly(2, 2'-(p, p'-biphenylene)-6, 6'-bis (4-phenyl quinoline) (PBPQ), three regions



(A, B & C) of steric hinderance due to the adjacent ortho-hydrogens of aromatic rings can be identified. We have systematically modified these regions to seek the effect of π -electron delocalization on the $\chi^{(3)}$ of these materials. The following structures are being investigated in this study:



We have also synthesized random copolymers of the conjugated rigid-rod polyquinolines in order to investigate the effect of disorder in the main chain of the polymers on their third-order optical nonlinearities. Copolymerization also provides a way to reduce or eliminate the crystallinity of the polymers and hence possibly reduce optical losses due to scattering.

EXPERIMENTAL

Synthesis: The monomers were synthesized according to the methods reported in literature: 3, 3'-dibenzoyl benzidine[4, 6]; 2, 5-dibenzoyl-1, 4-phenylene diamine[7]; 5-acetyl-2-amino benzophenone[8]; diacetyl stilbene[9]; diacetyl biphenylacetylene[10]. Diacetyl biphenyl and diacetyl benzene were obtained commercially and were purified[11].

A mixture of DCP/m-cresol was used as a polymerization medium and was synthesized as reported by Beever et al.[12]. The method of polymerization was similar to that adopted by Stille and coworkers[4]. Equal moles of each bis(amino ketone) and bis(keto methylene) monomers were reacted in DCP/m-cresol at 140°C under Ar for 48 hrs. The resulting polymerization dope was precipitated in 10% triethyl amine/ethanol mixture to obtain a pure polymer which was dried overnight at 80°C under vacuum. All of the polymers were obtained in high yield (>95%). The intrinsic viscosities obtained in each case are reported in Table 1.

Film preparation: Isotropic solutions of polyquinolines (1-3%) obtained in DCP/m-cresol (1:5) medium were used to cast thin films. These films were obtained by shearing a thin layer of polymer solution between two optically flat silica substrate (5 cm in diameter). The coatings on silica substrates were kept at 95°C for 5-7 hrs under vacuum to remove the solvent (m-cresol). The resulting thin films of polymer/DCP complex were precipitated in 10% triethyl amine/ethanol mixture and kept in this solvent overnight. Films of the pure polyquinolines were dried under vacuum at 95°C for 4-6 hrs.

$\chi^{(3)}$ measurements: THG experiments were performed with a picosecond laser system continuously tuneable in the range of 0.6-4 μ m. This source has been described in detail earlier[13]. For this work, we have used a repetition rate of 10 Hz and a pulsewidth of 30-50 ps. Using the method explained elsewhere[14], measurements were made in the fundamental wavelength range of 0.9-2.4 μ m. The reported $\chi^{(3)}$ values are the average values, corrected for absorption at the third harmonic wavelength and are obtained relative to $\chi^{(3)}$ for the fused silica ($= 2.8 \times 10^{-14}$ esu at 1.9 μ m). The error in $\chi^{(3)}$ values of the films, typically $\pm 20\%$, reflects mostly the error in film thickness measurement since the repeatability of individual results for each material is $\pm 5\%$.

RESULTS AND DISCUSSION

The absorption maxima of conjugated polyquinolines lie around 400 nm and the polymers are essentially transparent above 500 nm. Typical electronic absorption spectra of three derivatives of polyquinoline are shown in Figure 1. Optical Loss measurements on these polymers gave α values of the order 1-10 cm^{-1} in the region 0.8 to 2.0 μ m.

Table 1 shows the values of linear optical properties and intrinsic viscosities for seven homopolymers and three copolymers. The polymers exhibit decreasing band gaps and hence increasing degree of π -electron delocalization in the order: PSDA > PBADA > PBDA > PSPQ > PBAPQ > PBPQ. Introduction of biphenyl acetylene-linkage (in PBAPQ, PBADA) in place of biphenylene-linkage (in PBPQ, PBDA) has reduced the adverse effect of steric hinderance in the region A, which when replaced by stilbene-linkage (in PSPQ, PSDA) has resulted in further improvement of the π -electron delocalization. When structures II and III are compared, better electron delocalization is shown by III due to absence of the steric hinderance in region C of the latter. We expect that polymers IIIe and IIIf when synthesized, will exhibit the smallest band gaps among the polymers under study.

Figure 2 shows the wavelength dispersion of the $\chi^{(3)}(-3\omega; \omega, \omega, \omega)$ of the three homopolymers: PBPQ, PBAPQ, and PSPQ. The $\chi^{(3)}$ spectra of these polymers exhibit a resonance peak at about 1.2 μ m and off-resonance $\chi^{(3)}$ values in the region 1.8-2.0 μ m. Occurrence of a resonance peak at about three times the λ_{max} and absence of any absorption features in the 0.5-2.0 μ m range in their absorption spectra suggest that the peaks are due to three-photon resonance. Based on various theoretical models[15], which predict a strong dependence of $\chi^{(3)}$ on band gap of the material, one can expect increasing values of $\chi^{(3)}$ with the decreasing band gaps of the

reported polymers. However, we do not observe any significant effect of the structure in the off-resonant region where all of the polymers show about the same value of $\chi^{(3)} \sim 2 \times 10^{-12}$ esu. The values of $\chi^{(3)}$ increases above this by about an order of magnitude in the resonance region. $\chi^{(3)}$ at the resonance peaks for PBPQ, PBAPQ, and PSPQ are 1.92×10^{-11} , 2.66×10^{-11} , and 8.12×10^{-12} esu, respectively. In this resonance region, the effect of structures is much more pronounced but does not lie in the predicted order for the polymers. These results clearly indicate the presence of other factors which have stronger influence on $\chi^{(3)}$ than that of the band gap. Elucidation of these additional factors in future studies may result in possible approaches to enhance the $\chi^{(3)}$ of polymers without having to reduce the transparent region.

In the $\chi^{(3)}$ spectra of PBAPQ, PSPQ and their random copolymer (50:50), a resonance peak corresponding to three-photon resonance is observed in the copolymer as well as the homopolymers. Similar to the linear optical properties, third order nonlinear optical properties of the copolymer lie in between those of constituent homopolymers. $\chi^{(3)}$ at the resonance peak for PBAPQ/PSPQ is 1.78×10^{-11} esu which is very close to the molar average value of 1.74×10^{-11} esu calculated from the contributions of 50% each of PBAPQ and PSPQ. The disorder introduced in the main chain of the copolymer, apparently, does not have any influence on the optical nonlinearity of this series of polymers.

CONCLUSIONS

We have successfully synthesized a series of polyquinolines of systematically derivatized molecular structures and prepared their optical quality thin films. Reasonably large values of $\chi^{(3)} \sim 10^{-11}$ - 10^{-12} esu with significantly small optical losses (~ 1 - 10 cm $^{-1}$) were found for this class of polymers. From the wavelength dispersion of $\chi^{(3)}$, three-photon resonance and interesting structure-property relationships were observed. Although, there was no significant effect of structure on the nonresonant optical nonlinearities, resonant region indicated the effect of factors other than the band gap. The copolymer showed linear and nonlinear optical properties in between those of constituent homopolymers.

ACKNOWLEDGMENTS

Work at the university of Rochester was supported by the New York State Science and Technology Foundation, Amoco Foundation, and the National Science Foundation (Grant CHE-881-0024).

REFERENCES

- (a) Jenekhe, S. A.; Roberts, M. F.; Agrawal, A. K.; Meth, J. S.; Vanherzeele, H. *Mater. Res. Soc. Symp. Proc.* 1991, 214, pxxx; (b) Vanherzeele, H.; Meth, J. S.; Jenekhe, S. A.; Roberts, M. F. *Appl. Phys. Lett.* 1991, 58, 663; (c) Osaheni, J. A.; Jenekhe, S. A.; Vanherzeele, H.; Meth, J. S. *Chem. Mater.*, in press; (d) Jenekhe, S. A.; Lo, S. K.; Flom, S. R. *Appl. Phys. Lett.* 1989, 54, 2524; (e) Jenekhe, S. A.; Chen, W. C.; Lo, S. K.; Flom, S. R. *Appl. Phys. Lett.* 1990, 57, 126; (f) See parts 1, 3, 4 and 5, in this volume.
- Warsidlo, W.; Norris, S. O.; Wolfe, J. F.; Katto, T.; Stille, J. K. *Macromolecules* 1976, 9, 512.
- (a) Tunney, S. E.; Suenago, J.; Stille, J. K. *Macromolecules* 1983, 16, 1398; (b) Tunney, S. E.; Suenago, J.; Stille, J. K. *Macromolecules* 1987, 20, 258.
- (a) Stille, J. K. *Macromolecules* 1981, 14, 870; (b) Sybert, P. D.; Beever, W. H.; Stille, J. K. *Macromolecules* 1981, 14, 493.
- Unpublished results from our laboratory.
- Pelter, M. W.; Stille, J. K. *Macromolecules* 1990, 23, 2418.
- Imai, Y.; Johnson, E. F.; Katto, T.; Kurihara, M.; Stille, J. K. *J. Polym. Sci., Polym. Chem. Ed.* 1975, 13, 2233.
- Ning, R. Y.; Madan, P. B.; Sternbach, L. H. *J. Heterocycl. Chem.* 1974, 11, 107.
- Zimmermann, E. K.; Stille, J. K. *Macromolecules* 1985, 18, 321.
- Sutherland, D. M.; Stille, J. K. *Macromolecules* 1986, 19, 257.
- Norris, S. O.; Stille, J. K. *Macromolecules* 1976, 9, 496.
- Beever, W. H.; Stille, J. K. *J. Polym. Sci., Polym. Symp.* 1978, 65, 41.
- Vanherzeele, H. *Appl. Opt.* 1990, 29, 2246.
- Agrawal, A. K.; Jenekhe, S. A.; Vanherzeele, H.; Meth, J. S. *Chem. Mater.*, submitted.
- (a) Agrawal, G. P.; Cojan, C.; Flytzanis, C. *Phys. Rev. B* 1978, 17(2), 776; (b) Rustagi, K. C.; Ducuing, J. *Optics Commun.* 1974, 10, 258; (c) Pierce, B. M. *Mater. Res. Soc. Symp. Proc.*, 1988, 109, 109

Table 1 Linear optical properties of polyquinolines.

POLYMERS ([η] at 25°C; dl/g)	λ_{max} (film) (nm)	E_g (film) (eV)	λ_{max} (soln.) (nm)	log ϵ (soln.)
PPQ (0.95)	410	2.65	389	4.16
PBPQ (8.5)	394	2.81	429	4.83
PBAPQ (8.9)	399	2.72	436	4.86
PSPQ (31.3)	408	2.65	467	4.88
PBDA (6.85)	414	2.56	484	4.67
PBADA (7.65)	426	2.57	490	4.65
PSDA (30.3)	448	2.46	547	4.78
PBPQ/PBAPQ (25)	397	2.79	431	4.88
PBPQ/PSPQ (22.6)	402	2.72	440	4.77
PSPQ/PBAPQ (14.3)	404	2.72	445	4.81

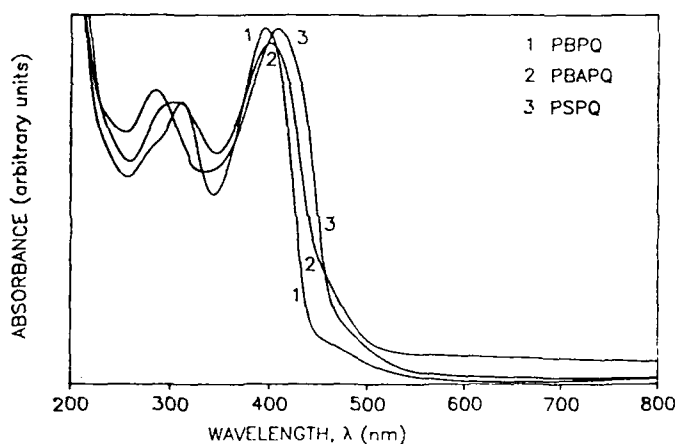


Figure 1 Electronic absorption spectra of thin films of PBPQ, PBAPQ and PSPQ.

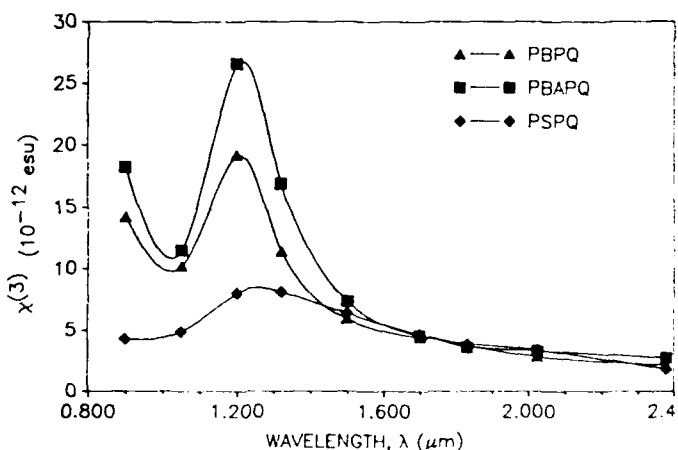


Figure 2 The $\chi^{(3)}(-3\omega; \omega, \omega, \omega)$ spectra of PBPQ, PBAPQ and PSPQ.

A Study of the Competition Between Electric Field Induced Molecular Ordering and Chemical Cross Linking in Vitrified Nonlinear Optical Polymer Films

J. D. Bewsher, G. R. Mitchell

Polymer Science Centre
University of Reading
Whiteknights
Reading RG6 2AF
U. K.

Introduction

Since the introduction of optical fibres there has been a movement to replace the traditional electronic based data manipulation systems with a much faster and more reliable system employing light. Traditionally the specialised switches and modulators required for such a system have been manufactured from optically nonlinear inorganic crystals such as LiNbO_3 and KDP. However with the need to produce integrated optical circuits on a sub-micron scale, these crystals have had to be rejected because of their bulk and their complicated processing routines.

Instead attention has been turned to organic materials^[1], where molecules with very large nonlinear optical properties can be synthesised and, with the support of polymer chemistry, used to produce films which are easily processible and ideal for integrated circuits.

The initial idea of introducing highly nonlinear guest molecules into a host polymer has proved to be quite successful in yielding operational devices^[2] but this regime does have its limitations. Although the nonlinearity of the guest molecules is high they can only ever be present in small concentrations before they phase separate from their host and crystallise to form light scattering centres reducing the performance of the device. Also the practice of thermopoling, the technique used to generate the noncentrosymmetric alignment of the NLO groups whilst effective has only limited long term applications. The glass transition temperature of most of the host materials used to date is not high enough to prevent the thermal relaxation of this induced molecular ordering (see Figure 1).

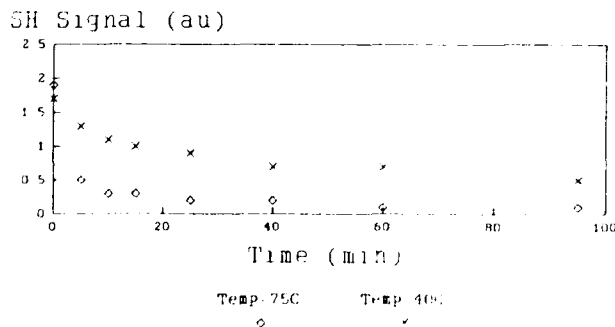


Figure 1: A Graph to Show Molecular Relaxation with Time

Another alternative is to use a polymeric material where the nonlinear units form part of the molecular chains, for example side groups^[3]. However these materials, although they contain a far higher concentration of NLO units, still suffer from the problem of a gradual relaxation of the noncentrosymmetric alignment.

Perhaps the most promising idea of recent years is to add functional groups onto a central nonlinear molecule^[4,5,6]. These individual units can then be aligned with an electric field and then chemical cross links formed between adjacent functional groups give rise to a long range, three-dimensional network, effectively locking in the induced molecular order. The glass transition temperature of such a system once linked will be extremely high, thereby reducing the effect of possible thermal relaxation of the molecular alignment.

As with previous materials the individual units that make up the prepolymer are heated to allow greater molecular mobility and to reduce the curing period. However at these higher temperatures the prepolymer becomes very fluid, leading to a drop in the resistivity of the material and a risk of electrical breakdown when the poling field is applied, resulting in damaged material. The solution to this problem so far has been to preclude the material, form some of the crosslinks between molecules thereby increasing the resistivity before the field is applied. However, precluding leads to restrictions on the molecular alignment, resulting in a material of reduced nonlinear optical performance. It is this apparent competition between the resistivity of the prepoled material and the effective poling of the NLO units that is the subject of this

Discussion

We have set out to explore this competition through two parallel programmes of activity. The first is a detailed experimental assessment of the levels of polar alignment which can be achieved using differing chemical configurations of the network and differing non-linear optical chromophores. The second approach is to model the various processes of chemical reaction and electric field alignment using a Monte Carlo type system.

The non-linear optical response of a particular material is directly proportional to the number density of active units, their non-linear optical susceptibility and the level of polar alignment. The model is concerned with evaluating the level of polar alignment commensurate with inherent chemical restraints of a polymer network. The chemical reaction of N reactive units to form a three dimensional cross-linked material remains a considerable problem within molecular modelling in its own right. We have therefore partitioned our model into two levels. The first of these is concerned with the detailed conformational interaction between the functional units. In essence what possible angular configurations are possible? The restrictions arising from the particular stereochemical geometry are related to detailed atomistic molecular modelling^[7]. Using various sampling techniques this modelling gives for any particular molecular pair the probabilities of each possible angle between the dipole moments of the non-linear optical chromophore. The

second part of the model is performed within a lattice approximation. Within the three dimensional system, chromophores N_c with functionality f and non-chromophoric N_n groups if appropriate are placed using Bernoullian statistics. Upon application of an electric field which may have some time dependence relating to the level of curing, the chromophores are assigned a Boltzmann type distribution of angles between the dipole moments μ^i and the electric field vector $\underline{E}(t)$. By Monte Carlo sampling techniques particular pairs of chromophores are examined and their angular correlation assessed. Through a standard acceptance test taking account of the probability of that angular correlation from the atomistic modelling, the units are connected or alternative action is taken. Since the energy of chemical reaction is high this will lead to modification of the alignment of the chromophores as curing proceeds. The basic output of the modelling is $\langle \psi \rangle$ where ψ is the angle between $\underline{E}(t)$ and μ^i , and the level of curing. These may be related to the SHG signal through a knowledge of the appropriate molecular parameters. Within the model the number of chromophores and their functionality represent important parameters and the results of variation of such parameters may be related to similar variation in the experimental series described above. For example at low concentrations of the multi-functional groups the non-linear optical response is linear with concentration (Figure 2), the key question is how to maintain this linearity. Using these approach we are able to build up a comprehensive appreciation of the structural features required to maximise $\langle \psi \rangle$ whilst maintaining a large number density of chromophores and long term stability of the non-linear optical response.

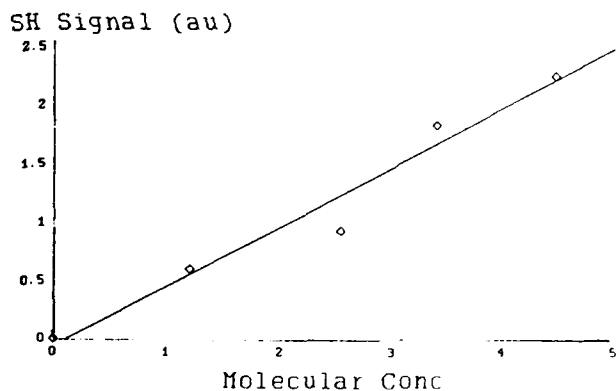


Figure 2: A Graph of Nonlinear Optical Response vs Concentration

Acknowledgements

This work is supported by the Science and Engineering Research Council (SERC), U. K.

References

1. K. D. Singer, S. J. Lalama, J. E. Sohn, "Organic Nonlinear Optical Materials", *Proc. SPIE*, vol. 578, pp. 130-136, 1985.

2. K. D. Singer, W. R. Holland, M. G. Kuzyk, G. L. Wolk, H. E. Katz, M. L. Schilling, P. A. Cahill, "Second-Order Nonlinear Optical Devices in Poled Polymers", *Proc. SPIE*, vol. 1147, pp. 233-244, 1989.

3. J. H. Wendorf, M. Eich, "Nonlinear Optical Phenomena in Liquid Crystalline Side Chain Polymers", *Mol. Cryst. Liq. Cryst.*, vol. 169, pp. 133-166, 1989.

4. M. Eich, B. Reck, D. Y. Yoon, C. G. Willson, G. C. Bjorklund, "Novel Second-Order Nonlinear Optical Polymers Via Chemical Cross-Linking-Induced Vitrification Under Electric Field", *J. Appl. Phys.*, vol. 66, no. 7, pp. 3241-3247, 1989.

5. B. Reck, M. Eich, D. Jungbauer, R. J. Twieg, G. C. Bjorklund, D. Y. Yoon, C. G. Willson, "Cross Linked Epoxy Polymers with Large and Stable Nonlinear Optical Susceptibilities", *Proc. SPIE*, vol. 1147, pp. 74-83, 1989.

6. D. Jungbauer, B. Reck, R. J. Twieg, D. Y. Yoon, C. G. Willson, J. D. Swalen, "Highly Efficient and Stable Nonlinear Optical Polymers Via Chemical Cross-Linking Under Electric Field", *Appl. Phys. Lett.*, vol. 56, no. 26, pp. 2610-2612, 1990.

7. RU-Prism Users manual, *University of Reading*, 1989.

METAL NANOCCLUSERS WITHIN BLOCK COPOLYMER MICRODOMAINS

G. S. W. Craig, R. E. Cohen, Y. Ng Cheong Chan, R. R. Schrock
Departments of Chemical Engineering and Chemistry
Massachusetts Institute of Technology
Cambridge, MA 02139

Introduction

Nanoscale metal clusters have physical, electrical, and optical properties that differ from those of the bulk metal. Quantum size effects that occur in metal clusters less than 100 Å in diameter can lead to interesting physical, electrical, and nonlinear optical behavior. For example, gold colloids have been shown to have large nonlinear susceptibilities. Physicists have predicted that $\chi^{(3)}$ for metal clusters scales with the inverse third power of the radius.¹ An ordered dispersion of small metal clusters in a nonconductive matrix leads to very large dielectric coefficients. As the concentration of the metal clusters reaches the percolation threshold, the dielectric constant increases dramatically.²

In the past, metal clusters have been synthesized by a variety of techniques, including hydrosols, evaporation, zeolitic encapsulation, laser ablation, and ion exchange/chemical reduction. There are inherent difficulties involved in placing particles generated by these techniques in a well-ordered array within a glassy matrix. Without kinetic barriers, nanoclusters can aggregate into bulk material. However, strong kinetic barriers, such as metal-polymer complexes, prevent true metal cluster formation.

Microphase separated block copolymers provide a well-ordered matrix in which a kinetic restraint, in this case the glass transition temperature, varies significantly between the two separate regions.³ When one of the blocks contains a detachable complexed metal atom in the repeat unit, and the other block has a significantly higher T_g , a cluster can form within each microphase separated region without the risk of aggregation. (See Figure 1.)

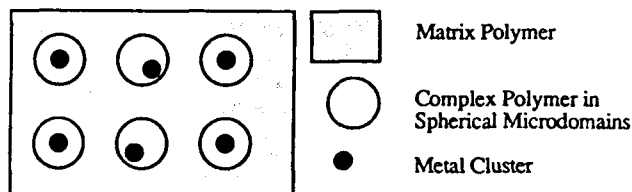


Figure 1: Metal clusters within polymer microdomains

Microphase separated systems can be annealed and oriented into a well-ordered matrix. Monodisperse microdomains of metal-containing polymers effectively restrict cluster size to a narrow range around the desired size. Because of these advantages, cluster formation within block copolymer microdomains is a potentially useful method for synthesizing metal nanoclusters dispersed throughout a nonconductive matrix, and for investigating the variation of optical and dielectric properties with cluster size.

Block Copolymer Synthesis

Ring opening metathesis polymerization of a strained cyclic olefin, such as methyltetracyclododecene (MTD) or norbornene (NBE), with a well-defined metal-alkylidene catalyst (I) yields a living, monodisperse homopolymer.⁴ Subsequent addition of the organometallic compounds palladium(allylbenzene)(cyclopentadienylmethylnorbornene) (PdAC_p^N) or platinum(trimethyl)(cyclopentadienylmethylnorbornene) ($\text{PtMe}_3\text{C}_p^N$) and termination with pivaldehyde results in a diblock copolymer in which each repeat unit in one of the blocks contains a metal complex. An example of the polymerization is shown in Figure 2.

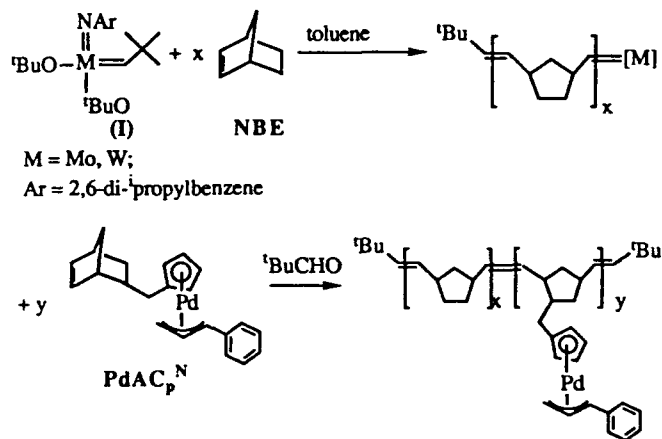


Figure 2: Ring opening metathesis polymerization of a diblock copolymer with a metal atom in one of the blocks.

When static cast from toluene, block copolymers of either MTD or NBE and PdAC_p^N or $\text{PtMe}_3\text{C}_p^N$ microphase separate at relatively low molecular weights. The microphase separation was characterized with small angle x-ray scattering (SAXS) and transmission electron microscopy (TEM). SAXS showed no long-range order within the plane of the cast film, and an interdomain spacing of 190 to 300 Å, depending on the molecular weight of the sample. Unlike TEM of hydrocarbon block copolymers, no staining agent is necessary for TEM of these diblocks. The metal atoms automatically stain the sample because of their greater electron density. To date, spherical and lamellar morphologies have been observed by TEM. A micrograph of a lamellar sample is shown in Figure 3.

Cluster Formation

The Pd or Pt clusters can be generated by reduction through exposure to hydrogen or UV radiation, respectively.⁵ For example, heating a sample consisting of spherical microdomains of poly(PdAC_p^N) in poly(MTD) at 100 °C under 60 psig H_2 leads to complete of cluster formation within the microdomains within 38 hours. The metal cluster formation was analyzed with wide angle x-ray scattering (WAXS). Initially, there are no peaks at 2θ values greater than 25°. After 18 hours of heating, the peaks

The fact that the Pd(111) scattering peak shape, intensity, and location do not change upon several days of heating shows that the poly(MTD) matrix, with a T_g of approximately 200C, is an effective barrier to interdomain cluster aggregation. In the case of cluster formation within a lamellar sample, as shown in the TEM micrograph in Figure 4, intradomain cluster aggregation is still possible. The size of the Pd clusters in this micrograph range from 20-40 Å. The polymer domains are not visible because the staining agent, the metal atoms, are no longer dispersed evenly throughout one domain. However, the clusters appear to line up like a string of pearls, suggesting that they remain within the original lamellar domain.

Acknowledgements

This work has been supported by NSF/MRL under Grant DMR 87-19217, through the CMSE at MIT. G.S.W.C. thanks the National Science Foundation for a Graduate Fellowship.

References

¹F. Hache, D. Ricard, and C. Flytzanis, *J. Opt. Soc. Am. B.*, **3**, 1647 (1986).

²D. J. Bergman and Y. Imry, *Phys. Rev. Lett.*, **59**, 1222 (1977).

³a) F.S. Bates, C. V. Berney, and R. E. Cohen, *Macromolecules*, **16**, 1101 (1983). b) J. Csernica, R. F. Baddour, and R. E. Cohen, *Macromolecules*, **20**, 2468 (1987).

⁴R. R. Schrock, S. A. Krouse, K. Knoll, J. Feldman, J. S. Murdzek, and D. C. Yang, *J. Mol. Cat.*, **46**, 243 (1988).

⁵O. Hackelberg and A. Wojcicki, *Inorg. Chim. Acta*, **44**, L63 (1980).



Figure 3: Lamellar microphase separation in a static cast film of (NBE)-(PdAC_p^N) diblock copolymer.

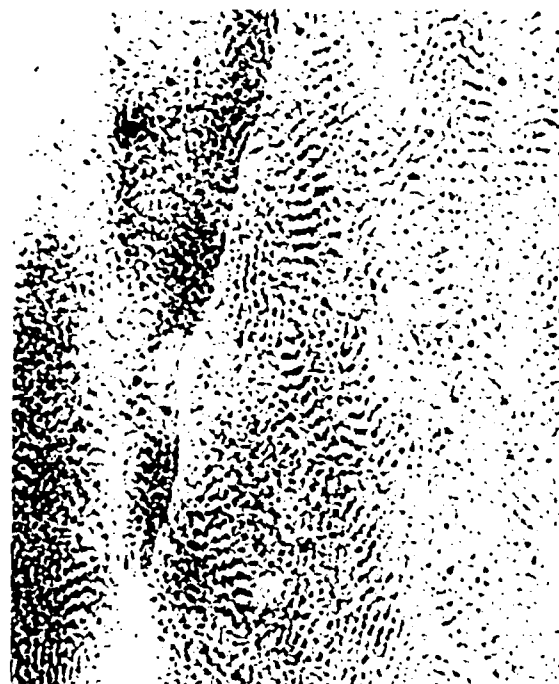


Figure 4: Palladium clusters in a poly(MTD) matrix.

References

- (1) J. D. Swalen, G. C. Bjorklund, S. Ducharme, W. Fleming, S. Herminghaus, D. Jungbauer, W. E. Moerner, B. A. Smith, R. Twieg, D. Yoon, G. Willson, Proc. SPIE 1337, 1 (1990)
- (2) M. Eich, B. Reck, D. Y. Yoon, C. G. Willson, G. C. Bjorklund, J. Appl. Phys. 66, 3241 (1989)
- (3) D. Jungbauer, I. Teraoka, D. Y. Yoon, B. Reck, J. D. Swalen, R. Twieg, C. G. Willson, IBM J. Res. Div. 7864, 72524 (1990) and J. Appl. Phys., in press
- (4) J. D. Swalen, R. Santo, M. Tacke, J. Fischer, IBM J. Res. Div. 21, 168 (1977)
- (5) M. Eich, A. Sen, H. Looser, G. C. Bjorklund, J. D. Swalen, R. Twieg, D. Y. Yoon, J. Appl. Phys. 66, 2559 (1989)

SYNTHESIS AND CHARACTERIZATION OF MONOMERS AND POLYMERS CONTAINING PHOTORESPONSIVE AZOBENZENE - BASED SIDEGROUPS

H. J. Haitjema, G. O. R. Alberda v. Ekenstein and Y. Y. Tan

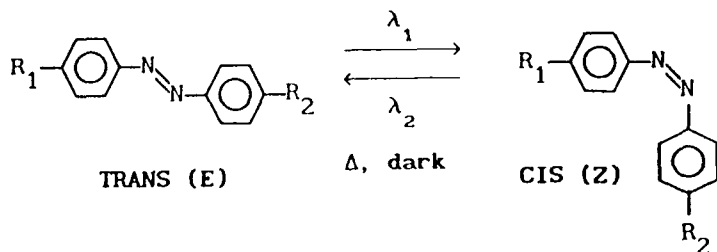
P. J. Werkman, A. J. Koldijk, T. S. Boer

State University of Groningen
Nijenborgh 16, 9747 AG Groningen
The Netherlands

The photochemical behavior of organic chromophores incorporated in polymeric materials is a topic of considerable scientific interest with numerous technological applications [1]. Light can be used as a signal, which can change physical and chemical properties of molecules in an on - off fashion. Photochromic molecules or moieties play an important role in such systems, in which light is absorbed that causes structural changes, which leads to the subsequent effects (i.e.: vision [2]). These effects are well known in biology and can explain the effect of light in many biological processes.

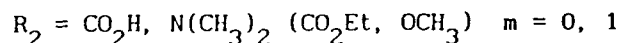
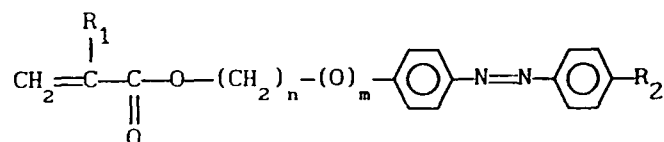
Recently these effects are also observed in synthetic polymers both in solution and in the solid state [3 - 6].

The cis - trans isomerization of the azobenzene chromophore is rather well investigated [8]. This cis - trans isomerization can be used to construct " optical switches" with respect to applications in optical (erasable) storage systems, or in display technology [5,7]. The reversible cis - trans isomerization can be envisioned as follows :



The isomerization is mainly dependent on λ_1 , λ_2 and the temperature (Δ). The isomerization (trans \rightarrow cis or cis \rightarrow trans) that is induced by irradiation at λ_1 or λ_2 , is called photoisomerization, while the isomerization caused by relaxation of the cis - isomer (thermodynamically unstable) in the dark to the trans - isomer (thermodynamically stable) is called the thermal isomerization. It is this isomerization, that we are interested in.

It is known, that the presence of a polymeric matrix effects the photoresponsive behavior of azobenzene compounds [6]. Photochromic processes in a solid matrix such as polymers generally proceed with considerable deviations from what is expected from the behavior in solution. But these effects are already rather well understood. What we are interested in, is what happens to the photoresponsive behavior (kinetics) of the azobenzene chromophores in the case of the existence of a special interaction with the matrix. The type of these interactions may be ionic interactions, or hydrogen bonding (formation of polymeric complexes). The monomers that we aimed to synthesize and polymerize, are of the following type :



We expect that the kinetics of the photoresponsive behavior of the azobenzene groups with CO_2H or $\text{N(CH}_3)_2$ as end groups might deviate from normal kinetics on interaction with respectively (poly) - base or (poly) - acid type polymers (in solution or in film).

Preliminary experiments indicate that there are effects that can be detected in case of the presence of these interactions.

Sofar we have studied the thermal isomerization of azobenzene based compounds (monomeric, polymeric) in solution with other end groups than CO_2H or $\text{N(CH}_3)_2$. The results of the experiments comply with the results of similar experiments published in literature. The thermal isomerizations follow normal first - order kinetics.

One typical feature of the azobenzene compounds with CO_2H or $\text{N(CH}_3)_2$ end groups in solution (DMF) is that they behave like azobenzene-based pH - indicators, like methylorange or methylred.

What the exact effect of this phenomenon will be on the photoresponsive behavior, is yet to be investigated.

ACKNOWLEDGEMENTS

This investigation is supported by the Dutch Ministry of Economic Affairs, Innovation-oriented Research Programme on Polymer Composites and Special Polymers (IOP-PCBP). We thank B. Hesp (State University of Groningen, Physical Department) for building the apparatus for photoresponsive measurements.

LITERATURE

- [1] Guillet, J. E. "Polymer Photophysics and Photochemistry: An Introduction to the Study of Photoprocesses in Macromolecules", Cambridge University Press, New York 1985
- [2] Dewey, A. G.
Opt.Eng. 23, 230 (1984)
- [3] Ciardelli, F. ; Carlini, C. ; Solaro, R. ; Altomare, A. ; Pieroni, O. ; Houben, J. L. and Fissi, A.
Pure & Apl.Chem., 56 (3), 329-42 (1984)
- [4] Ueno, A. ; Adachi, K. and Nakamura, J.
J.Polym.Sci.Polym.Chem., 28, 1161-70 (1990)
- [5] Ikeda, T. ; Miyamoto, T. ; Kurihara, S. ; Tsukada, M. and Tazuke, S.
Mol.Cryst.Liq.Cryst., 182B, 357 (1990)
- [6] Eisenbach, C. D.
Ber.Bunsenges.Phys.Chem., 84, 680-90 (1980)
- [7] LeBarney, P. ; Ravaux, G. ; Dubois, J. C. ; Parneix, J. P. ; Nieumo, R. ; Legrand, C. and Levelot, A. M. in "Molecular and Polymeric Optoelectronic Materials : Fundamentals and Applications", edited by G. Khanarian,
Proc.SPIE-int.Soc.Opt.Eng., 682, 56 (1986)
- [8] Ross, D. L. and Blanc, J.
Photochromism by cis-trans isomerism in "Techniques of Chemistry", edited by G. H. Brown, Wiley-Interscience, New York 1971, vol.III, p.p.471

Poling and Chemical-Binding of Glass-Embodied Chromophores in Supported Sol-Gel Thin-Film Glasses for Second Harmonic Generation

Y. Haruvy[†], J. Byers, and S.E. Webber
The Department of Chemistry and Biochemistry
& Center for Polymer Research
The University of Texas at Austin, Austin, TX, 78712, USA.

Introduction

Second-harmonic generation (SHG) is facilitated by materials that combine a donor-acceptor (DA) molecular system which is conjugated via hybrid π -molecular orbitals with a non-centrosymmetric distribution of molecules¹. The first property is characterized by a very high hyperpolarizability (β) and exists in a wide variety of molecules². The second characteristic can be attained, in principle, in one of two ways: either by using a pure enantiomer of chiral molecules or chiral crystals, or by a non-centrosymmetric packing of symmetric donor-acceptor molecules which possess at least one asymmetric axis.

Many attempts have been published to facilitate non-centrosymmetric packing of donor acceptor molecules and polymers. While most of these methods maintain the first layers almost perfectly ordered, the ordering decreases with an increasing number of layers³ and practical devices with substantial SHG are difficult to obtain. An alternative route is to embody the SHG-active molecules in a host matrix and orient them to produce a non-centrosymmetric pattern. The most convenient route to generate this non-centrosymmetric ensemble of conjugated molecules is by poling them with an intense electric-field^{4,5}. This must be done under conditions which allow sufficient molecular mobility to enable the desired orientation. Poling must be followed by a decrease in the mobility in order to retain the non-centrosymmetric pattern after the electric field is removed.

The salient problem of SHG materials prepared by this method is the spontaneous random reorientation of the poled molecules. This so-called "relaxation" of the poled species occurs after the poling field is removed and leads to a decay of the SHG properties within typical half-times of 1-10 days. The mechanism of this "relaxation" differs from one system to another. In some cases the poled species were encaged in the host-matrices but not chemically bound to them and thus, remained free to reorient⁶. Others have poled species chemically bound to the host matrix as pendant groups of a polymeric backbone. Even so, the poled species could still reorient via several rotation modes⁷. Recently, the incorporation of donor-acceptor conjugated molecules into the backbone of epoxy-polymers was reported⁸. In these studies, the prepolymers were simultaneously subjected to the poling field and to temperatures high enough to induce curing of these epoxies. The resultant polymers exhibited a fairly stable SHG, since most of the DA molecules were attached to the polymeric backbone via two bonds and were less mobile as a consequence.

We have recently introduced a new fast sol-gel method for the preparation of supported thin-film glasses, which are capable of encaging high concentrations of discrete guest molecules^{9,10}. The present work focussed on the selection, incorporation and encaging of SHG molecules in these thin-films. The investigation of various combinations of simultaneous poling, curing and chemical-binding of SHG molecules is discussed

Materials

Methyltrimethoxysilane (MTMS), utilized as the sole monomer for the sol-gel preparations, and chlorotrimethylsilane (CTMS), used for the preparation of silylated model compounds were purchased from Aldrich. The following SHG molecules with high β values were incorporated in the sol-gel matrices: 4,4' diaminodiphenylsulfone (DDS), *p*-nitroaniline (PNA) ($\beta = 35 \times 10^{-30}$ esu), and 4-amino-4'-nitroazodiphenyl (Disperse-Orange-DO) were purchased from Aldrich (AR); and 4-dimethylamino-4'-nitrostilbene (DANS) ($\beta = 450 \times 10^{-30}$ esu) was purchased from Kodak (AR). Sol-gel catalysts were hydrochloric acid (Baker, AR) and dimethylamine (Kodak, AR). All the materials were used without further purification. SHG measurements to date have emphasized PNA-doped sol-gel glasses.

Synthesis

The preparation of the supported thin-film glasses was described in detail in the previous communications^{9,10}. This synthetic route comprises, in principle, the hydrolysis of MTMS with stoichiometric quantity of water in the presence of HCl as catalyst, followed by its polymerization to polymethylsiloxane (PMSO). The ~5 min. reaction is followed by spin-casting onto the support and curing for a few hours (at 60-70°C) to a few days (at room temperature). Samples for poling were freshly prepared and cast before applying the poling field.

Poling

The set-up used for poling consisted of a "DC High Voltage Insulation Tester" of Lanagan & Hoke Inc., capable of supplying up to 15 kV and 500 μ A. Gel samples, freshly cast on a metallic support, were placed a flat electrode which was grounded. The high voltage electrode was a tungsten rod ground to a sharp point and was placed at a distance of 0.5 to 2 cm above the gel. The high voltage was increased gradually until reaching the maximum value without arcing. Typically the poling was carried out at 14 kV and 5-10 μ A. The poling was continued until the surface of the gel appeared cured, as manifested by loss of gloss.

SHG Measurements

The set-up used for measurements of the SHG of the gel-embodied poled molecules is shown in Figure 1. The beam from a mode-locked Nd:YAG laser was incident at 60° from the surface normal and focused to a 0.1 mm² spot. The pulsing rate was 76 MHz with a time profile per pulse of ~100 ps fwhm. The average energy per pulse was ~0.1 mJ. The laser radiation was filtered from the outgoing beam using a cooled Ni(NO₃)₂ aqueous solution liquid filter and followed by a Corning color glass filter. The second harmonic signal at 532 nm was then focussed into a glass fiber optic bundle and brought to the input slit of an Instruments, SA H-10 monochromator with appropriate optical matching to the monochromator f/number.

The detection scheme used was a time resolved photon counting method that allows separation of background noise and SHG signal. Photon counts from a cooled PMT (dark counts of 3 Hz) triggered a time-to-amplitude converter (TAC) start pulse. The stop pulse was obtained from a fast photodiode triggered from the laser pulse. The output of the TAC is proportional to the time difference between the start and stop pulse. This output from the TAC is then digitized by a Multichannel analyzer and a count added to the appropriate time channel. A time profile of the SHG signal was thus obtained. An example profile is shown in Figure 2. The flat noise background line was subtracted and the SHG pulse profile integrated to obtain the desired data. Using this method counting rates of as little as 1 count per second result in high signal to noise ratios.

Results

a) Encaging Donor-Acceptor Molecules in PMSO Glass

Most of the chromophores used were only slightly soluble in the siloxane precursor, due to their polar nature. A typical reaction mixture was: 1g MTMS, 0.2g HCl (10⁻² M) and 2 mg of the chromophore. Upon heating this stirred reaction mixture to 80°C, methanol was produced and complete dissolution of all the ingredients occurred, yielding a clear solution (reaction (1)).



Following our sol-gel procedures^{9,10}, the hydrolysis and polymerization are continued until a weight loss of ca. 500 mg (MeOH) is attained and the viscous polymer is spin-cast.

With less soluble chromophore such as DDS reprecipitation occurred following extensive loss of methanol. At this point the methanol concentration becomes too low to maintain dissolution, while the degree of polymerization is not high enough to encage the chromophores. This problem was highly aggravated when we tried to achieve high loadings (5-15% w/w) of chromophores in the sol-gel recipes (which correspond to ca. 10-30% in the final glass). An additional observation was a decrease in the reaction rate. This can be attributed to the protonation of the amino group of the chromophore and loss of the catalyst. This problem was successfully overcome by modifying the reaction in several ways. The concentration of HCl has to be increased in order to accommodate both protonation of the amino-chromophore molecules and catalysis of the sol-gel reaction. However, this approach cannot be applied at high loadings of the chromophore: adding too much acid at the early stages of the polymerization results in the formation of a grainy polymer film rather than a viscous fluid.

However we found that the regular acid concentration could be employed and the reaction rate enhanced by elevating the temperature to 83-85 °C. The appropriate amount of 1M acid (ca. equimolar to the chromophore) was added, while stirring the sol. When the methanol weight loss reached ca. 35% of the monomer weight the resultant viscous liquid was cast onto the support and spun.

Many chromophores have been introduced into polymeric matrices and poled in order to maintain a non-centrosymmetric chromophore array with SHG properties. It is generally believed that post-poling relaxation processes are the cause of SHG deterioration with time and therefore, chemical binding of the SHG molecules to the matrix while being poled is extremely desirable. This is the situation for amino compounds incorporated into a sol-gel glass, although we have not established that all amino groups are covalently bound. Diamino molecules may be preferred for our goal since they can become bound in two sides and hence, are less subjected to post-poling relaxation processes. Since the binding reaction is reversible, we have to provide appropriate conditions to drive it to the right: 1) to separate the H⁺ from the Si-bound amine as soon as possible to impede reopening of the bond; 2) to ensure a water-lean environment to impede rehydrolysis of the Si-NH bond. The latter condition is inherent to all the fast sol-gel recipes.

b) SHG Measurements of PNA in sol-gel glasses

The SHG behavior of PNA-loaded PMSO glasses is a complex function of sol-gel preparation conditions and poling. The clarity of these films depends on the PNA loading and the rate of curing. For example, for PNA contents greater than ca. 4 wt. % and thicker films (ca. 10-20 μm) some turbidity is obvious, which we assume to be due to colloidal or microcrystalline PNA. These films demonstrated SHG with or without corona poling. In fact in the central portion of the disk where the poling is strongest the SHG was often weaker than near the disk edge. We believe this effect arises because the corona discharge has an accelerating effect on the PMSO curing rate¹¹. The tendency for precipitation or crystallization of the PNA depends on the rate of cross-linking and/or methanol/water ratio present in the PMSO glass (see reaction (1)). In films of this type the SHG signal varied strongly across the face of the disk, presumably increasing when the beam encountered a region with a higher density of crystallites. These films demonstrated little or no SHG when the PNA content was reduced to ca. 3 wt.% unless they were poled. For this loading the films are clear to the eye and we presume that no colloids or crystallites are present.

Thinner films (ca. 1-2 μm) can be prepared by varying the H₂O and HCl content in the sol-gel reaction and increasing the spinning rate during spin-casting. These films were prepared with ca. 3 wt. % of PNA and are very clear and respond strongly to corona poling. In this case we believe we have molecularly dispersed PNA and these molecules have been oriented by the electric field. A thinner film has several effects: 1) the electric field is ca. 10x larger than the thicker films described above; 2) the rate of curing is modified since methanol escape is faster; 3) the effect of poling on sol-gel curing may be different¹². These films have a SHG efficiency as large as the thicker film despite the smaller amount of PNA and smaller path length of the 1064 nm light through the glass. In all cases the strength of the SHG signal is approximately 2 to 10 times stronger than a comparable powdered sample of urea and the 532 nm (green) light is easily visible to the naked eye.

It seems peculiar that the higher loading samples exhibit SHG without poling since the crystal habit of PNA is reported to be centrosymmetric¹³. According to Kurtz and Perry¹⁴ the SHG efficiency of a centrosymmetric powder should be zero. We speculate that incorporation of PNA in these spun glasses induces a non-centrosymmetric aggregation. These and related phenomena for other SHG molecules in these sol-gel glasses will be reported.

Acknowledgement

The authors would like to acknowledge the financial support of the State of Texas Advanced Technology Program (Grant number 003658-394). Quentin Hibben and Douglas Kiserow have assisted with various aspects of some of the measurements reported here.

References

† On sabbatical leave from Soreq NRC, Yavne, 70600, Israel

- 1 Non-linear Optical Properties of Organic and Polymer Materials, Williams, D.J. Ed.: ACS Symposium Series 233, 1983
- 2 Prasad, P.N.; Reinhardt, B.A. Chem. Mater. 1990, 2, 660
- 3 Swalen, J.D. Thin Solid Films 1988, 160, 197
- 4 Mortazavi, M.A.; Knoesen, A.; Kowel, S.T. J. Opt. Soc. Am. B. 1989, 6, 733
- 5 Hampsch, H.L.; Torkelson, J.M.; Bethke, S.J.; Grubb, S.G. J. Appl. Phys. 1990, 67, 1037
- 6 See references 4 and 5 for example.
- 7 Eich, M.; Sen, A.; Looser, H.; Bjorklund, G.C. Swalen, J.D.; Twieg, R.; Yoon, D.Y. J Appl. Phys. 1989, 66, 2559
- 8 Eich, M.; Reck, B.; Yoon, D.Y.; Willson, C.G.; Bjorklund, G.C. J. Appl. Phys. 1989, 66, 3241
- 9 Haruvy, Y.; Webber, S.E. Chem. Mater. (in press)
- 10 Haruvy, Y., Heller, A.; Webber, S.E. "Supported Sol-Gel Thin-Film Glasses Embodying Laser Dyes. II. Three Layer Waveguide Assemblies", to be presented at the Sept. 3-6, 1991 SPIE Conference, Boston, MA
- 11 This effect is the subject of continuing investigation.
- 12 The rate of the sol-gel curing may be tuned by a combination of H₂O and HCl contents and the temperature at which the pre-gel is formed.
- 13 Trueblood, K.N.; Goldfish, E.; Donohue, J. Acta Cryst. 1961, 14, 1009
- 14 Kurtz, S.K.; Perry, T.T. J. Appl. Phys, 1968, 39, 3798

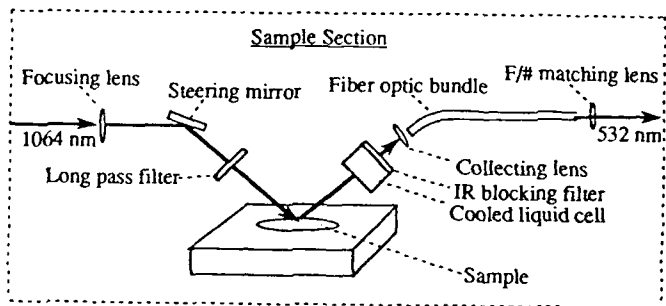
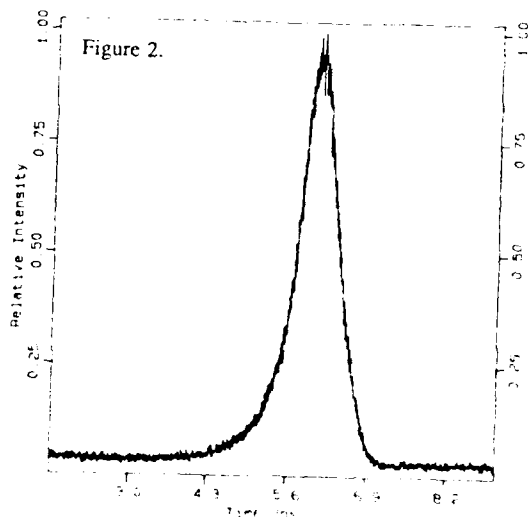


Figure 1 Optical Setup for SHG measurements

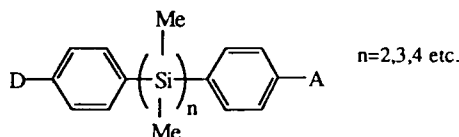


Model molecules with donor-acceptor units intermediated by silicon chains

*Diny Hissink, Jeannet Brouwer, Rien Flipse
and Georges Hadziioannou.*

*Laboratory of Polymer Chemistry, Department of Chemistry,
University of Groningen, Nijenborgh 16, 9747 AG Groningen,
The Netherlands.*

In our research program we aim to synthesize materials transparent in the visible spectrum and with high non-linear optical (NLO) properties. The dye molecules we decided to synthesize are end-capped with donor and acceptor groups, having the following general structure:



D and A are respectively an electron donor and acceptor group. This kind of DA molecules are previously reported by Mignani et al.¹ We intend to introduce these dyes in a polymer matrix, either attached chemically or dispersed physically. Here we present only the initial work on the dye synthesis and characterization.

In most compounds, previously reported², the donor and acceptor groups are intermediated by a conjugated π -system. For many applications e.g. frequency doubling of the fundamental wavelength of a 820 nm laser, complete transparency in the visible is required.

We have chosen a silicon backbone, because of its good transparency and (σ - σ^*) conjugation through the Si-Si bonds, in order to obtain materials with high NLO properties.

The donor and acceptor groups will enhance the electron transport through the silicon chain. The donor group can be functionalized, in order to connect the "dye" to a polymer matrix. With use of spectroscopic techniques like UV and fluorescence we investigated the electronic properties of these materials and the relation to their structure and NLO properties.

Experimental.

All reactions were carried out under an inert atmosphere of argon or nitrogen. The solvents (THF and diethylether) were distilled under nitrogen from LiAlH_4 . The synthesis of the donor-acceptor compounds was carried out using the standard Schlenk techniques.

dichlorosilane

1,2-dichlorotetramethyldisilane and 1,4-dichlorooctamethyltetrasilane were prepared following the procedure reported by Sakurai³.

Grignard reagentia

To a suspension of magnesium in freshly distilled THF, a solution of 4-bromodimethylaminobenzene or 4-bromofluorobenzene in 175 ml freshly distilled THF was added dropwise. 4-trifluoromethylbenzene was dissolved in diethylether. After complete addition the mixture was refluxed overnight and filtered.

Donor-acceptor compounds (DA)

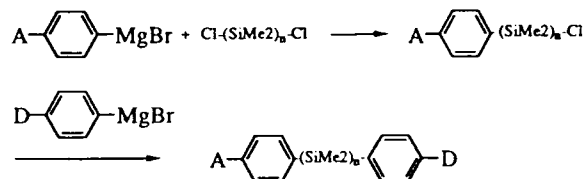
FN2, FN4, and CF3N2 (see next column) were synthesized using the following procedure:

One equivalent of the acceptor grignard reagent solution was added dropwise to a solution of 1 equivalent of the dichlorosilane in freshly distilled THF.

During the addition the reaction mixture was cooled at 0 °C. The reaction mixture was stirred overnight at room temperature. One equivalent of the donor grignard reagent solution was added dropwise to the reaction mixture which was cooled at 0 °C. The reaction was stirred overnight at room-temperature. After removing the solvent, diethylether was added to the crude product. The salt was removed by filtration. The solution was washed 3 times with water. The organic layer was dried over MgSO_4 . The solvent was removed by evaporation, and after crystallization from diethylether (-20 °C) the product was isolated. Yield: FN2 - 40%, CF3N2 - 50%, FN4 - 60%.

Results and Discussion.

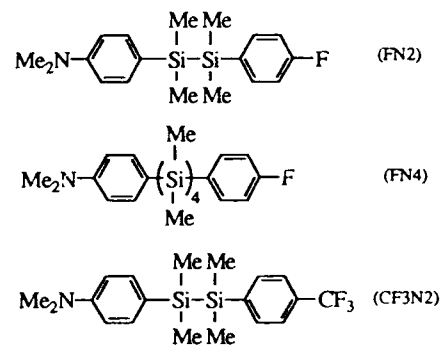
The general synthetic method of these DA compounds is presented in Scheme 1.



Scheme 1.

This reaction can also be inverted.

In this way we prepared the following three compounds:



We used fluor (F) and trifluoromethyl (CF3) as acceptors, because these groups give stable molecules. The above materials were characterized with spectroscopic techniques such as NMR (^1H , ^{13}C , ^{19}F , ^{29}Si), IR (CCl_4) UV and fluorescence. The crystal structures of molecules FN2 and CF3N2 were determined with X-Ray. The phenyl groups are ordered trans towards each other, with a tetrahedral configuration of the silicon atoms.

The electronic properties of these materials were investigated. Table I gives the absorption maxima of FN2, FN4, and CF3N2 and of their analog silicon compounds, without donor and acceptor groups. We used solvents of different polarity. The solvatochromic shifts of the absorption bands at maximum wavelength are very small (1-2 nm), when the solvent is changed from apolar (cyclohexane) to polar (acetonitrile).

When a methyl group on each silicon atom of hexamethyldisilane is replaced by a phenyl group, λ_{max} increases with about 30 nm. This band shifts also 30 nm with respect to the $^1\text{L}_A$ absorption band of benzene. The phenyl group effectively lengthens the conjugated system and would therefore be expected to cause an increase in λ_{max} . The influence of the phenyl rings on the absorption maxima has been reported elsewhere.⁴

With increasing chain length (from 2 to 4 silicon atoms) the position of the maximum absorption band has a bathochromic shift of 15 nm, caused by a longer conjugation length. If a phenyl group is substituted by a dimethylamino group at the para position, λ_{\max} is observed at 272-274 nm with a high molar absorptivity ($\epsilon = 50000$)⁵. We found also that FN2, FN4, and CF3N2 have a maximum absorption at about 273 nm. Consequently, the kind of substituent at the second phenyl ring (H, F or CF3) and the increasing chain length have no influence on the position of λ_{\max} . The absorption can be assigned to a local ($\pi-\pi^*$) transition of the dimethylaminophenyl group. We do not observe Charge-Transfer bands in the UV spectra, which means that the energy needed for a local transition is lower than for a direct Charge-Transfer from the donor to acceptor group.

We measured the emission spectra of FN2, FN4, and CF3N2 in four different solvents: cyclohexane, diethylether, THF, and acetonitrile. The solvatochromic shifts of the CT emission bands are related to the change in dipole moment from ground to excited state, $\Delta\mu$, which can be calculated using the Lippert equation⁶:

$$\nu_{ab}-\nu_{fl} = 2/hc (\mu_e-\mu_g)^2 / A^3 \Delta f + c$$

$$\Delta f = (D-1)/(2D+1) - (n^2-1)/(2n^2+1)$$

where ν_{ab} and ν_{fl} are respectively the absorption and emission maxima, A the Onsager radius of solutes⁷, Δf the solvent parameter, D the dielectric constant, n the refractive index, h Planck's constant and c the velocity of light. The slope of a plot of $\nu_{ab}-\nu_{fl}$ vs Δf gives the value of $\Delta\mu$. FN2, CF3N2, and FN4 show emission bands in the fluorescence spectra at about 350 nm with a small solvatochromic effects. These can be assigned to a local excited emission state of the dimethylaminophenyl ring. CF3N2 shows a second emission band with a large solvatochromic shift, which can be assigned to a Charge-Transfer band (350 nm (cyclohexane); 398 nm (diethylether); 445 nm (THF) and 518 nm (acetonitrile). Figure 1 shows the plot of $\nu_{ab}-\nu_{fl}$ vs Δf .

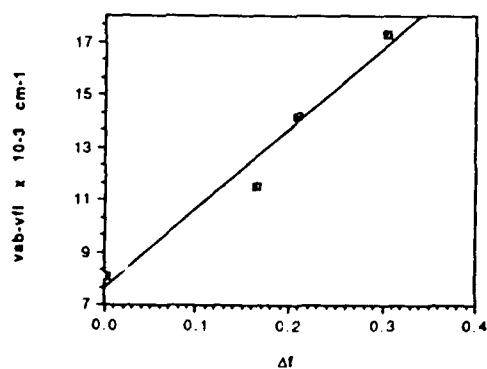


Figure 1: Solvatochromic effect of CF3N2.

We used solvents with different Δf -values: 0.001 (cyclohexane); 0.166 (diethylether); 0.210 (THF); 0.304 (acetonitril).

The slope is 30477 cm^{-1} . Thus $\Delta\mu$ is found to be 27D. This value of $\Delta\mu$ is very large compared to other asymmetric silanes⁸. e.g.: $\text{Ph}(\text{SiMe}_2)_2\text{Me}$ has $\Delta\mu = 4.3 \text{ D}$ and other D-A molecules e.g. p-dimethylamino-p-nitrostilbene (DANS) has $\Delta\mu = 24\text{D}$ ⁶.

The fluorescence emission experiments led us to believe that CF3N2 has a complete charge separation in the excited state. Preliminary β -measurements have been made and the results look promising. More detailed experiments are under way.

Conclusions.

We synthesized materials with interesting spectroscopic properties and promising NLO properties. By increasing the chain length and using stronger acceptors we hope to obtain materials which will have high NLO properties. The relation of β -values to the spectroscopic and structural properties of the new DA molecules reported will be studied in the future.

Acknowledgement.

This work was financially supported by the Dutch Ministry of Economical Affairs, Innovation-oriented Research Programme on Polymer Composites and Special Polymers (IOP-PCBP, Project BP 108).

References.

- 1) Mignani, G., et. al. *Organometallics*, 9 (1990) 2640-2643.
- 2) Chemla, D.S.; Zyss, J. Eds. *Nonlinear Optical Properties of Organic Molecules And Crystals*; Academic Press: Orlando, FL, 1987.
- 3) Sakurai, H.; Tominaga, M.; Watanabe, T., and Kumada, M., *Tetrahedron Lett.*, 45 (1966) 5493.
- 4) Gilman, H.; Atwell, W.H.; Schwebke, G.L., *J. Organomet. Chem.*, 2 (1964) 369.
- 5) Kelling, H., *Z. Chem.*, 7 (1967) Vol. 6.
- 6) Lippert, E., *Z. Elektrochem.*, 61 (1957) 962.
- 7) Onsager, L., *J. Am. Chem. Soc.*, 58 (1936) 1486.
- 8) Sakurai, H.; Sugiyama, H. and Kira, M., *J. Phys. Chem.*, 94 (1990) 1837-43.

Table 1: Maximum wavelengths (nm) of di- and tetrasilanes in cyclohexane and acetonitrile.

Compound	solvent	λ_{\max}	ϵ	λ_{\max}	ϵ
Me ₆ Si ₂	c-hexane	201.4	3150		
	acetonit.	212.8	640		
Ph ₂ Si ₂	c-hexane	205.7	18300	236.5	18000
	acetonit.	213.0	11550	236.4	16650
Ph ₂ Si ₄	c-hexane	202.4	25900	250.8	21600
	acetonit.	213.1	18500	250.7	21400
FN2	c-hexane	209.4	36400	272.0	29300
	acetonit.	214.2	19200	273.3	28100
FN4	c-hexane	220.0	24800	273.8	37000
	acetonit.	213.9	21900	274.7	29400
CF ₃ N ₂	c-hexane	205.7	24400	272.8	27500
	acetonit.	213.9	17500	273.6	23800

(220-240 nm: shoulder)

Novel Third Order NLO Materials from 96% Quinoline

Robert V. Honeychuck

Department of Chemistry, George Mason University,
Fairfax, Virginia 22030, and Chemistry Division,
Naval Research Laboratory, Washington, D.C. 20375

Introduction

Polymers have been formed from quinoline in the presence of trimethyl boron¹ and ZnCl₂ and protonic acids,² and via glow discharge.³ The formation of thin films by simple heating and evaporation of quinoline has apparently not been investigated. We present here a description of films formed by this method from 96% quinoline and 96% quinoline containing solutes.

Experimental

Surface profiles were obtained on a Tencor Alpha-Step 250 instrument. Infrared spectra were done on KBr pellets using a Perkin-Elmer 1800 FTIR machine. Proton NMR spectra were obtained on a JEOL FX90Q instrument at 90 MHz, in CDCl₃ unless otherwise stated, and were referenced to internal TMS. Thermal analyses were done in N₂ on DuPont 951 TGA or 910 DSC machines, using the Thermal Analyst 2100 system. Third order nonlinear optical susceptibilities were measured at 1.064 μm using degenerate four wave mixing. The phase conjugate reflectivity of the polymer film 5a, solutions of the precursor materials, and the solvents were measured relative to CS₂ using apparatus and methods that were previously described.⁴

Poly(1,4-cyclohexylene carbonate) (3) of nominal molecular weight 600 was obtained from Polysciences, Inc., Warrington, PA. The molecular weight specified by Polysciences is meant to be qualitative. The type of molecular weight is not given.

Results and Discussion

When 96% quinoline (1, Fig. 1) is heated in air at 200°C for 3 days it darkens appreciably. The resulting solution can be evaporated on a glass slide at 65°C to give a homogeneous thin film, 2, of high optical quality. The infrared spectrum of 2 exhibits absorptions in the aliphatic C-H stretching region as well as the aromatic region. Aliphatic groups are present in the ¹H NMR of the unheated 96% quinoline starting material. As the quinoline solvent evaporates from the slides, alkylated species remain if they are less volatile. The weight of material remaining after evaporation was 2.8% of the starting weight, roughly corresponding to the 4% of non-quinoline components originally present.

The peak at 1724 cm⁻¹ and the broad absorption from 2500 to 3300 cm⁻¹ for 2 suggests that carboxyl groups are present, possibly from oxidation of methyl groups. The possible intermediate in a methyl to carboxyl transformation, an aldehyde, is not present in the unheated starting material, as evidenced by the lack of peaks in the δ 11.0-11.5 region of the ¹H NMR.⁵

The ¹H NMR of 2 in DMSO-d₆ exhibits the expected complex aromatic region from δ 7 to 9. In addition, a broad, low peak is visible between δ 2.25 and 2.40. This peak is not due to an impurity in the DMSO-d₆, as a solvent blank shows.

Thermogravimetric analysis indicates that 2 may contain some unsubstituted quinoline, with onset of weight loss at 153°C. Quinoline boils at 237°C. The DSC of 2 on the first pass exhibits a broad 1st order endotherm at 119° followed by many sharp

endotherms between 120 and 150°C. These features disappear on the second pass. In a melting point capillary this material forms a viscous black liquid gradually between 80 and 100°C. A melting endotherm was not evident in this range in either DSC pass. Material 2 is soluble in N,N-dimethylformamide, quinoline, and dimethyl sulfoxide, suggesting that if it is polymeric in nature, it is not crosslinked.

Quinoline (96%) is an excellent solvent for poly(1,4-cyclohexylene carbonate) (3) above its melting point of 50°C, and for synthetic mesoporphyrin IX dimethyl ester (4a). The latter is a porphyrin with side chains containing only alkyl groups, plus two ester functionalities. When an approximately 1:1 molar solution of the polycarbonate and diester was heated in 96% quinoline at 200°C and subsequently evaporated at 65°C, a brown material resulted. This sample, 5a, prepared on a microscope slide, was reflective, hard, and flat. It ranged in clarity from transparent at one end to cloudy in the middle to opaque at the other end.

The surface profile of a sample of 5a was obtained. It provides information about the flatness and thickness of the film, attributes important for optical studies. The thickness could not be determined from measurement at the edge of the film on the profilometer because the material had a thick lip wider than 2 mm, the maximum available probe travel. In addition, an attempt to determine the thickness by light microscopy (focusing on the top and bottom of the film) gave questionable results. Instead, a scratch was made with a razor blade perpendicular to the direction of the profilometer probe travel. The scratch extends down to the glass, and some of the material removed appears as a positive peak. The profile exhibits a maximum surface variation normal to the surface of 0.10 μm, with the probe traveling parallel to the surface a distance of 2 mm. The scratch reveals the flat glass of the substrate, a commercial microscope slide. In a separate experiment, the slide alone showed a maximum variation of 0.01 μm, and a scratch made the same manner had a depth of 0.14 μm. Thus the scratch in the material in Fig. 2 represents primarily the thickness, 2.92 μm, of the organic film, determined at the point of laser impingement (see below).

The infrared spectrum of 5a, taken in a KBr pellet, shows primarily peaks associated with the polycarbonate and the quinoline-derived material. In particular, the carbonyl frequencies (Table 1) indicate that the major contributor is 2.

Table 1. Carbonyl stretching frequencies.^a

	$\nu_{C=O}$, cm ⁻¹
4a	1735
3	1739
1	b
2	1724
5a	1724

^aAll spectra taken in KBr pellets on a Perkin-Elmer 1800 FTIR. All intensities are strong unless otherwise noted.

^bQuinoline (96%) has very weak absorptions at 1718 and 1734 cm⁻¹.

The ¹H NMR spectrum of material 5a is most easily understood by comparison with the spectra of the starting materials. The most prominent feature of the spectrum of mesoporphyrin IX dimethyl ester, taken in chloroform-d, is in the methyl singlet

region. Theoretically there should be 6 singlets; in practice 4 peaks and 2 shoulders appear, entirely between 3.5 and 3.7 ppm. Poly(1,4-cyclohexylene carbonate) shows peaks between 0.9 and 2.0 ppm, and between 3.4 and 4.1 ppm. The spectrum of 5a in the same solvent shows the quinoline-derived material at 2.4 ppm and between 6 and 9 ppm, and the polycarbonate between 1 and 4 ppm. The porphyrin methyls may contribute to the 3.4 to 3.7 ppm region. The entire spectrum is characterized by broad peaks except for the TMS and residual CHCl_3 peaks.

The appropriate thermal analysis studies were done. Thermogravimetric analysis of the porphyrin alone indicates remarkable stability, with no weight loss at 378°C. The onset of decomposition was at 411°C, with 54% of the weight remaining at 492°C. Loss of the 8 groups around the porphyrin nucleus would give 50.8% residual weight.

Poly(1,4-cyclohexylene carbonate) shows a gradual decrease in weight after melting at 50°. This is probably associated with polymerization and subsequent boiling of cyclohexanediol (bp 270°C), and boiling of remaining polycarbonate of MW 600 at 350°. The product material (5a) has a TGA which most closely resembles those of the polycarbonate and the quinoline-derived material. The steepest portion has an onset at 248°, near the boiling point of quinoline and the melting point of the product material.

The DSC of 5a on the first pass exhibits a broad endotherm centered at 61°C followed by a strong exotherm with an onset at 190°C. In a melting point apparatus, some of the material melts at 225-230°C, forming a black solid in a black liquid. The second DSC pass is essentially featureless, suggesting that polymerization may have occurred during the first pass.

The third order nonlinear optical susceptibilities of some of these materials have been measured at 1.064 μm . The results are given in Table 2. The $\chi^{(3)}$ for the polycarbonate-porphyrin-quinoline polymer film (5a) was substantially larger than that of any of the components. Among the polymer precursor materials, the $\chi^{(3)}$ for 96% quinoline was surprisingly large. It was about 4 times larger than that of the related molecule α -picoline⁶ and about half that of CS_2 . The $\chi^{(3)}$ of the porphyrin, 4a, in solution was indistinguishable from that of the solvent; only an upper limit for the molecular hyperpolarizability of this material was found.

Table 2. Nonlinear optical properties.

	$\chi^{(3)}$ χ_{xxxx} , esu ^a	α , cm ⁻¹ b	$\langle \gamma_{xxxx} \rangle$, esu ^c
4a ^d	3×10^{-14}		$< 3 \times 10^{-34}$
5a	6×10^{-12}	400	
1	2×10^{-13}	<1	

^aThird order optical susceptibility with all polarizations parallel.

^bAbsorption coefficient.

^cThird order hyperpolarizability with all polarizations parallel.

^d 3×10^{-2} M solution in CHCl_3 .

Conclusions

Films from 96% quinoline and from 96% quinoline with poly(1,4-cyclohexylene carbonate), meso-porphyrin IX dimethyl ester, and d(II)mesoporphyrin IX dimethyl ester have been cast via heating and subsequent evaporation. The films are approximately 3 μm thick, with a maximum variation normal to the surface of 0.10 μm in 2 mm

of surface travel. The optical quality of the samples formed from 96% quinoline alone is excellent, and variable from the quinoline/solute combinations. The third order nonlinear optical properties of some of these materials have been examined. The response of the porphyrin-containing materials may be due primarily to the porphyrins or to the 96% quinoline-derived material; this awaits measurements of the 96% quinoline-derived material 2.

Acknowledgements

The author gratefully acknowledges the support of the ONT/DEW Hardened Materials Block Program at NRL and the American Society for Engineering Education, which provided a Summer Faculty Research fellowship. The assistance of Robert F. Cozzens of the NRL Chemistry Division, James S. Shirk and J. Ryan Lindle of the NRL Optical Sciences Division, and Bruce D. Sartwell of the NRL Condensed Matter and Radiation Sciences Division is greatly appreciated.

References

- Smirnov, R.F.; Tikhomirov, B.I.; Bitsenko, M.I.; Yakubchik, A. I. *Vysokomol. Soedin., Ser. A* 1971, 13, 1618.
- Topchiev, D.A.; Popov, V.G.; Kabanov, V.A.; Kargin, V.A. *Izv. Akad. Nauk SSSR, Ser. Khim.* 1964, 391.
- Bradley, A.; Hammes, J.P. *J. Electrochem. Soc.* 1963, 110, 15.
- Shirk, J.S.; Lindle, J.R.; Bartoli, F.J.; Hoffman, C.A.; Kafafi, Z.H.; Snow, A.W. *Appl. Phys. Lett.* 1989, 55, 1287.
- Pouchert, C.J. "The Aldrich Library of NMR Spectra," 2nd ed., Vol. 2, Aldrich Chemical Co., Milwaukee, 1983; 744D, 745A.
- Phu Xuan, N.; Ferrier, J.-L.; Gazengel, J.; Rivoire, G. *Opt. Comm.* 1984, 51, 433.

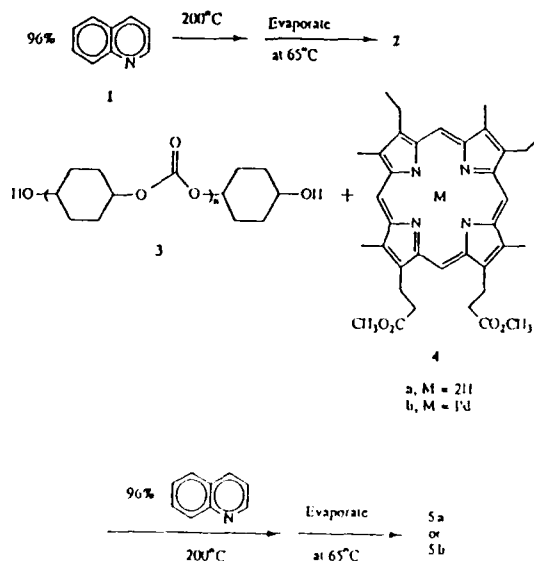


Fig. 1. Preparation of materials 2, 5a, and 5b.

CUBIC NONLINEAR OPTICS OF POLYMER THIN FILMS.
5. WAVELENGTH DISPERSION OF THE $\chi^{(3)}$ OF
POLY(P-PHENYLENE BENZOBISTHIAZOLE) BASED
MOLECULAR COMPOSITES

Samson A. Jenekhe* and Michael F. Roberts
Center for Photoinduced Charge Transfer
and Department of Chemical Engineering
University of Rochester
Rochester, NY 14627-0166
and

Herman Vanherzele and Jeffrey S. Meth
DuPont Central Research & Development Department
P.O. Box 80356, Wilmington, DE 19880-0356

Introduction. As originally conceived [1-5], a molecular composite is a material system in which a high strength, high modulus, rigid-rod polymer is molecularly dispersed in the matrix of a flexible-coil polymer. This concept of a molecular composite was introduced with the aim of obtaining materials with enhanced mechanical properties by molecular-level reinforcement of the rigid-rod polymer, such as poly(p-phenylene benzobisthiazole) (PBZT), with highly entangled flexible-coil materials [1-5]. Unfortunately, these attempts have been fraught with difficulties associated with processing of the molecular composites, for example: low critical concentrations for phase separation [2,3a]; phase separation during coagulation [3b]; and degradation of the flexible-coil polymer in the concentrated acid solvents used [4].

Our primary interest in molecular composites is in developing novel approaches to their processing [6] and in their nonlinear optical (NLO) properties [7]. We view the molecular composite (MC) concept as an important approach to tailor the NLO properties of polymers. Molecular composites as third order NLO materials allow the ready investigation of effects of composition, morphology, and intermolecular structure on both the third order optical susceptibility $\chi^{(3)}$ and linear optical properties such as optical loss (α) and index of refraction (n).

In this paper we will report our detailed study of the third order NLO properties of the molecular composites of the conjugated rigid-rod polymer PBZT with flexible-coil polyamides, nylon 66 and poly(trimethyl hexamethylene terephthalamide) (PTMHT), prepared using the novel approach of complexation mediated processing from organic solvents [6]. We will discuss the wavelength dispersion of the $\chi^{(3)}$ of PBZT/nylon 66 and PBZT/PTMHT composites as determined by picosecond third harmonic generation (THG) in the wavelength range 0.8-2.4 μ m. We will also discuss the composition dependence of the nonresonant $\chi^{(3)}$ of these composites at 1.9 μ m.

Although early measurements of the $\chi^{(3)}$ of PBZT indicated that this polymer has a large third order optical nonlinearity [8,9], there was a major inconsistency between the two reported values of $\chi^{(3)}$. Some of the possible sources for the one order of magnitude difference between the reported $\chi^{(3)}$ values of PBZT [8-10] include optical quality of the films, possible protonation of the films by the acidic processing solvents, poor estimate of the film thickness and index of refraction, and the difference in wavelength and measuring techniques. A recent study of the NLO properties of PBZT and PBZT/Zytel composite [10] attempted to address some of these problems but acknowledged that possible residual acid in the films and hence protonation of the PBZT by the methanesulfonic acid solvent makes it difficult to attribute the recently measured $\chi^{(3)}$ to the pure PBZT [10].

Experimental. The PBZT sample had an intrinsic viscosity of 18 dl/g in MSA at 30°C and was kindly given to us by the Air Force Materials Laboratory, Dayton, OH. Nylon 66 of intrinsic viscosity 1.0 dl/g was obtained from Polysciences Inc., Warrington, PA, and PTMHT of intrinsic viscosity 0.9 dl/g was obtained from Scientific Polymer Products, Ontario, NY. (Both $[\eta]$ values of the polyamides were measured in m-cresol at 40°C). Nitromethane (99+%) and Aluminum (III) Chloride (99.9%) (Aldrich) were used as received.

Details of the complexation of these polymers and their subsequent dissolution in organic solvents have been described in detail elsewhere [6,11,12] and in a forthcoming publication [6c] and

will not be repeated here. In summary, $AlCl_3$ complexes of the desired polymer composites were prepared in nitromethane, in a glove-box under a nitrogen purge.

Thin films of the molecular composites of PBZT/nylon 66 and PBZT/PTMHT were prepared by shearing thin films of their solutions between two 1 mm thick optically flat silica substrates (5 cm in diameter). The coatings on the silica substrates were immersed in deionized water overnight to remove the aluminum chloride. This was followed by drying in a vacuum oven at 60-70°C for 12-16 hours. Composites prepared in this way were characterized by differential scanning calorimetry (DSC), thermogravimetric analysis (TGA), UV-Visible and FTIR spectroscopy, and optical and scanning electron microscopy, and were found to be uniform, homogeneous, non-phase separated materials of the desired composition [6c].

The electronic absorption spectra of thin films of PTMHT, PBZT, and 1:1 PBZT:nylon 66, and 1:1 PBZT:PTMHT are shown in Figure 1, where the ratios in the composites are mole ratios of polymer repeating units. The film thickness of these composites was not measured and therefore their electronic spectra were normalized relative to the λ_{max} (437 nm) of the pure PBZT for comparison. The absorption bands of the pure conjugated polymer PBZT (203, 255, 437, and 468 nm) were retained in the composites. No absorption features were observed above 500 nm in the spectra of Figure 1.

The THG measurements of the magnitude of $\chi^{(3)}$ ($-3\omega, \omega, \omega$) of the PBZT/nylon 66 and PBZT/PTMHT composites and pure components PBZT and PTMHT were made by using a previously described laser system [13] and THG procedure [7]. In the present study the THG experiments were performed at a fundamental wavelength of 0.8-2.4 μ m.

Results and Discussion. Figure 2 shows the composition dependence of the off-resonant $\chi^{(3)}$ of PBZT/nylon 66 and PBZT/PTMHT molecular composites at 1.9 μ m. The PBZT/nylon 66 composites show a linear dependence of $\chi^{(3)}$ with mole fraction of the optically active component PBZT, as expected for a three-dimensional isotropic material. The $\pm 20\%$ error in the $\chi^{(3)}$ value of each sample is due mostly to error in film thickness measurement since the repeatability of individual result for each sample is $\pm 5\%$. The composition- $\chi^{(3)}$ relationship for the PBZT/PTMHT composites, shown in Figure 2, exhibit a nonlinear dependence. The greater than linear increase of $\chi^{(3)}$ with mole fraction of PBZT in PBZT/PTMHT composites is attributed to a partial ordering to the PBZT molecules by the PTMHT host matrix. These results of the effects of the host matrix and composition on the $\chi^{(3)}$ of molecular composites are particularly interesting in that they demonstrate that a suitable choice of the host matrix material can, through morphological control of the order of the guest NLO polymer, enhance the magnitude of $\chi^{(3)}$.

In Figure 3 is shown the wavelength dispersion of the $\chi^{(3)}$ of PBZT and its 1:1 composites with nylon 66 and PTMHT in the wavelength range 0.8-2.4 μ m. The $\chi^{(3)}$ spectra of all three materials exhibit a strong resonance feature that can be attributed to a multiphoton process. The peak position of this resonance in $\chi^{(3)}$, 1.3 μ m ($\sim 1eV$), suggests that it is a three-photon resonance with the first excited state which has a peak at 437 nm as seen from the electronic spectra of Figure 1. The three-photon resonance enhanced $\chi^{(3)}$ of the pure PBZT at 1.3 μ m is $8.31 \pm 1.66 \times 10^{-11}$ esu and that of the 1:1 PBZT/PTMHT and 1:1 PBZT/nylon 66 was $\sim 5.2 \times 10^{-11}$ and $\sim 4.3 \times 10^{-11}$ esu, respectively.

In a forthcoming paper [7b] we will use a theoretical model to analyze and fit the $\chi^{(3)}$ data of PBZT and its molecular composites.

Conclusions. Optical quality thin films of PBZT and its molecular composites with two flexible-coil polyamides, nylon 66 and PTMHT, have been prepared from their soluble Lewis acid-base complexes in organic solvents and their third order nonlinear optical properties investigated by picosecond third harmonic generation in the wavelength range 0.8-2.4 μ m. The composition- $\chi^{(3)}$ relationship was found to be linear in PBZT/nylon 66 composites and nonlinear in the case of PBZT/PTMHT. The greater than linear $\chi^{(3)}$ dependence on mole fraction of PBZT in PBZT/PTMHT composites was attributed to the host matrix induced ordering of the conjugated

PBZT molecules. From the measured $\chi^{(3)}$ spectra of the pure PBZT and its molecular composites it was found that the cubic optical nonlinearity was enhanced by a strong three-photon resonance with a peak at $1.3\mu\text{m}$. These results confirm our belief that polymer based molecular composites represent an important approach to the optimisation of cubic NLO materials for photonic applications and are excellent model systems for probing structure- $\chi^{(3)}$ relationships.

Acknowledgements. Work at the University of Rochester was supported by the New York State Science and Technology Foundation, Amoco Foundation, and National Science Foundation (Grant CHE-881-0024).

References

1. Helminiak, T.E. *ACS Div. Org. Coatings and Plastic Chem. Preprints* 1979, 40, 475.
2. Hwang, W.-F.; Wiff, D.R.; Banner, C.L. *J. Macromol. Sci. - Phys.* 1983, B22(2), 231.
3. (a) Hwang, W.-F.; Wiff, D.R.; Verschoore, C. *Polym. Eng. Sci.* 1983, 23, 789. (b) Hwang, W.-F.; Wiff, D.R.; Verschoore, C.; Price, G.E.; Helminiak, T.E.; Adams, W.W. *Polym. Eng. Sci.* 1983, 23, 784.
4. Chuah, H.H.; Tan, L.-S.; Arnold, F.E. *Polym. Eng. Sci.* 1989, 29, 107.
5. Wiff, D.R.; Helminiak, T.E.; Hwang, W.-F. in: *High Modulus Polymers*, A.E. Zachariades and R.S. Porter, Eds., Marcel Dekker: New York, 1988, Chapter 8.
6. (a) Roberts, M.F.; Jenekhe, S.A. Paper presented at the 33rd IUPAC Int. Symp. on Macromolecules, July 8-13, Montreal, Canada. (b) Roberts, M.F.; Jenekhe, S.A. *Chem. Mater.* 1990, 2, 629-631. (c) Roberts, M.F.; Jenekhe, S.A. *Chem. Mater.*, to be submitted.
7. (a) Vanherzele, H.; Meth, J.S.; Jenekhe, S.A.; Roberts, M.F. *Appl. Phys. Lett.* 1991, 58, 663. (b) Vanherzele, H.; Meth, J.S.; Jenekhe, S.A.; Roberts, M.F. To be submitted.
8. Rao, D.N.; Swiatkiewicz, J.; Chopra, P.; Ghosal, S.K.; Prasad, P.N. *Appl. Phys. Lett.* 1986, 48, 1187.
9. Garito, A.F.; Teng, C.C. *Proc. Soc. Photo-Opt. Instrum. Eng.* 1986, 613, 146.
10. Lee, C.Y.-C.; Swiatkiewicz, J.; Prasad, P.N.; Mehta, R.; Bai, S.J. *Polymer*, in press.
11. Jenekhe, S.A.; Johnson, P.O.; Agrawal, A.K. *Macromolecules* 1989, 22, 3216
12. Jenekhe, S.A.; Johnson, P.O. *Macromolecules* 1990, 23, 4419.
13. Vanherzele, H. *Appl. Optics* 1990, 29, 2246.

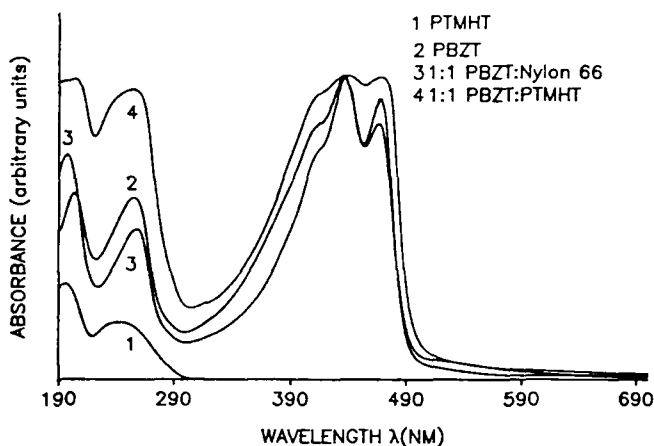


Figure 1 Electronic absorption spectra of thin films of PTMHT, PBZT, PBZT/nylon 66 (1:1), and PBZT/PTMHT (1:1).

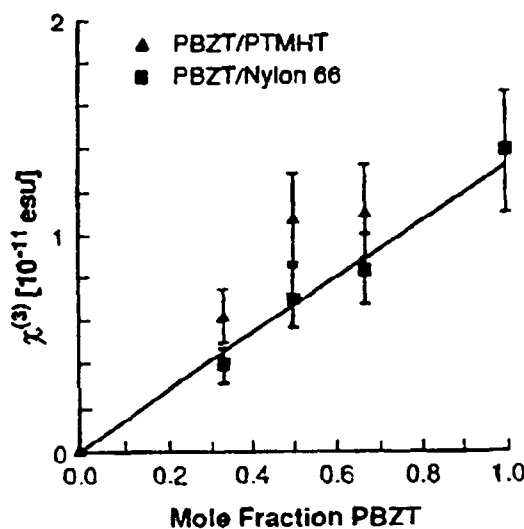


Figure 2 Composition dependence of the $\chi^{(3)}$ of PBZT/nylon 66 and PBZT/PTMHT composites at $1.9\mu\text{m}$.

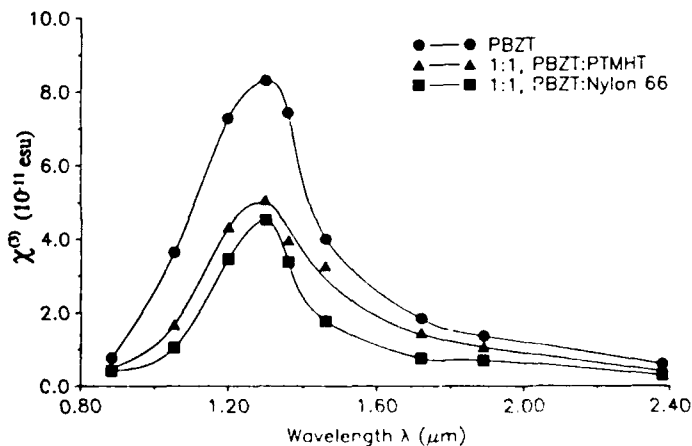
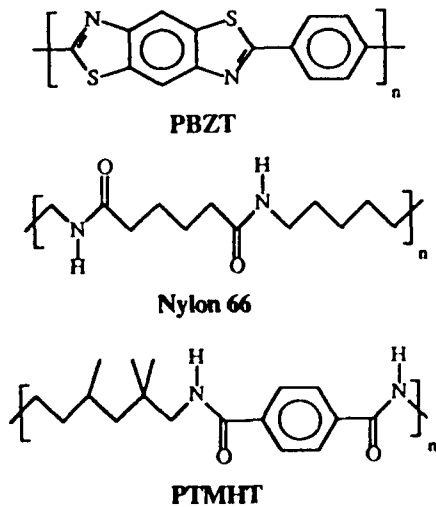


Figure 3 The $\chi^{(3)}$ spectra of PBZT and its molecular composites with nylon 66 and PTMHT.

MEASUREMENTS OF THE OPTO-ELECTRIC PROPERTIES OF MOLECULES OF POTENTIAL USE IN PHOTOACTIVE POLYMERS BY TIME RESOLVED MICROWAVE CONDUCTIVITY (TRMC).

S.A. Jonker and J.M. Warman

IRI, Delft University of Technology, Mekelweg 15, 2629 JB Delft, The Netherlands.

1. Introduction

The recent interest in the nonlinear optical properties of organic molecules has necessitated a better understanding of their photophysical properties. In particular the two state model for the molecular hyperpolarizability, β , predicts that this parameter, which is responsible for second harmonic generation, is amongst other things, proportional to the difference in dipole moment of the first excited singlet state and ground state ($\mu_s - \mu_0$). Information about the dipole moment changes occurring on photoexcitation of molecules in dilute solution in non-polar solvents can be provided by the time-resolved microwave conductivity (TRMC) method. A brief description of the TRMC-technique and examples of its applications are given below.

1. Technique

A solution of ca. 0.1 mM of the molecule of interest is photoexcited by a 308 nm laser pulse of 5 ns FWHM and an intensity of ca. 10 mJ/cm². The transient change in microwave conductivity (dielectric loss) of the medium on flash photolysis is monitored with nanosecond time resolution. This change is related to the dipole moments of the photoexcited solute molecule in the ground and excited state, μ_0 and μ_s respectively, by

$$\Delta\sigma = \frac{(\mu_s^2 - \mu_0^2)}{\tau_r} \frac{(\epsilon + 2)^2}{27k_B T} F(\omega\tau_r) N_s \quad (1)$$

In (1), k_B is the Boltzmann constant; ϵ is the relative dielectric constant of the solvent; N_s is the concentration of excited molecules; τ_r is the rotational relaxation time of the dipole and ω is the radian microwave frequency. The function $F(\omega\tau_r)$ is the Debye relaxation term. Knowing the light intensity and the optical characteristics of the solution, the concentration of the excited state (N_s) and hence the parameter $(\mu_s^2 - \mu_0^2)/\tau_r$ can be determined¹. In addition, by measurement of the background dielectric loss of the solution as a function of concentration of ground state molecules (N_0) the parameter μ_0^2/τ_r can be determined from (2). If the value of μ_0 is known then μ_s can be calculated from the two measurements assuming the relaxation time to be the same for the two states. The relaxation time can also be estimated.

$$\Delta\sigma = \frac{\mu_0^2}{\tau_r} \frac{(\epsilon + 2)^2}{27k_B T} F(\omega\tau_r) N_0 \quad (2)$$

TRMC provides therefore identification and quantification of dipolar excited states and their kinetics. The technique is unique in that it can monitor both singlet and triplet excited states at the same time. TRMC provides in addition information on the motional freedom of chromophoric molecules.

3. Results and Discussion

3.1 Amino-Nitro compounds. Figure 1 shows transient microwave conductivity traces for solutions of compounds ANF and DANF in benzene.

From this figure it is apparent that methylation of the anilino nitrogen strongly influences the molecular photophysics. The dimethylamino derivative DANF, clearly displays a short lived dipolar singlet component followed by a much longer lived triplet signal. In the case of ANF, the triplet signal is seen to be much larger indicating a considerably greater intersystem crossing efficiency. Also the singlet lifetime determined from the fluorescence decay is substantially increased by dimethyl substitution from 1.9 to 3.6 ns. Similar effects but less pronounced are found for ANS and DMANS as is shown by the parameters listed in Table I.

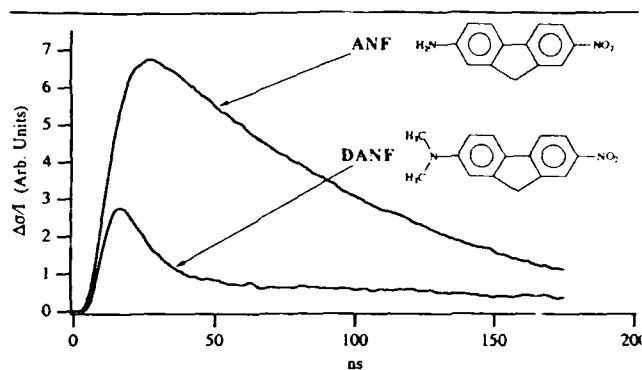


Figure 1: Transient microwave conductivity traces for solutions of compounds ANF and DANF in benzene.

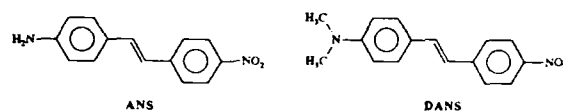


TABLE I: Estimates of the S1 and T1 lifetimes, the intersystem crossing efficiency Φ_{isc} and dipole moments of ground and excited state.

Compound	τ_{S1} (ns)	Φ_{isc}^a	μ_{S0} (Debye)	μ_{S1} (Debye)
ANF	1.9	0.65	5.4	20
DANF	3.6	0.08	6	23
ANS	2.5	0.08	5.1	18
DANS	2.8	0.03	6.6	24

a) on the basis of $\mu_{T1} = \mu_{S1}$

3.2 Alkoxy-cyano-biphenyl compounds. Figure 2 shows transient microwave conductivity traces for solutions of compounds HOCNBP and MAPCNBP in benzene.

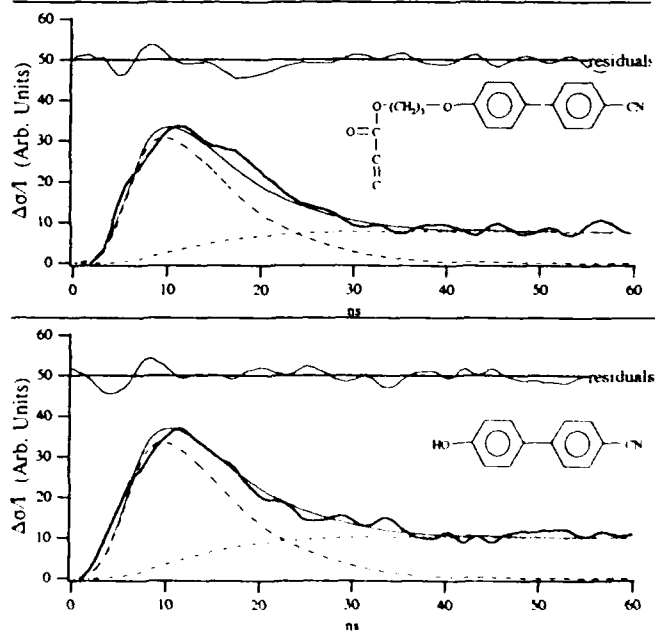


Figure 2: Transient microwave conductivity traces for solutions of compounds MAPCNBP (upper part) and HOCNBP (lower part) in benzene. Also shown are the calculated convolution fits (—), with separate triplet (---) and singlet (- - -) contributions.

As is evident from figure 2 the absolute magnitude and the form of the transients observed for these two compounds are similar. Both are characterised by the formation of a, short lived dipolar singlet state with a lifetime of ~ 1 ns and a long lived dipolar triplet state with a lifetime of > 500 ns. For $\mu_T = \mu_S$, Φ_{isc} is determined to be approximately 0.02. The photophysics of the hydroxy-cyano-biphenyl chromophore would appear therefore to be very little influenced by propylmethacrylate substitution at the hydroxy group in contrast to the marked effect of methyl substitution at an amino donor site mentioned above.

Taking for the unsubstituted chromophore an S_1 lifetime of 1.0 ns together with a ground-state dipole moment of 4.8 D and a dipole relaxation time of 86 ps (determined from the ground state dielectric loss, Eqn. 2) results in a value of 12.4 D for the dipole moment of the S_1 state from the TRMC transient, i.e. considerably lower than for the nitro-amino compounds. In view of the apparent lack of change in the photophysics of the chromophoric units we take the excited state dipole moment to be the same for the substituted compound. Using this we can derive a value for the dipole relaxation time of 111 ps for the propylmethacrylate derivative from the TRMC transients. This value is not significantly different to the 86 ps found for the unsubstituted chromophoric unit. Because of the flexibility of the substituents there is apparently little perturbation of the motional freedom of the hydroxy-cyanobiphenyl unit.

Future research will focus on the photophysical properties and motional freedom of the donor-acceptor chromophores attached to a polymer backbone.

References

- (1) De Haas, M.P. ; Warman, J.M. *Chem. Phys.* 1982, 73, 35.

MACROMOLECULAR CHROMOPHORIC ASSEMBLIES WITH ENFORCED POLARITY: INORGANIC AND HETEROCYCLIC LINKAGES

H.E. Katz, M.L. Schilling, C.E.D. Chidsey, T.M. Putvinski, W.L. Wilson, G.R. Scheller, W.T. Lavell. AT&T Bell Laboratories, Murray Hill, NJ 07974.

Research on noncrystalline second order nonlinear optical materials has focussed increasingly on the magnitude and stability of the polar orientation required of the active molecular subunits. Joining these subunits together in a head-to-tail fashion can lead to enhancements in both qualities, since the orienting force might act cooperatively upon an ensemble of subunits, and the motion required to randomize the orientation of a polar aggregate is much less probable than for individual molecules. Here, we describe two approaches to polar chromophore aggregates. The first results in a thermally stable self-assembled multilayer of polar azo dyes, while the second produces covalently head-to-tail-linked polar chromophores in which the molecular moments are constrained to be highly additive.

I. Polar zirconium organophosphate self-assembled multilayers

Self assembly has already been considered for the construction of films with extensive polar order.¹ We have recently demonstrated a simpler method for polar multilayer self-assembly based on zirconium phosphate layered structures.² These layers are robust and insoluble, and show no evidence of deterioration in quality with the number of monolayers deposited. Our three-step deposition method is a modification of the two-step method developed by Mallouk³ for preparing symmetrical multilayers. A hydroxyl-terminated surface is first treated with POCl_3 to give a phosphate-terminated surface. This is then treated with aqueous Zr(IV) to form a zirconium-terminated surface. Finally, the latter is treated with a hydroxy-organophosphonic acid to form a new hydroxyl-terminated surface. We now extend this technique to construct multilayers from a hydroxy-phosphonic acid that contains a polar azo chromophore, **1**. Figure 1 illustrates the expected multilayer structure, which was expected to show substantial second-order nonlinear optical susceptibilities.

Silicon and glass substrates were prepared for organophosphonate deposition according to conditions optimized previously.⁴ After oxidative treatment with H_2O_2 - H_2SO_4 solution (CAUTION: this reacts violently with organic material), the substrates were exposed to a solution of (3-aminopropyl)trimethoxysilane (1% v:v) in anhydrous octane at reflux for 10 min. The resulting 30-Å-thick film provided an amino-terminated surface that was phosphorylated with 0.2 M POCl_3 and 0.2 M collidine in acetonitrile at room temperature for 5-10 min. The phosphoramidate-terminated surfaces were washed with H_2O and immersed in 5 mM aqueous ZrOCl_2 for 5 min; previous experiments have shown that the zirconation step is essentially instantaneous.

Substrates with zirconated surfaces were immersed for 10 min in solutions of 1.5 mM **1** (synthesized by azo-coupling of 4-aminophenylphosphonic acid to *N,N*-bis(2-hydroxyethyl)aniline) in EtOH in capped jars heated just below the boiling point. This treatment was sufficient to obtain maximum thickness. At room temperature, several hours were required for complete coverage. The hydroxyl end groups on the dyes were phosphorylated and zirconated as described for the priming sequence, and the dye deposition was repeated, creating a multilayer. The thickness of the multilayer films on silicon was monitored by ellipsometry and UV-vis spectrometry. The thickness per layer, 16 Å, is slightly less than the theoretically predicted 20 Å based on the model in Figure 1. This thickness was reproduced consistently from layer to layer.

Observation of second harmonic generation from this multilayer assembly (1.064 μm fundamental) confirms that the layers are in fact polar ordered, as was expected from the method and conditions of their preparation. No second harmonic output was observed from layers of the centrosymmetric compound quaterthiophenediphosphonic acid, consistent with expectations that a polar chromophore is necessary for second harmonic generation, and proving that the observed second harmonic output is not an artifact of the inorganic interlayers. Additional experiments in which input and detector polarizations were varied indicated that both *zz* and *zx* tensor components contribute to the signal.

II. Piperidinylimino-linked polar chromophores

Oligomers consisting of head-to-tail-linked, dipolar, pi-conjugated monomers have been of interest as electrically polarizable elements in polymeric second order nonlinear optical materials.⁵ If these oligomers could be made rigid and linear, they should be orientable by electric fields to give materials with larger polar order parameters than similar materials containing corresponding monomers, because the oligomer dipole moment would be the sum of all the constituent monomer moments, leading to an enhanced orientational polarizability. The resulting orientation should be more stable than for small or nonrigid dipoles because of the large volume of matrix material that would have to move during orientational randomization.

We have reported semirigid polar oligomers based on piperazinamide linkers,⁶ in which each segment may sweep out a 110° cone angle with respect to its neighbor. Although the angle is rigorously defined, the dipolar additivity between segments is much less than it would be if the angle were closer to 180°, and the rotational freedom around the cone leads to multiple conformations in oligomers larger than dimer. Here, we propose the 4-piperidinylimino group, which combines a parallel divalent imine acceptor with a 1,4-disubstituted six-membered ring donor, as a novel link between dipolar segments, with the ultimate aim of incorporating this linker in a polymer such as **2**. So far, we have synthesized bis chromophores **3** and **4**, as well as single chromophores **5** and **6**. We show via dipole moment measurements that the dipoles on either side of the imine link are almost perfectly additive, i.e. the bonds to the internal donor and acceptor supplied by the link, as well as the principal moments of the segments, are virtually parallel.

The dimeric chromophores were synthesized as shown in Figure 2.⁷ Compounds **5** and **6** were synthesized from the appropriate aldehydes and cyclohexylamine in toluene. The dipole moments of **3-7** determined in dioxane solution from plots of dielectric constant vs. weight fraction of solute⁸ (linear correlation coefficients of >0.997) are 9.2, 10.6, 2.7, 4.8, and 6.8 D, respectively. Clearly, the dipole moments for models of the segments of **3** add up to a value (9.5 D) that nearly equals the dipole moment of **2**, and is within experimental error of that moment. Significant additivity is also indicated for **4**. Molecular modelling (MOPAC) predicts a phenylene-phenylene angle for **2** of 150-180°, which is consistent with the observed additivity of the moments. The apparent additivities could have been diminished slightly because the axis of the benzaldimine chromophore moment is not entirely coincident with the 1,4-axis of the phenylene unit, and small contributions from C-N single bonds may slightly influence the moments as well.

We expect polymers with structures like **1** to be highly dipolar rigid rods, by virtue of the significant dipole moment contributed by each segment and the nearly perfect projection of the moments along the rigid rod axis assured by the imino connector. Efforts to synthesize these polymers are currently in progress.

Synthesis, Poling and Optical Characterization of Polyurethanes Bearing NLO-active Chromophores

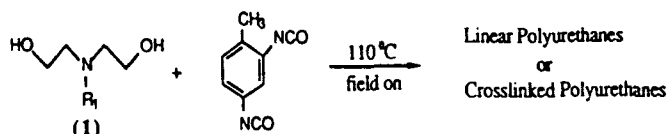
P. Kitpichai, R. Laperuta, Jr., G.M. Korenowski and G. E. Wnek, Department of Chemistry, Polymer Science and Engineering Program, Rensselaer Polytechnic Institute, Troy, New York 12180-3590; I. Gorodisher, 3M Science Research Laboratory, St. Paul, MN 55144-1000.

Introduction

Recently organic and polymeric materials have been of particular interest due to their promising potential applications in optical information processing and telecommunications.^{1,2} This interest has arisen from the promise of attractive combinations of optical, structural, and mechanical properties. Organic and polymeric materials can exhibit considerably high optical damage thresholds and broad transparency ranges. In addition, the ability to prepare numerous derivatives implies that properties can be tuned to meet specific requirements. Because of their processability into various forms, polymer seem particularly attractive for applications in nonlinear optics.

Popular approaches for the generation of polymers exhibiting second harmonic generation (SHG) include poling linear polymers³ or networks⁴ containing dissolved, NLO-active chromophores, or polymers to which suitable chromophores have been covalently attached.⁵ We have considered approaches for the preparation of polymer films capable of second harmonic generation where electric field poling of is carried out during polymerization and film formation using monomers bearing NLO-active chromophores. In previous preprint,⁶ we demonstrated this idea with the simultaneous synthesis and poling of a polyurethane derived from *N,N*-bis-(2-hydroxyethyl)-*p*-nitroaniline and 1,6-diisocyanatohexane. Solidification to glassy thin films is complete within a few seconds owing to the fast kinetics of isocyanate/alcohol reactions.

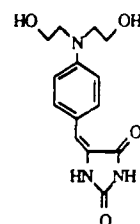
The present paper describes in more detail the synthesis and optical characterization of some of these new polymers. The general approach is outlined in Scheme 1.



The diols (1) are typically comprised of a bis-(2-hydroxyethyl)aniline moiety connected at the para position to acceptors such as nitro, tricyanovinyl, *p*-nitroethenyl, cyclobutene dione, and imidazolidine dione. We note that these diols may also have utility as dyes in a variety of step-growth polymers. We have prepared about twelve new diols bearing NLO-active chromophores, and the synthesis of one of these will be described in detail later. A new triol capable of network formation during polymerization and poling will also be described, and the stability of the SHG response from polyurethanes derived from the diol and triol will be compared. Pu recently proposed the use of the cyclobutene-dione moiety as a promising new electron acceptor group,⁷ and the triol utilized in the present study employs this acceptor along with an aniline donor. The diol we discuss below contains an imidazolidine dione as an acceptor, which to our knowledge has not been examined previously. The diol and triol were reacted with commercially available diisocyanates, in particular 2,4-toluene diisocyanate (TDI), in an electric field as outlined in Scheme 1. A corona generated at the tip of a sharp tungsten needle was used for poling.

Experimental

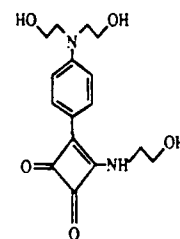
5-[4-[*N,N*-Di(2-hydroxyethyl)amino]benzylidene]imidazolidine-2,4-dione, 1a.



1a

A mixture of 2 g (9.57 mmol) of *N,N*-Di(2-hydroxyethyl)-*p*-aminobenzaldehyde,⁸ 0.96 g (9.57 mmol) of hydantoin and 3 drops of piperidine in 25 ml of ethanol was heated under reflux for 20 hours. The mixture was cooled and yellow product was collected and recrystallized from water. Yellow crystals were obtained (m.p. 239–40°C). UV: λ_{\max} (EtOH) = 388 nm. ¹H NMR (DMSO-*d*₆): δ vs. TMS: 6.69 (d), 7.43 (d): aromatics; 3.30–3.70 (m): methylene protons; 6.31 (s): methine proton; 7.70 (s), 10.41 (s): NH; 4.80 (s): OH.

4-(3-amino-1-propanol)-3-[*N,N*-Di(2-hydroxyethyl)aniline]-cyclobutene-1,2-dione, 1b.



1b

A solution of 8.89 g (49 mmol) of *N,N*-Di(2-hydroxyethyl)aniline in 49 ml dichloromethane was added dropwise to the mixture of 3.68 g (24.5 mmol) 1,2-dichlorocyclobutenedione⁹ and 3 ml (0.245 mmol) of boron trifluoride etherate in 15 ml of dichloromethane at 5–10°C with stirring. After the addition was completed, the mixture was stirred for another 4 hours at 5–10°C. The solvent was evaporated out and the residual viscous liquid was poured into 150 ml of ice water containing 2 drops of concentrated hydrochloric acid. An orange powder was precipitated. The mixture was filtered and washed well with cold water. The product was purified by column chromatography and recrystallized from chloroform. Orange crystals of 4-chloro-3-[*N,N*-Di(2-hydroxyethyl)aniline]-cyclobutene-1,2-dione were obtained (m.p. 136–8°C). ¹H NMR (CD₃CN-*d*₃): δ vs. TMS: 8.05 (d), 6.94 (d): aromatics; 3.61–3.73 (m): methylene protons; 3.29 (s): OH.

Next, a mixture of 0.295 g (1 mmol) of 4-chloro-3-[*N,N*-Di(2-hydroxyethyl)aniline]-cyclobutene-1,2-dione, 0.15 g (1 mmol) of 3-amino-1-propanol and 10 ml of absolute ethanol was heated under reflux for 10 minutes. After cooling in an ice bath, the yellow product 1b was separated and crystallized from absolute ethanol (yellow crystals, m.p. 198–9°C). UV: λ_{\max} (EtOH) = 399 nm. ¹H NMR (DMSO-*d*₆): δ vs. TMS: 6.80 (d), 7.83 (d): aromatics; 1.76 (m), 3.73 (m), 3.43–3.69 (m): methylene protons; 8.69 (t): NH; 4.53 (t), 4.80 (t): OH.

Synthesis and poling of polyurethanes derived from 1a and 1b and TDI.

An equimolecular amount of diol and diisocyanate was dissolved in 10 ml of distilled tetrahydrofuran (THF). Ten drops of the solution were deposited onto a 1 mm thick transparent microscope slide (Fisher, Premium) coated on the opposite side with aluminium. The slide was immediately placed 0.7 cm under a sharpened tungsten needle electrode charged at 10 kV and the mixture was then heated at 110°C for 20 minutes. A bright yellow polymer film formed in a few seconds. The heat was then shut off and the polymer was allowed to cool to room temperature and finally the electric field was terminated. The Al coating was removed using dilute HCl. Polymer film thickness was measured with a profilometer (Alpha-Step 200), and each sample yielded thickness

values in the range of $\sim 1 \mu\text{m}$.

Second harmonic generation (SHG) measurements. The second harmonic generation (SHG) at 532 nm of the poled polyurethanes was measured in transmission. The incident source was the 1064 nm fundamental of a Q-switched DCR-2A Quanta-Ray Nd:YAG laser operating at a 10 Hz repetition rate and a 9 ns pulse duration.

In the SHG experiment the monochromatic, near Gaussian pump beam with a diameter of 0.9 cm was immediately directed through a Glan-Taylor polarizer to select linearly, vertically polarized light. A 10% beamsplitter was employed before the polymer sample to direct a fraction of the beam into a stationary polycrystalline quartz reference. The collimated beam propagating through the beamsplitter was then incident on a 20 cm focal length lens which was positioned 20 cm in front of the 0.2 m McPherson monochromator.

The polymer sample were mounted on a rotation stage in between the entrance of the monochromator and the lens, and rotated around a horizontal axis at about 1 degree/sec. P-polarization was selected by having the incident beam impinge perpendicularly to the horizontal rotation axis as the sample was rotated from an angle of incidence of $+80^\circ$ to -80° . After the sample two IR absorbing Schott KG-1 glass filters and a polarizer were utilized to allow only the vertically polarized signal through to monochromator entrance.

At the monochromator exit slit, the optical signal was detected by a cooled RCA c31034 photomultiplier tube. After preamplification, the signals from individual laser pulses were measured and digitized using a Stanford Research System gated integrator Model SR250 and Model SR245 Computer Interface Module. The processed signals from the laser pulses were then digitally stored.

Pulse to pulse laser intensity variations were removed by monitoring the SHG generated in the quartz reference. The detection of the SHG produced in the reference was the same as that for the sample's signal.

The refractive indices of the polymer film prepared from diol 1a and TDI are 1.620 (532 nm) and 1.565 (1064 nm); those for the polymer prepared from triol 1b and TDI are 1.602 (532 nm) and 1.544 (1064 nm). These values were determined at the University of Lowell (Prof. S. K. Tripathy's laboratory).

SHG stability. The SHG intensity was measured as a function of time after poling at room temperature. As a further test of the SHG stability, the sample was heated to 100°C and the SHG intensity was monitored continuously at a fixed angle ($\phi = 56^\circ$).

Results and Discussion

Figure 1 shows a Maker-fringe curve (p-p measurement) obtained from a poled, crosslinked¹¹ polyurethane prepared from 1b and TDI. The second harmonic coefficient was calculated from the angular dependence of the second harmonic (SH) intensity and the formalism of Jerphagnon and Kurtz for uniaxial materials, assuming also that $d_{31} = d_{24} = d_{15} = 1/3d_{33}$.^{3,10} The SHG coefficient for the network polymer was determined to be $d_{33} = 7.81 \times 10^{-9}$ esu. The SH intensity of the poled crosslinked polyurethane is extremely stable. For example, no relaxation of SH intensity is observed even during one hour at 100°C . The polymer prepared from the diol 1a and TDI is less stable, experiencing slow decay of SH intensity over a six month period at room temperature as shown in Figure 2. The d_{33} values obtained shortly after poling and ~ 6 months after poling are 8.74×10^{-9} and 6.03×10^{-9} esu, respectively. The temporal response is somewhat better than those of other poled, linear polymers, and may be due to hydrogen bonding between urethane and/or imidazolidine dione units assisting to retard depolarization. The T_g of this polymer is about 178°C from differential scanning calorimetry. The polymer is soluble in THF, arguing against crosslinking during synthesis via allophanate formation or reactions at the imidazolidine dione.

In summary, we believe the in-situ poling and polymerization of diisocyanates and NLO-bearing diols and triols represents a useful approach for the synthesis of NLO-active polymer films having attractive optical properties and temporal stability.

Acknowledgements

We thank the Air Force Office of Scientific Research and DARPA for generous support, and Prof. Sukant Tripathy and members of his group for the refractive index measurements.

References and Notes

1. D. S. Chemla and J. Zyss eds., *Nonlinear Optical Properties of Organic Molecules and Crystals*, Academic Press, New York, 1987.
2. D. J. Williams ed., *Nonlinear Optical Properties of Organic and Polymeric Materials*, ACS Symposium Series No. 233, 1983.
3. K. D. Singer, J. E. Sohn, and S. J. Lalama, *Appl. Phys. Lett.*, **49**, 248 (1986).
4. M. A. Hubbard, T. J. Marks, J. Yang, and G. K. Wong, *Chem. Mater.*, **1**, 167 (1989).
5. C. Ye, T. J. Marks, J. Yang, and G. K. Wong, *Macromolecules*, **20**, 2322 (1987).
6. P. Kitipichai, R. LaPeruta, Jr., G. M. Korenowski, G. E. Wnek, I. Gorodisher and D. R. Uhlmann, *Polym. Prepr.*, **30**, 176 (1989).
7. L. S. Pu, in *Materials for Nonlinear Optics*, S. R. Marder, J. E. Sohn and G. D. Stucky, eds., ACS Symp. Ser. No. 455, ACS, Washington, Ch. 22 (1991).
8. A. K. Sen and C. C. Price, *J. Org. Chem.*, **24**, 125 (1959).
9. R-C. De Selins, C. J. Fox, and R. C. Riordan, *Tetrahedron Lett.*, 781 (1970).
10. J. Jerphagnon and S. K. Kurtz, *J. Appl. Phys.*, **41**, 1667 (1970).
11. The film derived from triol 1b is insoluble; films derived from diols will usually dissolve in common solvents.

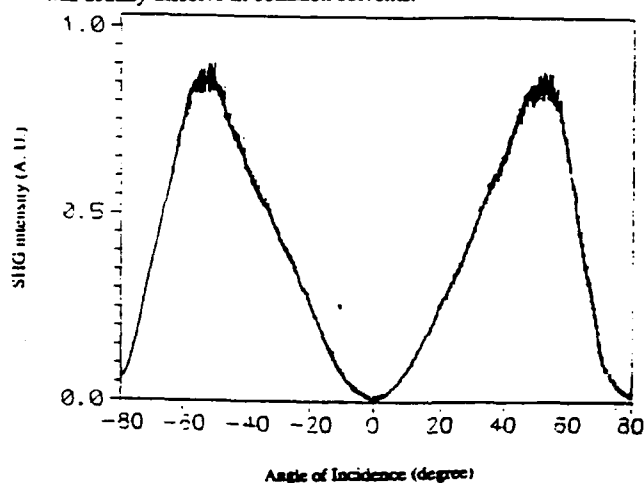


Figure 1. Fringe pattern of crosslinked polyurethane prepared from 1b and TDI.

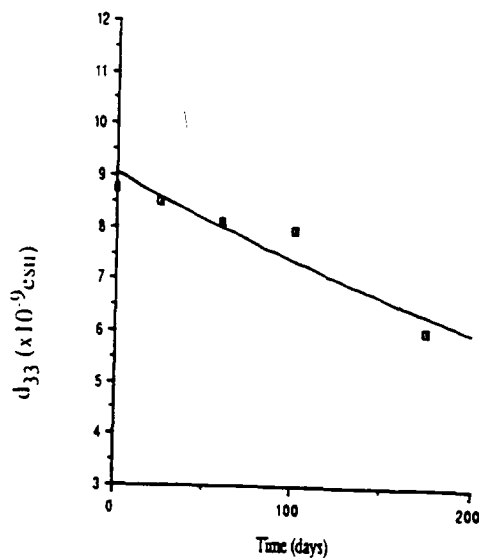


Figure 2. Second-harmonic coefficient of poled polyurethane prepared from diol 1a and TDI, measured as a function of time at ambient temperature.

OPTICAL FOUR-WAVE MIXING IN A SILVER COLLOID-POLYMER COMPOSITE

R. LaPeruta, P. Kitipichai, G. E. Wnek, and G. M. Korenowski, Department of Chemistry, Rensselaer Polytechnic Institute, Troy, New York 12180.

INTRODUCTION

Increasing interest in applications of nonlinear optical (NLO) processes has stimulated research aimed at developing materials possessing large third order nonlinearities. This focus on third order NLO materials is a direct result of the large number of different four-wave mixing (FWM) processes which can be exploited in applications. One example of a FWM process is optical phase conjugation. Optical phase conjugation can be used to restore distorted optical wave fronts and has potential applications in laser amplification and laser fusion as well as in optical image restoration.

All FWM processes result from the third order NLO polarization, $P^{(3)}$.

$$P^{(3)} = \chi^{(3)} : E_1 E_2 E_3 \quad (1)$$

The magnitude of $P^{(3)}$ in a given material is directly proportional to the product of the electric fields of the incident light waves. $P^{(3)}$ is also proportional to the third order NLO susceptibility, $\chi^{(3)}$. It is $\chi^{(3)}$ which is characteristic of the optical medium.

In this paper, we undertake the first work on the development of NLO composites constructed from noble metal nanoparticles in NLO polymer hosts. As separate classes of materials, both the organics and metal nanoparticles show promise as NLO materials. When combined to form composites, interactions between the polymer host and entrapped metal nanoparticles can potentially be used to produce large optical nonlinearities. Tailoring the size and shape of the metal particles to increase local fields internal to the composite and having charge transfer interactions between the polymer and metal particles are several mechanisms by which an increase in the nonlinear polarizabilities can be achieved. We present the first synthetic preparation of a polymer/silver nanoparticle composite, its characterization, and the measurement of $|\chi^{(3)}|$ for degenerate four-wave mixing (DFWM) at selected wavelengths.

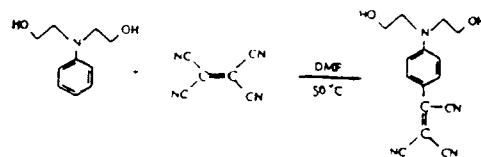
EXPERIMENTAL

A: Synthetic Preparations

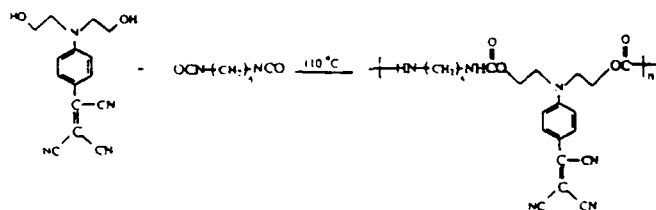
Silver colloids were prepared by reduction of silver ions with lithium borohydride. This preparation was a slight variation of the method developed by Creighton et al (1979).¹ This involved the drop-wise addition of 33.33 ml of 1×10^{-3} M AgNO_3 solution over the course of 10 minutes to 100 ml of a freshly prepared 2×10^{-3} M LiBH_4 solution while constantly stirring. The solution became faint yellow in color upon the addition of the silver nitrate solution. The silver colloids have an absorbance maximum at ~ 397 nm corresponding to the surface plasmon resonance of the silver.

The silver colloids were further characterized in terms of size and shape by transmission electron microscopy. The average diameter of the silver sols used in the polymer/colloid composite was determined from transmission electron microscopy to be 11.46 ± 3.74 nm.

A N,N-di-(2-hydroxyethyl)-p-tricyanoethylaniline monomer (tricyano) for the polyurethane preparation was synthesized according to the following reaction



In 10 ml of a silver colloidal solution (6×10^{-6} volume fraction of silver), 1.5 mg of the tricyano monomer was dissolved. The water was removed by rotary evaporation over 30 minutes at 50°C followed by vacuum drying at room temperature for 12 hours. The sample was dissolved in tetrahydrofuran and 0.05 g of additional tricyano monomer was added to the solution. A stoichiometrically correct quantity of 1,6-diisocyanatohexane (corresponding to 1:1 ratio of monomers) was added to the resulting solution followed by vigorous stirring. Homogeneous mixtures of the two solutions were made using various relative concentrations of the two in order to vary the silver particle concentration in the resulting composite. Approximately, 1 ml of a given mixture was placed on a BK-7 glass slide and the solvent was allowed to evaporate at room temperature. The subsequent monomer mixes were heated to 110°C to polymerize and form the composite via the following reaction



B: Degenerate Four-Wave Mixing

The experimental arrangement for the phase conjugation measurements is shown in Figure 1a. The measurements were performed at the three wavelengths 532 nm, 562 nm and 570 nm. The 532 nm source was the second harmonic from a Quanta-Ray Q-Switched DCR-2A Nd:YAG laser operating at 10 Hz with a 6-7 ns pulse duration. The 562 and 570 nm lines were obtained from a Quantel TDL50 dye laser operating with Rhodamine 590. The dye laser was pumped with a Quantel Q-Switched YG581C-20 Nd:YAG laser operating at 20 Hz. The pulse duration of the dye laser was 6 ns. In the DFWM experiment, the two pump beams were counterpropagating and the optical fields were coupled into the glass/thin film composite waveguide by 1 cm right angle prisms as shown in Figure 1b. The probe beam was 6° off the pump beam axis. All incident beams were vertically polarized. The intensities of the two pump beams were varied from 2.83×10^{12} to 8.74×10^{13} erg/cm². The probe beam intensity was varied from 1.42×10^{11} to 4.37×10^{12} erg/cm². The phase conjugate signal beam was focused into a 0.2 m McPherson monochromator with a 20 cm focal length lens. At the monochromator exit slit, the optical signal was detected by a calibrated and cooled RCA C31034 photomultiplier tube. After preamplification, the signal from individual laser pulses was measured and digitized using a Standford Research System gated integrator Model SR250 and Model SR245 Computer Interface Module. The processed signals from the laser pulses were then digitally stored.

RESULTS AND DISCUSSION

The colors of the polyurethane/silver nanoparticle composite and the polyurethane polymer are very different. The polymer is dark red-violet while the composite material is light yellow. UV-visible spectra for the polymer and the polymer/silver composite, volume fraction of silver 5×10^{-6} , are shown in Figure 2.

Degenerate four-wave mixing measurements were made on thin films of this polymer/composite material (volume fraction of silver $\sim 5 \times 10^{-2}$). These measurements were performed in the thin film waveguide arrangement previously described. Table 1 lists values of $|\chi^{(3)}|$ at the wavelengths of 532 nm, 562 nm, and 570 nm which were obtained from these measurements. To extract a value of $|\chi^{(3)}|$, the intensity of the signal beam in the four-wave mixing experiment was measured and a reflectivity R was determined. This reflectivity is related to $|\chi^{(3)}|$ by Equation 2.²

$$R = \left[\frac{2\pi\omega}{cn} \right]^2 |\chi^{(3)}|^2 (8\pi/cn)^2 L^2 I_f I_b \quad (2)$$

R , the reflectivity, is the ratio of signal power to incident probe power and I_f and I_b are the intensities of the forward and backward pump light beams, respectively. L is the optical path length through the composite. From power dependence studies, the value of n in Equation (1) was determined to be 2.

The maximum value measured, $|\chi^{(3)}| = (3.65 \pm 1.09) \times 10^{-10}$ (esu), was at 532 nm and was appreciably larger than $|\chi^{(3)}|$ measured for a silver colloidal solution. At 532 nm, a sol solution containing an approximately equal volume fraction of silver nanoparticles as that found in the composite yielded a magnitude of $|\chi^{(3)}| = (0.963 \pm 0.503) \times 10^{-10}$ (esu).

In comparing the composite to silver nanoparticles in water, it is not known whether the larger value of $|\chi^{(3)}|$ for the composite is the result of polymer/metal particle interactions. It is possible that this increase in $|\chi^{(3)}|$ is from an additional nonlinearity from the polyurethane. DFWM measurements were also performed on polyurethane films. No DFWM signals were observed. This lack of a DFWM signal could be the result of several factors. One possible factor is that DFWM signals could have been absorbed by the polymer. A second possibility is that the polymer may possess a small $|\chi^{(3)}|$ with respect to DFWM.

The extent to which polymer/silver nanoparticle interactions contribute to $|\chi^{(3)}|$ of the composite is not determined at this time. Evidence was found, however, that indicates strong interactions exist between the functional groups of the polymer and the silver particles. This evidence implies that these interactions are potentially responsible for an increase in the optical nonlinearity of the composite.

In the composite preparation, the diol bearing a tricyanovinyl moiety of the polymer was introduced to the silver colloidal solution. It was observed that the tricyano monomer stabilized the silver nanoparticles. Without the monomer, the silver particles agglomerate and precipitate over time. Also, during evaporation of a sol solution, particle agglomeration was observable. However, with the addition of the monomer, there was no evidence that the silver particles were agglomerating.

Raman spectra of the tricyano monomer in a sol solution showed a vibrational Raman band at $\sim 530 \text{ cm}^{-1}$. This band is assigned to a Ag-cyano stretching mode³ and indicates the tricyano monomer is chemisorbed to the silver nanoparticles. This also suggests that other strong interfacial interactions (such as charge transfer) between the polymer and silver nanoparticles can exist.

In the composite, it appears that the polymer is strongly interacting with the entrapped silver nanoparticles through the cyano functional group. Solution NMR studies show absorptions by the aromatic ring protons of the tricyanovinyl moiety, are slightly shifted upfield for the composite with respect to those observed for the

polymer sample. This is indicative of greater electron density in the aromatic rings in the polyurethane/silver nanoparticle composite in comparison to the polyurethane. In the composite material, cyano groups are apparently interacting with the silver nanoparticles. The result is the reduction of the electron withdrawing capabilities of the cyano groups.

In addition, FTIR spectra of the polymer versus the composite show a decrease in the strength of the free C≡N stretching band ($\sim 2250 \text{ cm}^{-1}$) for the composite indicating fewer free cyano functional groups. This additional evidence points to chemisorption of the polymer to the silver particles and existence of interactions between these two components of the composite.

In summary, the first of a new class of polymer/noble metal nanoparticle composite materials was synthesized and characterized. With respect to DFWM, this composite exhibits a larger $|\chi^{(3)}|$ than that measured for either of its component parts alone. Interactions between the polymer functional groups and the entrapped metal particles are believed to be the origin of the increase in optical nonlinearity.

ACKNOWLEDGEMENTS

G. E. Wnek wishes to thank DARPA for support of this work. G. M. Korenowski thanks the DARPA funded Optoelectronics Technology Center and the Office of Naval Research for their support.

REFERENCES

1. J. A. Creighton, C. G. Blatchford and M. G. Albrecht, *J. Chem. Soc. Faraday II* 75, 790 (1979).
2. J. T. Remillard and D. G. Steel, *Opt. Lett.* 13, 30 (1988).
3. F. Farha and R. T. Iwamoto, *Inorg. Chm.* 4, 844 (1965).

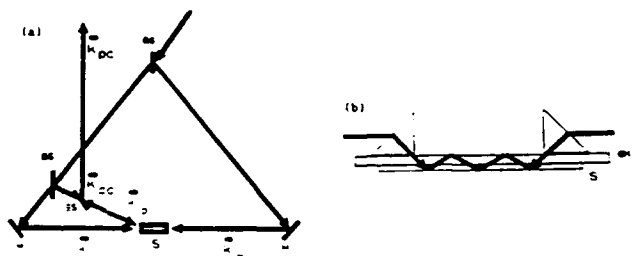


Fig. 1. Experimental arrangement for phase conjugation. BS (beam splitter), M (mirror), S (sample), BK 7 (glass substrate), and k (wavevector). Subscripts f, b, p and pc correspond to the forward pump, backward pump, probe and phase conjugate light beams, respectively. (a) is a top view and (b) is a side view.

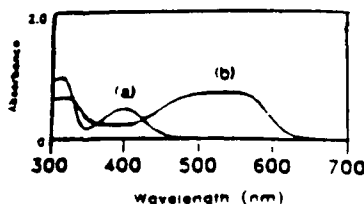


Fig. 2. UV-Vis of (a) composite and (b) polyurethane.

Table 1	
Wavelength	$ \chi_{\text{eff}}^{(3)} $ (10^{-10} esu)
532 nm	3.65 ± 0.82
562 nm	0.791 ± 0.276
570 nm	0.586 ± 0.198

Novel Photoactive Liquid Crystal Polymers
C.H.Legge., M.J.Whitcombe., A.Gilbert. and
G.R.Mitchell.

Polymer Science Centre,
University of Reading,
Whiteknights,
Reading RG6 2AF.,
U.K.

1. Introduction.

The liquid crystalline state is characterised by long-range orientational correlations of molecular groups which are usually described in terms of an order parameter, S . A wide variety of optical phenomena, such as changes in refractive index, may be induced in liquid crystalline materials, either through variation in S or by manipulation of the director n . In addition to the well known electric and magnetic effects known in nonlinear optics these induced changes may come about via photochromic units which are mixed in with the mesogen: Upon irradiation at an appropriate wavelength it is possible for some photochromic molecules to undergo a shape change via isomerisation. This change can disrupt the local ordering of the liquid crystalline units and consequently change the properties of the material. By combining both units into a polymer it is possible to utilise polymeric properties, such as their processability and glass transition, whilst maintaining the liquid crystalline properties of the low molar mass analogues.

In this report we present some novel liquid

crystalline copolymers in which we are able to manipulate the order parameter S and the director n through selective irradiation with light. In particular we are able to photoinduce an isothermal phase transition from the orientationally ordered liquid crystalline state ($0 < S < 1$) to the isotropic phase where $S = 0$ in copolymer 1 whilst in copolymer 2 we are able to change the direction of n with respect to some initial predefined orientation. Photocontrol of both S and n has been reported recently for polymeric liquid crystal systems [1-6]. In essence all of these reports utilise the possibility of optically pumped geometric isomerisation in which the structural effects of isomerisation have been exploited rather than directly using the photochromic properties. In such liquid crystalline systems the photoactive units may be present as a small fraction of the total material.

The changes in S and n for the copolymers studied occur due to photoinduced isomerisation of the photoactive units (E-Z isomerisation). In copolymer 1 the chromophore unit is non-mesogenic in nature and photoisomerisation results in a depression of T_{11} as a direct consequence of a change in S . In copolymer 2, however, the chromophore is mesogenic. In this case the isomerisation results in a rotation of the mesogenic/photoactive units (change in n).

2. Results

2.1. Naphthyl System

The copolymer 1 was prepared by free

radical polymerisation of the appropriate monomers as described elsewhere [7 and 8]. This copolymer with $R^1:R^2=9:1$ exhibited a nematic phase with $T_{11}=66^\circ\text{C}$ and $T_i=25^\circ\text{C}$. The chromophore, R^1 , can undergo E-Z isomerisation about the ethylenic bond. Films (ca. $18\mu\text{m}$ thickness) were prepared on both surface treated and untreated glass slide substrates. The copolymer was melted between the substrate and a glass cover slip (thickness ca. 0.1mm) followed by pressing in a clamp. The phase behaviour of these prepared copolymer films was evaluated using conventional thermo-optic procedures. Wavelength selective irradiation of these films was achieved using a 150W Xe arc lamp incorporating an infrared filter and a grating monochromator together with a variable temperature stage which allowed in-situ irradiation [9]. Spatial selectivity in irradiation was achieved through the use of masks.

Films prepared as outlined above were irradiated using a narrow band (40nm) of wavelengths centred on 340nm for 30min to achieve E-Z isomerisation. Figure 1 shows the change in transmitted light, as a function of temperature, passing through the sample in the polarising microscope. The sample was viewed so that half of the area represented the irradiated part of the sample and the other half the unirradiated. From this graph we can see that two transitions are present, due to each of the irradiated and unirradiated areas, and shows a depression in the transition temperature of -3°C . Analysis of UV-VIS curves taken from solutions of irradiated and unirradiated films leads to the result that under the irradiation

conditions specified the film is optically pumped to 36%E isomer (film initially contained 100%E).

As a result of the depression in T_{11} it is possible to hold a film which has irradiated and unirradiated areas at a temperature, T (Figure 1), such that we can observe areas of isotropic and liquid crystalline material. This gives the potential for storage of data into the film. By selection of an appropriate mask which can be laid on the film, areas of film may be defined as irradiated, or unirradiated. Then by heating the film to T it is possible to read out the data with either polarised or unpolarised light as a contrast image of liquid crystalline and isotropic phases. The image can then be frozen into the film by quenching to below the glass transition [8].

2.2. Azobenzene System

The copolymer 2 was prepared by a similar route to that described for the Naphthyl system. This copolymer with $R^1:R^2=9:1$ exhibited a nematic phase, with $T_{11}=77^\circ\text{C}$ and $T_i=24^\circ\text{C}$. The chromophore, R^1 , can undergo E-Z isomerisation about the nitrogen double bond. Films were prepared in the same way as for the Naphthyl system using surface treated glass slides to define an initial orientation for the copolymer. The sample was annealed at 65°C to fully develop the surface alignment, and irradiated with the polarisation state of the beam set parallel to the surface alignment of the film for 30min with the wavelength centred on 350nm . Thermo-optic analysis of the film using the polarising

Synthesis of Block Copolymers of Poly(styrene) and Poly(arylate) and their optical properties

by
Hiroshi Ohishi, Shinji Inaba, Masanao Kawabe, and Masao Kimura

R&D Laboratories-1, Nippon Steel Corporation
1618 Ida, Nakahara-ku, Kawasaki 211 Japan

1. Introduction

Since the optical information storage systems such as Laser Vision, Compact Disk and Magnetic Optical Disk are developing quickly, interest in polymers suitable for optical applications has grown enormously.

Poly(arylate)(PAR), a poly(ester) from bisphenol-A (BPA) and mixture of terephthalic acid/isophthalic acid (1:1 mol. ratio), is a high performance polymer which has high thermal resistance, impact strength and optical transparency. However, PAR shows poor processability because of its high melt viscosity, and what is worse for optical applications, PAR generates positive intrinsic birefringence during the processing such as injection molding and extrusion, with the retained orientation of molecules after the cooling.

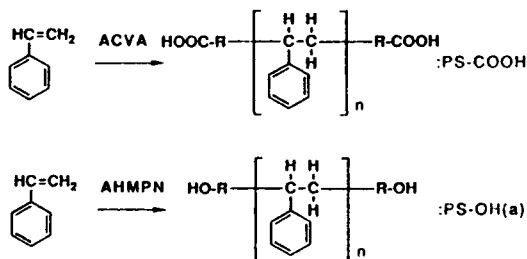
On the other hand, poly(styrene)(PS) has high optical transparency and negative birefringence, so birefringence would be reduced by blending PAR and PS(1). However, in the blends of PS and PAR, the size control of phase within 1 μ m, which is the focused laser spot diameter of optical drive apparatus, is difficult because of their poor compatibility. Therefore chemical bondings would be required between PS and PAR molecules.

The purpose of this report is to propose new synthetic methods of block copolymers(PS-b-PAR) of PS and PAR and to introduce their optical properties.

2. Experiments

1) Synthesis of functional macromers of PS

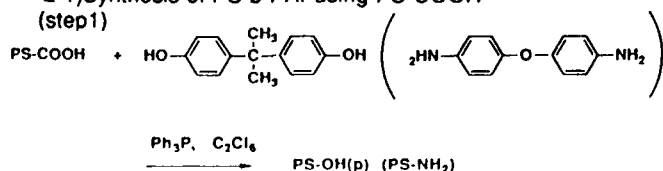
Two kinds of functional macromers of PS were synthesized by radical polymerization using functional azo-radical initiators. One was the carboxyl terminated PS(PS-COOH), synthesized at 363K using 4,4'-Azobis(4-cyanovaleric acid) (ACVA). Another was the alcoholic hydro-oxidal terminated PS(PS-OH(a)), polymerized at 383K using 2,2'-Azobis[2(hydroxymethyl)-propionitrile] (AHMPN). In both synthetic processes the initiators were continuously added to the reactor during polymerization.



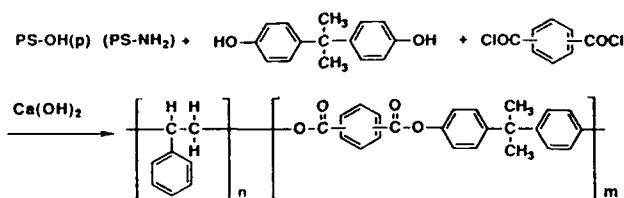
2) Synthesis of PS-b-PAR

PS-b-PAR were prepared by the following reaction processes.

2-1) Synthesis of PS-b-PAR using PS-COOH



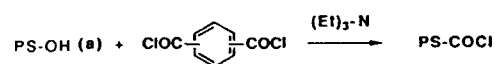
(step2)



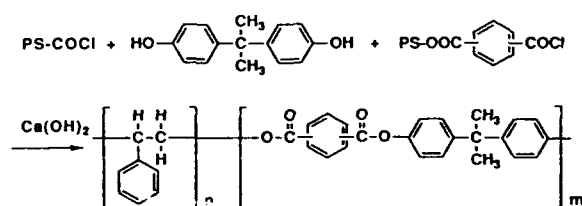
Because reactivity of carboxylic groups of PS-COOH is much inferior to that of chloroformyl groups of Isophthaloyl dichloride (IPCOCI)/Terephthaloyl dichloride(TPCOCI), carboxylic groups have to be changed into more reactive groups before polycondensation. In the step1 they were coupled with excess BPA or 4,4'-diaminodiphenyl ether(DAPE) by direct condensation method with triphenylphosphine and hexachloroethane(2), and phenolic hydro-oxidal terminated PS (PS-OH(p)) or amino terminated PS (PS-NH₂) were prepared. In the step2 PS-b-PAR were synthesized by solution polycondensation method with calcium hydroxide(3).

2-2) Synthesis of PS-b-PAR using PS-OH(a)

(step1)



(step2)



Because alcoholic hydro-oxidal groups are inferior to phenolic hydro-oxidal groups in reactivity, in the step1 PS-OH(a) were reacted with excess IPCOCI/TPCOCI with triethylamine(4) and chloroformyl terminated PS (PS-COCI) were synthesized. The step2 was the same as 2-1).

3) Characterization of PS macromers and PS-b-PAR

Molecular weight distributions of PS macromers and PS-b-PAR were measured by Gel Permeation Chromatography (GPC), calibrated by mono molecular weight distribution PS, made by Waters Corp. Functionalities of PS-COOH were estimated by neutralize titration and those of PS-OH(a) were calculated by NMR measurement of PS-OH(a) silylated by trimethylchlorosilane. The formation of PS-b-PAR was confirmed by NMR measurement using the materials of which unreacted PS were excluded by Soxhlet's extracting using cyclohexane for 26hr.

4) Measurement of birefringence of PS-b-PAR

100 μ m films of PS-b-PAR were casted from tetrachloroethane solution, and drawn from 10% to 50% at 483K. Birefringences of drawn films were measured by a polarized microscope using white light source.

5) Determination of melt viscosity of PS-b-PAR

Viscosities of PS-b-PAR were estimated by a flow tester at 513K.

3. Results and discussion

1) Synthesis of PS macromer

As it is extremely important to control molecular weight distribution, we had reported to add functional chain transfer reactors such as succinic acid peroxide is effective(5). However, it turned out that molecular weight distribution could be controlled without any chain transfer reactors by adding the initiators continuously at the adjusted conversion(fig.1). The number of functional groups of PS macromers were from 1.2 to 2.5 per one macromer molecule.

2) Synthesis of PS-b-PAR

From NMR analysis, two kinds of proton peaks were observed; one was attributable to PS and another to PAR(fig.2). Transparent PS-b-PAR films were prepared by both 2-1) and 2-2). In these reaction processes PS-b-PAR were synthesized at the room temperature and the ordinary pressure and reactive ratios of PS macromers were higher than 85%.

3) Birefringences of PS-b-PAR

Birefringences of 50% drawn films, of which PS-composition were from 40% to 60%, were about 1/100 lower than that of PAR, although the birefringences of block polymers containing P 30%PS were not low(fig.3). Therefore from 40% to 60% PS-composition would be required for optical applications.

As differences between stress relaxation times of PS and PAR have a great influence on the birefringences (6), the relationship between micro phase structures and birefringences of PS-b-PAR has been studied now.

4) Melt viscosity of PS-b-PAR

The melt viscosities of PS-b-PAR decreased as PS-composition increased(fig.4). When PS-composition was 50%, the melt viscosity of PS-b-PAR became about 1/1000 lower than that of PAR. Although in the case of PAR the injection temperature must be higher than 600K because of its high viscosity, to get transparent moldings was difficult owing to their heat decompositions. As viscosity of PS-b-PAR, whose PS-composition was 50%, was low enough even at 513K, they could be injection molded at 513K, and transparent moldings would be easily obtained.

4. Summary

New synthesis methods of transparent PS-b-PAR using functional macromers of PS were proposed at the room temperature and the ordinal pressure; reactive ratios of PS were higher than 85%.

The birefringences of 50% drawn films of PS-b-PAR and melt viscosities of PS-b-PAR were measured; the birefringences of PS-b-PAR were about 1/100 less than that of PAR, when PS-composition were from 40 to 50%. The melt viscosities of PS-b-PAR decreased as PS-composition increased. When PS-composition was 50%, it was about 1/1000 lower than that of PAR.

Because of their low birefringences and melt viscosities PS-b-PAR would be suitable material for optical applications.

5. References

- 1) H. Saito and T. Inoue, J. Polym. Sci., B, Polym. Phys. Ed., 25, 1629(1987)
- 2) S. Kitayama, K. Sanui, and N. Ogata, J. Polym. Sci., Polym. Chem. Ed., 22, 2075(1984)
- 3) European Patent EPU15828
- 4) A. Ueda, Y. Agari, S. Nagai, N. Minami and T. Miyagawa Chem.

- Express, 4 193(1983)
 5) M. Kawabe, M. Kimura, Polym. Prep. Jpn. Vol. 27 No2 312(1988)
 6) H. Miyashita, G. Aoki, H. Saito and T. Inoue, Polym. Prep. Jpn. 38, 3539(1989)

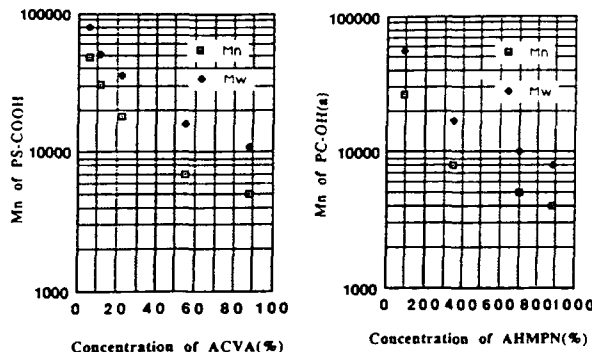


Fig. 1 Relationship between Concentration of ACVA (AHMPN) and Mn and Mw of PS-COOH(PS-OH). Mw; weight average molecular weight.

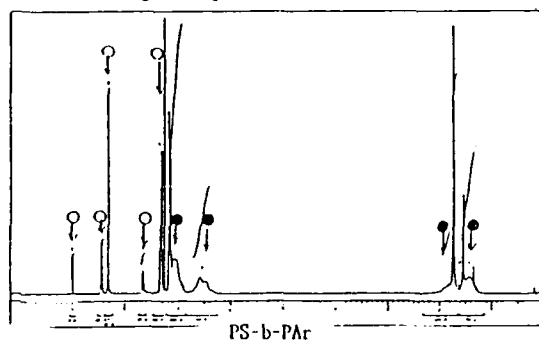


Fig. 2 NMR measurement of PS-b-PAR
 ● was attributable to PS, ○ to PAR

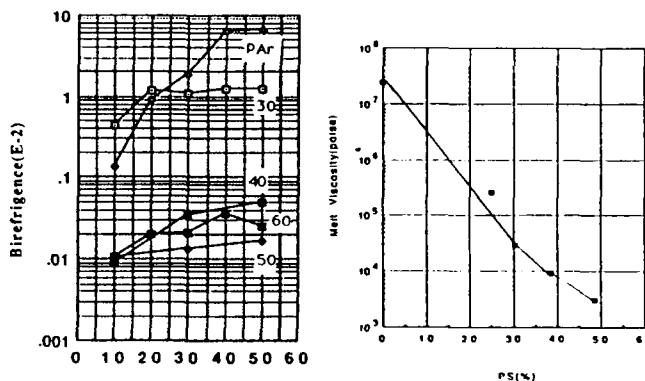


Fig. 3 Relationship between Drawing Ratio and Birefringences of PAR and PS-b-PAR. The number is PS-Composition.

Fig. 4 Relationship between PS-Composition and Melt Viscosities of PS-b-PAR (Mw=100000). Temperature; 513K, Shear Shear Rate; 5/sec. Melt viscosities were estimated by the following formula.

$$\mu = 100000 \cdot \mu_{ps} \cdot (100000/M_w)^{2.4}$$

CUBIC NONLINEAR OPTICS OF POLYMER THIN FILMS.
4. STRUCTURE- $\chi^{(3)}$ RELATIONSHIPS IN POLYANILINES
AND DERIVATIVES

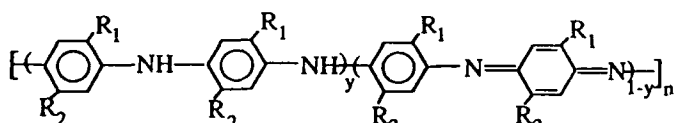
by
John A. Osaheni and Samson A. Jenekhe*
Center for Photoinduced Charge Transfer
and Department of Chemical Engineering
University of Rochester
Rochester, NY 14627-0166

and
Herman Vanherzele and Jeffrey S. Meth
DuPont Central Research & Development Department
P.O. Box 80356, Wilmington, DE 19880-0356

Introduction. Our current interest in understanding the structure-property relationships in conjugated polymers as electronic, optical, and nonlinear optical materials has led us to a systematic investigation of the structure- $\chi^{(3)}$ relationships in different classes of polymers [1]. Polyanilines represent a versatile family of polymers with interesting electronic, linear optical, and electrochemical properties which can be varied by addition or removal of electrons or protons on the polymer backbone and through derivatization of the p-phenylene rings [2-3].

In order to study the structure- $\chi^{(3)}$ relationships in polyanilines I, the oxidation state 1-y, can be varied from the fully reduced (1-y=0) polyleucoemeraldine base to the fully oxidized (1-y=1) polypernigraniline base. Also, the p-phenylene rings that alternate with the nitrogens in the polymer backbone can be derivatized with different substituents (R_1 , R_2) as in Ia - Ie. Furthermore, the measured $\chi^{(3)}$ of the polyanilines can also be compared to or contrasted with the known nonlinear optical properties of other p-phenylene ring polymers such as poly(p-phenylene vinylene) [4] and those of other quinoid ring polymers [5].

In this paper, we report our picosecond third harmonic generation investigation of the wavelength dependent $\chi^{(3)}$ of spin coated thin films of polyaniline and its derivatives, Ia - Id, in their emeraldine base forms (1-y=0.5). We will focus our discussion here mainly on polyemeraldine base (PEMB, Ia) and poly(o-toluidine) base (POTB, Ib). The complete results for the other derivatives will be presented.



I

- | | | |
|----|------------------------|---------|
| Ia | $R_1 = R_2 = H$ | (PEMB) |
| Ib | $R_1 = CH_3, R_2 = H$ | (POTB) |
| Ic | $R_1 = OCH_3, R_2 = H$ | (PMAB) |
| Id | $R_1 = SO_3H, R_2 = H$ | (PSAB) |
| Ie | $R_1 = R_2 = OCH_3$ | (PDMAB) |

Experimental. Polyemeraldine salt (hydrochloride) (PEMS) was prepared by the chemical oxidation of aniline with ammonium persulfate in 1M HCl in air using the literature method [6] and was subsequently converted to the emeraldine base form (PEMB) by stirring it in 0.1M NH_4OH solution. Using a similar approach, poly(o-toluidine) [7], poly(2-methoxyaniline), and poly(2,5-dimethoxy aniline) were prepared by chemical oxidation of o-toluidine, 2-methoxyaniline, and 2,5-dimethoxyaniline, respectively.

The intrinsic viscosity of PEMB and POTB in methanesulfonic acid at 40°C was 1.63 and 0.72 dL/g, respectively, which are typical of high molecular weight polyanilines [8]. The oxidation state, 1-y, can be estimated from the relative intensities of the infrared absorption bands at $\sim 1600\text{ cm}^{-1}$ (quinoid) and $\sim 1500\text{ cm}^{-1}$ (benzenoid) [9]. Using this approach, we have estimated the 1-y in the PEMB and POTB thin films to be ~ 0.44 and ~ 0.42 , respectively.

The thin films for the third harmonic generation (THG) experiments were prepared by spin-coating of N-Methyl-1-pyrrolidone (NMP) solutions of the polymers onto optically flat fused silica substrates (5 cm in diameter). The thickness of the PEMB and POTB films was typically 27 nm and 58 nm, respectively. The electronic absorption spectra of thin films of PEMB and POTB are shown in Figure 1. The electronic spectra indicate a blue shift of the spectrum of POTB relative to that of PEMB in accord with previous observations [10,11]. On the other hand, 2-methoxy substitution on the p-phenylene rings causes the electronic spectrum (not shown) to red shift relative to 2-methyl substitution in POTB as expected because of the stronger electron releasing effect of OCH_3 than CH_3 .

The THG experiments were performed by using a picosecond laser system which is continuously tunable in the range 0.6 - 4.0 μm [12]. The detailed THG procedure for the measurement of the third-order optical susceptibility $\chi^{(3)}(-3\omega; \omega, \omega, \omega)$ with this laser system has also been described in detail elsewhere [1a-1d]. The THG experiments were performed at a fundamental wavelength of 0.9-2.4 μm . The reported $\chi^{(3)}$ values are average values, corrected for absorption at the third harmonic wavelength, and obtained relative to the $\chi^{(3)}$ for fused silica (2.8×10^{-14} esu at 1.9 μm) [13]. The error for the reported $\chi^{(3)}$ values is $\pm 20\%$ and is due mostly to the error in film thickness measurement. The repeatability of individual results for each material is $\pm 5\%$.

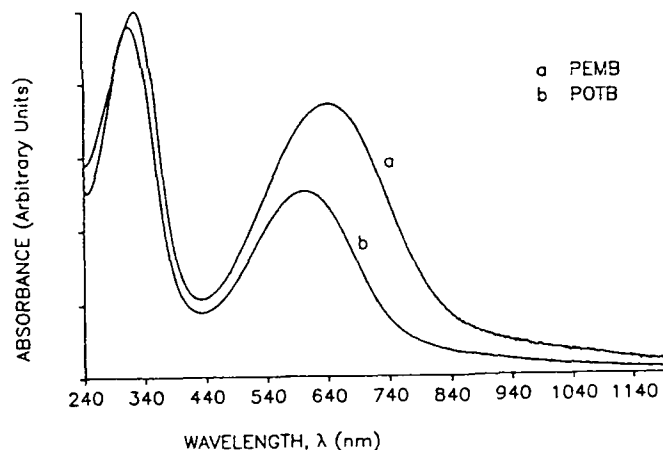


Figure 1 Electronic absorption spectra of thin films of PEMB and POTB.

Results and Discussion. Figure 2 shows the wavelength dispersion of the $\chi^{(3)}(-3\omega; \omega, \omega, \omega)$ of PEMB and POTB thin films in the wavelength range 0.9-2.4 μm . From the $\chi^{(3)}$ spectra, we see that the cubic optical nonlinearity of these polyanilines is large and compare favorably with the reported $\chi^{(3)}$ of some conjugated polymers [4]. The observed resonance feature in the $\chi^{(3)}$ spectra of Figure 2 are attributed to multiphoton processes since the electronic absorption spectra of the polymers in Figure 1 did not exhibit any absorption features in the 0.9-3.0 μm region. The resonance peak position in the $\chi^{(3)}$ spectra of PEMB and POTB at $\sim 1.8\mu\text{m}$ suggests that the peak is due to three-photon resonance.

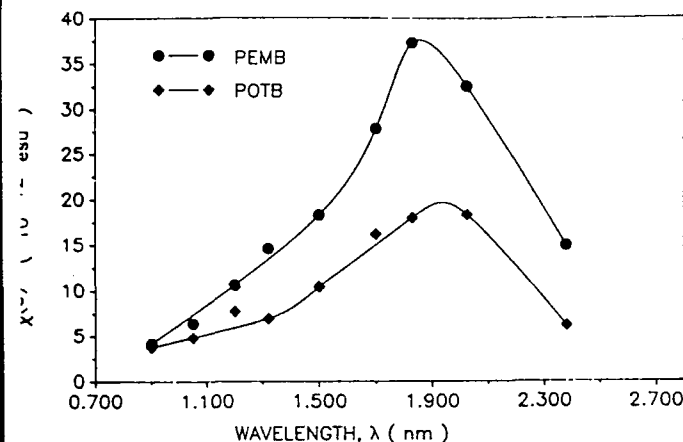


Figure 2 The $\chi^{(3)}(-3\omega, \omega, \omega, \omega)$ spectra of PEMB and POTB.

It is interesting to note from the $\chi^{(3)}$ spectra of the polymers in Figure 2 that the magnitude of the $\chi^{(3)}$ of POTB is smaller than that of PEMB in the wavelength range 0.9–2.4 μm . Near the resonance peaks, the $\chi^{(3)}$ of PEMB is a factor of 2 greater than that of POTB. The origin of this difference in the magnitude of the third-order optical susceptibility of PEMB and POTB can be traced to the observed difference in the electronic spectra of the polymers in Figure 1. The electronic absorption spectrum of POTB is blue shifted from that of PEMB due to a decrease in the electron delocalization arising from the increase in the torsional angle between the adjacent p-phenylene rings [7]. Such a decrease in the electronic delocalization can be expected to adversely affect the $\chi^{(3)}$ as observed in going from PEMB to POTB. The observed reduction of $\chi^{(3)}$ with 2-methyl substitution on the phenylene ring, of the parent polyemeraldine base, at the same level of oxidation, suggests that derivation is important in understanding the structure- $\chi^{(3)}$ relationships in polyanilines. The effects of other ring substituents on the $\chi^{(3)}$ of the polyanilines which are currently under investigation will be presented.

The effect of the oxidation state $1-y$, on the $\chi^{(3)}$ of polyaniline appears to be large although it is yet to be fully investigated. The fully reduced base ($1-y=0$) is expected to have a small $\chi^{(3)}$ because the sp^3 -hybridized nitrogen prevents electron delocalization. Thus, the bond additivity model is expected to work well, and the $\chi^{(3)}$ is expected to be close to any substituted benzene ring. So, even though the polyleucoemeraldine base has not yet been measured due to its ready oxidation in air, its $\chi^{(3)}$ can be estimated to be about that of aniline, which as a $\chi^{(3)}=1.7 \times 10^{-13}$ esu $=5.7 \times 10^{-36}$ esu [14]. This apparent two orders of magnitude increase in $\chi^{(3)}$ in going from zero to intermediate oxidation state ($y \approx 0.44$) is understandable considering the increase in electronic delocalization and the greater polarizability of the quinoid rings in PEMB compared to the all-benzenoid rings in polyleucoemeraldine base. In fact, similar effects of oxidation on the $\chi^{(3)}$ of polythiophene methylene and polythiophene methine system have been observed [5]. Hence it can be expected that further oxidation of polyaniline to the fully oxidized ($1-y=1$) polypyrrograniline might result in enhanced $\chi^{(3)}$.

Conclusions. We have investigated the third-order nonlinear optical properties of polyanilines and derivatives by picosecond third harmonic generation in the wavelength range 0.9–2.4 μm in an effort to establish the structure- $\chi^{(3)}$ relationships for this class of polymers. Our results show that the optical nonlinearities of the polyanilines are large and compare favorably with other conjugated polymers. For example, the three-photon enhanced $\chi^{(3)}$ of PEMB and POTB at 1.83 μm was found to be 3.73×10^{-11} and 1.8×10^{-11} esu, respectively. The results suggest a strong dependence of the optical nonlinearities on both the oxidation state and the derivation of the p-phenylene rings of polyanilines.

Acknowledgement. Work at the University of Rochester was supported by the New York State Science and Technology Foundation, Amoco Foundation, and National Science Foundation (Grant CHE-881-0024).

References

- (a) Jenekhe, S.A.; Roberts, M.; Agrawal, A.K.; Meth, J.S.; Vanherzeele, H. *Materials Research Soc. Proc.* vol. 214, in press. (b) Vanherzeele, H.; Meth, J.S.; Jenekhe, S.A.; Roberts, M.F. *Appl. Phys. Lett.* 1991, 58, 663. (c) Osaheni, J.A.; Jenekhe, S.A.; Vanherzeele, H.; Meth, J.S. *Chem. Mater.* 1991, in press. (d) Agrawal, A.K.; Jenekhe, S.A.; Vanherzeele, H.; Meth, J.S. *Chem. Mater.*, submitted. (e) Parts 1–3 in the series, this volume.
- McDiarmid, A.G.; Chiang, J.C.; Hatpern, M.; Huang, W.S.; Mu, S.L.; Somasiri, N.L.D.; Wu, W.; Yaniger, S.I. *Mol. Cryst. Liq. Cryst.* 1985, 121, 173.
- (a) Sun, Y.; McDiarmid, A.G.; Epstein, A.J. *J. Chem. Soc. Chem. Commun.* 1990, 529. (b) dos Santos, M.C.; Brédas, J.L. *Phys. Rev. Lett.* 1989, 62, 2499.
- (a) Kaino, T.; Kubodera, K.I.; Tomura, S.; Kurihara, T.; Saito, S.; Tsutsui, T.; Tokito, S. *Electron. Lett.* 1987, 23, 1095. (b) Kaino, T.; Saito, S.; Tsutsui, T.; Tokito, S. *Appl. Phys. Lett.* 1989, 54, 1619.
- (a) Jenekhe, S.A.; Lo, S.K.; Flom, S.R. *Appl. Phys. Lett.* 1989, 54, 2524. (b) Jenekhe, S.A.; Chen, W.C.; Lo, S.K.; Flom, S.R. *Appl. Phys. Lett.* 1990, 57, 126.
- McDiarmid, A.G.; Chiang, J.C.; Richter, A.F.; Somasiri, N.L.D. In: Alcaicer, L.; Ed. *Conducting Polymers*, Reidel: Dordrecht, Holland, 1987, pp. 105–120.
- Wei, Y.; Fock, W.W.; Wnek, G.E.; Ray, A.; McDiarmid, A.G. *J. Phys. Chem.* 1989, 93, 495.
- Cao, Y.; Andreatta, A.; Heeger, A.J.; Smith, P. *Polymer* 1989, 30, 2305.
- Lu, F.L.; Wudl, F.; Nowak, M.; Heeger, A.J. *J. Am. Chem. Soc.* 1986, 108, 8311.
- Wudl, F.; Angus, Jr., R.O.; Lu, F.L.; Allemand, P.M.; Vachon, D.J.; Nowak, M.; Liu, Z.X.; Heeger, A.J. *J. Am. Chem. Soc.* 1987, 109, 3677.
- Asturias, G.E.; McDiarmid, A.G.; McCall, R.P.; Epstein, A.J. *Synth. Metals* 1989, 29, E157.
- Vanherzeele, H. *Appl. Optics* 1990, 29, 2246.
- Buchalter, B.; Meredith, G.R. *Appl. Optics* 1982, 3221.
- Meredith, G.R.; Buchalter, B.; Hanzlik, C. *J. Chem. Phys.* 1983, 78, 1543.

OPTO-ELECTRONIC PROPERTIES AND SECOND HARMONIC GENERATION BY σ -BOND SEPARATED DONOR-ACCEPTOR MOLECULES

W. Schuddeboom, B. Krijnen, J.W. Verhoeven,
Laboratory of Organic Chemistry, University of Amsterdam, Nieuwe
Achtergracht 129, 1018 WS Amsterdam, The Netherlands

E.G.J. Staring, G.L.J.A. Rikken,
Philips Research Laboratories, PO Box 80000, 5600 JA, Eindhoven,
The Netherlands

H. Oevering
DSM Research, PO Box 18, 6061 MD, Geleen, The Netherlands

S.A. Jonker
IRI, Delft University of Technology, Mekelweg 15, 2629 JB Delft,
The Netherlands

1. Introduction

Until now it has been well established that structures which incorporate an electron rich donor group and an electron deficient acceptor group, interconnected by a conjugated π -system, in general give rise to large molecular second order effects (e.g. 4-nitroaniline has a prototype molecular structure [1]). The contribution (β_{ct}) of the important low lying charge transfer state (resulting in a large change in dipole moment upon excitation to the first excited state as well as in a high oscillator strength for the corresponding electronic transition [2]) to the molecular hyperpolarizability is described using a simple two level model (eqn 1), where it has been assumed that μ_{ge} and $\Delta\mu_{ge}$ have the same direction (one dimensional model):

$$\beta_{ct} = \frac{4\pi^2}{(h\omega_0)^2} |\mu_{ge}|^2 \Delta\mu_{ge} \left[\frac{\omega_0^4}{[\omega_0^2 - 4\omega^2][\omega_0^2 - \omega^2]} \right] \quad (1)$$

It can be shown that very efficient molecules are those with a large transition dipole moment (μ_{ge}) and a large difference between ground and excited state dipole moments ($\Delta\mu_{ge}$). The factor between square brackets is the so called dispersion factor, where ω_0 is the absorption angular velocity and ω the excitation angular velocity.

We now report the results of a study on the nonlinear optical properties of bichromophoric molecules 1 and 2 (see Fig. 1) [3]. These molecules consist of a phenyl substituted nitrogen electron donor and an electronegatively substituted ethylene acceptor interconnected by a saturated hydrocarbon unit which, classically speaking, isolates the chromophores from each other.

2. Experimental

The syntheses and photophysical measurements of compounds 1 and 2 have been described elsewhere [4,5]. Electric field induced second harmonic generation on polymethylmethacrylate films, containing typically 1% wt of the compounds under study, at a fundamental wavelength of 1064 nm was measured under constant corona-poling (ca. 1.2 MV/cm).

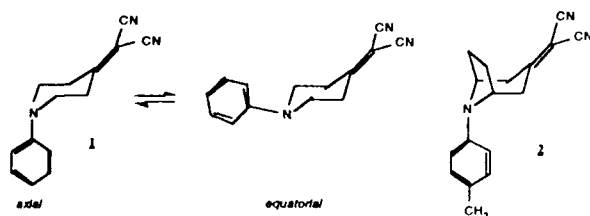


Figure 1: Structures of 1 and 2.

3. Results and discussion

To check the validity of the two level model we have to calculate β_{ct} and com-

pare the outcome with β_{exp} .

3.1 Determination of β_{exp}

Comparison of the second-harmonic intensities measured with a known sample (quartz) allowed calculation of the innerproduct of the ground state dipole moment μ_g and the molecular hyperpolarizability ($\mu_g\beta_{exp}$) and with knowledge of μ_g we could extract β_{exp} as compiled in Table I. Ground state dipole moments of the molecules 1 and 2 were calculated employing the SCF-MO semi-empirical AM1 method as described in ref. [3].

3.2 Determination of β_{ct}

From absorption and X-ray diffraction measurements Krijnen et al. [4, 5] concluded that for molecules like 1 and 2 significant electronic interaction between the chromophores occurs via the intervening σ -bonds. As discussed earlier, this interaction manifests itself in the long wavelength absorption (and the corresponding emission) of these compounds (see Fig.2), which demonstrate that in spite of the lack of direct π -conjugative interaction between the donor and acceptor sites a low lying intramolecular charge transfer state is available, a feature generally considered to be essential for second order nonlinear optical properties.

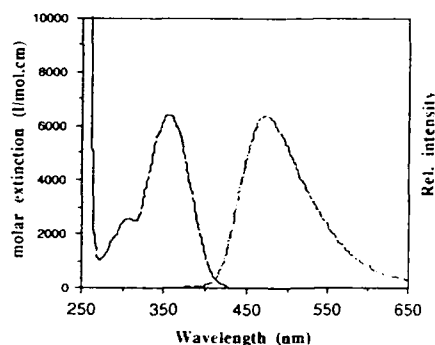


Figure 2: Electronic absorption (—) and emission (---) spectra of 2 in n-hexane.

It was shown by Krijnen et al. [4,5], that through bond interaction is optimized for: an axial orientation of the phenyl group in systems like 1 and 2. Evidently such an axial orientation is more highly populated in the tropane derivative 2, where the additional bridging ethylidene unit sterically destabilizes the equatorial orientation of the phenyl group, than in 1. This difference in conformation has been demonstrated to result in stronger charge transfer absorption of the tropane derivative and now also may be inferred to be related to the higher β value. It is therefore of interest to investigate the applicability of the two level model underlying eqn (1) for estimating the CT contribution to the molecular hyperpolarizability of 1 and 2.

For the evaluation of β_{ct} , knowledge of the change in dipole moment of the molecules between their electronic ground state (μ_g) and their electronically excited state (μ_e) is required and also the transition dipole moment μ_{ge} .

Calculation of $\Delta\mu_{ge}$

The present compounds display a very large solvatochromism of their fluorescence and a minor solvatochromism of the absorption. This is typical for charge transfer systems with a small dipole moment in the ground state (μ_g) and a large dipole moment in the emissive excited state (μ_e). It has been shown: [6,7] that treating the molecular dipole as a point dipole and the solvent as a continuous dielectricum, the change in dipole moment between ground and excited state ($\Delta\mu_{ge} = \mu_e - \mu_g$ in Debye) can be derived from the solvatochromic shifts of the absorption and emission frequencies (ν_a resp. ν_f in cm^{-1}) via:

$$\nu_a - \nu_f = \text{const} + 2(f-f') \left[(\mu_e - \mu_g)^2 / hc \rho^3 \right] \quad (2)$$

In eqn (2) f and f' are parameters related to the solvent static dielectric constant (ϵ) and refractive index (n) as $f = (\epsilon - 1)/(2\epsilon + 1)$ and $f' = (n^2 - 1)/(2n^2 + 1)$, while ρ (in Å) represents the effective radius of the solvent cavity occupied by the molecule.

by plotting the difference of the fluorescence and absorption intensities versus the solvent parameters ($f-f'$) a linear correlation should be found. From the slopes of these correlations $\Delta\mu_{ge}^{opt}$ can then be calculated if known. The results compiled in Table 1 show that upon excitation the moment for the present systems increases by 16.5 ± 0.5 Debye units.

Measurements

In order to obtain an independent check of the viability of the changes in dipole moments thus obtained, we have also performed some preliminary measurements with the time resolved conductivity (TRMC) technique [8], which allows direct observation of the formation and decay of (di)polar species in non-polar solvents. The following relationship between the conductivity and the change in dipole moment exists:

$$\Delta\sigma = \frac{(\mu_e^2 - \mu_g^2)}{\tau_r} \frac{(\epsilon + 2)^2}{27k_B T} F(\omega\tau_r) N_s \quad (3)$$

(3), k_B is the Boltzmann constant; ϵ is the relative dielectric constant of the solvent; μ_e and μ_g are respectively the dipole moment of the excited state and ground state of the molecule; N_s is the concentration of excited molecules; τ_r is the rotational relaxation time of the dipole and ω is the radian wave frequency. The function $F(\omega\tau_r)$ is the Debye relaxation term, depending on the light intensity and the optical characteristics of the solution, the concentration of the S_1 state (N_s) and hence the parameter $(\mu_e^2 - \mu_g^2)/\tau_r$ can be determined.

As can be seen from Table 1 the values determined from the CT fluorescence with the solvent polarity show excellent agreement with the results of the TRMC measurements.

Calculation of μ_{ge}

The oscillator strength (F) of the charge transfer transition (see Table 1) was calculated from the absorption spectra via eqn. (4):

$$F = 4.3 \cdot 10^{-9} \epsilon_{\max} \Delta\nu_{1/2} \quad (4)$$

ϵ_{\max} is the maximum molar absorption coefficient and $\Delta\nu_{1/2}$ is the width of the absorption band (in cm^{-1}), which then can be related to the transition dipole moment μ_{ge} (5):

$$F = 4.7 \cdot 10^{-29} \nu_{\max} |\mu_{ge}|^2 \quad (5)$$

ν_{\max} is the maximum of the charge transfer absorption band (in cm^{-1}) and μ_{ge} is the transition dipole moment.

The calculated β_{CT} values are compared with the experimental molecular hyperpolarizabilities in Table 1. β_{CT} is seen to account for a major component of the total hyperpolarizability, thus substantiating the hypothesis that the hyperpolarizability of the present systems is mainly governed by the presence of the through-bond charge transfer interaction. We have shown before [4,9], that the CT interaction of systems such as those presented here derive part of its intensity from coupling to higher (locally) excited states, implying that a simple two-level model cannot be expected to describe quantitatively the hyperpolarizability connected to this transition.

Table 1: Absorption maximum ν_{\max} (cm^{-1}), molar extinction (ϵ in $\text{Lmol}^{-1}\text{cm}^{-1}$), half-width ($\Delta\nu_{1/2}$ in cm^{-1}) and oscillator strength F of the intramolecular charge transfer transition of 1 and 2 (in *n*-hexane 20°C), AM1 calculated ground state dipole moment (μ_g), difference in ground state dipole moment and first excited state dipole moment, calculated from both absorption and emission shifts $\Delta\mu_{ge}^{opt}$ (eqn 2) and TRMC measurements (benzene) $\Delta\mu_{ge}^{TRMC}$ and finally the via eqn (1) calculated CT contribution of the total hyperpolarizability β_{CT} (in 10^{-30} esu) and the experimental hyperpolarizability β_{exp} (in 10^{-30} esu) determined from the electric field induced second harmonic generation measurements employing AM1 calculated ground state dipole moments.

ν_{\max}	ϵ	$\Delta\nu_{1/2}$	F	μ_g (AM1)	$\Delta\mu_{ge}^{opt}$	$\Delta\mu_{ge}^{TRMC}$	β_{CT}	β_{exp}
19.41	2970	2749	0.057	4.1	16.1	16.8	3.7	6.4
18.09	6390	3119	0.115	3.4	16.0	17.0	9.1	26.7

4. Conclusions

We have demonstrated that molecules in which donor and acceptor are connected by a saturated σ -bond system (D- σ -A) can exhibit efficient second harmonic generation, probably as a result of through bond interaction. It should be noted that a similar mechanism has been proposed earlier to explain SHG by the mono N-oxide of diazabicyclooctane [10], for which, however, no β value appears to have been determined. The β value now estimated for 2 is comparable to D- π -A molecules such as *p*-nitroaniline. In the context of a two-level model, it is evident that the present D- σ -A systems derive their remarkably large molecular hyperpolarizability mainly from a high value of $\Delta\mu_{ge}$, corresponding to complete charge separation in the excited state as opposed to virtually none in the ground state. For fully conjugated systems of comparable size $\Delta\mu_{ge}$ is expected to be less, due to significant mixing of the charge-transfer state into the ground state. On the other hand, however, the transition dipole moment, μ_{ge} , for a π -conjugated system will in general be larger, implying a trade-off between $\Delta\mu_{ge}$ and μ_{ge} as a function of the electronic interaction between donor and acceptor sites.

At the moment it is hard to say what degree of electronic interaction will establish optimum conditions for achieving high molecular hyperpolarizability and it is therefore of considerable interest to investigate systems in which the interaction is systematically varied between the extremes presented by pure π -conjugation and mere through-sigma-bond interaction.

References

- [1] J.F. Nicoud and R.J. Twieg in: *Nonlinear Optical Properties of Organic Molecules and Crystals*, Vol. 1, eds. D.S. Chemla and J. Zyss (Academic Press, New York 1987) p. 227
- [2] D.J. Williams, *Angew. Chem.* 96, 637 (1984).
- [3] W. Schuddeboom, B. Krijnen, J.W. Verhoeven, F.G.J. Staring, G.L.J.A. Rikken and H. Oevering, *Chem Phys. Lett.*, accepted for publication
- [4] B. Krijnen, H.B. Beverloo, J.W. Verhoeven, C.A. Reiss, K. Goubutz and D. Heijdenrijk, *J. Am. Chem. Soc.* 111, 4433 (1989).
- [5] B. Krijnen, Thesis, University of Amsterdam, Amsterdam, (1990).
- [6] E. Lippert, *Z. Elektrochem.* 61, 962 (1957).
- [7] P. Suppan, *J. Photochem. Photobiol.* 50, 293 (1990).
- [8] M.P. de Haas and J.M. Warman, *Chem. Phys.* 73, 35-53 (1982).
- [9] P. Pasman, F. Rob and J.W. Verhoeven, *J. Am. Chem. Soc.* 104, 5127 (1987).
- [10] a. P. Mihailovic, P. Bassoul and J. Simon, *Chem. Phys. Lett.* 141, 462 (1987).
b. J. Simon, P. Bassoul and S. Norvez, *New J. Chem.* 13, 13 (1989).

Side Chain Copolymers for Third Order Nonlinear Optical Applications

James R. Sounik, Robert A. Norwood, Jacquelyn Popolo, Douglas Holcomb
Robert L. Mitchell Technical Center
Hoechst Celanese Corporation
86 Morris Ave, Summit, New Jersey 07901

Introduction

Organic polymeric materials have received much attention for applications in nonlinear optical devices. Most recent work has focused on the electro-optic applications of glassy polymeric materials in optical waveguide devices whereas the development of all optical waveguide devices has suffered from the lack of highly active materials which can be easily processed [1-3]. There have been a number of reports in the literature on the $\chi^{(3)}$ activity of porphyrin derivatives, namely tetrabenzporphyrins, phthalocyanines and naphthalocyanines, that show relatively high third order nonlinear optical responses. These molecules are planar π -conjugated systems that have sharp absorption bands in the visible and near infrared and exhibit excellent thermal and chemical stabilities. Most studies have examined these dyes in solution [4-6], sublimed thin films [7,8] or in Langmuir Blodgett thin films [7,9]. Some silicon phthalocyanines have been made into siloxane copolymers that show high third order susceptibilities [10,11]. It would be desirable to develop materials containing these types of porphyrin derivatives that show high activity as well as processability similar to those polymeric materials being developed for electro-optic applications. Here we present the chemistry and nonlinear optical properties of a series of silicon phthalocyanine methylmethacrylate copolymers prepared by the modification of the central silicon atom.

Results and Discussion

Polymer Chemistry. The synthesis of the diacrylate silicon phthalocyanine monomer (1) follows directly from dihydroxysilicon phthalocyanine, figure 1. Since the monomer is a crosslinking agent, concentrations above 15 percent of the phthalocyanine monomer by weight in the copolymer showed gel formation or gave intractable solids. Copolymers of lower concentrations gave materials that were easily isolated. Synthesis of the monoacrylate silicon phthalocyanine monomer requires the synthesis first of the symmetrically substituted silicon phthalocyanine followed by the hydrolysis of one of the nonreactive groups to give the hydroxy silicon phthalocyanine. This compound can then be reacted to give the unsymmetrically substituted monoacrylate, figure 2. Copolymerizations with methylmethacrylate were carried out in chlorobenzene using AIBN as the radical initiator. Concentrations from 1 to 10 percent by weight of the silicon phthalocyanine monomer have so far been made for both the mono and diacrylate monomers. Table 1 shows typical composition and molecular weight data obtained for these types of copolymers. The glass transition temperatures are slightly higher than that of polymethylmethacrylate (PMMA) and the molecular weights range from 40,000 to 300,000.

These copolymers can be easily formed into micron thick thin films by spin coating from cyclohexanone or *o*-xylene and can be compression molded into millimeter thick disks. In all cases, the strong Q band absorption remains very similar to the absorptions found in solution for the monomers, figure 3. This is unlike the data seen for guest/host materials of phthalocyanines in PMMA which show limited solubility of the dye in the polymer and shifts and broadening of the absorption bands. These copolymers show low absorption at wavelengths higher than 800 nm and can give thin films which may be used for waveguide devices at these wavelengths.

Nonlinear Optical Characterization. Degenerate four wave mixing (DFWM) in the conventional phase-conjugate geometry was used to perform the measurements on thin film samples of the copolymers spin-coated onto glass slides. The laser pulses used for the experiment were 5-6 psec long, 598 nm wavelength, repetition rate of 10 Hz, and maximum individual pulse energies at the sample on the order of 10-20 μ J. The diagonal component of the third order nonlinear susceptibility $\chi_{xxxx}^{(3)}$ is measured by studying the intensity dependence of the phase conjugate signal as a function of input laser intensity. One expects that the signal should go as the cube of the intensity input to the apparatus, but this will only hold for unsaturated nonlinearities. The following expression, appropriate for thin film samples, was used to determine $\chi^{(3)}$:

$$\frac{\chi_S^{(3)}}{\chi_R^{(3)}} = \left(\frac{n_S}{n_R}\right)^2 \left(\frac{L_R}{L_S}\right) \frac{\alpha_S L_S}{e^{-\alpha_S L_S/2}(1 - e^{-\alpha_S L_S})} \sqrt{\frac{C_S}{C_R}}$$

where n_S and n_R are the refractive indices of the sample and the reference (100 μ m of carbon disulphide), L_S and L_R the lengths of the sample and reference, respectively; α_S the absorption coefficient of the sample, and C_S and C_R the sample and reference DFWM signals for low pump intensities. The ratio C_S/C_R was averaged for low pump intensities and the error in this procedure is estimated to give an uncertainty in $\chi_{xxxx}^{(3)}$ of 10%.

In the present case $n_S = 1.44$ (anomalous dispersion), $n_R = 1.6246$, $L_R = 100 \mu$ m, $L_S = 2 \mu$ m, $\alpha_S L_S = 2.02$, and $C_S/C_R = 20.2$. Using the literature value for $\chi_{xxxx}^{(3)}$ of CS_2 at 532 nm ($= 6.8 \times 10^{-13}$ esu), we find that $\chi_{xxxx}^{(3)}$ for the SiPc/MMA 10:90 bisacrylate copolymer is 7.7×10^{-10} esu, however we stress that this is only accurate for pump intensities such that the nonlinearity is unsaturated; at higher intensities the measured $\chi_{xxxx}^{(3)}$ diminishes, approaching 10^{-10} esu. Figure 4B illustrates that while the phase conjugate signal of CS_2 increases with power following a monotonically polynomial, that of the copolymer begins to saturate at a fairly low intensity, indicating significant excited state population effects at this point. At low intensities, the majority of the response of the silicon phthalocyanine copolymer can primarily be attributed to ultrafast electronic hyperpolarizabilities and fast decay from excited states, as demonstrated in Figure 4A where the time resolved DFWM response of the copolymer is compared to that of CS_2 . The origin of the residual response is being investigated and could result from either one- or two-photon absorption effects.

Experimental

Methods of Analysis. Instrumentation: NMR spectra were obtained on either a Varian XL200 spectrometer, and chemical shifts were reported in ppm downfield relative to tetramethylsilane. All NMR samples were solutioned in $CDCl_3$ unless noted otherwise. Polymer molecular weights were determined on a Waters 201 GPC equipped with a Waters 410 RI and a Viscotek Model 100 differential viscosity detector, and the mobile phase was tetrahydrofuran. Molecular weights were calculated from a Universal calibration curve. Thermal analysis was done using a DuPont 9900-910 Thermal Analyzer. Melting points were obtained on a Melt-Temp II capillary melting point apparatus and are uncorrected.

Bis(3-methacryloxypropylidimethylsiloxy) silicon phthalocyanine (1). A mixture of dihydroxysilicon phthalocyanine (2.10 g) [12], 3-methacryloxypropylidimethylchlorosilane (3.09 g) and distilled dried pyridine (75 mL) was stirred at 50° C for 48 hours. The chlorosilane was distilled under vacuum prior to use. The mixture was filtered and the filtrate was diluted with a 1:1 ethanol/water solution (100 mL). The solid was isolated, washed with methanol (50 mL), vacuum dried (rt, 12 hr) and weighed (2.96 g, 86%): MP 170-172° C; IR (Nujol) 1714 (s, C=O), 1336 (s), 1250 (m, SiCH₃), 1158 (s), 1123 (s), 1081 (s), 1044 (s, Si-O-Si), 736 (s); ¹H NMR δ 9.65 (m, Pc-H), 8.34 (m, Pc-H), 5.75 (s, C=CH), 5.41 (s, C=CH), 2.73 (t, γ -CH₂), 1.73 (s, CH₃), -0.95 (m, β -CH₂), -2.23 (m, α -CH₂), -2.84 (s, SiCH₃).

Bis(tri-*n*-hexylsiloxy) silicon phthalocyanine (2). A mixture of tri-*n*-hexylsilanol (14.9 g), sodium methoxide (2.67 g) and absolute ethanol (50 mL) was reduced to an oil under vacuum. This oil was added to a mixture of dichlorosilicon phthalocyanine (15.10 g) and distilled dried 1,2,4-trimethylbenzene (70 mL). The resulting suspension was refluxed for 1 hr and was filtered hot (whatman #54). The filtrate was allowed to cool (12 hr) and was diluted with methanol (350 mL). The solid was isolated by filtration, washed with methanol (100 mL), vacuum dried (room temp., 12 hr) and weighed (22.06 g, 79%): MP 175° C (Lit [12] 175° C); IR (Nujol) 1525 (s), 1325 (s), 1125(s), 1080 (s), 1038 (s, Si-O-Si), 725 (s).

Hydroxy(tri-*n*-hexylsiloxy) silicon phthalocyanine (3). This procedure is a modification of a procedure described by Batzel [13]. A mixture of (2) (15.05 g), trichloroacetic acid (6.27 g) and distilled dried toluene (120 mL) was refluxed for 1 hr. The resulting solution was concentrated under vacuum and was then added to a mixture of 5:1 pyridine/water (60 mL) and was stirred for 2 hr at 62° C. The suspension formed was concentrated under vacuum and diluted with methanol (100 mL). The solid was isolated by filtration, washed with methanol (100 mL), dried under vacuum (room temp., 12 hr) and weighed (9.45 g, 84%): IR (Nujol) 3500 (w, OH), 1340 (s), 1125 (s), 1037 (m, Si-O-Si), 740 (s).

(3-methacryloxypropylidimethylsiloxy)(tri-*n*-hexylsiloxy) silicon phthalocyanine (4). A mixture of (3) (4.43 g), 3-methacryloxypropylidimethylchlorosilane (3.43 g), tri-*n*-butylamine (2.88 g) and distilled dried toluene (100 mL) was stirred at room temperature for 48 hr. The solution was concentrated under vacuum and was diluted with methanol. The solid was isolated by filtration, dried under vacuum (rt, 12 hr) and weighed (4.30 g, 80%) MP 120° C; IR (Nujol)

1714 (s, C=O), 1336 (s), 1250 (m, SiCH₃), 1158 (s), 1123 (s), 1081 (s), 1044 (s, Si-O-Si), 736 (s): ¹H NMR δ 9.66 (m, Pc-H), 8.34 (m, Pc-H), 5.75 (s, C=CH₂), 5.41 (s, C=CH₂), 2.74 (t, γ-CH₂, C3 chain), 1.74 (s, CH₃), 0.79 (m, ε-CH₂), 0.67 (t, δ-CH₂), 0.36 (m, δ-CH₂), -0.02 (m, γ-CH₂, C6 Chain), -0.99 (m, β-CH₂, C3 chain), 1.27 (m, β-CH₂, C6 Chain), -2.27 (m, α-CH₂, C3 chain), -2.43 (m, α-CH₂, C6 chain), -2.84 (s, SiCH₃).

Copolymer Synthesis, General Methods. A general method was used for copolymerization of the silicon phthalocyanine monomers with methylmethacrylate. The silicon phthalocyanine monomer, methylmethacrylate and dry distilled chlorobenzene were purged with argon for two hours while being heated. AIBN as 3 to 5 mole percent was added and the reaction was heated for 18 to 72 hr under an inert atmosphere. Precipitation of the product was done in methanol and the solid was isolated by filtration, dried (vacuum, 50° C, 12 hr) and weighed. The yields were generally greater than 70% based on the silicon phthalocyanine monomer.

Acknowledgments

We gratefully acknowledge the support of the Air Force Office of Scientific Research.

References

- 1) R. DeMartino, S. Jacobson, B. Feuer, G. Khanarian, D. Karim, J. Stamatoff, C. C. Teng, H. Yoon, "Non-Linear Optical Polymers for Active Optical Devices", Materials Research Society Symposium Proceedings, 1989, 134, 641.
- 2) J. Stamatoff, R. DeMartino, D. Haas, G. Khanarian, H. Man, R. Norwood, H. Yoon, *Angew. Makro. Chem.*, 1990, 183, 151.
- 3) R. DeMartino, "Polymers for Nonlinear and Electro-optic Applications", in *Fine Chemicals for the Electronics Industry II: Chemical Applications for the 1990s*, edited by D.J. Ando and M.G. Pellatt, Royal Society Special Publication, 1991, 88, 223.
- 4) J. Wu, J. Heflin, R. Norwood, K. Wong, O. Zamani-Khamiri, A. Garito, P. Kalyanaraman and J. Sounk, *J. Opt. Soc. Am. B*, 1989, 6(4), 709.
- 5) J. Shirk, J. Lindle, F. Bartoli, C. Hoffman, Z. Kafali and A. Snow, *Appl. Phys. Lett.*, 1989, 55(13), 1287.
- 6) D. Rao, F. Aranda, J. Roach and D. Remy, *Appl. Phys. Lett.*, 1991, 58(12), 1241.
- 7) M. Cassettevans, M. Samoc, J. Pflieger and P. Prasad, *J. Chem. Phys.*, 1990, 92(3), 2019.
- 8) Z. Z. Ho, C. Y. Ju and W. Hetherington, *J. Appl. Phys.* 1987, 62(2), 716.
- 9) A. Kaltbeitzel, D. Neher, C. Subeck, T. Sauer, G. Wegner and W. Caseri, "Electronic Properties of Conjugated Polymers III", Springer-Verlag, 226, (1989)
- 10) T. Sauer, W. Caseri and G. Wegner, *Mol. Cryst. Liq. Cryst.*, 198
- 11) C. Subeck, D. Neher, A. Kaltbeitzel, G. Duda, T. Arndt, T. Sauer and G. Wegner, "Nonlinear Optical Effects in Organic Polymers", Kluwer Academic, 162,185, (1989).
- 12) B. Wheeler, G. Nagasubramanian, A. Bard, L. Schectman, D. Dinniny, M. Kenney, *J. Am. Chem. Soc.*, 1984, 106, 7404.
- 13) D. Batzel, PhD. Thesis, Case Western Reserve University, 1990.

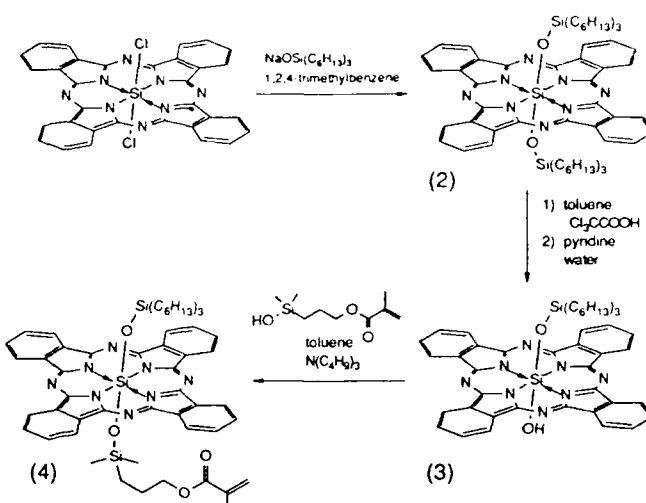


Figure 2. Synthesis of (3-methacryloxypropyldimethylsiloxy)(tri-*n*-hexylsiloxy) silicon phthalocyanine.

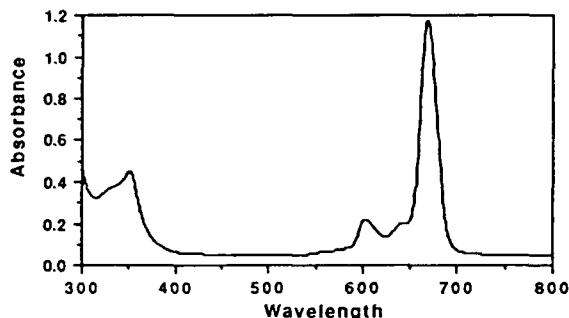


Figure 3. UV-Vis-NIR spectra of a 0.36 μm thin film of a 10% by weight silicon phthalocyanine/methylmethacrylate copolymer on glass.

Table 1

Monomer	Reaction Temp (°C)	Comp. ¹	Comp. ² (NMR)	Tg (°C)	Molecular Weight
bisacrylate	70	10:90	10.9:89.1	130	307,000
bisacrylate	70	5:95	5.5:94.5	112	192,000
bisacrylate	70	1:95	1.4:98.6	121	41,000
monoacrylate	70	10:90	9:91	117	99,000

¹Composition of monomers in reaction as weight percent. (wt Pc:wt MMA)
²Composition of copolymer as analyzed by integration of NMR as weight percent. (wt Pc:wt MMA)

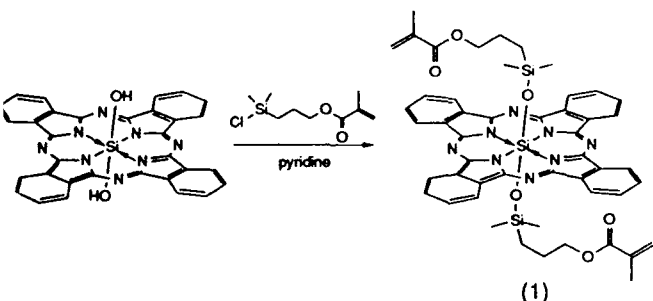


Figure 1. Synthesis of bis(3-methacryloxypropyldimethylsiloxy) silicon phthalocyanine

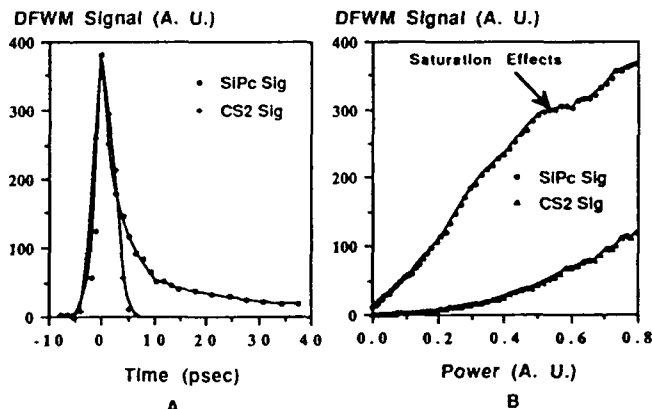


Figure 4. A) Decay of DFWM signal as a function of backward pump delay for SiPc/MMA 10:90 bisacrylate copolymer. B) Power dependence of DFWM signal in SiPc/MMA 10:90 bisacrylate copolymer and 100 μm carbon disulphide.

QUANTITATIVE STUDY OF MOLECULAR ORIENTATION OF HEMICYANINE
LANGMUIR-BLODGETT FILMS BY FOURIER TRANSFORM INFRARED
SPECTROSCOPY AND SECOND HARMONIC GENERATION

W-F. A. Su*, T. Kurata, H. Nobutoki and H. Koezuka

Mitsubishi Electric Corporation
Materials and Electronic Devices Laboratory
Japan 661

*Westinghouse Electric Corporation
Science and Technology Center
Pittsburgh, Pennsylvania 15235

INTRODUCTION. The Langmuir-Blodgett (LB) technique has the ability to organize molecules into highly ordered monolayers and to manipulate a multilayer film toward a desired architecture. By this technique specific physical and chemical properties of materials can be easily controlled, compared with other techniques such as vacuum evaporation. The LB technique has the potential for fabricating next generation novel devices operating at an extremely small scale for information processing, transmission and storage.¹ The structure of assembled LB films needs to be quantitatively evaluated in order to understand the relationship between molecular orientation and the characteristics of a specific device.

Among the various analytical methods applicable to thin organized films, such as LB films, FTIR provides the most convenient and useful way. In particular, several attempts have been made to apply infrared reflection absorption (RA) spectroscopy to molecular orientation analysis.^{2,4} Chollet et al. had quantitatively analyzed the structure of thin films by comparing peak intensities of RA spectra with those of transmission spectra.² However, they had assumed that the enhancement factor for the RA spectra on a metal surface was virtually independent of wavenumber. Recently this analytical method has been further improved by Takenaka et al.⁴ They calculated infrared intensities and enhancement factors using the rather rigorous optical formalism for the multilayer films developed by Hansen.⁵

The detection of second harmonic generation (SHG) gives another powerful tool to investigate the molecular orientation in LB films. The SHG signals can be observed even from a single monolayer on a substrate.⁶ The amphiphilic hemicyanine dye (Figure 1) has attracted much attention as an organic nonlinear material because of its large molecular hyperpolarizability. Girling et al. had first reported that hemicyanine dye LB films had generated large SHG.^{7,8} From the analysis of SHG data, the tilt angle of the hemicyanine dye chromophore was calculated, although the tilt angle of the long alkyl chain could not be estimated.^{7,9} Many studies using the SHG technique have been conducted for hemicyanine dye LB films to determine the molecular configuration as described above.⁷⁻¹¹ On the other hand, little work using the FTIR method has been conducted for hemicyanine dye LB films. Stroeve et al.¹² reported the molecular orientation of hemicyanine using FTIR. Two types of samples were studied: Z-type multilayer hemicyanine LB films and alternate layers of hemicyanine and arachidic acid LB films. By comparing the peak intensities of transmission spectra with those of RA spectra qualitatively, they concluded that the orientation of hemicyanine was closer to normal when it was interleaved with arachidic acid.

In this paper, we report the quantitative evaluation of the molecular orientation of hemicyanine LB films by FTIR spectroscopy for the alkyl chain and the chromophore individually. We also show that a SHG Maker fringe method is very useful in the investigation of molecular orientation.

EXPERIMENTAL. A Kyowa Kaimen Kagaku Model HBM-AP Langmuir trough was employed for hemicyanine LB film fabrication. The water subphase contained CaCl₂ and NaHCO₃ (pH=6.0) and was maintained at 20°C. All the infrared spectra were measured by JOEL JIR-100 FTIR spectrometer equipped with a MCT detector. A Q-switched Nd:YAG laser (Quantel YG-571, 1.06 μm, 10 Hz repetition, FWHM 10nsec) was utilized for SHG Maker fringe measurements (Figure 2). More detailed experimental descriptions are going to be presented in a

formal technical paper which will be submitted to *Langmuir* for publication.

RESULTS AND DISCUSSION. The results of the FTIR and SHG are discussed separately as follows.

FTIR Measurement. In the transmission spectra of FTIR, the electric field vector is parallel to the film surface, so the infrared radiation only probes the vibrations having components of their transition moments in the plane of the film. On the other hand, the electric field vector perpendicular to the sample surface is enhanced in the RA spectroscopy, so that the infrared radiation selectively probes those vibrations that have components of their transition moments normal to the film. Therefore, the functional group orientation of the film molecule can be evaluated by comparing the transmission spectra to the RA spectra.^{4,13,14}

A series of nonpolarized and polarized infrared transmission spectra of LB films was measured. Those spectra had the same peak height which was independent of infrared beam polarizations, so the distribution of hemicyanine molecules is in-plane isotropic. Figure 3 shows polarized infrared transmission and RA spectra of a multilayer film consisting of five hemicyanine monolayers. The absorption bands assignments are summarized in Table I. In the transmission spectrum, both the symmetric CH₂ stretching band (2850 cm⁻¹) and the antisymmetric CH₂ stretching band (2918 cm⁻¹) are stronger than those in the RA spectrum. The transition moments of the antisymmetric and the symmetric CH₂ stretching bands are perpendicular to the long alkyl chain axis, so the alkyl chain axis is considered to be approximately aligned along the surface normal. This conclusion is further supported by the fact that the symmetric CH₂ stretching band (2871 cm⁻¹) was observed only in the RA spectrum. The splitting for the CH₂ scissoring band can be used as a criterion in distinguishing the lateral packing of the alkyl chains.¹⁴ In our case the CH₂ scissoring band of the hemicyanine LB film appears as a singlet at 1470 cm⁻¹ in the transmission spectrum. Thus, the alkyl chains of the hemicyanine dye LB film are considered to be in a hexagonal subcell packing where each chain freely rotates around its alkyl long axis.¹⁴ This conclusion means that the alkyl chain is in-plane isotropic.

In the case of the in-plane aromatic ring (C=C) stretching band, the absorption was shown to be much stronger in the RA spectrum than in the transmission spectrum, indicating that this transition moment is directed away from the substrate normal. The evaluation of the hemicyanine chromophore orientation requires the knowledge of the relationship between the transition moment direction and the chromophore molecular axis. This consideration will be discussed later.

Because the molecular orientation of the hemicyanine LB film is considered to be uniaxially distributed around the surface normal, the quantitative evaluation of each functional group orientation of the hemicyanine in the LB films can be conducted according to Takenaka et al.^{4,14} They suggested that the orientation of the transition moment of the specific vibration could be evaluated by equation (1), assuming the uniaxial distribution of the transition moment around the surface normal *z* with the angle ψ .

$$\frac{A_T}{A_R} = \frac{\sin^2 \psi}{2m_z \cos^2 \psi + m_x \sin^2 \psi} \quad (1)$$

The film surface is the *xy*-plane, and infrared beam incidence in the RA measurements is in the *xz*-plane. *A_T* and *A_R* are the absorbances of the specific band in the transmission and RA spectra, respectively. The *m_z* and *m_x* are the enhancement factors along the *z* and *x* axes of the RA intensity to the transmission intensity. The values of *m_z* and *m_x* can be estimated by comparing the calculated absorbances of transmission and RA spectra using Hansen's formulas.⁵ Those values, whose calculation procedure was described in Ref. 4, depend on the complex refractive indices of the film and the substrate, the thickness of the film, the infrared light incident angle in the RA measurements and the infrared wavelength. Our LB film

samples can be regarded as a 3-phase plane-bounded system both for the transmission and the RA measurements. For the transmission measurement where the incident angle is zero, the system is air/LB film/CaF₂. The known values, n₁(air)=1.0 and n₂(CaF₂)=1.415, were used as refractive indices for the first phase and the third phase, respectively. For the RA measurements, the system is air/LB film/silver; n₂(Ag)=0.62+25.1i was used as the complex refractive index of the third phase, a silver layer.¹⁶ The incident angle for our RA measurements was set to be 80°. The refractive index of the second phase, a 5-monolayer LB film, was assumed to be 1.50, the same as that of stearic acid⁴, because the effect of the hemicyanine chromophore on the refractive index should be small in the infrared region, that is far from the characteristic absorption band of the chromophore in the visible region. The observed thickness of LB film by X-ray diffraction was 15.7nm. Table II shows the tilt angles of each transition moment determined for three specific bands, and also the calculated enhancement factor. The wavenumbers of the absorption bands in the RA spectra varied slightly from the corresponding wavenumbers in the transmission ones due to anomalous dispersion in the real part of the refractive index originating from each absorption. However, these differences were not very large, so we used the wavenumber of the absorption band in the transmission spectra to calculate tilt angles.

The tilt angles of the transition moments of the antisymmetric and symmetric CH₂ stretching band have been calculated to be 72° and 75°, respectively using equation (1) (Table II). We called them α and β . The directions of the transition moments of the antisymmetric and the symmetric CH₂ stretching bands and the long alkyl chain axis are perpendicular to each other. The tilt angle of the alkyl chain axis from the surface normal, γ , can be evaluated by the following orthogonal relationship among α , β and γ :

$$\cos^2 \alpha + \cos^2 \beta + \cos^2 \gamma = 1 \quad (2)$$

By substituting $\alpha = 72^\circ$ and $\beta = 75^\circ$ into equation (2), the tilt angle of the alkyl chain axis was calculated as 24°.

The tilt angle of the transition moment of the aromatic ring was calculated to be 43° using equation (1). To confirm the chromophore tilt angle of the hemicyanine dye, the relationship between the transition moment and the chromophore molecular axis should be made clear, as previously described. Thus, vibrational analysis has been carried out for a model molecule (p-methyl aniline). The direction of the transition moment of the aromatic ring vibration mode of the model molecule was determined using Gatrix. The MNDO molecular orbital method was used to optimize the molecular structure.¹⁶ The results have shown that vibrational frequency resulting from the aromatic ring =C band was 1659 cm⁻¹, which is close to the measured value 1589 cm⁻¹, and the direction of its transition moment lies completely along the molecular axis. These results indicate that the direction of the aromatic ring transition moment of hemicyanine is in an agreement with the direction of the hemicyanine chromophore axis.

From the estimated tilt angles (Table II), the molecular configuration of the hemicyanine LB film is illustrated in figure 4.

SHG Measurement. Figure 5 shows the typical SHG Maker fringe patterns of a monolayer deposited on both sides of a glass substrate. The appearance of the fringe pattern is attributed to the interference between the second harmonic radiation derived from the monolayers on both sides of the glass substrate. For all the SHG measurements, only the p-polarized harmonic radiation was observed for p-(P-P) and s-(S-P) polarization of the fundamental wave. The SHG intensity increased with the incident angle, which is defined as the angle from the surface normal. In addition, the SHG signals were independent of the rotation in the sample plane. This result is consistent with the fact that the absorption band intensities in the FTIR transmission spectra were isotropic in the sample plane.

These observations indicate that the nonlinear optical polarization has no components in the film plane and is in-plane isotropic. The LB films, therefore, have only two independent tensor components of nonlinear optical coefficient, that is, d_{33} and d_{31} ($= d_{32} = d_{24} = d_{15}$)

according to Kleinman symmetry.^{17,18} The effective nonlinear optical coefficient is expressed by the product of nonlinear optical coefficient d and projection factor $p(\theta)$ as shown in the following equations (3) and (4), for P-P and S-P polarizations, neglecting the local field factor:

$$d \times p(\theta) = d_{33} \sin^3 \theta + 3d_{31} \cos^2 \theta \sin \theta \quad (\text{P-P polarization}) \quad (3)$$

$$d \times p(\theta) = d_{31} \sin \theta \quad (\text{S-P polarization}) \quad (4)$$

where θ is the incident angle of the fundamental wave.

Coefficients d_{33} and d_{31} can be calculated from the above equations using a quartz glass as a reference. In order to evaluate the chromophore tilt angle, ψ , and the molecular hyperpolarizability β , a simple distribution model was applied.¹⁹ The model carries the following assumptions: (1) the molecule has one main component of β and the molecular axis is consistent with the direction of the main component of β , (2) the molecular axis is inclined at an angle ψ to the surface normal with random azimuthal angle. These assumptions are rational for our systems which have only two independent nonlinear optical coefficients and are in-plane isotropic. In this model the nonlinear optical coefficients are expressed as the following equations:

$$d_{33} \left(\frac{1}{2} \chi_{zzz} \right) = \frac{1}{2} N \beta \cos^3 \psi \quad (5) \quad d_{31} \left(\frac{1}{2} \chi_{zxx} \right) = \frac{1}{4} N \beta \sin^2 \psi \cos \psi \quad (6)$$

where N is the number of molecular density, which was calculated from the monolayer thickness (31.3Å) and the monolayer molecular area (33.1Å²). Using the above equations, the estimated molecular hyperpolarizability, β , is 63 x 10⁻³⁰ esu and the molecular tilt angle, ψ , is 44°.

The estimated β value is of the same order as the reported value, that is 43°. The estimation of molecular hyperpolarizability, β , included many unreliable factors, for example: the local field factor was neglected in this case. Thus, it is difficult to compare those values obtained in other experiments. However, the tilt angle value is reliable, because its determination does not depend on the local field factor. The determined tilt angle, 44°, is consistent with the tilt angle of the hemicyanine chromophore, which is estimated to be 43° from FTIR measurements.

CONCLUSION. The molecular orientation of hemicyanine LB films was studied quantitatively by FTIR spectroscopy. The tilt angles of the alkyl chain and of the chromophore were found to be 24° and 43°, respectively. The SHG Maker fringe measurement is very sensitive and can probe the molecular orientation of one monolayer. The tilt angle of molecular hyperpolarizability, that is, the chromophore axis, was estimated to be 44° using a simple distribution model analysis. The SHG result supports the FTIR evaluation. By using two methods, the molecular orientation of LB film can be measured with precision and accuracy.

ACKNOWLEDGEMENTS. We would like to thank Dr. A. Tsumura and Mr. I. Karino for their valuable help and discussions.

REFERENCES.

1. *Langmuir-Blodgett Films*, ed. by Roberts, G., Plenum Press: New York, 1990.
2. Chollet, P.A.; Messier, J.; Rosilio, C., *J. Chem. Phys.*, 1976, **64**, 1042.
3. Allara, D. L.; Nusso, R. G., *Langmuir*, 1985, **1**, 45, 52.
4. Ugemura, J.; Kamata, T.; Kawai, T.; Takenaka, T., *J. Phys. Chem.*, 1990, **94**, 62.
5. Hansen, W. N., *J. Opt. Soc. Am.*, 1988, **58**, 380.
6. Koesuka, H.; Kurata, T.; Tsumura, A.; Fuchigami, H., *Mat. Res. Soc. Symp. Proc.*, 1989, **173**, 691.
7. Girling, I. R.; Cade, N. A.; Kolinsky, P. V.; Montgomery, C. M., *Electron. Lett.*, 1985, **21**, 169.
8. Girling, I. R.; Cade, N. A.; Kolinsky, P. V.; Earle, J. D.; Cross, G. H.; Peterson, I. R., *Thin Solid Films*, 1985, **132**, 101.

9. Girling, I. R.; Cade, N. A.; Kolinsky, P. V.; Jones, R. J.; Peterson, I. R.; Ahmad, M. M.; Neal, D. B.; Petty, M. C.; Roberts, G. G.; Feast, W. J., *J. Opt. Soc. Am.*, 1987, **B4**, 950.
10. Marowsky, G.; Chi, L. F.; Mobius, R.; Steinhoff, R., *Chem. Phys. Lett.*, 1988, **147**, 420.
11. Kajikawa, K.; Shiota, K.; Takesue, H.; Fukuda, A.; *Jpn. J. Appl. Phys.*, 1990, **29**, 513.
12. Stroeve, P.; Saperstein, D. D.; Rabolt, J. F.; *Thin Solid Films*, 1989, **179**, 529.
13. Cheung, J.; Rubner, M. F., *Polymer Preprint*, 1990, **31(1)**, April, 404.
14. Kawai, T.; Umemura, J.; Takenaka, T., *Langmuir*, 1990, **6**, 872.
15. Ordal, M. A.; Long, L. L.; Bell, R. J.; Bell, S. E.; Bell, R. R.; Alexander, Jr., R. W.; Ward, C. A., *Appl. Opt.*, 1988, **22**, 1099.
16. Dewar, M.J.S.; Thiel, W., *J. Am. Chem. Soc.*, 1977, **99**, 4890.
17. Kleinman, D. A., *Phys. Rev.* 1962, **126**, 1977.
18. Williams, D. J., *Nonlinear Optical Properties of Organic Molecules and Crystals*, Vol. 1, ed. by Chema, D. S. and Zyss, J., Academic, New York, 1987, p. 406.
19. Heints, T. F.; Chen, C. K.; Ricard, D.; Shen, Y. R., *Phys. Rev. Lett.*, 1982, **48**, 478.

Table I Assignments of FTIR Main Peaks of Hemicyanine 5-Monolayer LB Film

Wavenumber (cm ⁻¹)	RA	Assignment
2958	2966	antisym. CH ₂ stretching
2918	2922	antisym. CH ₂ stretching
--	2871	sym. CH ₂ stretching
2850	2852	sym. CH ₂ stretching
1628	1643	vinyllic C=C stretching
1589	1599	aromatic ring C=O stretching
1470	1468	CH ₂ scissoring
1178	1176	aliphatic C-N stretching

Table II Calculated Enhancement Factors and Tilt Angles for Specific Transition Moments of Hemicyanine LB Film

Assignment	Wavenumber (cm ⁻¹)	Transmission	RA	A _T /A _S	E _r	E _s	ψ(°)
ν _a (CH ₂)	2918	2922	0.95	0.0595	4.79	73	
ν _s (CH ₂)	2850	2852	1.47	0.0570	4.82	75	
ν(C=C)	1589	1599	0.09	0.0185	5.06	43	

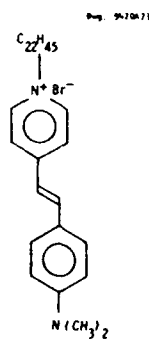


Fig. 1-Structure of Amphiphilic Hemicyanine Dye

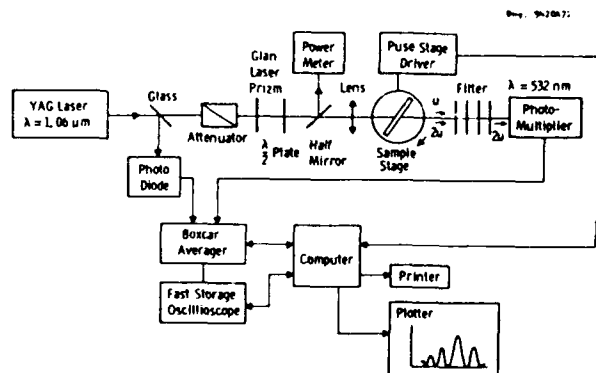


Fig. 2-Experimental Configuration for Maker Fringe Measurement

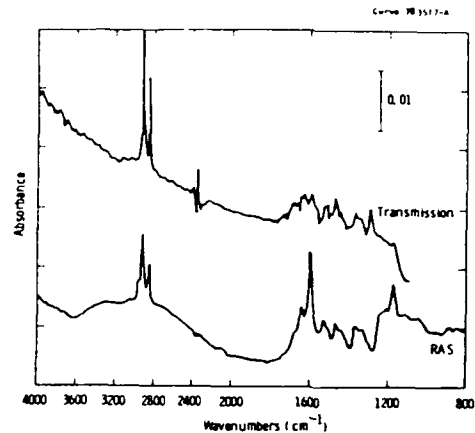


Fig. 3-Infrared Transmission and Reflection Spectra of 5-Monolayer Hemicyanine L-B Film

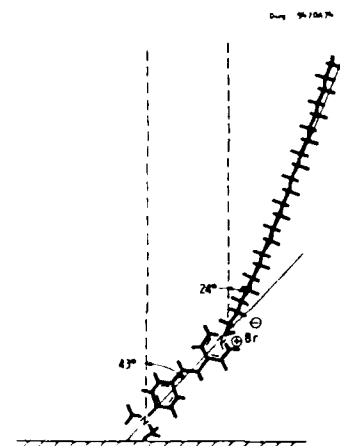


Fig. 4-Molecular Orientation of Hemicyanine L-B Film

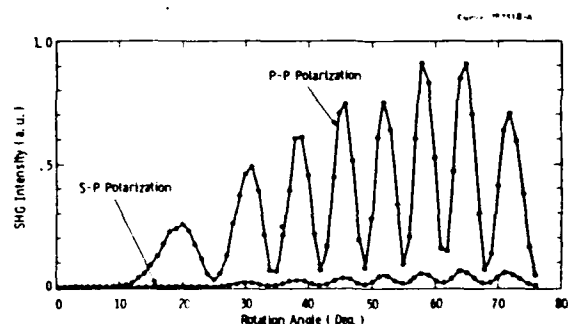


Fig. 5-Typical SHG Maker Fringe Pattern of Hemicyanine Dye Monolayer

INTERNAL ELECTRIC FIELD AND DYE ORIENTATION IN PVDF/PMMA BLEND

Naoto Tsutsumi, Yoshiaki Ueda and Tsuyoshi Kiyotsukuri
 Department of Polymer Science & Engineering
 Kyoto Institute of Technology
 Matsugasaki, Sakyo, Kyoto 606, JAPAN

Introduction

Hill et al.¹⁾ recently demonstrated that the internal electric field E_i created by the preferentially oriented polar crystals of the copolymer of vinylidene fluoride and trifluoroethylene (VDF-TrFE copolymer) can orient polar molecules which dissolve in the amorphous region of the copolymer. Using guest molecules which have non-linear optical (NLO) properties, they showed that such poled copolymer films exhibit second harmonic generation (SHG) arising from the oriented NLO molecules. Tsutsumi et al.²⁾ have also studied E_i created between the β -crystallite dipoles of the VDF-TrFE copolymer using the electrochromic peak shift of dye dissolved in the copolymer.

Polyvinylidene fluoride (PVDF) and polymethylmethacrylate (PMMA) blends have known to be compatible in all blend ratios.³⁾ Furthermore there are a few reports on β -crystallite formation in a melt-quenched PVDF/PMMA blend at some blend ratio.⁴⁾⁵⁾

We measured E_i created between the β -crystallite dipoles of β -PVDF in PVDF/PMMA (80/20) blend with the same procedure applied to the VDF-TrFE copolymer²⁾ and estimated the orientation of dyes by E_i from the dichroic ratio of dye. In this study, we report the effects of E_i on thermal aging and annealing and the orientation of dye by E_i .

Experimental

PVDF (Kureha, KF-polymer, $M_v = 141,000$, $M_n = 64,000$) and PMMA (Mitsubishi Rayon, Acrypett-VHK, $M_v = 168,000$, $M_n = 96,400$) were used. 4-Dimethylamino-4'-nitrostilbene (DANS) from Eastman Kodak Co. was crystallized from amyl alcohol.

The polymers were mechanically melt blended at 200°C and films were melt-pressed between 50 μ m thick films of Uplex (Ube Industry, Japan) on a heated press to a thickness between 40 to 70 μ m. The melted films were quenched into liquid nitrogen.

The solute probe DANS was introduced by soaking the polymer films in n-propyl alcohol solutions saturated with DANS at the boiling point of the alcohol (97°C) for 4 h followed by drying overnight at room temperature in vacuum. The concentration of DANS in the blend was 5.0 - 6.5 mmol/l.

The blend films were poled by applying a constant voltage for 1 h at 80°C in the nitrogen atmosphere to aluminum electrodes which had been evaporated onto opposing surfaces of the films. Pyroelectric response was determined by measuring the current generated upon heating and cooling the poled film at a measured rate, usually 0.1 - 0.8°C/min in the vicinity of 30°C.

UV-visible spectra of the films were measured on a Shimadzu model UV-2101PC spectrophotometer and measured spectra data were stored in a computer for analysis.

Data Analysis

E_i was calculated using the equation of

$$\frac{1}{(1-f)} \left[\frac{A(v, E)}{v} - A(v, 0) \right] / v = \frac{G(u)}{1-G(u)} \times \left[-3C \frac{\partial A(v, 0)/v}{\partial v} + 1.5C^2 \frac{\partial^2 A(v, 0)/v}{\partial v^2} \right] \quad (1)$$

where

$$G(u) = 1 - 3 \coth(u)/u + 3/u^2 \quad (2)$$

$$u = E_i \mu_g / kT \quad (3)$$

$$C = (k T \Delta \mu) / (h c \mu_g) \quad (4)$$

μ_g : dipole moment of DANS in the ground state, k : Boltzmann's constant, T : absolute temperature, $\Delta \mu$: the difference between the dipole moments in the excited state and in the ground state, h : Planck's constant, c : the speed of light.

The first and second derivatives of $A(v, 0)/v$ were evaluated as a function of v to determine the value v_H , for which the right hand side of equation (1) was zero. When $\partial \{A(v, 0)/v\} / \partial v = (C/2) \partial^2 \{A(v, 0)/v\} / \partial v^2$, a value of $(1-f)$ was chosen to make the spectra of the poled and unpoled samples intersect at v_H , i.e., $A(v_H, E) / \{(1-f)v_H\} = A(v_H, 0) / v_H$. Having normalized the curves at v_H , the difference in absorbance between the two spectra at several other values of v were then determined, the derivatives were evaluated at the corresponding values of v as required for equation (1) and the quantity $[G(u) / \{1-G(u)\}]$ was evaluated from a linear least squares fit. From $G(u)$ and equation (2), a value of u was obtained from which E_i was evaluated.

The degree of orientation F of dye to the direction of electric field (to the sample thickness) was estimated as follows. Modified dichroic ratio D of $(I_{\parallel} / I_{\perp})^P / (I_{\parallel} / I_{\perp})^0$ was measured, tilting the sample film, where I_{\parallel} and I_{\perp} are the absorbances parallel to and perpendicular to the tilting axis, respectively, and superscripts of P and 0 mean poled and unpoled. Then F was estimated using the conventional equation of $F = (1-D) / (1+2D)$ with D extrapolated to the tilting angle of 90°.

Results and Discussion

Figure 1 shows the effect of poling on the absorption spectrum of the dissolved DANS. It is apparent that the poling causes the slight shift of maximum peak in spectrum to longer wavelength, which shows the electronic state of DANS dissolved in the amorphous region is subject to the strong internal electric field created between the β -PVDF crystallite dipoles. The decrease of absorption intensity by poling is mainly due to the reorientation (alignment) of DANS to the internal field. After normalizing the poled DANS spectrum using the procedure described in the section of Data Analysis, internal electric field was calculated.

Figure 2 shows the plots of E_i and C_{pyro} after the poled sample film was stored at room temperature for the indicated aging time. The poling was carried out to apply a constant field of 0.5 MV/cm at 80°C for 1h in the nitrogen atmosphere. E_i decayed in the several hours after poling and almost leveled off in a few days. E_i of 1.3 MV/cm immediately after poling leveled off to ca. 1.0 MV/cm. It is noted that E_i is twice larger than the poling field of 0.5 MV/cm. C_{pyro} also decayed and leveled off in the same manner. Decrease of E_i in the initial several hours is due to the accumulation of ionic countercharges at crystal-amorphous interface described below or the loss of the instable charges induced under high field poling.¹⁾

Table I shows E_i and C_{pyro} as well as F values, compared with the corresponding results of VDF-TrFE copolymer. VDF-TrFE copolymer was poled at room temperature. Although E_i 's of both systems are almost the same, C_{pyro} and F of PVDF/PMMA are smaller than those of VDF-TrFE copolymer. The difference of both C_{pyro} and F is ascribed to the difference of mobility of dye in the amorphous region due to the difference of glass transition temperature of both systems. Higher applied field produced higher E_i and C_{pyro} , probably because of the achievement of higher ordered state of β -PVDF

crystallite dipoles.

Figure 3 shows E_i and C_{pyro} after the poled film is annealed for two hours each at successively higher temperatures. C_{pyro} monotonically decreases with increasing annealing temperature, whereas the decreased E_i up to 60°C changes to increasing until it falls down again above 90°C. The WAXS results did not show any significant change of crystallite structure, crystallite size and crystallinity. Thus the decrease of E_i and C_{pyro} with increasing annealing temperature is ascribed to the relaxation of the aligned crystallite dipoles. The increase of E_i after annealing to the vicinity of 90°C is attributed to the loss of the accumulated ionic countercharges. The slight increase of E_i after heating to the vicinity of 80°C was measured in the VDF-TrFE copolymer, and it was explained by the loss of the localized F^- ion at crystal-amorphous interface which is generated during high field poling²⁾. Thus PVDF/PMMA blend is also considered to generate F^- ion under high field poling, which is localized at the interface, and the loss of the localized F^- ion is responsible to the increase of E_i .

The effect of the difference of the crystal form on E_i was studied. A melt and slowly cooled PVDF/PMMA film shows the crystal form of type II (α -PVDF). The result of E_i and C_{pyro} are also listed in Table I. It is clear that E_i created by α -PVDF crystallite dipoles is smaller than that by β -PVDF one, which is consistent with the results of C_{pyro} . The smaller net dipole moment of α -crystallite phase is responsible to the smaller values of E_i and C_{pyro} .

Conclusion

It was found that the β -PVDF crystallite dipoles in the PVDF/PMMA blend create the strong internal electric field which aligns the dye semipermanently. Further this blend has the good optical quality of almost not scattering light in the visible region. These properties will guarantee this blend as one of the candidate of the SHG material.

Acknowledgements

The authors are sincerely grateful to Mr H. Horibe, Mitsubishi Electric Co., Japan, for preparing blend sample. This work is supported in part by a Grant-in-Aid for Scientific Research No. 02750635, from Ministry of Education, Science and Culture, Japan.

References

- 1) J.R.Hill, P.Pantelis and G.J.Davies, *Ferroelectrics* 76, 435 (1987)
- 2) N.Tsutsumi, G.T.Davis and A.S.DeReggi, *Bull. Am. Phys. Soc.* 34, 981 (1989); *Macromolecules* submitted.
- 3) T.Nishi and T.T.Wang, *Macromolecules* 8, 909 (1975).
- 4) C.Leonard, J.L.Halary, L.Monnerie, D.Broussoux, B.Servet and F.Micheron, *Polym. Commun.* 24, 110 (1983).
- 5) H.Horibe, F.Baba and S.Etoh, *Polym. Preprints Jpn.* 38, 3533 (1989).

Table I. Results of E_i and C_{pyro} and F

	E_i (MV/cm)	C_{pyro} (nC/cm ² K)	F
PVDF/PMMA (β -form)	1.9 - 2.0	0.35 - 0.5	0.01 - 0.02
VDF-TrFE Copolymer	2.0	1.3	0.05 - 0.1
PVDF/PMMA (α -form)	0.56 - 0.7	0.13 - 0.17	

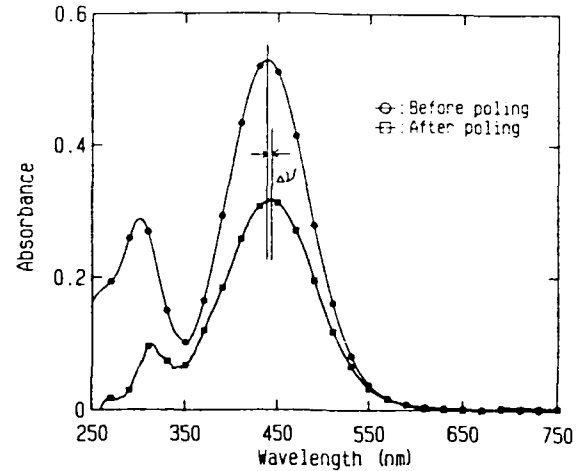


Figure 1. Absorption spectra of DANS in PVDF/PMMA before and after poling. Poling field is 0.8 MV/cm.

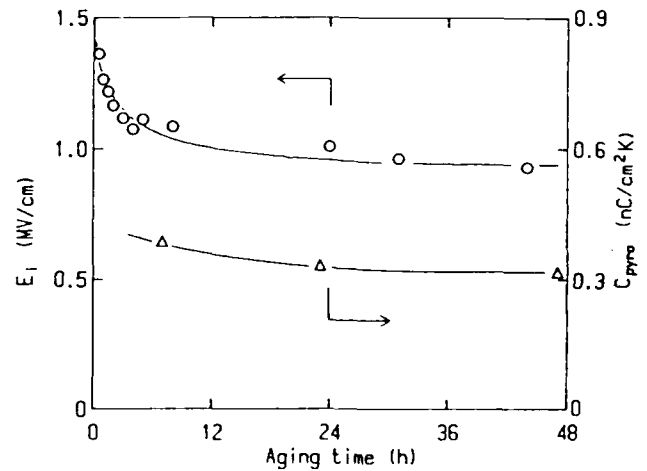


Figure 2. Dependence of E_i and C_{pyro} on aging time at room temperature.

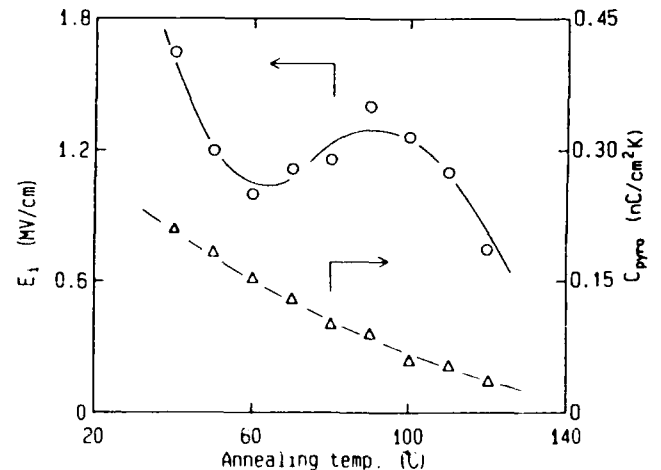


Figure 3. Dependence of E_i and C_{pyro} on annealing temperature

CUBIC NONLINEAR OPTICS OF POLYMER THIN FILMS.
3. STRUCTURE- $\chi^{(3)}$ RELATIONSHIPS IN CONJUGATED
AROMATIC POLYAZOMETHINES

Chen-Jen Yang and Samson A. Jenekhe*
Center for Photoinduced Charge Transfer
and Department of Chemical Engineering
University of Rochester
Rochester, NY 14627-0166

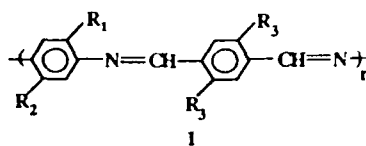
and
Herman Vanherzeele and Jeffrey S. Meth
DuPont Central Research & Development Department
P.O. Box 80356, Wilmington, DE 19880-0356

Introduction. The conjugated aromatic polyazomethines are thermally stable film- and fiber-forming materials that exhibit good mechanical strength, thermotropic liquid crystallinity, and lyotropic liquid crystallinity in concentrated sulfuric or methanesulfonic acid [1-3]. Although these features of the aromatic polyazomethines have been investigated for many years [1-3], the detailed structure and solid state properties of this class of polymers have not been studied because of their general *insolubility* except in strong concentrated acids in which they rapidly degrade due to the hydrolysis of the Schiff base ($-\text{CH}=\text{N}-$). We recently reported the preparation of soluble complexes of a series of conjugated aromatic polyazomethines and their solution processing to optical quality thin films suitable for characterization of linear optical, nonlinear optical, and electronic properties of the polymers [4]. Here, we will report on our study of the third-order nonlinear optical properties of a series of homopolymers and random copolymers of the conjugated aromatic polyazomethines.

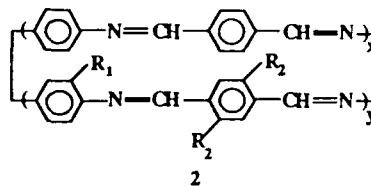
Our interest in these aromatic Schiff base polymers as third-order nonlinear optical materials is based in part on their unique structure and their relationship to other *p*-phenylene polymers. The conjugated aromatic polyazomethines are isoelectronic with poly(*p*-phenylene vinylene) and derivatives whose electronic structure and nonlinear optical properties have been widely investigated [5-9]. For example, films of PPV and its 2,5-dimethoxy derivative have a $\chi^{(3)}$, measured by third harmonic generation, of 7.8×10^{-12} and 5.4×10^{-11} esu, respectively, at $1.85 \mu\text{m}$ [7]. Highly oriented PPV films have a $\chi^{(3)}$ of 1.5×10^{-10} esu at $1.85 \mu\text{m}$ [9]. Similarly large third order optical nonlinearities can be expected in conjugated aromatic polyazomethines. On the basis of the theoretically predicted anharmonicity effect on $\chi^{(3)}$ [10], the aromatic polyazomethines might be expected to have larger optical nonlinearities compared to their corresponding vinylene-linked polymers due to the anharmonicity arising from a nitrogen replacing one CH in vinylene links.

We have synthesized and prepared thin films of a series of homopolymers 1 and random copolymers 2 in order to investigate the structure- $\chi^{(3)}$ relationships in this class of conjugated polymers. This paper reports our picosecond third harmonic generation measurement of $\chi^{(3)}$ and its wavelength dispersion in selected members of 1 and 2. Trends in the structure- $\chi^{(3)}$ correlations for all the homopolymers and random copolymers will be presented.

Experimental. All the monomers used, whether synthesized or purchased, were rigorously purified prior to polymerization. All the polymers were prepared by the solution polymerization of aromatic diamines with aromatic dialdehydes. Details of the synthesis and characterization of the polymers are described elsewhere [4]. The following are typical synthetic procedures. **Copolymer PPI/PMPI (2a):** This copolymer was prepared by solution polymerization of 1.0677 g (8.74 mmol) 2-methyl-1,4-phenylenediamine, 0.9453 g (8.74 mmol) 1,4-phenylenediamine and 2.3450 g (17.48 mmol) terephthalaldehyde in the presence of 1 g LiCl in a 50 mL 1:1 HMPA/NMP solution at room temperature. After purification and vacuum drying the yield was 3.647 g (98%). ^1H NMR of PPI/PMPI: ($\text{CD}_2\text{NO}_2/\text{GaCl}_3$) 2.80, 8.10, 8.30, 8.70, 9.70, and 9.83 ppm. **PMOPI (1d).** 1.4339 g (13.26 mmol) 1,4-phenylenediamine was reacted with 2.5724 g (13.26 mmol) 2,5-dimethoxyterephthalaldehyde in 40 ml 1:1 HMPA/NMP and 0.8 g LiCl under nitrogen purge at room temperature. After 48 hrs polymerization time, the polymer was precipitated, washed repeatedly with water and methanol and dried



- 1a. $R_1 = R_2 = R_3 = \text{H}$ (PPI)
1b. $R_1 = \text{CH}_3, R_2 = R_3 = \text{H}$ (PMPI)
1c. $R_1 = \text{OCH}_3, R_2 = R_3 = \text{H}$ (MO-PPI)
1d. $R_1 = R_2 = \text{H}, R_3 = \text{OCH}_3$ (PMOPI)
1e. $R_1 = \text{OCH}_3, R_2 = \text{H}, R_3 = \text{OCH}_3$ (MO-PMOPI)
1f. $R_1 = R_2 = \text{OCH}_3, R_3 = \text{OCH}_3$ (DMO-PMOPI)
1g. $R_1 = R_2 = \text{H}, R_3 = \text{OH}$ (PHOPI)



- 2a. $R_1 = \text{CH}_3, R_2 = \text{H}$ (PPI/PMPI)
2b. $R_1 = \text{H}, R_2 = \text{OCH}_3$ (PPI/PMOPI)

under vacuum to afford an orange powder (3.25 g, 92% yield). ^1H NMR of PMOPI: 4.50, 8.20, and 9.60 ppm.

Thin films of the polymers were prepared on optically flat fused silica substrates (5 cm in diameter) from either soluble GaCl_3 complexes in nitromethane or di-*m*-cresylphosphate (DCP) complexes in *m*-cresol [4]. Figure 1 shows the electronic absorption spectrum of the parent aromatic polyazomethine, 1a (PPI). This electronic spectrum shows that PPI absorbs in the visible with λ_{max} at 405 nm and an optical bandgap (E_g) of 2.50 eV. 2,5-dimethoxy substitution of every other *p*-phenylene ring in PPI significantly red shifts the electronic absorption spectrum as observed in Figure 1 for the spectrum of PMOPI (1d). The λ_{max} and E_g of PMOPI are 450 nm and 2.34 eV, respectively. Other substitutions in the aromatic polyazomethines produced expected variation in the linear optical properties λ_{max} and E_g . The polymer 1g, for example, has a λ_{max} and E_g values of 494 nm and 2.07 eV, respectively.

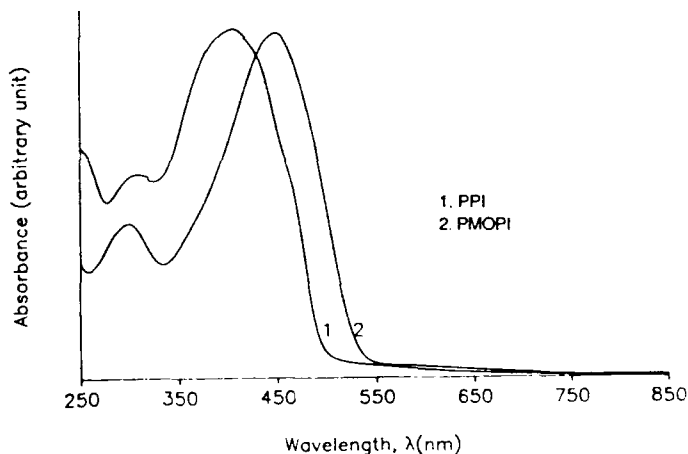


Figure 1 Electronic absorption spectra of thin films of PPI and PMOPI.

The third harmonic generation (THG) measurements of the magnitude of $\chi^{(3)}(-3\omega, \omega, \omega, \omega)$ were made by using a picosecond laser system continuously tunable in the range 0.6–4.0 μm [11] and following the procedure previously described [12]. The THG experiments in the present study were performed at a fundamental wavelength of 0.9–2.4 μm . The reported $\chi^{(3)}$ values are average values, corrected for absorption at the third harmonic wavelength, and obtained relative to the $\chi^{(3)}$ for fused silica (2.8×10^{-14} esu at 1.9 μm) [13]. The error for the reported $\chi^{(3)}$ values is $\pm 20\%$ due mostly to the error in film thickness measurement. The repeatability of individual results for each sample was $\pm 5\%$.

Results and Discussion. The wavelength dispersion of the magnitude of the third order susceptibility $\chi^{(3)}(-3\omega, \omega, \omega, \omega)$ of PPI and PMOPI thin films in the wavelength range 0.9–2.4 μm is shown in Figure 2. The nonresonant $\chi^{(3)}$ values for PPI and PMOPI were $\sim 2 \times 10^{-12}$ and $\sim 1 \times 10^{-11}$ esu, respectively, at 2 μm wavelength. The magnitude of the nonresonant cubic optical nonlinearity of PMOPI is a factor of 5 larger than that of the parent aromatic polyazomethine, PPI. This enhancement of the nonresonant third order optical properties of PPI by dimethoxy substitution can be explained by the greater electron delocalization in PMOPI as evidenced by its smaller bandgap.

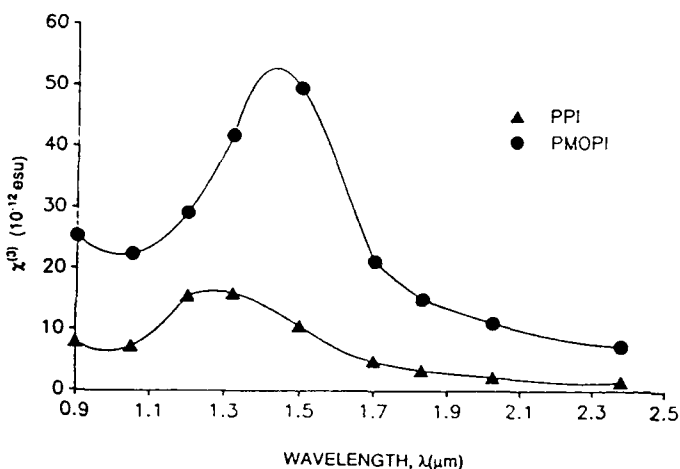


Figure 2 The $\chi^{(3)}$ spectra of two aromatic polyazomethines (PPI and PMOPI).

The $\chi^{(3)}$ spectra of PPI and PMOPI in Figure 2, exhibit a resonance feature that can be attributed to multiphoton processes since the electronic spectra of the polymers did not show any absorption features in the wavelength range 0.80–3 μm . The resonance peak in the $\chi^{(3)}$ spectra of PPI and PMOPI was $\sim 1.2 \mu\text{m}$ and $\sim 1.35 \mu\text{m}$, respectively, and hence suggests a three-photon resonance as the origin of the observed peak in the wavelength dispersion of the third order susceptibility. The magnitude of the three-photon enhanced $\chi^{(3)}$ of PPI and PMOPI was 1.6×10^{-11} and 5.0×10^{-11} esu, respectively. Thus, three-photon resonance enhancements results in about one order of magnitude increase for PPI and a factor of 5 increase for PMOPI above the nonresonant optical nonlinearities of these two aromatic polyazomethines.

In the $\chi^{(3)}$ spectrum of PHOPI, two resonance peaks were observed and similar in line shape to the two peaks observed in the electronic absorption spectrum of the polymer. The nonresonant $\chi^{(3)}$ of PHOPI was $\sim 2 \times 10^{-12}$ esu at 2.4 μm which is the same as the unsubstituted parent polymer PPI. The three-photon resonance enhanced $\chi^{(3)}$ increased by a factor of only ~ 5 above the nonresonant value. The observed nonresonant and resonant optical nonlinearities of PHOPI are very surprising when compared to those of PPI and PMOPI. Since the electron delocalization in PHOPI, as measured by the λ_{max} and E_g values, is greater than in PPI and PMOPI, it was anticipated that the magnitude of $\chi^{(3)}$ in PHOPI will also be larger. Instead, it was observed that the optical nonlinearity in PHOPI is

about the same as in PPI but significantly less than in PMOPI. These results suggest that an important structural factor, other than electron delocalization, is also at play in the magnitude of the cubic optical nonlinearities of the polymers. The effects of other ring substituents and substitution patterns and random copolymerization on the cubic nonlinear optics of conjugated aromatic polyazomethines will be presented.

Conclusions. We have prepared optical quality thin films of a series of homopolymers and copolymers of aromatic polyazomethines and investigated their cubic nonlinear optical properties by picosecond third harmonic generation in the wavelength range 0.9–2.4 μm in order to understand the underlying structure- $\chi^{(3)}$ relationships. The results shown that the magnitude of the third order optical susceptibility of the conjugated aromatic polyazomethines, as measured by THG, was about 10^{-12} to 10^{-11} esu off-resonance and about 10^{-11} to 10^{-10} esu with three-photon resonance enhancement. In some series of the polymers $\chi^{(3)}$ was observed to increase with increasing electron delocalization as measured by λ_{max} and E_g . However, it was found that this relationship does not hold in some members of the conjugated polymers 1 and 2.

Acknowledgment. Work at the University of Rochester was supported by the New York State Science and Technology Foundation, Amoco Foundation, and National Science Foundation (Grant CHE-881-0024).

References

- (a) G.F. D'Alelio, J.V. Crivello, R.K. Schoenig and T.F. Huemmer, *J. Macromol. Sci. A1*, 1161 (1967). (b) G.F. D'Alelio, W.F. Strazik, D.M. Feigl and R.K. Schoenig, *J. Macromol. Sci. Chem. 2*, 1457 (1968).
- P.W. Morgan, S.L. Kwolek and T.C. Pletcher, *Macromolecules* 20, 729–739 (1987).
- (a) B. Millaud, A. Thierry and A. Skoulios, *Mol. Cryst. Liq. Cryst., Lett.* 41, 263 (1978). (b) C. Noel and J. Billard, *Mol. Cryst. Liq. Cryst., Lett.* 41, 269 (1978).
- (a) C.J. Yang and S.A. Jenekhe, *Chem. Mater.*, submitted. (b) C.J. Yang and S.A. Jenekhe, in preparation.
- S. Antoun, F.E. Karasz, and R.W. Lenz, *J. Polym. Sci. A: Polym. Chem.* 26, 1809–1817 (1988).
- H. Eckhardt, L.W. Shacklette, K.Y. Jen, and R.L. Elsenbaumer, *J. Chem. Phys.* 91, 1301–1315 (1989).
- (a) T. Kaino, K.I. Kubodera, S. Tomura, T. Kurihara, S. Saito, T. Tsutsui, and S. Tokito, *Electron. Lett.* 23, 1095 (1987). (b) T. Kaino, S. Saito, T. Tsutsui and S. Tokito, *Appl. Phys. Lett.* 54, 1619 (1989).
- (a) B.P. Singh, P.N. Prasad and F.E. Karasz, *Polym.* 29, 1940 (1988). (b) J. Swiatkiewicz, P.N. Prasad, F.E. Karasz, M.A. Druy and P. Glatkowski, *Appl. Phys. Lett.*, 56, 892–894 (1990).
- C. Bubeck, A. Kaltbeitzel, R.W. Lenz, D. Neher, J.D. Stenger-Smith, and G. Wegner, In: J. Messier, F. Kajzar, P. Prasad, and D. Ulrich, Eds., *Nonlinear Optical Effects in Organic Polymers* (Academic Publishers, Dordrecht, Holland, 1989) pp. 143–147.
- S.C. Mehendale and K.C. Rustagi, *Opt. Commun.* 28, 359 (1979).
- H. Vanherzeele, *Appl. Optics* 29, 2246 (1990).
- (a) H. Vanherzeele, J.S. Meth, S.A. Jenekhe and M.F. Roberts, *Appl. Phys. Lett.* 58, 663 (1991). (b) J.A. Osaheni, S.A. Jenekhe, H. Vanherzeele and J.S. Meth, *Chem. Mater.* 3, No. 2, p. xxx (1991).
- B. Buchalter and G.R. Meredith, *Appl. Optics* 21, 3221 (1982).